27TH Annual Conference Proceedings

Lithium Battery Technology Conference

ALTA Metallurgical Services, Melbourne, Australia

www.altamet.com.au

PROCEEDINGS OF

ALTA 2023 LITHIUM-BATTERY TECHNOLOGY SESSIONS

5 May 2023

Perth, Australia

978-0-6458390-4-3

ALTA Metallurgical Services Publications

Lithium-Battery Conference

LITHIUM & BATTERY TECHNOLOGY KEYNOTE

VALUE ADDING OPPORTUNITIES FOR AUSTRALIAN BATTERY CRITICAL MINERALS

By

[1,2]Jacques Eksteen,

[1]Western Australian School of Mines, Minerals, Energy & Chemical Engineering

[2]Future Battery Industry CRC

Presenter and Corresponding Author

Jacques Eksteen
Jacques.Eksteen@curtin.edu.au

ABSTRACT

Critical minerals, metals and materials cover a highly diverse range of materials which share some commonality in geopolitical and mineral economic constraints, but no commonality with regards to processing, metallurgy or even markets. Even within the same market, such as energy storage, there is very little overlap with regards to chemistry, or processing. For energy and battery-related critical minerals there are however some common constraints that have to be considered during value addition such as ESG drivers (particularly around decarbonisation, ethical sourcing), ultra-high product purity, and the focus on material properties beyond chemical purity (in comparison to the conventional mineral processing industries). Ultimately, we need to remove the criticality of Critical Metals & Minerals though sustainable, diversified supply chains where redundancy is baked into the supply chains from raw materials to final products, without single countries or jurisdictions exerting near-complete control over the supply chains.

Within the Australian context, some progress has been made with regards to refining of concentrates to battery chemicals, most notably lithium hydroxide and nickel sulphate which are now produced at an industrial scale. Yet, the level of innovation has been fairly low, and production has been pretty much according to standard processing pathways used elsewhere. The stock markets remain sceptical about new technologies and process innovation is implicitly discouraged when finance is sought. Conversely, juniors and mid-tiers (and even some Tier-1 producers) have over-hyped project potential and severely underestimated the timelines to market, further reinforcing the market scepticism. Market valuations of companies involved in battery metals and materials refining reflects that the industry as a whole has fallen victim to the Dunning-Kruger effect with realism setting in after a period of initial hype followed by disillusionment.

Nonetheless, there are significant opportunities for process intensification during value addition that should be considered. The drive to decarbonise value chains is particularly important and is being supported by battery producers and governments. Furthermore, given the relative scarcity of some of the battery critical metals, such as nickel, lithium and cobalt and vanadium, process development to utilise lower grade materials, whether lower grade concentrates, tailings, or scrap is essential to ensure sustainable future supply of these metals.

This presentation will touch upon some of the opportunities to add value to our battery critical metals while intensifying our processes for refining, improving ESG credentials, and broadening the resource and reserve base.

Keywords: Critical Metals, Battery Metals, Lithium, Nickel, Cobalt, Processing, Decarbonisation, ESG

Context: Critical Minerals/Metals as Group

- Critical Minerals (CMs): An mineral economic term, not a technical one.
- Geopolitical drivers are typical in risks to supply chains disruptions which makes minerals critical if those minerals are essential for modern technologies, and in particular for the modern energy transition.
- Prices are volatile and supplies are at risk due to many possible disruptions by single (or a few) big players along value chain
- Some part of the value chain normally passes through a country that often threatens free market operation and known geopolitical risks
- Processing and chemistries very diverse. No commonality exists that would allow generalisation across the wide range of CMs. Even when they are used in the same application, e.g. batteries, there is no similarity amongst battery CMs of lithium, nickel, manganese, high purity alumina and graphite (and/or phosphate in the case of LFP batteries).
  - Their geological occurrence, mineralogy, mining, waste products, chemistry, processing and refining differ widely.
- Some CMs, such as Li-bearing spodumene is viewed as an industrial mineral of the lithophile group of elements. Others, such as nickel, belongs to the chalcophile group of elements and scarcer base metals. The Platinum Group Metals (PGMs), essential in the green hydrogen equipment supply chain, are extremely scarce and also classified as precious metals. Unlike gold, PGMs are critical and gold not.
- Many CMs are by-products from the primary production of other minerals.

Natural Flake Graphite

Spodumene (Li)

HPA (Alumina)

Pentlandite (Ni)

Platinum

The pictures shaping the world of battery minerals/metals

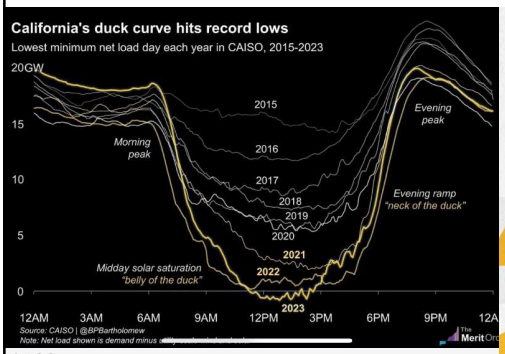

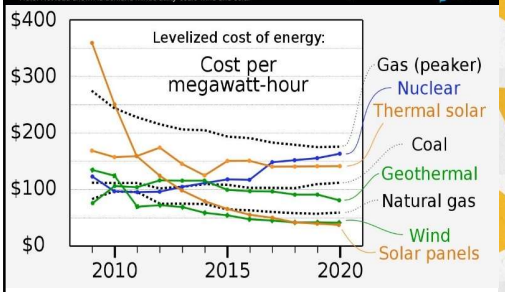

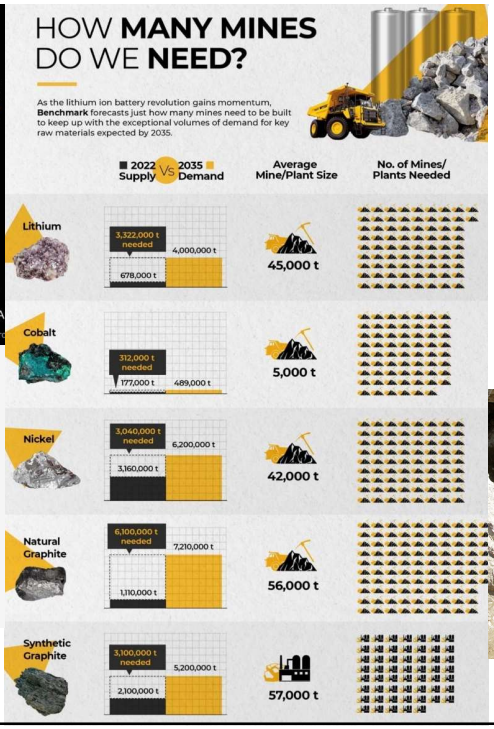

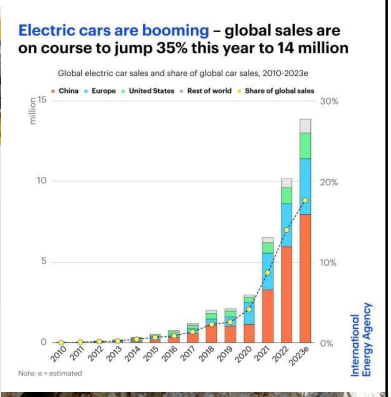

China still dominates the batter material supply chains

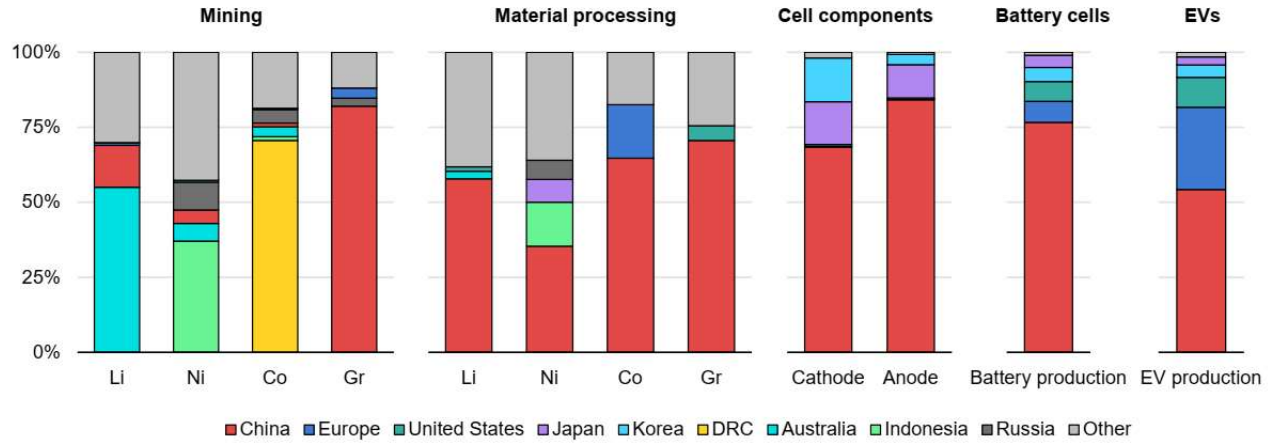

Graph sourced from IEA Report (www.iea.org): "Global Supply Chains of EV Batteries", 2022

CMs in the Energy Transition, Defense, and Advanced Technology Markets (EU Example)

It is ***important to remove the criticality*** of CMs. Criticality is alleviated through redundancy in the supply chain and parallel pathways to remove bottlenecks.

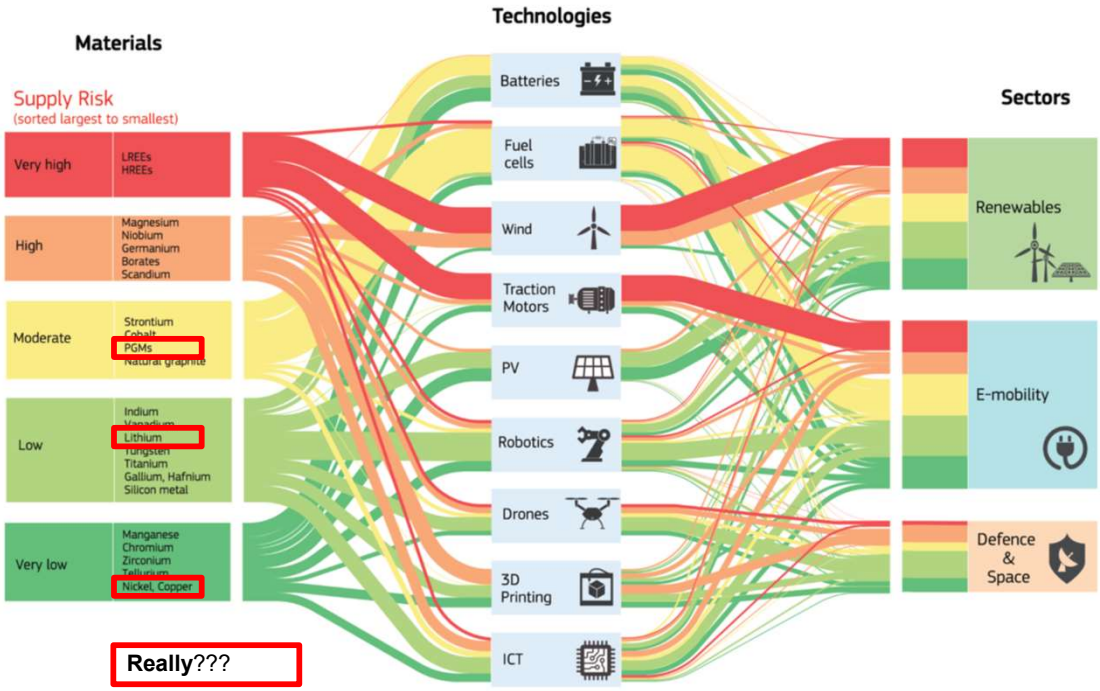

Demand Growth in some Critical Minerals / Metals / Materials

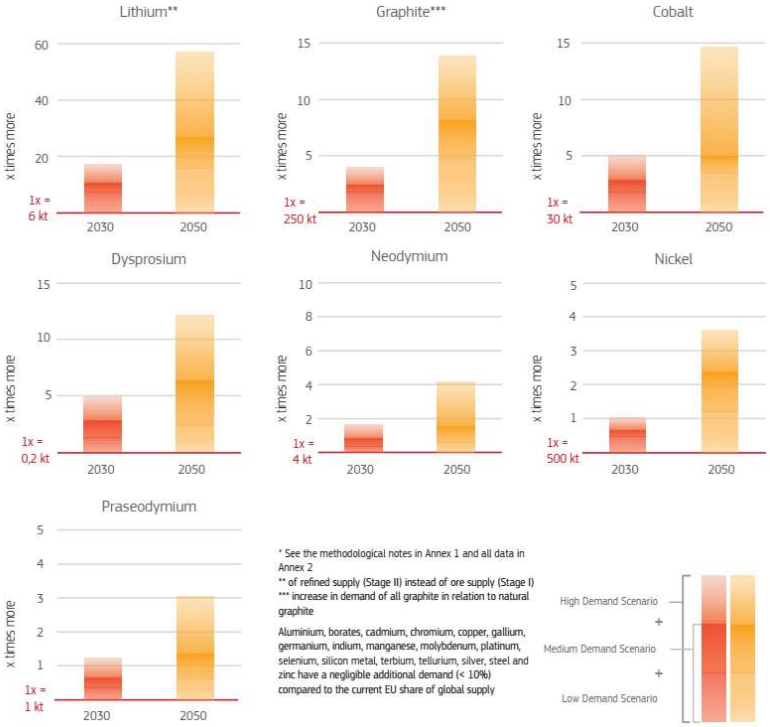

Innovation and the vulnerability to disruption:

Comparing the supply chain vulnerabilities of clean energy technologies

While innovation is often seen as positive, high rates of change and disruption may lead to “Osborne Effect”

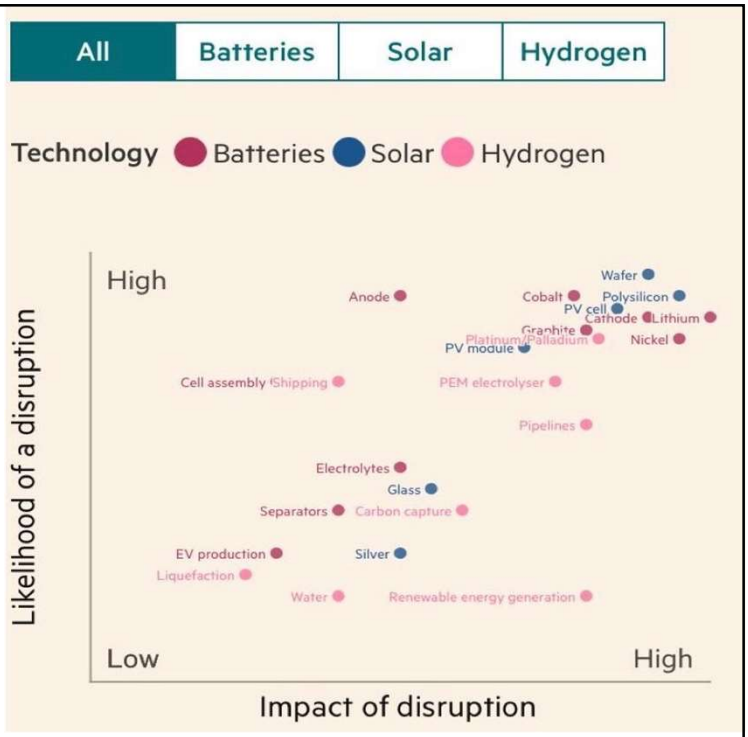

Source: International Energy Agency

Anticipated changes in battery chemistries (excluding flow batteries):

Battery cathode chemistries include:
Na-ion = sodium-ion.
LNMO =lithium nickel manganese oxide.
LMO = lithium manganese oxide.
LFP = lithium iron phosphate.
LNO = lithium nickel oxide.
LMR-NMC = lithium-manganese-rich NMC.
NMC = lithium nickel manganese cobalt oxide.
NMC-highNi includes: NMC811 and NMC9.5.5.
NMC-medNi includes: NMC532, NMC622 and NMC721.
NMC-lowNi includes: NMC333.
NMCA = lithium nickel manganese cobalt aluminium oxide.
NCA = lithium nickel cobalt aluminium oxide.
NCA+ includes: NCA85, NCA90, NCA92 and NCA95

*Sourced from IEA

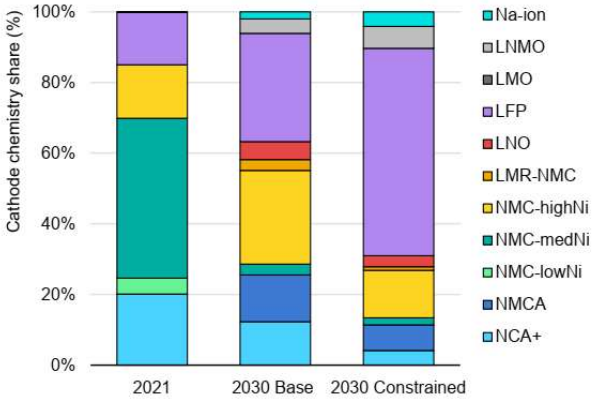

Graph sourced from IEA Report (www.iea.org): "Global Supply Chains of EV Batteries", 2022

The disconnect in timelines to establish bring new capacity online

Graph sourced from IEA Report (www.iea.org): "Global Supply Chains of EV Batteries", 2022

There is a significant disconnect between the time to bring new EV manufacturing or battery production into production versus bringing new mines and refining capacity into production

Critical Minerals, Metals & Materials (C3M's) in the Clean Energy Transition: Environment, Social & Governance (ESG) as a common driver & context

- These C3Ms are key enablers of clean energy transition:
  - batteries, hydrogen, ammonia, solar PV, wind turbines, electric motors and generators/dynamo'.
- Clean energy target requires supply chain of C3Ms to be clean, be ESG compliant, and align with global SDG's.
- This implies decarbonisation of scope 1, 2, and 3 emissions of CO_2. In addition, the sourcing should be ethical, have ethical and responsible labour practices, and minimise impacts on potable water use, communities, and waste generation.
  - Mine electrification is happening apace to lower Scope 1 & 2 the missions, but refining and conversion to high concentration materials required to lower Scope 3 emissions, e.g. associated with shipping/transport.
  - Carbonation of mineral wastes with point source emissions of CO_2 can lead to both sequestration and valorisation.
  - Waste must be valorised where it is generated as far a possible and not end up in landfill.
- Circularity does not only imply end-of-life only but reuse and repurpose throughout the value chain.
- Electrification from a renewable grid would be instrumental to decarbonise mining, processing and refining as well as advanced materials production.
- These ESG drivers and decarbonisation determine the context for our mine and process design.
- In this light we will look at two examples:
  - Decarbonisation and electrification of spodumene conversion to LiOH.
  - Process intensification and decarbonisation of nickel and cobalt from disseminated sulphide resources

Sustainability in battery supply chains

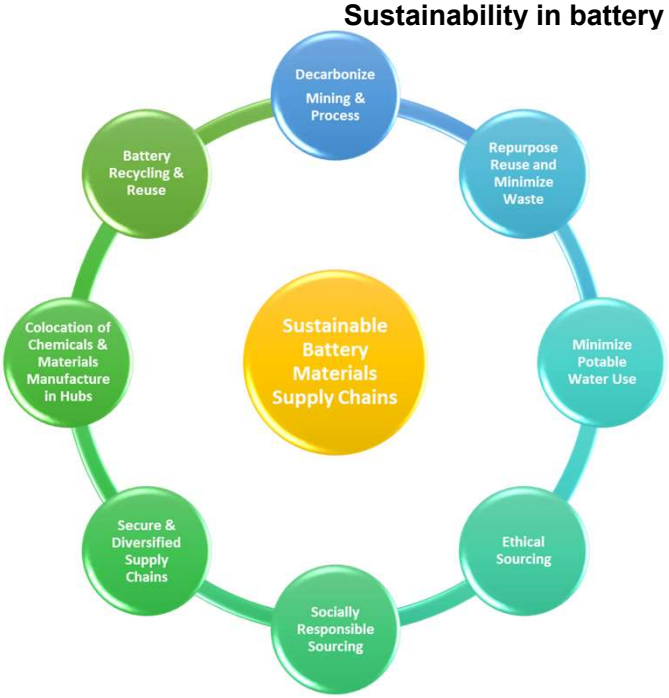

Supply Side Constraints:

- Limited accessible Ni-Co-Mn-Li geologies
- Geopolitical stability
- Community & regional conflicts :Water use
- Community & regional conflicts: Waste
- Extent to which mining & processing can be made net-zero in terms of CO2 emissions
- Poor metallurgical processing recoveries and yields
- Ensuring "green" processes are in place to produce refined lithium, nickel and graphite
- Single, or limited, dominant players in the supply chain

The battery metal demand tsunami

- Li's use is ubiquitous in cathode active materials, electrolyte and (sometimes) as anode material.
- Al is used as a foil in the cathode current collector but is also present in the cathode active materials, separator, and cathode and anode coatings (as high purity alumina).
- Fe appears in LFP and LFMP battery chemistries
- Cu foil is used as anode current collector, but it also underpin the global "electrify everything" drive
- Not shown here are the metals such as vanadium in redox flow batteries for stationary energy storage systems
- Phosphorus is used in Li-ion electrolytes ($LiPF_6$) and in LFP and LFMP battery cathode materials
- In addition to the battery metals, the Rare Earths are important, particularly for the magnets in electrical motors (EV's) and wind turbines for electrical power generation

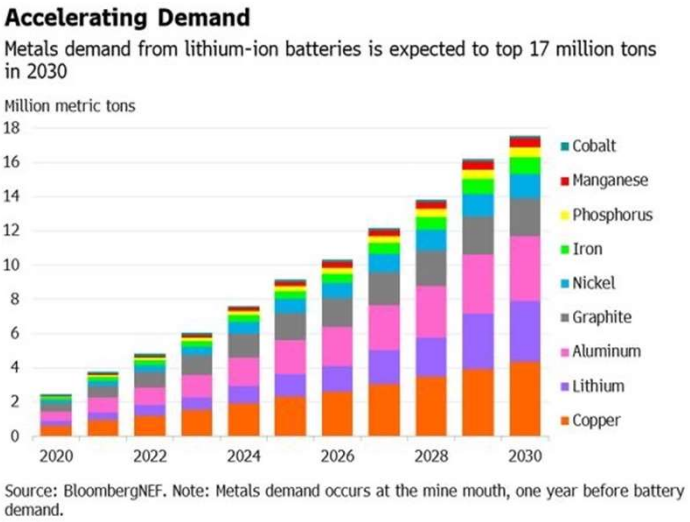

The production of the renewable technologies and energy storage technologies should be sustainable and should have a minimal carbon footprint

Contributions to Carbon Intensity of NMC LiB's

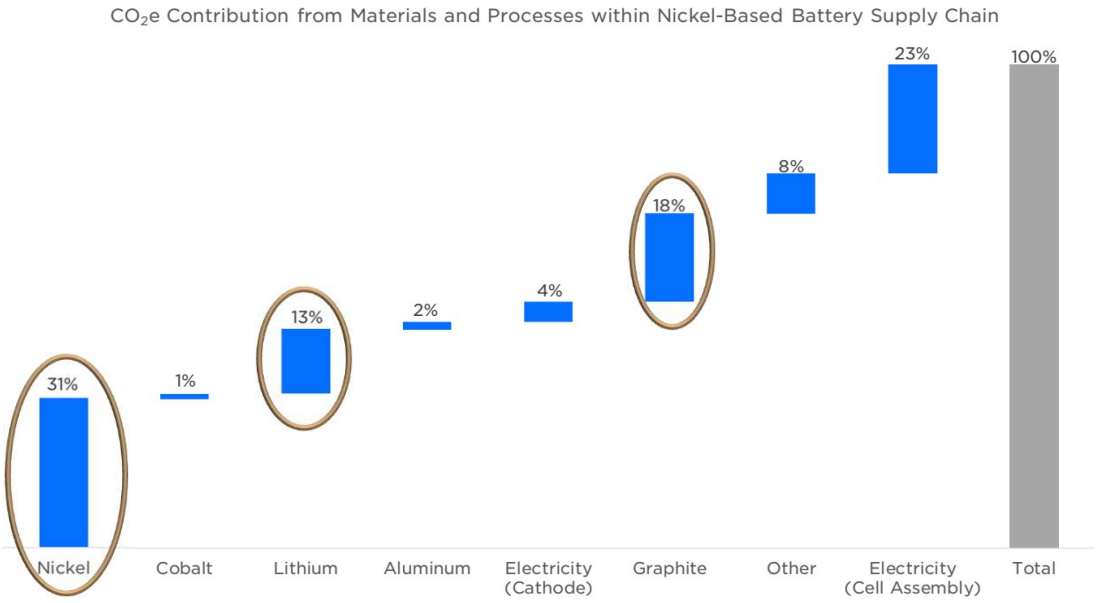

Major Carbon Contributors: Nickel, Lithium and Graphite

- Nickel, lithium and graphite all derive from ores that needs to be:
  - Mined
  - Crushed
  - Ground/milled
  - Concentrated through gravity & flotation technology
- The recoveries that can be achieved upstream in the concentrator is often constrained by the grade requirements of the downstream process (calcination, smelting, pressure leaching, spheroinisation in the case of graphite)
- Scope 1,2 & 3 emissions need to be evaluated, including the production of reagents, transport & energy mix
- Poor concentrator recovery implies that a significant amount of the energy used in crushing & grinding is wasted in unrecovered material to the tailings dam
  - *Just increasing the metallurgical recovery already significantly lowers the carbon footprint per metal unit produced*
- Finding metallurgical methods that can eliminate smelting (and its grade constraints), perform calcination in ways that minimize interparticle contact and clinkering, and improves spheroinisaton and graphitization yields (or replace synthetic graphite with high-yield, spheroinised natural graphite) can significantly lower the carbon footprint
- While improvements in heat transfer and fluid flow in the various thermal devices may lead to improvements, the extent of these improvements are highly dependent on the metallurgical and mineralogical nature of the materials (metal of interest and gangue minerals)

Multifaceted approach to decarbonization in lithium processing

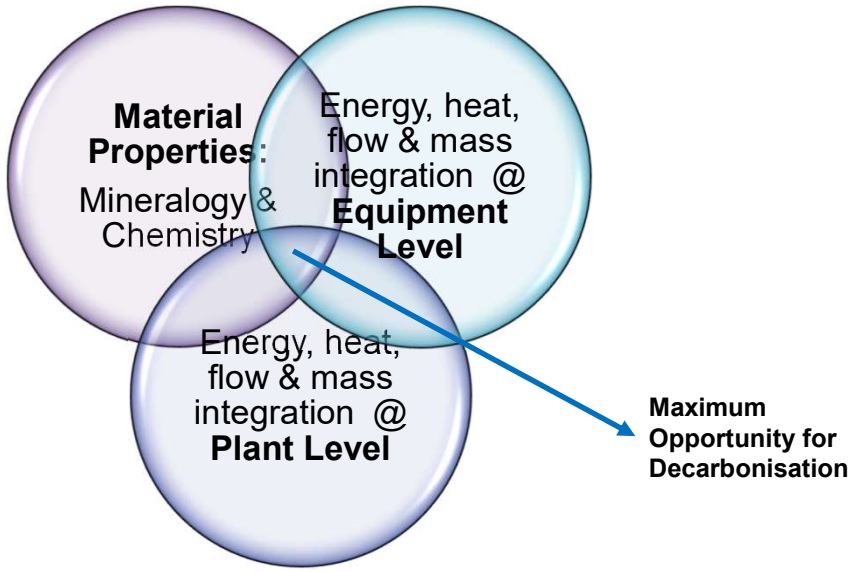

Major lithium mineral deposits (≥0.1 Mt Li)

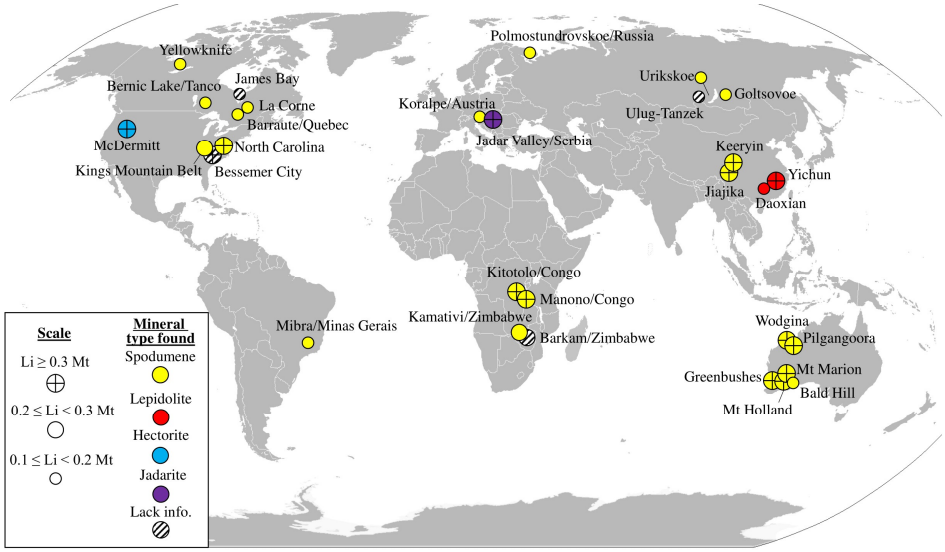

Typical lithium-bearing concentrate

Spodumene concentrate (Greenbushes, WA)

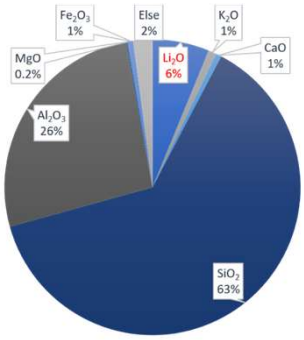

- Higher lithium grade
- Simpler compositions
- Less impurities

Lepidolite concentrate (Yichun, China)

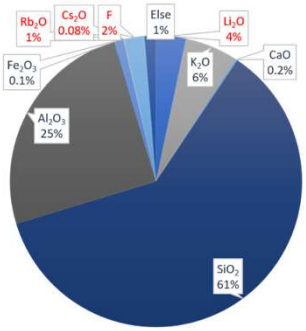

- Lower lithium grade
- Value-added rubidium, cesium
- Harmful fluorine

Zinnwaldite concentrate (Zinnwald, Germany)

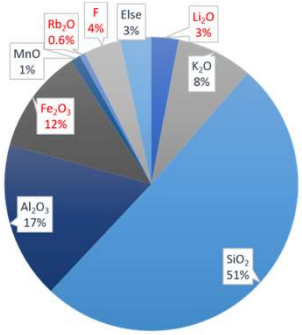

- More lower lithium grade
- Value-added rubidium
- Harmful fluorine
- High iron content

Conventional H_2SO_4 roasting method

- Proven effective to β-spodumene (con. H_2SO_4) and lepidolite (~85% H_2SO_4)
- Voluminous residue to be treated
  - Al-Si based residue, silica;
  - Calcium sulfate, calcium carbonate, Mg/Mn/Al/Fe hydroxides
- Noticeable lithium loss during impurity removal, *esp*. for lepidolite
- Flooded sodium sulphate by-product
- Lepidolite
  - Release of HF, SiF_4 gases
  - Further treatment of mixed alums (K, Rb, Cs)

Fluorine-based leaching methods

- Proven effective to α-spodumene, β-spodumene and lepidolite
- Options:

Hydrofluoric acid (HF) | **HF/ fluorosilicic acid (H_2SiF_6) + H_2SO_4** | **Fluorite (CaF_2) + H_2SO_4**

- Energy saving (75-230 °C), and high extractions;
- Fluorine removal better as early as possible, *e.g.* before alum crystallization;
- More sensible for silicate minerals with fluorine originally contained;
- Future research on mechanism, equipment design, safety control, *etc*;

Alkali roasting/autoclaving methods

- Proven effective to α-spodumene, β-spodumene and lepidolite;
- Alkali options:
  - Caustic (NaOH)
  - Lime/limewater ($CaO/Ca(OH)_2$)
- Caustic autoclaving for α-spodumene
  - Phase transfer (~1050 °C) avoided
  - High caustic consumption, *e.g.* 0.6 tonne caustic/tonne feed (5.5% Li_2O)

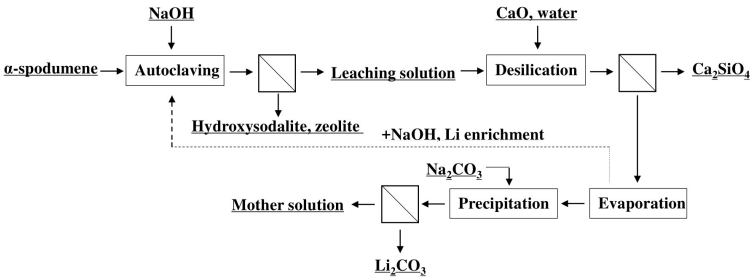

- Alkaline (caustic, lime/limewater/limestone) treatment is also capable of directly producing LiOH product.

Salt roasting/autoclaving methods

- Proven effective to β-spodumene, lepidolite and zinnwaldite;
- No considerable Na_2SO_4 problem
- Salt options:
  - Sulphate: K_2SO_4, **Na_2SO_4**, $FeSO_4$
  - Chloride: $CaCl_2$, NH_4Cl, NaCl
    - ✓ Capable of directly producing LiCl product
  - Carbonate: Na_2CO_3, $CaCO_3$
    - ✓ Followed by carbonation (CO_2) or conversion leaching (*e.g.* $Ca(OH)_2$);
  - Mixture of any above
- Fluorine may form fluorite (CaF_2) and/or Ca-Si-F compound ($Ca_4Si_2O_7F_2$), reporting to

Future research/trends

- Spodumene: still the main mineral source of lithium
  - Modification/improvement of H_2SO_4 method;
  - Direct treatment of natural spodumene;
  - Direct production of LiOH;
- Fluorine-based methods
  - Treatment of fluorine-containing waste;
  - Recycling/reuse of fluorine;
  - Indirect use of HF;
  - Reaction mechanism, equipment design, safety control.
- Towards comprehensive utilization - K, Al, Rb, Cs, F
  - Utilization of voluminous residue, *esp*. Al-Si based residue in the case of ion-exchange;
  - The key to compete with spodumene for lepidolite.

Lithium recovery from spodumene

	Acid method				Alkali method	
Major reagent	H_2SO_4	HF	H_2SO_4+HF	CaF_2+ H_2SO_4	NaOH	CaO/ $Ca(OH)_2$
Way of processing	Roasting	Leaching	Leaching	Leaching	Roasting/ autoclaving	Autoclaving
Spodumene type processed	β-spodumene	α/β-sposumene	α-spodumene	α-spodumene	α-sposumene	β-spodumene
Temperature of processing	~250 °C	~130 °C/ 75 °C	100 °C	~230 °C	600 °C fusion/ 250 °C autoclaving	100-205 °C
Representative ref.	Conventional	Kuang et al., 2012; Rosales et al., 2014	Guo et al., 2017	Kuang et al., 2012; Griffith et al., 2018	Sugyeong, 2018; Xing et al., 2019;	Mcintosh, 1946

Fluorine-based methods

Capable of processing α-spodumene

List of references

Lithium recovery from spodumene: High level approaches

	Sulphate method	Carbonate method	Chlorinating method	
Major reagent	K_2SO_4/ Na_2SO_4	Na_2CO_3/$CaCO_3$/ CO_2	Cl_2	$CaCl_2$/NH_4Cl/NaCl
Way of processing	Roasting/autoclaving	Autoclaving	Roasting	Roasting/autoclaving
Spodumene type processed	β-Spodumene	β-Spodumene	β-Spodumene	β-Spodumene
Processing Temperature	~1150 °C roasting/ 230 °C autoclaving	200-225 °C	1100 °C	900 °C roasting/ ~250 °C autoclaving 1000 °C roasting, H_2O leach
Representative ref.	Zeelikman et al., 1966; Kuang et al., 2018	Chen et al., 2011; Tiihonen et al., 2019 Haynes, B. & Mann, J., 2017	Barbosa et al., 2014	Gabra et al., 1975; Barbosa et al., 2015 Fosu et al

List of references

Lithium recovery from spodumene: Alternative Thermal Treatments

Review of spodumene processing techniques by heat treatment.

Type of roasting	Roasting			Leaching		Product
	Additive	Temp., °C	Time, min	Reagent	Efficiency	
Sulfation	$(NH_4)_2SO_4$	150–370	–	NH_3 (aq.)	–	Li_2SO_4
	$CaSO_4 + CaCO_3$	1000–1150	120–180	H_2O	85–90	Li_2SO_4
	$Na_2SO_4 + CaO$	–	–	$Na_2SO_4 + CaO$	93.3	Li_2SO_4
	$Na_2SO_4 + NaOH$	200–300	–	$Na_2SO_4 + NaOH$	90.7	Li_2SO_4
Carbonation	$CaO + H_2O$	100–205	60	H_2O	~97	LiOH
	$CaO + H_2O$	1000–1230	–	H_2O	80	LiOH
	Na_2CO_3	150–250	10–120	H_2O	~94	Li_2CO_3
	$Na_2CO_3 + NaCl$	~923	120	H_2O	70	Li_2CO_3
Chlorination	Cl_2	1100	150	–	–	LiCl
	$CaCl_2$	900	120	H_2O	90.2	LiCl
	$MgCl_2$-$CaCl_2$.12H_2O	550–1200	120	H_2O, HCl	50–90	LiCl
	KCl, NaCl	1000–1050	15–60	H_2O/HCl	85–97.5	LiCl
	$CaCl_2$	800–1200	180–720	Alcohol	96.5–98.5	LiCl
	NH_4Cl	250–750	–	Cold water	97–98	LiCl
Fluorination	NaF	600	120	HF	90	LiF

Kundu, T., et al., 2023, Powder Technology 415 (2023) 118142

Lithium recovery from spodumene: Generalized Flowsheets

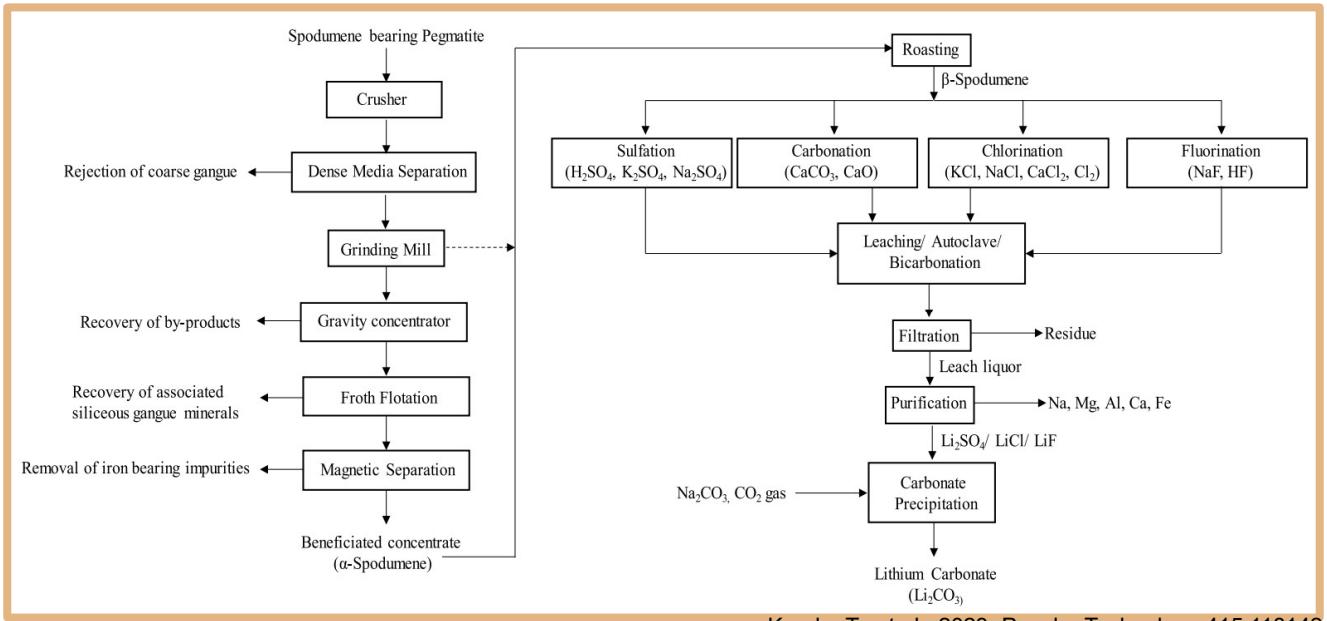

Kundu, T., et al., 2023, Powder Technology 415,118142

Lithium: Towards decarbonization of concentrating and refining (beyond "Electrify Everything")

- Crushing & grinding in the concentrator are major energy consumers:
  - Significantly improving metallurgical recovery leads to less valuable material going to tailings that have been blasted, hauled, crushed & milled and significantly lowers the energy input per ton of metal unit that leaves the mine gate
  - However, better separation normally requires better liberation that is obtained at finer grinds
- Increasing mica contamination leads to surface fusion i.e., sintering and poor spodumene conversion. I.e., calcination energy is wasted as, no matter the energy input, the target conversion is not obtained
- Increasing fines lead to increasing elutriation losses, particularly where fuels and combustion gases increase gas flow
- At 1100 ºC, radiation heat transfer is the dominant heat transfer mode (compared to conduction & convection)
- Particle-particle and particle-gas contact play a less dominant role
- The more particle-particle contact occurs (number of particles and duration of contact), the higher the opportunity for sintering and clinkering
- Rotary kilns, originally developed for lower value limestone and cement may not be fit for purpose for spodumene that trades around $7,000 - $8,000 per tonne. Rotary kilns increases particle-particle contact and the opportunity for sintering & clinkering. Combustion gases leads to fines elutriation and reprocessing
- *Vertical flash calcination* with indirect heating eliminates most of these challenges, allowing integration of mineralogy and metallurgical knowledge with concentrator-to-refinery optimization based on a different equipment design, thereby minimizing sintering, maximizing conversion and minimizing fines elutriation and reprocessing, leading to significant better energy utilization to achieve conversion

Vertical Flash Calcination Technology (Calix Ltd, Australia)

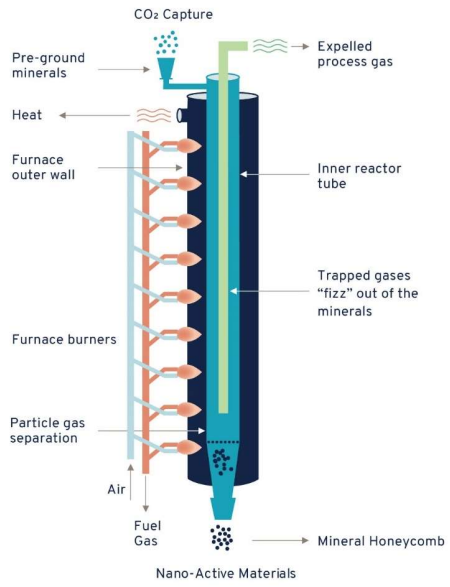

- Sector/stage-wise heating – thermal profile control
- Can be fully electrified
- Ideal for finer particles (<200 micrometre)
- Longer residence time due to serpentine particle movement rather than straight drop.
- Thermophoresis is used to move particles with thermal gradients. It leads to particles moving away from shot side-walls.
- No combustion gases in calcination zone (minimise particle elutriation)
- Elimination of clinkering
- Allows processing of fines

Nickel from Disseminated Sulfide Ultramafic Resources

CONVENTIONAL Ni PROCESSING OPTIONS

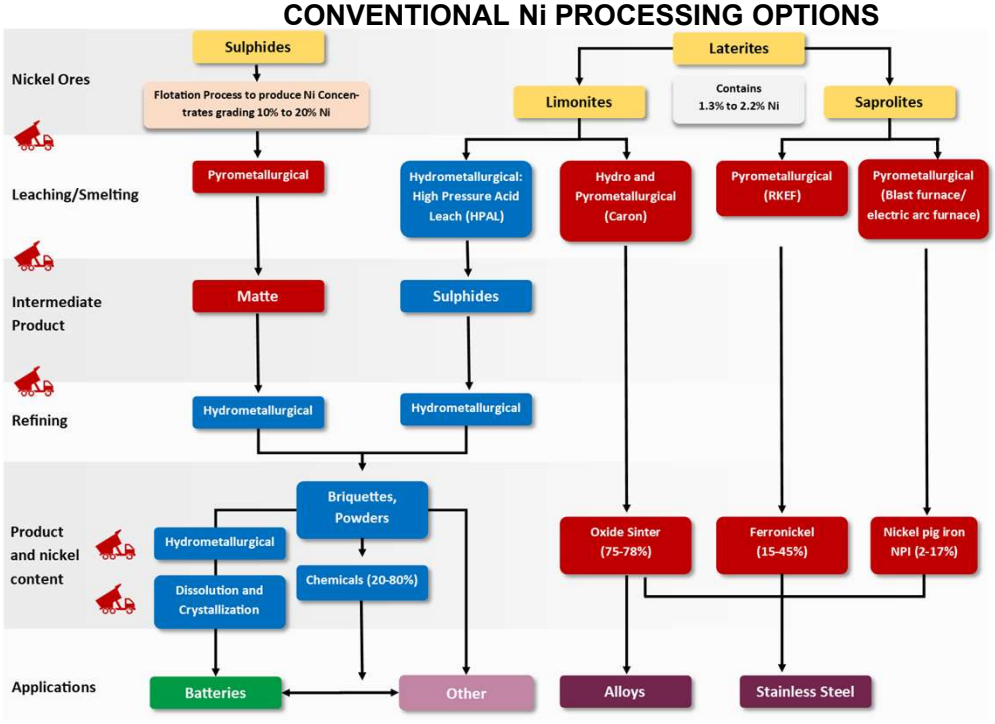

Schmidt, Buchert, Schebek, 2016. Investigation of the primary production routes of nickel and cobalt products used for Li-ion batteries. Resources, Conservation and Recycling, 112: 107-122

Nickel: Cutting the carbon footprint in nickel production (for disseminated sulfide resources)

- Nickel extraction, concentrating and refining ⇨ large carbon footprint.
- WA Ni ores, particularly disseminated sulfides derived from ultramafic deposits are interlocked in gangue minerals high in magnesium and iron which both pose challenges in the smelter furnaces and converters
- Concentrate grade constraints by the smelter lead to very high losses of nickel and cobalt to tailings (40-50%).
- A direct leach & recovery technology using mildly alkaline glycine solutions was developed at Curtin University. This allowed the following outcomes:
  - Direct leaching of nickel and cobalt from rougher concentrates, fines, slimes, ores and tailings possible, nearly doubling saleable metal units for the same energy input during comminution & mining
  - Selectivity improved as insignificant iron and magnesium was dissolved
  - As metal sulfates rather than metallic nickel was required, it provided a direct hydrometallurgical pathway to battery chemicals
  - Carbonation of magnesium-rich ores and tailings is a fitting technology as the alkaline environment doesn't lead to decomposition of carbonate minerals, leading to permanent sequestration of CO@ from point sources
  - Glycine, a non-toxic, cheap reagent that is recovered and recycled in the process, is deployed
  - The GlyLeach™ process is currently being optimized and is due to be piloted in the coming two years.
- This is an example of how knowledge of mineralogy, novel chemistry and process flowsheet design can lead to significant decarbonization while achieving other sustainability and metallurgical objectives

Ni and Co losses in conventional processing of disseminated sulfides

- MgO (slag liquidus, viscosity impact) and FeS (matte aisle logistics) specification in smelters constrains nickel and cobalt recovery at concentrator.
- Large Co losses occur during matte converting that are hard to recover.
- Cleaner tails still contain high amounts of ground sulfide that is an environmental problem.

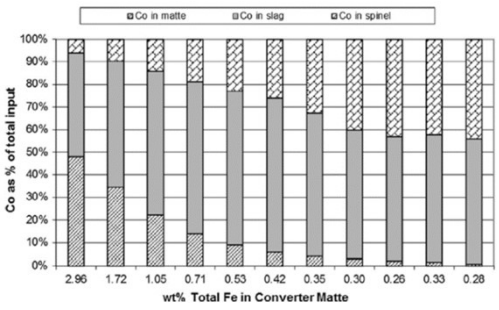

*Cobalt loss to matte is for a PGM-Ni-matte in P-S Converter.

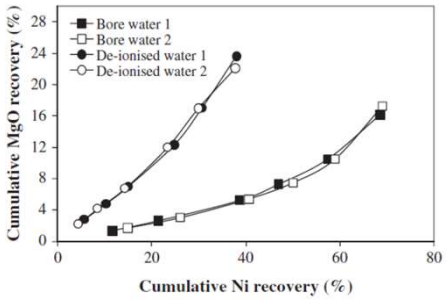

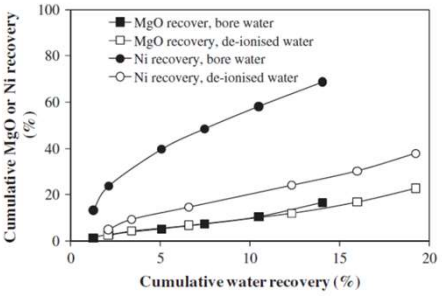

Some of the hurdles

Conventional processing of nickel resources is accompanied with many metallurgical challenges:

- Aggressive non-recyclable reagents
- Often poor flotation recoveries to meet smeltable concentrate specifications
- High temperature (ferronickel / nickel pig iron) or high pressure (HPAL) approaches required
- Poor cobalt recoveries, particularly for smelting & converting routes
- Reagents are typically not recycled and reused leading to poor circularity of materials
- Exotic materials of construction required, particularly for HPAL
- Poor ability to recover associated precious metals (e.g., Au, Pt, Pd), and poor payabilities
- Significant “smearing” of contaminants across the extraction and refining, e.g., Fe, Mn, Mg, Cr, Al, Si, As, Se, and Te
- Complicated multistage extraction routes, often better targeted towards metallic nickel production for the stainless-steel market or crude MHP production.

Towards “Green” Nickel and Cobalt - Process Requirements:

- Lead to significantly higher recoveries of Ni & Co
  - Given the carbon footprint of the mining operations and comminution circuits, lost Ni translates directly into a large carbon penalty
- Use environmentally friendlier reagents, and reagents that are less corrosive
- Allow the reprocessing of tailings, including pyrrhotite tailings and allow processing of ores and concentrates
- Bypass the requirement for smelting and converting, or pressure leaching or pressure reduction to metallic nickel
- Sidestep any route that requires intermediate, MHP, MSP, matte and metallic Ni production to produce Ni & Co sulfates directly
- Eliminate contaminants such as Fe, Mg, As, Se, SiO2, $Al_xSi_yO_z$ as early as possible in the process without “smearing” them across multiple process steps.
  - Every unwanted element not eliminated at the start leads to recovery losses later

Attributes of the alkaline glycine process

Reagent is non-toxic	Reagent recovery and reuse is easy and cost-effective	It can be operated under dilute and concentrated modes
It is environmentally benign	The reagent cost is low (< AUD 2000/tonne)	It is chemically stable under alkaline conditions (compared to cyanide, thiosulfate, etc.)
It has a high affinity for: Ni, Co, Cu, Au, Ag, Pd, Pt, Zn, Pb, Cd	It can be used synergistic with cyanide (for precious metals)	The precious metal glycinate complexes adsorb well onto activate carbon
Given the alkaline operation, there is no or very limited interaction with acid consuming materials	It can be applied in various leach modes (such as heap, in-situ, vat and agitated tank leaching)	The alkaline operation allows low cost materials of construction
Highly soluble, but non-hygroscopic crystals	No transportability & logistics, trade restrictions	Ease of base metals removal / recovery
Thermally stable	Non-volatile	Simple chemistry
Insignificant Fe, Mn, Mg, Si, Al, Cr dissolution (excellent gangue rejection)	Cu- glycinate is a good oxidant	No pH changes required between base and precious metals leaching stages

Leach evaluations on different nickel-bearing materials: LG concentrate, Ores, Tailings & Slimes

Alkaline glycine leach extractions of ores, tailings and concentrates

Alkaline Glycine leach extractions were performed at:

- Room Temperature
- Atmospheric Pressure
- Controlled dissolved oxygen levels / Redox
- Controlled (maintained) pH
- Results reflect outcomes of batch tests
- Resin-in-pulp / resin-in-leach and counter-current transfer can further improve results
- Different alkalizing agents used, depending on nature of material treated

Sample	Rougher concentrate 1	Rougher concentrate 2	Ore 1	Ore2	Cleaner Tails 1	Cleaner Tails2	High Pyrrhotite slimes
Ni	6.13	6.02	0.78	1.67	0.886	0.79	4.075
Fe	9.12	33.5	5.89	11.4	5.24	6.43	26.50
Ca	0.49	0.33	0.55	1.49	0.39	0.20	2.975
Mg	16.29	4.04	22.9	5.92	22.25	22.2	4.465
S	6.04	27.6	0.83	7.04	1.15	1.70	15.30
Mn	0.08	0.09	0.05	0.11	0.06	0.06	0.120
Co	0.11	0.179	0.014	0.048	0.021	0.019	0.132
Zn	0.03	0.012	0.008	0.011	0.001	.023	0.021
As	0.03	0.007	0.007	0.005	0.0045	.007	BDL
Cu	0.29	0.301	0.13	0.10	0.0185	0.215	2.00

Test ID	Rougher Concentrate 1	Rougher Concentrate 2	Ore 1	Ore 2	Cleaner Tailings 1	Cleaner Tailings 2	High pyrrhotite Slimes
Solid, %	30	10	40	30	30	30	10
Initial pH	10.2	10.2	10.2	10.2	10.2	10.2	10.2
Gly:Ni mole ratio	4:1	4:1	4:1	4:1	4:1	4:1	4:1
Residence time, hours	72	72	48	72	48	48	72
Ni Extraction, % of total Ni	90.2	81.9	69.1	74.8	62.5	80.1	81.5
Co Extraction, % of total Co	85.7	16.5	65.3	27.5	64.5	72.6	71.9

The leachates obtained showed high selectivity of Ni and Co over Fe, Mg, As, Ca, Mn.

Test ID	Element	Ni	Co	Fe	Ca	Mg	S	Mn	Zn	As	Cu
Cleaner Tails 1	Final solution assay, mg/L	2070	52.8	BDL	118	79.8	3200	BDL	0.8	BDL	48.8
Cleaner Tails 2	Final solution assay, mg/L	2805	63.8	1.5	30.5	25.3	3860	BDL	11.0	BDL	118
High pyrrhotite Slimes	Final solution assay, mg/L	3500	100	19.6	12.8	7.4	3770	BDL	BDL	BDL	646
Ore 1	Final solution assay, mg/L	4100	80.5	BDL	50.6	36.5	4820	BDL	2.5	BDL	318
Ore 2	Final solution assay, mg/L	4020	27.2	11	78.6	78.4	7760	BDL	9.0	0.11	213
Rougher Concentrate 1	Final solution assay, mg/L	7560	147	3.4	10.8	22.4	9860	DBL	15.8	0.07	316
Rougher Concentrate 2	Final solution assay, mg/L	5080	30.8	115	5.5	2.6	9750	BDL	0.4	0.21	169

- Cobalt leaching mostly congruent with nickel leaching
- Silica levels BDL (not shown)
- Sulfur leaching congruent with nickel leaching
- BDL: Below detection limit (by ICP OES)

Metal recovery from solution, reagent recycle and metal separation:

- Glycine leachates are recovered from solids using filtration
- Excellent primary extraction of Ni, Co, and Cu is possible with either:
  - Ion exchange resin (for leachates from ores and tailings)
  - Solvent extraction (for leachates from concentrates)
  - Metal recovery onto resin or to SX extractant is as the divalent cation
  - Glycine remains in the barren raffinate and is recycled (with sulfate) back to leach
  - Ni, Co and Cu are stripped from resin or SX extractant using sulfuric acid
  - Ni, Co and Cu sulfates are separated in acidic sulfate medium using conventional solvent extraction technologies (e.g. Cyanex 272 for Ni-Co separation)
  - Final pure nickel sulfate, cobalt sulfate and copper sulfate can be crystallised, or transferred (minus copper) for mixed hydroxide cathode precursor manufacture
- Dissolved sulfate can be removed and differentially crystallised as the sulfates of any of K, Na, NH_4^+ or Ca

Option 1 (for Concentrates and high sulfide materials): GlyAmm based

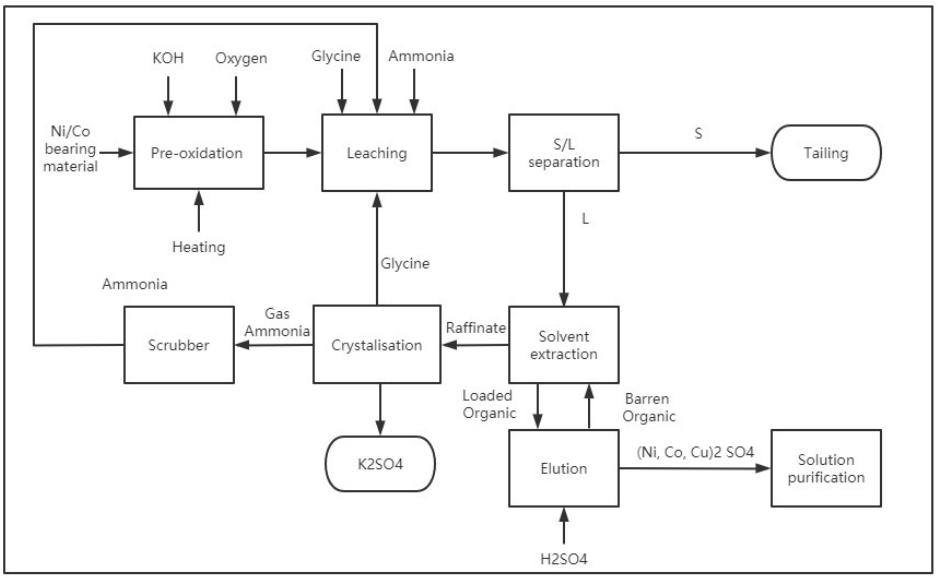

Conclusions:

Alkaline glycine technology provides an ideal pathway to produce “Green” nickel and cobalt

- It allows maximum recovery of nickel and cobalt with minimal co-extraction of impurities
- It allows pathways directly to nickel and cobalt sulfate without the need for smelting, converting, or pressure leaching
- It eliminates most of the typical problematic contaminants, such as iron, magnesium and manganese from the first extraction stage
- It operates under similar processing conditions, and with similar equipment to gold leaching circuits
- A detracting factor is leach residence time (around 24 hours) leading to more tankage
- Glycine recycle is simple, minimising reagent costs
- Processes can be used with saline water
- Applicable to various grades, but optimal for ores & concentrates with nickel grades of between 0.3% - 7.0% Ni
- Various alkalising agents can be considered (hydroxides of K, Na, NH_4^+, Ca, or carbonates of K, Na, NH_4^+)
- Good palladium recoveries can be obtained using GlyLeach™ / GlyCat ™, when associated with pentlandite

Towards better sustainability and decarbonization in mattery metal value chains

Decarbonization is achieved through:

- Novel process chemistry and process mineralogical understanding
  - E.g., glycine use in nickel processing
  - Mineral carbonation and CO_2 sequestration in nickel ore processing
- Maximizing recoveries and conversions through fit-for-purpose equipment design
  - E.g., indirectly heated vertical flash calcination of spodumene
- Maximizing recoveries through novel chemistry
- Simplifying across the whole value chain (e.g., mine, concentrator, pyrometallurgical conversion and refinery) and reviewing overall process integration, e.g.:
  - direct leaching of nickel to produce battery metals chemicals and
  - processes that allows fines processing in spodumene conversion

To ensure greater sustainability we have to:

- Increase processing efficiencies and recoveries
- Reuse and recycle reagents and water
- Use what nature provides us
- Electrify what we can with renewable sources & energy storage
- Maximize the use of non-toxic and benign reagents
- Understand the interactions between mineralogical and chemical properties and materials interactions (particle-particle and particle-gas) in equipment, and opportunities to unlock inter-business unit bottle necks

COMPLY OR COLLAPSE:
THE DILEMMA FACING THE LITHIUM-ION BATTERY INDUSTRY

By

Adrian Griffin
adrian.griffin@lithium-au.com

Future Technology Trust

ABSTRACT

Lithium-ion batteries occupy pole position in terms of the world's transition to green energy, including e-mobility alternatives to traditional transport options. This position is buoyed by the immediacy of the need for carbon neutrality, long lead times for the development of alternative technologies and the immense scale of investment in current and committed infrastructure involved, which in turn requires a satisfactory return on capital. Today, these drivers appear paramount in initiating the changes required to achieve net-zero, but what factors detract from such adjustments? Which are most likely to influence the evolution of the lithium-ion battery supply chain and, indeed, battery chemistries of the future – and can the current industry compromise and/or evolve to meet future demand?

A profusion of legislation/policies in the European Union, the United States, China, India and other major jurisdictions will profoundly impact the ways in which supply chains for lithium-ion batteries – and what comprises them – are managed. ESG legislation and reporting already influence the availability of credit, as well as perceived financial risk. Embedded within this plethora of actual and potential regulation are lifecycle analyses, calculations of carbon footprint and the need for sustainability.

Examination of the lithium-ion battery lifecycle highlights two areas of vulnerability in terms of the industry's survival. They are:

- the sustainability of raw material inputs (primarily 'battery metals'), and
- battery recycling rates and efficiencies.

Both areas are the focus of much debate, some related to restrictions in the trading of goods lacking appropriate ESG credentials. The electric vehicle (e-mobility) industry in particular will be subject to the imposition of 'battery passports', designed to track battery lifecycles and ensure regulatory compliance. Markets for non-compliant batteries will be severely restricted.

Meanwhile, raw materials are already susceptible to supply chain deficits, carbon footprint assessments and ESG credibility. The *US National Blueprint for Lithium Batteries 2021-2030* encourages widespread substitution of nickel and cobalt in lithium-ion batteries by 2030 to assuage such restrictions. Difficulties in marketing products produced from Australian, and perhaps other, spodumene, may also arise, due to the currently poor sustainability (recovery) profile of this material, resulting from the inability of downstream processing to handle fine spodumene feed. This poor resource utilisation (the alienation of fine spodumene during current processing practices) could drive a change to other battery chemistries (sodium-ion batteries?) or more sustainable sources of lithium, including direct lithium extraction from brines.

Although the issues raised above are certainly complex, two promising technologies are already tackling the issue of converting fine spodumene into lithium chemicals, to improve resource recovery and utilisation and provide a pathway to greater sustainability and ESG amenability.

This paper outlines some of the compliance issues that will affect the lithium-ion battery supply chain and ways in which the industry can not only comply with legislative requirements but also improve its financial performance. Technologies that enhance efficiency and reduce reliance on new raw material inputs will be crucial to that. Two outstanding technologies are being developed to improve sustainability of spodumene production, and tackle recovery losses resulting from unmarketable fine spodumene. One is pyrometallurgical, the Midstream process being developed by Pilbara Minerals and Calix, and the other is hydrometallurgical, the LieNA® process, being commercialised by Lithium Australia Limited.

Keywords: ESG, legislation, sustainability, lithium, battery

Future drivers of the battery industry

- The drive towards net zero has produced a plethora of policy and legislation.
- Although reporting of sustainability is now a requirement in the EU, somewhat ironically **"sustainability" is not defined** in the legislation.
- Interaction of various Acts and policies points to a common sustainability factor: **carbon footprint.**
- Progressive introduction of compliance will probably result in a practical definition of "sustainability" by 2026.

Warning

- **Low recovery of spodumene from Australian pegmatite operations poses a real sustainability compliance risk for marketing concentrates, lithium chemicals, or downstream products, manufactured from Australian spodumene.**

Europe spearheads the move to lithium sustainability

Let's take a look as the major policies

Rate of policy introduction

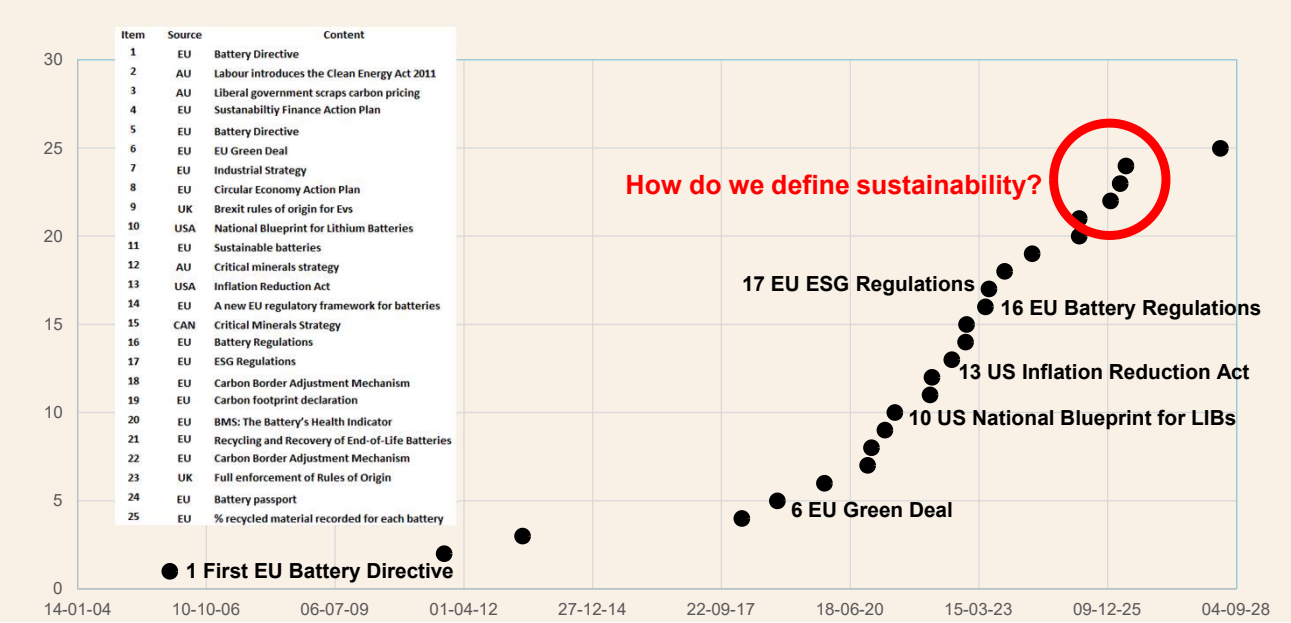

EU Battery Regulations, May 2023

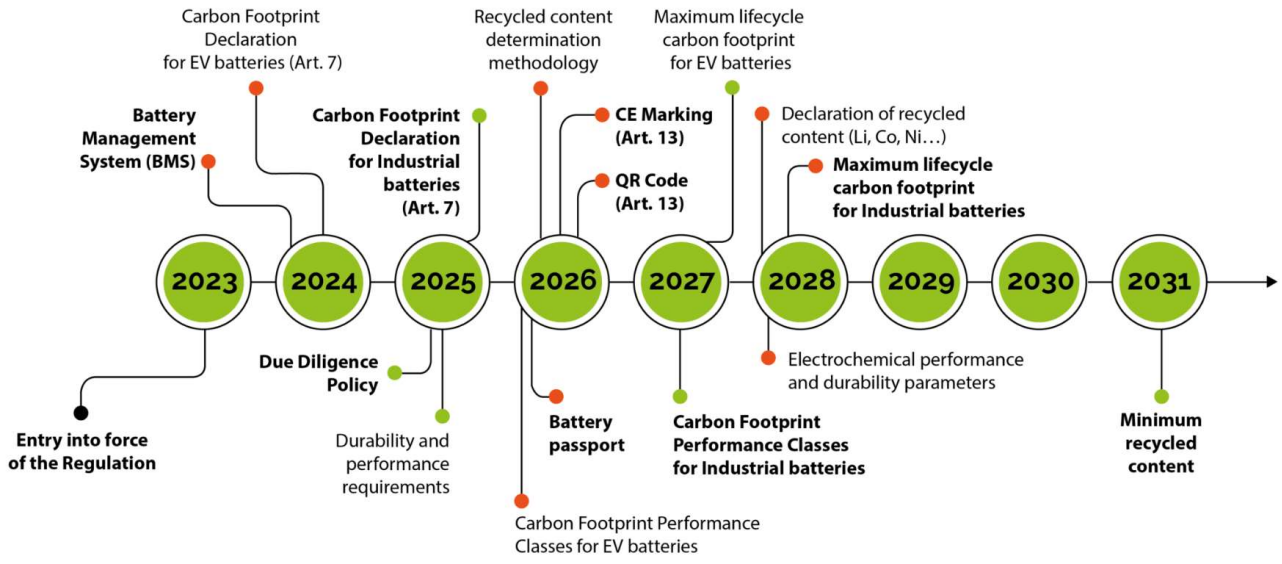

Source:https://www.flashbattery.tech/en/new-european-battery-regulation/

EU Sustainability Reporting (ESG regulations)

- Corporate sustainability directives (CSRD) require large EU companies and public-interest entities to disclose information on their annual ESG performance.
- Reporting requires upstream and downstream supply chain impacts to be assessed.
- Sustainable Finance Disclosure Regulation (SFDR) and the Taxonomy Regulation, require disclosure of the sustainability characteristics of investment products, to assist end investors in making more informed investment decisions.
- **EU Carbon Border Adjustment Mechanism (Oct 2023) will attempt to level the impacts of environmental supply chain sensitivity.**
- Suppliers into the EU to comply as though they were EU companies.
- 4000 Australian companies require compliance.
- **Spodumene producers and subsequent products to be affected.**

EU Carbon Border Adjustment Mechanism Oct 2023

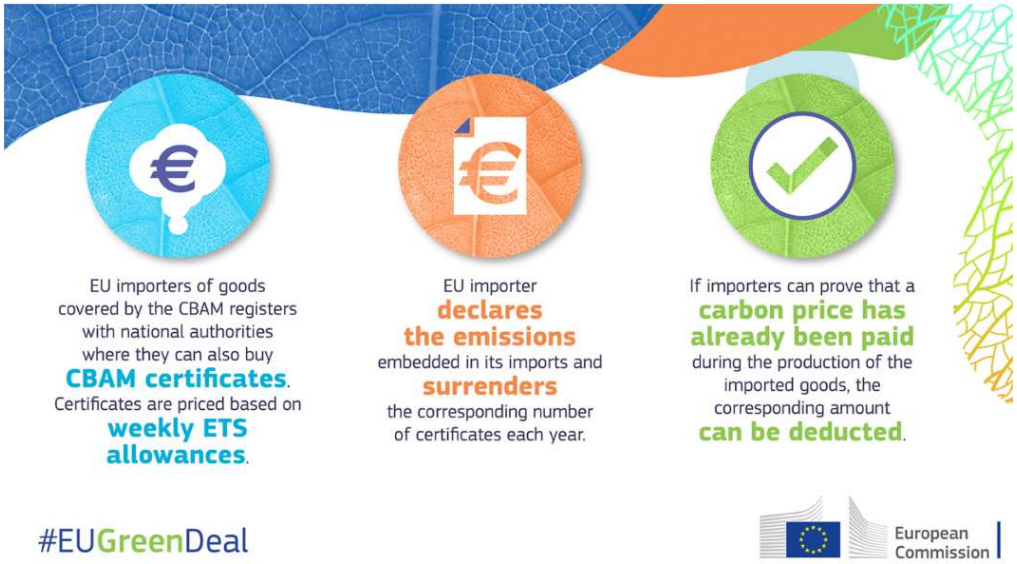

Global Carbon Pricing

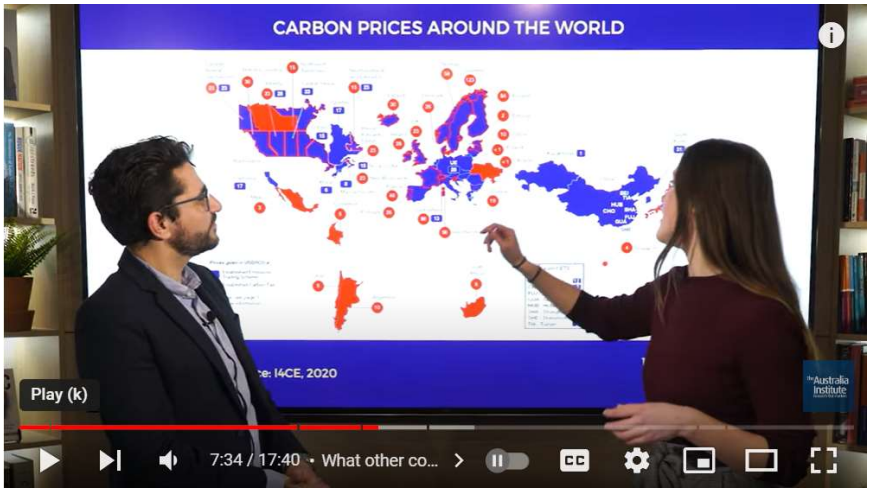

Australian climate policies will be dictated by foreign powers.
Revenue from taxes to go offshore.

EU Battery Regulations, May 2023

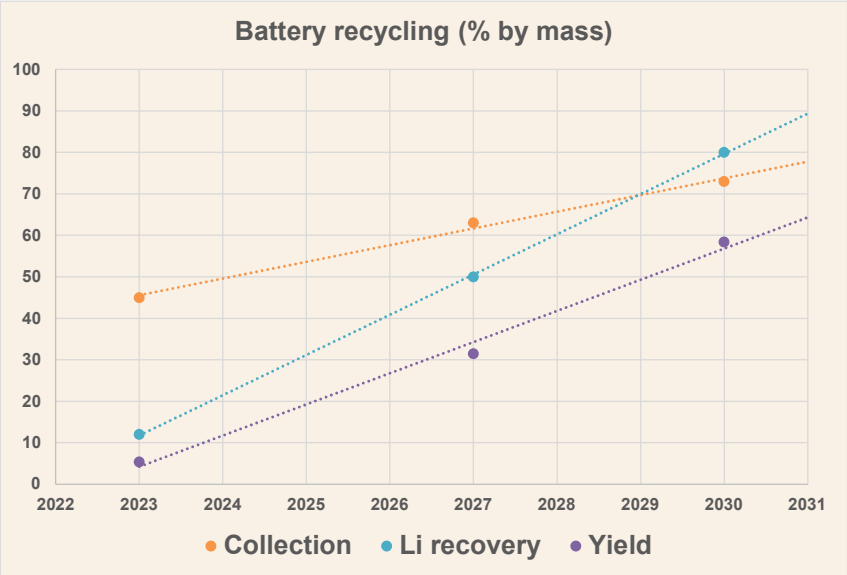

- All batteries collected must be recycled.
- Today 30% of battery mass and 40% of EVs must be sourced from within EU/UK; rising to 45/60% by January 2024.
- Likely 80,000tpa recycled lithium carbonate equivalent required to meet EU mandatory requirements by 2030.
- Globally, recycled lithium is set to make up around 10% of the lithium supply in 2031, rising to over 20% in 2036 (Benchmark).

EU Battery Passport May 2026

Passport to carry digitally recorded battery data and history

- Battery type & unique identification (manufacturer, serial number etc).
- Date of manufacture and sale.
- Chemical composition including list of toxic substances.
- Recycled raw materials contained in the battery.
- Information and activities related to repair, reuse and dismantling.
- End-of-life treatment, recycling and recovery methods.

EU Regulations 2028

full LCA CO_2 reporting

How is the battery industry being managed in the USA?

Policies are clearly focused on securing supply, developing domestic battery production capability, reducing emissions and getting on top of inflation.

USA – reinforcing the National Battery Blueprint

Source:https://www.energy.gov/eere/vehicles/articles/national-blueprint-lithium-batteries

- The USA National Blueprint for Lithium Batteries is strongly supported by the Inflation Reduction Act, 2022.
- The IRA provides a framework of subsidies, grants and tax breaks to stimulate the clean energy industry.
- The IRA is heavily oriented towards developing domestic supply chains, stimulating the battery industry and providing tax incentives
- The IRA requires that EV manufacturers source 40% of critical battery minerals domestically or with free trade partners by 2024 increasing to 80% in 2026. This strongly favours the use of Australian sourced lithium.

Process problems and potential solutions

If we don't act, Australia will squander a once in a century opportunity

A move towards lithium sustainability

- Sustainability evaluations must cover the entire supply chain including mining, concentration, transport, conversion etc. BUT there is no substitute for maximizing the recovery of contained lithium units within an orebody.
- Downstream improvements include:
  - Minimising transport impact,
  - Using renewable energy,
  - Recycling product.
- We must strive towards maximising the value of our resources and to do this we need to **maximise recovery**.
- The lithium industry has arisen by amalgamation of legacy technologies, but the time has come to **design production systems fit for purpose**.

The spodumene carbon footprint problem

- Historically Australian spodumene production has been geared towards the requirements of the Chinese spodumene converters (chemical producers).
- Stage 1 of conventional chemical conversion is counter-current roasting in rotary kilns.
- The critical particle size for kiln throughput is generally around 75µm.
- An enormous amount of the carbon footprint to produce spodumene concentrates is expended on the mining, comminution and rejection of material that cannot meet converter specifications i.e. below the critical particle size.
- A disproportionate quantum of the carbon footprint must then be assigned to the commercial concentrate.
- Material reporting to tailings is notionally assigned a zero carbon footprint.

Solving the recovery problem – reducing CO_2 footprint

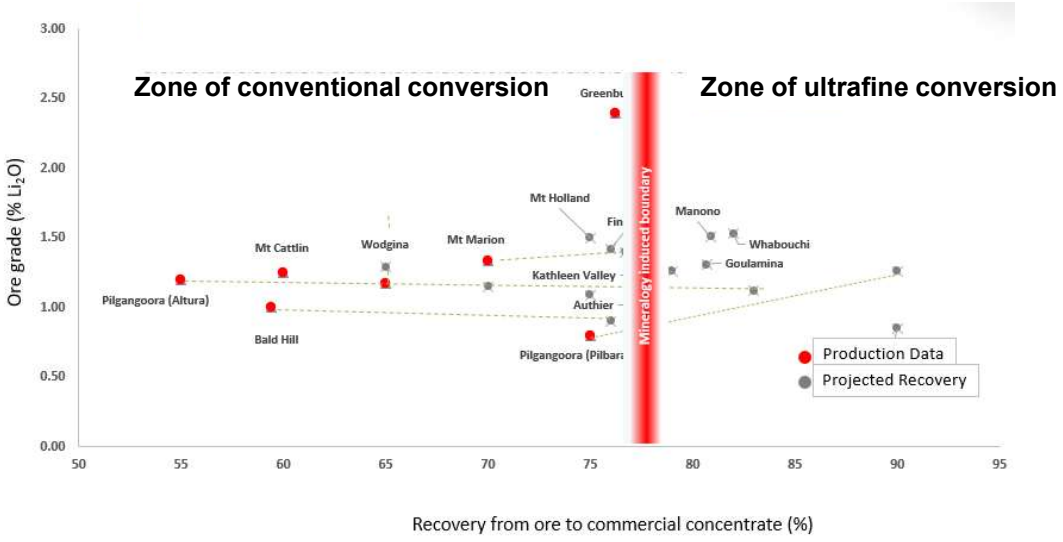

Source: historic data c 2018

What needs to be improved?

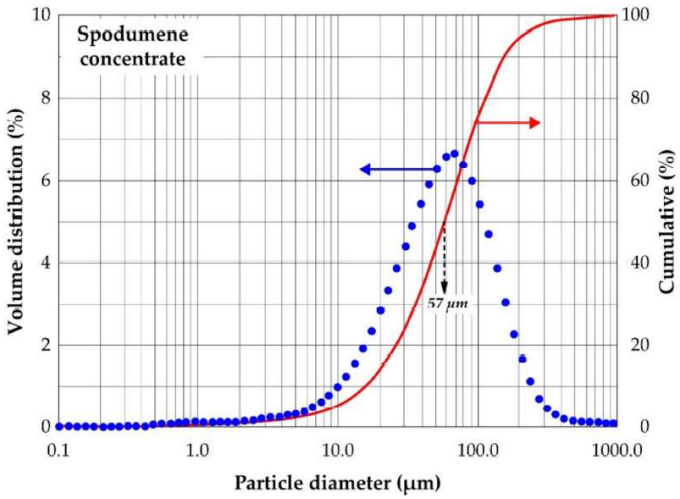

Source: Fosu, A.Y. et al. Physico-Chemical Characteristics of Spodumene Concentrate and Its Thermal Transformations. Materials **2021, 14, 7423**. https://doi.org/10.3390/ma14237423

What's in the sample?

- Sample from Pilbara region of WA.
- Mass yield from ore to concentrate 85%.
- Only about 40% of the **concentrate** exceeds a particle size of 75µm.

What's happening elsewhere?

- Recoveries to concentrate as low as 30%
- CO_2 footprint of resulting commercial concentrates is consequently very high.
- Discarded fines ultimately being exported carry a zero CO_2 production footprint.

Two promising solutions to the problem

Lithium Australia's caustic conversion – LieNA®
and
Calix & Pilbara Minerals' flash calcination

Alternative #1 – Lithium Australia - LieNA® process

- LieNA® is a caustic conversion process.
- Requires no roasting.
- Ideally suited to fine and low-grade spodumene.
- Capable of recovering lithium from any form of spodumene but best for material not suited to conventional conversion.
- Developed in conjunction with ANSTO.
- Partially funded through Australian government grant (CRC-P).
- Pilot plant commissioning August 2023
- Choice of end product – carbonate, hydroxide, phosphate etc. with potential to feed directly into LFP cathode production.
- Lithium phosphate output preferred to minimize carbon footprint (elimination of energy intensive evaporation).

LieNA® comparison with conventional conversion

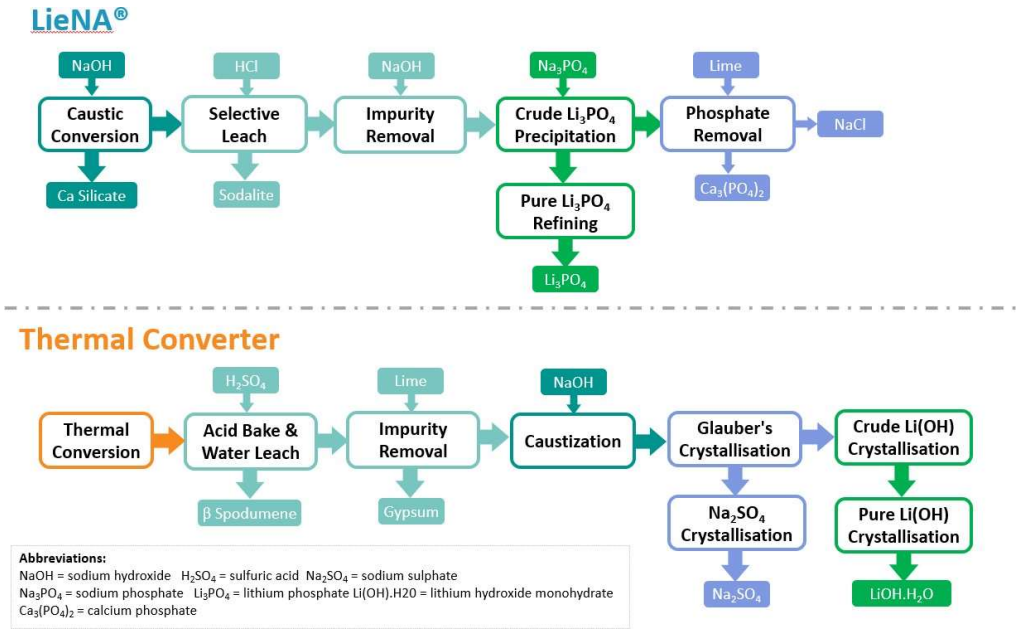

Abbreviations:
NaOH = sodium hydroxide H_2SO_4 = sulfuric acid Na_2SO_4 = sodium sulphate
Na_3PO_4 = sodium phosphate Li_3PO_4 = lithium phosphate Li(OH).H20 = lithium hydroxide monohydrate
$Ca_3(PO_4)_2$ = calcium phosphate

Alternative #2 – Calix flash calcination

- Like LieNA®, the Calix' flash calcination process is focused on maximizing the commercial recovery of lithium from spodumene deposits.
- The process is being developed as a JV between Pilbara Minerals and Calix.
- Advantages:
  - As a process addition, it aids in optimizing the recovery of mined lithium units.
  - Electrically powered, it has potential to utlilize renewable energy and reduce carbon footprint.
  - High conversion rates from α to β spodumene.
  - Lithium recoveries > 90%
  - Can take advantage of the expanding market for lithium phosphate materials.
  - 8-10 fold reduction in shipping mass if the process is established next to the spodumene concentrator.
  - Production of high-value lithium salt, close to the spodumene source, will retain more value for local producers and reduce the carbon footprint of the final consumer product.

Alternative #2 – Calix flash calcination

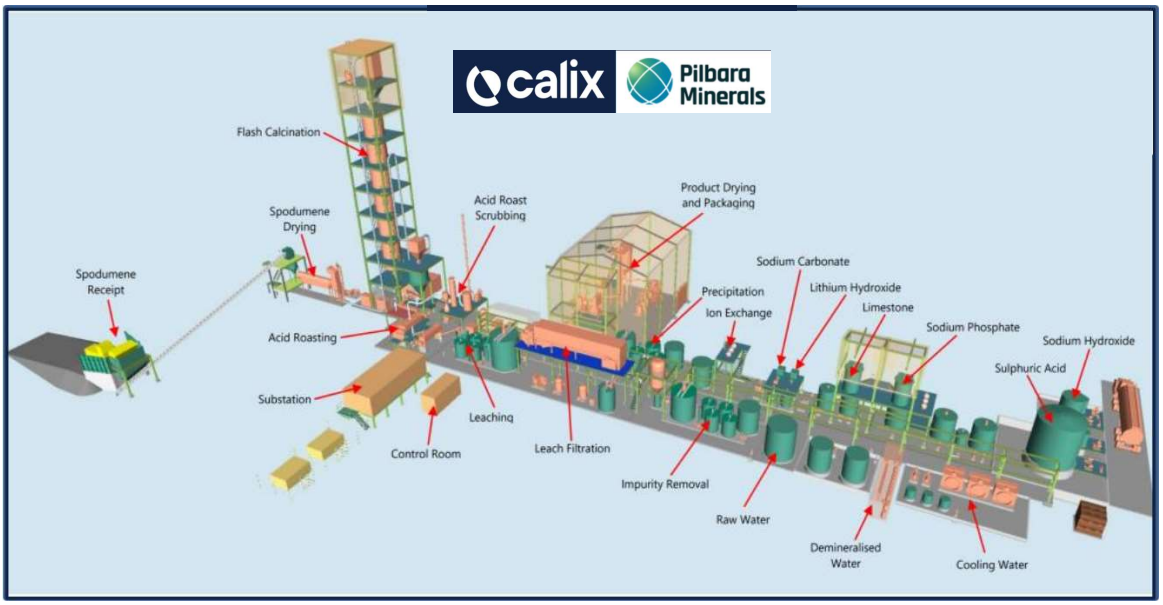

Source: Calix

Conclusion – dodging the bullets

A wakeup call to the industry to improve sustainability and profitability

Conclusion

- Australian lithium products are in danger of being alienated from EU markets on the basis of Australia having no domestic carbon tax and spodumene concentrate producers having a high carbon footprint.
- Foreign companies are seizing the opportunity and buying fine Australian spodumene which can be accounted for as having a zero production carbon footprint. It can also be marketed as a recycled product.
- Utilising the fine spodumene to fill surplus installed battery production capacity can open the EU markets to offshore entities and impede Australia's ability to capitalize on the current opportunity.
- Without addressing the sustainability issues in the lithium supply chain, Australia will be restricted to US and Chinese markets.
- Advanced technologies can alleviate the sustainability compliance issues faced by Australia and maintain competitive access to all markets – **LieNA® and Calix.**
- The Australian government needs to work with the lithium industry to implement policies addressing competitive pressures in international markets.

LITHIUM EXTRACTION FROM A-SPODUMENE BY HYDROALKALINE TREATMENT: RECENT PROGRESS AND OUTSTANDING CONSIDERATIONS

By

Bogdan Z Dlugogorski

Energy and Resources Institute, Charles Darwin University, Australia

Presenter and Corresponding Author

Bogdan.Dlugogorski@cdu.edu.au

ABSTRACT

Over the last five years, several hydrometallurgical processes have emerged to extract lithium from *α*-spodumene, by digesting this mineral with solutions of concentred NaOH or KOH, 20 – 50 %, at temperatures between 250 and 300 °C, under pressure to contain the reacting systems, for residence time of 4 to 24 h, with or without a CaO dopant [1-5]. These processes aim to decarbonise the refining of lithium, by avoiding the decrepitation (phase inversion) of *α*-spodumene to *β*-spodumene. The decrepitation constitutes the most energy intensive step in processing of *α*-spodumene to lithium chemicals in the Chinese and the nascent Australian refineries. The application of CaO, either to induce a more effective decomposition of *α*-spodumene or to precipitate silicon-based impurities from the leachate, represents the key technological advancement of the new processes.

While the hydroalkaline digestion yields high Li recovery of ca 90 %, examination of literature indicates enlarged requirements for feedstock chemicals, increased by-product streams for disposal and more contaminated pregnant liquor solutions for downstream separation and purification. The processes comprise up to three pH swing operations, including the original hydroalkaline digestion step, acid dissolution of precipitated lithium species, followed by the removal of impurities that requires switching back to basic pH. Although analogies exist with the Bayer process for refining bauxite to alumina, there are also important differences, including slower kinetics and elevated silica to alumina ratios, which make Li refining more complicated and challenging than that of alumina. The hydroalkaline processes work by the dissolution-precipitation reactions, rather than by the ion exchange mechanism, which defines the leaching of *β*-spodumene with strong acids. Recycling streams cannot be avoided as they serve to recover the unreacted hydroxides and to intercept part of extracted Li, which deports to the aqueous phase in the digestion treatment. Thus, it appears that the hydroalkaline processes need to overcome important practical hurdles prior to being able to challenge the established position of the sulphuric acid digestion in the refining industry and the rising popularity of the analcime-type operations [6,7]; the latter involving the pressure leach of *β*-spodumene with solutions of Na_2CO_3 or NaCl, with straightforward purification to battery grade $LiOH{\cdot}H_2O$ or Li_2CO_3.

From these perspectives, this contribution examines the main aspects of the new processes, including

(i) formation of aqueous and solid species arising in digestion reactions
(ii) feedstock and by-product intensity
(iii) digestion kinetics
(iv) type and removal of impurities
(v) effect of recycling of aqueous streams on energy demands, as well as
(vi) Li recoveries in comparison with those of the sulfuric-acid and analcime operations.

[1] Song Y, Zhao T, He L, Zhao Z, Liu X. 2019. A promising approach for directly extracting lithium from *α*-spodumene by alkaline digestion and precipitation of phosphate. Hydrometallurgy 189, 10514.
[2] Qiu S, Liu C, Yu J. 2022. Conversion from *α*-spodumene to intermediate products Li_2SiO_3 by hydrothermal alkaline treatment in the lithium extraction process. Minerals Engineering 183, 107599.
[3] Qiu S, Zhu Y, Jiang Y, Liu C, Yu J. 2022. Kinetics and mechanism of lithium extraction from α-spodumene in potassium hydroxide solution. Industrial and Engineering Chemistry Research 61, 15103-15113.
[4] Napier A, Griffith C. 2021. Caustic Conversion Process, US Patent 20210180155A1.
[5] Xing P, Wang C, Zeng L, Ma B, Wang L, Chen Y, Yang, C. 2019. Lithium extraction and hydroxysodalite zeolite synthesis by hydrothermal conversion of *α*-spodumene. ACS Sustainable Chemistry & Engineering 7, 9498-9505.
[6] Tiihonen M, Haavanlammi L, Kinnunen S, Kolehmainen E. 2020. Outotec lithium hydroxide process – a progress update. ALTA 2020 Uranium-REE-Lithium Conference. Perth, Australia.
[7] Alhadad M F, Oskierski H C, Chischi J, Senanayake G, Dlugogorski B Z. 2023. Lithium extraction from *β*-spodumene: A comparison of keatite and analcime processes. Hydrometallurgy 215, 105985.

Keywords: Hydroalkaline digestion of α*-spodumene; Pressure leach; Refining of* α*-spodumene to lithium chemicals; Feedstock and energy intensity in Li refining; Byproducts from Li refining*

Presentation outline

1. Introduction

- Decarbonisation of spodumene refineries
  - Decrepitation (calcination)
  - Evaporation/crystallisation
- Spodumene reactivity
- Sulfuric acid process
- Technologies that avoid decrepitation

2. Hydroalkaline processes

- Filtrate based
  Li partitions mostly to leach solution
  - Digestion conditions
  - Sellable byproducts in residue
  - Li separation and recycling
- Residue based
  Li partitions mostly to leach residue
  - Digestion conditions and byproduct species in residue
  - Acid leach
  - Li separation and recycling

3. Quantities that matter

- Lithium recovery
- Feedstock intensity
- Byproduct intensity
- Energy intensity
- Capex

4. Conclusions

- Comparison with the sulfuric acid process
- Problems solved
- Outstanding problems

Decarbonisation of spodumene refineries

Decrepitation (calcining), evaporation and crystallisation

- The *embodied* emissions of CO_2 from the supply chain of lithium chemicals, especially lithium hydroxide ($LiOH{\cdot}H_2O$) refined from spodumene, exceed those from brines, by about a factor of three, i.e., 15 t CO_2/(t $LiOH{\cdot}H_2O$) for processing spodumene, in comparison to 5 t CO_2/(t $LiOH{\cdot}H_2O$) for the Chilean production from brines.
- The EU will commence implementing carbon tariffs starting from 2023.
- These tariffs have potential to discriminate against electric vehicles equipped with batteries containing lithium chemicals refined from spodumene, because of their high embodied emissions of CO_2.
- The most CO_2 intensive steps in the supply chain of lithium hydroxide monohydrate (or Li_2CO_3) refined from spodumene concentrates are the decrepitation (calcining) and evaporation/crystallisation steps.
- The decrepitation step involves phase inversion of α-spodumene (aka spodumene) to β-spodumene; a question naturally arises about circumventing this step or change the design of the kiln to operate on renewable energy (outside the scope of this presentation).

Grant A, Deak D, Pell R, *The CO2 Impact of the 2020s' Battery Quality Lithium Hydroxide Supply Chain* (2023); https://www.jadecove.com/research/liohco2impact (assessed 3 May 2023)

Sulfuric acid process (SAP)

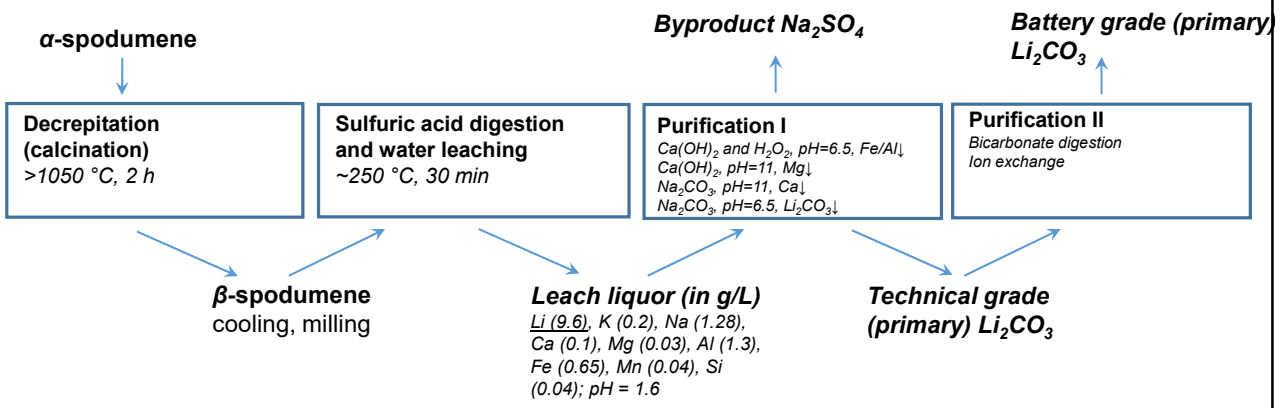

Tan I K S, Process for Production of Lithium Carbonate, WO 2011/082444 A1
La Brooy S and Harman G, Removal of minor and trace impurities from lithium leach liquors, ALTA 2018, 19-26 May, Perth, Australia
Dlugogorski B Z, Recovery of lithium from spodumene−energy and environmental considerations. Lithium and Battery Metals Conference. Perth, Australia; https://ris.cdu.edu.au/ws/portalfiles/portal/57188333/Dlugogorski_Alkaline_Pressure_Leaching_for_conference_proceedings.pdf, 2018

Sulfuric acid process (SAP)

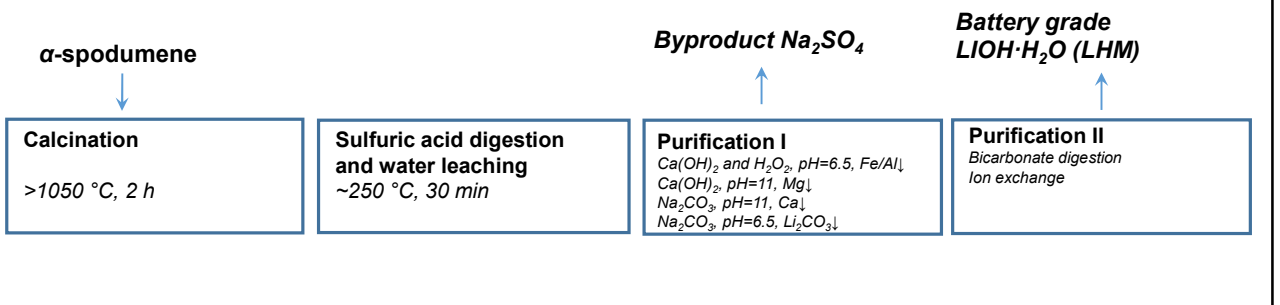

Problem 1
Energy intensity

Problem 2
Waste disposal: acidic aluminosilicates from leaching and impurities precipitated in Purification I, SO_x

Problem 3
Energy intensity
Feedstock intensity: concentrated H_2SO_4, $Ca(OH)_2$, Na_2CO_3 (in addition to Na_2CO_3 needed for precipitation of Li_2CO_3)

Problem 4
Byproduct recycling: Na_2SO_4

SAP works well; steep-learning curve to produce battery-grade LHM; well-oiled technology.

Dlugogorski B Z, Recovery of lithium from spodumene−energy and environmental considerations. Lithium and Battery Metals Conference. Perth, Australia; https://ris.cdu.edu.au/ws/portalfiles/portal/57188333/Dlugogorski_Alkaline_Pressure_Leaching_for_conference_proceedings.pdf, 2018

Technologies that avoid decrepitation

(no phase inversion of *α*-spodumene to *β*-spodumene)

1. Leaching *α*-spodumene with HF (Kuang et al, 2012) or HF/H_2SO_4 (Guo et al, 2019)
2. Roasting *α*-spodumene with NaOH at 320 °C (Han et al, 2022)
3. Digesting *α*-spodumene concentrated solution of NaOH (hydroalkaline treatment; today's presentation)

Guo H, Yu H, Zhou A, Lu M, Wang Q, Kuang G, Wang H, Kinetics of leaching lithium from *α*-spodumene in enhanced acid treatment using HF/H_2SO_4 as medium, *Trans Nonferrous Met Soc China 29*(2), 407−415 (2019).

Han s, Sagzhanov D, Pan J, Vaziri Hassas B, Rezaee M, Akbari H, Mensah-Biney R, Direct extraction of lithium from **α-spodumene by salt roasting-leaching process, *ACS Sustain Chem Eng* 10, 13495-13504 (2022).**

Kuang G, Chen Z, Guo H, Li M, Lithium extraction mechanism from *α*-spodumene by fluorine chemical method, *Adv Mat Res 524−527*, 2011−2016 (2012).

Outside the scope: alkaline treatment of lepidolite

Mulwanda J, Senanayake G, Oskierski H, Altarawneh M, Dlugogorski B Z, Leaching of lepidolite and recovery of lithium hydroxide from purified alkaline pressure leach liquor by phosphate precipitation and lime addition, *Hydrometallurgy 201*, 105538 (2021).

Presentation outline

1. Introduction

- Decarbonisation of spodumene refineries
  - Decrepitation (calcination)
  - Evaporation/crystallisation
- Spodumene reactivity
- Sulfuric acid process
- Technologies that avoid decrepitation

2. Hydroalkaline processes

- Filtrate based
  Li partitions mostly to leach solution
  - Digestion conditions
  - Sellable byproducts in residue
  - Li separation and recycling
- Residue based
  Li partitions mostly to leach residue
  - Digestion conditions and byproduct species in residue
  - Acid leach
  - Li separation and recycling

3. Quantities that matter

- Lithium recovery
- Feedstock intensity
- Byproduct intensity
- Energy intensity
- Capex

4. Conclusions

- Comparison with the sulfuric acid process
- Problems solved
- Outstanding problems

Strategies

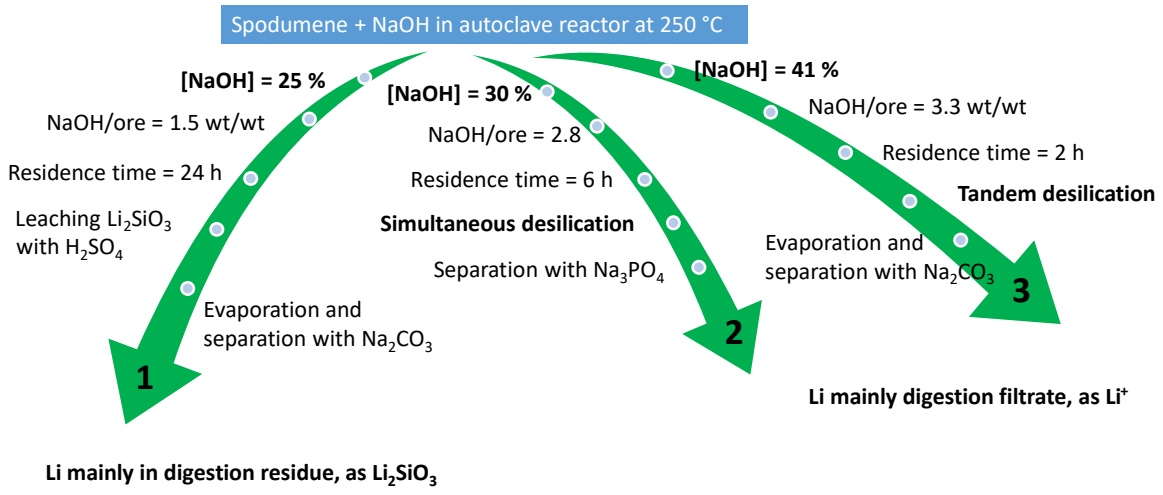

Hydroalkaline processes

1. (Residue based with tandem leaching) Qiu S, Liu C, Yu J, Conversion of α-spodumene to intermediate product of Li_2SiO_3 by hydrothermal alkaline treatment in the lithium extraction process, *Miner Eng* 183, 107599 (2022)
2. (Filtrate based with simultaneous desilication) Song Y, Zhao T, He L, Zhao Z, Liu X, A promising approach for directly extracting lithium from α-spodumene by alkaline digestion and precipitation as phosphate, *Hydrometallurgy* 189, 105141 (2019)
3. (Filtrate based with tandem desilication) Xing P, Wang C, Zeng L, Ma B, Wang L, Chen Y, Yang C, Lithium extraction and hydrosodalite zeolite synthesis by hydrothermal conversion of α-spodumene, ACS Sustain Chem Eng 7, 9498-9505 (2019)

Patents

- Catovic E, *Caustic Digestion Process*, AU 2017306576 B2, Date of filing 2 Aug 2017
- Napier A, Griffith C, Caustic Conversion Process, US 2021/0180155 A1, PCT filed 24 July 2019

Hydroalkaline processes

Three process

- Qiu et al, 25 % NaOH
- Song et al, 30 % NaOH
- Xing et al, 41 % NaOH

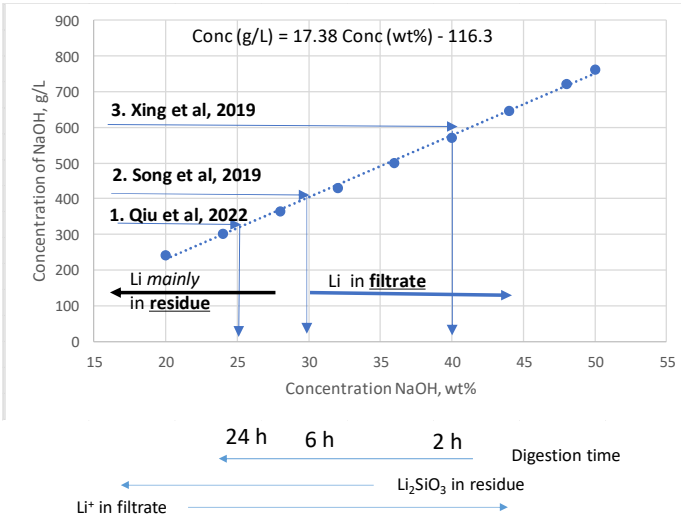

Similarities:
T = 250 °C for all
Small particle size

Key differences:
1. [NaOH] (%)
2. Residence time (h)
3. Li in filtrate or (mainly) in residue

---- *next slide* ----

4. NaOH/ore (g/g)
5. S/L (mL/g)
6. Desilication (yes/no, if yes, simultaneous or tandem)
7. Li separation

Hydroalkaline processes

	***T*, °C**	**[NaOH], %**	***t*, h**	**Li part in digestion**	**NaOH/ore, g/g**
1. Qiu et al	250	25	24	Mainly residue	1.5
2. Song et al	250	30	6	Filtrate	2.8
3. Xing et al	250	41	2	Filtrate	3.3

	***S/L*, mL/g**	**Desilication, Y/N**	**Li separation**	**Leaching, Y/N**
1. Qiu et al	4.7	?	Evaporation, Na_2CO_3	Y
2. Song et al	7.0	Y (simul)	Na_3PO_4	N
3. Xing et al	5.0	Y (tandem)	Evaporation, Na_2CO_3	N

	Particle size, µm
1. Qiu et al	D_{50} = 17.2
2. Song et al	D_{50} = 15.3
3. Xing et al	≈ 30

Presentation outline

1. Introduction

- Decarbonisation of spodumene refineries
  - Decrepitation (calcination)
  - Evaporation/crystallisation
- Spodumene reactivity
- Sulfuric acid process
- Technologies that avoid decrepitation

2. Hydroalkaline processes

- Filtrate based
  Li partitions mostly to leach solution
  - Digestion conditions
  - Sellable byproducts in residue
  - Li separation and recycling
- Residue based
  Li partitions mostly to leach residue
  - Digestion conditions and byproduct species in residue
  - Acid leach
  - Li separation and recycling

3. Quantities that matter

- Lithium recovery
- Feedstock intensity
- Byproduct intensity
- Energy intensity
- Capex

4. Conclusions

- Comparison with the sulfuric acid process
- Problems solved
- Outstanding problems

Overall refinery mass balance for sulfuric acid process

t

Energy intensity

Decrepitation: 1.53 ± 0.05 MJ/kg ore (thermodynamic value)

Compare to 2.3 MJ/kg to evaporate or 4.2 kJ/(kg °C) to heat water. Average heat capacity of spodumene is 1.2 kJ/(kg °C).

Abdullah A, *Thermal Treatment of Spodumene (LiAlSi2O6) for Lithium Extraction*, PhD Dissertation, Murdoch University, 2018

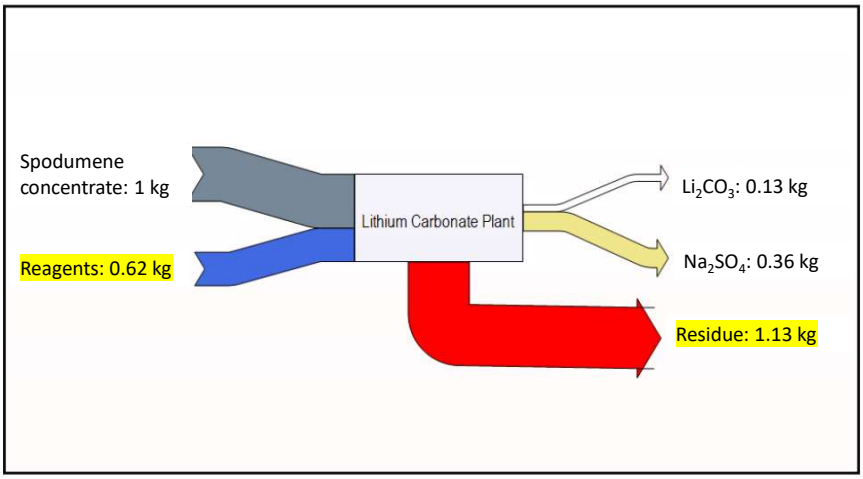

Harman G, Trends and developments in lithium processing, ALTA 2022

Feedstock, byproduct and energy intensity of Process 2

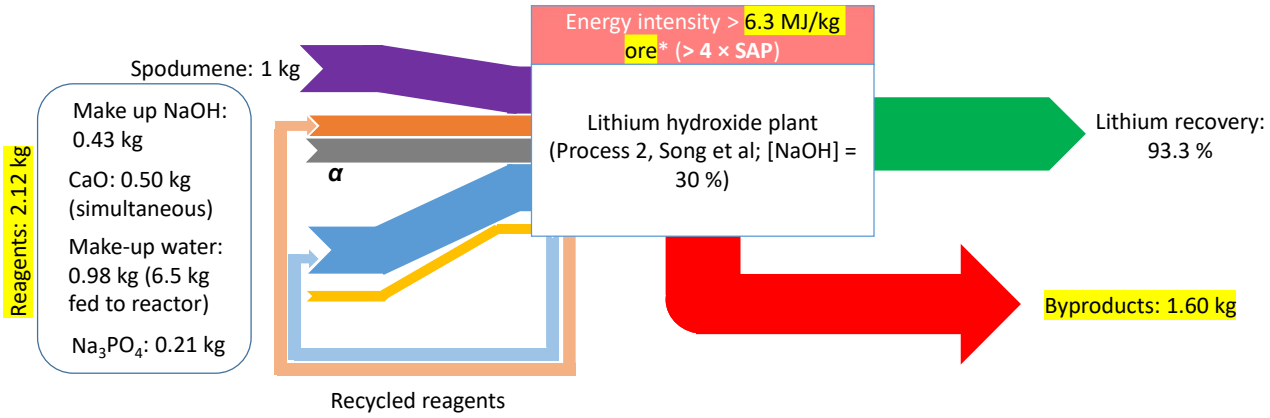

*Based on heating the water between 20 °C and 250 °C.

Feedstock, byproduct and energy intensity of Process 3

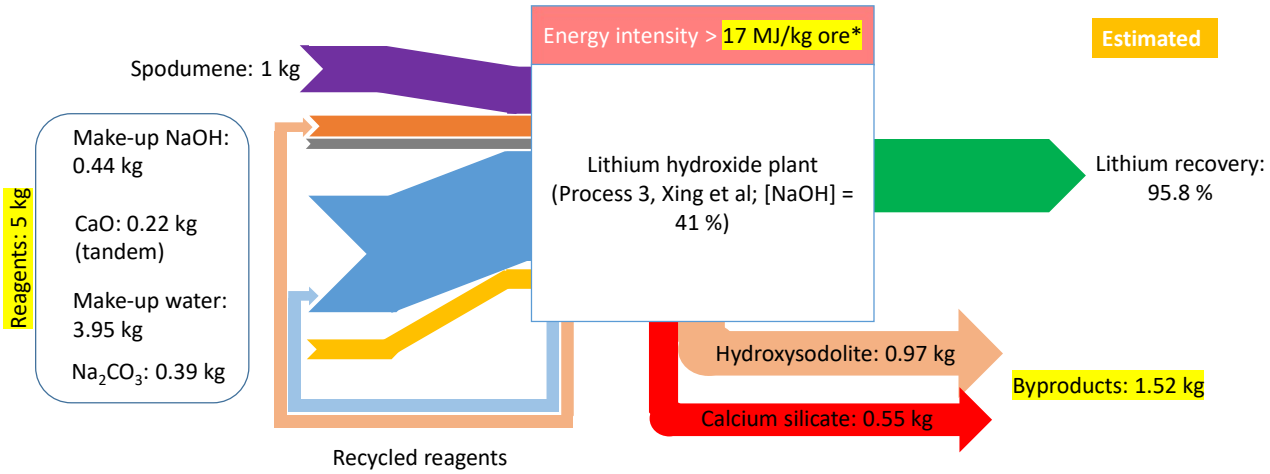

*Based on heating the water between 20 °C and 250 °C and evaporating the water to concentrate the filtrate.

Cost of evaporation and concentration of Li

In present lithium refineries, [Li] from the sulfuric acid bake and water leaching is about 10 g/L.

If a hydroalkaline treatment requires to concentrate Li from, say, around 2.7 g/L to 10 g/L, this incurs significant operating cost

2 kg H_2O	2.3 MJ	\$10	7 g Li	10^6 g $LiOH{\cdot}H_2O$	=	\$770
10 g Li	1 kg H_2O	1000 MJ	42 g $LiOH{\cdot}H_2O$	1 t $LiOH{\cdot}H_2O$		1 t $LiOH{\cdot}H_2O$

Once one accounts for efficiencies in energy and Li extraction, the cost > \$1000/1 t LHM.

If evaporation is required as part a process replacing the decrepitation kill, this defeats the purpose of decreasing the emission of embedded CO_2.

Capex

1. Industry appears to settle on multiples of 25 kt $LiOH{\cdot}H_2O$/y trains
2. This translates to ≈190 kt spodumene, concentrate treated per year, or 542 t/day;
3. Process 2 has 10.5 t charge per 1 t concentrate, with two runs a day, a 200 t autoclave can process 38 t SC a day, considering 6 h residence time and time for charging, heating and discharging
4. This corresponds to a battery of 15 autoclaves, each with charge capacity of 200 t

Residence time appears to be critical for capex; perhaps Process 2 can be accelerated by digestion with solutions of > 40 % NaOH.

Presentation outline

1. Introduction

- Decarbonisation of spodumene refineries
  - Decrepitation (calcination)
  - Evaporation/crystallisation
- Spodumene reactivity
- Sulfuric acid process
- Technologies that avoid decrepitation

2. Hydroalkaline processes

- Filtrate based
  Li partitions mostly to leach solution
  - Digestion conditions
  - Sellable byproducts in residue
  - Li separation and recycling
- Residue based
  Li partitions mostly to leach residue
  - Digestion conditions and byproduct species in residue
  - Acid leach
  - Li separation and recycling

3. Quantities that matter

- Lithium recovery
- Feedstock intensity
- Byproduct intensity
- Energy intensity
- Capex

4. Conclusions

- Comparison with the sulfuric acid process
- Problems solved
- Outstanding problems

Conclusions

1. Comparing with the sulfuric acid process: (i) New technology; dramatic break with learnings since 1950s; (ii) Feedstock intensive (by ≈ 70 % in comparison to SAP, excluding process water, for Process 2); (iii) Byproduct intensive (by ≈ 40 % in comparison to SAP, for Process 2); (iv) Recycle – consumption of NaOH ≈ 15 % per pass, for Process 2; (v) Long residence time increases CAPEX; (vi) Energy intensive (probably around 4 × as intensive as SAP); *There is no energy savings!*

2. Problems solved: (i) Chemistry works well; (ii) Nearly complete data set available for at least one process (Process 2; Song et al.); (iii) Desilication and NaOH recycling required; (iv) Identified weak points of the technology; (v) Evaporation needed to produce (low purity) Na_2CO_3 for further separation is a major energy requirement; (vi) Lithium recovery > 90 %

3. Outstanding problems: (i) Optimisation of residence time; (ii) Integration of separated lithium (low purity Na_2CO_3) into the purification circuits of existing refineries, or development of industrial technologies for converting Li_3PO_4 to LHM or LC; (iii) CAPEX – number and cost of unit operations, recycling; (iv) Handling of byproducts; (v) Future research should focus on recycling and separation of Li from the filtrate, and on more detailed economic assessment; (vi) Unclear mechanisms at atomic level, their knowledge would help optimise the process

DESIGN OF CRYSTALLISATION PLANTS FOR THE PRODUCTION OF BATTERY GRADE LITHIUM HYDROXIDE

By

[1]Katherine Lombard, [2]Nipen M. Shah and [1]Dave Rogans

[1]JordProxa Pty Ltd, South Africa
[2]JordProxa Pty Ltd, Australia

Presenter and Corresponding Author

Katherine Lombard
klombard@jordproxa.com

ABSTRACT

The rapid rise in demand for long-range, fast charging batteries for the electric vehicle market has resulted in simultaneous rapid growth in the supply chain for battery feed materials. As the energy density of the resulting batteries increases, so too does the requirement for ultra-high purity battery feedstocks.

Differing geologies and upstream chemistries result in a broad range of impurities in the feed solutions to lithium hydroxide monohydrate (LHM) crystallisation plants. These challenging and various feeds require careful assessment to develop flowsheets optimised for each application. The primary focus is on achieving stringent and ever-increasing product purity requirements, whilst concurrently minimising capital and operating costs, and lithium losses to the extent practical. Sophisticated simulation software and extensive test work are employed to develop robust flowsheets to process these differing feed chemistries and achieve the plant objectives outlined before.

This paper briefly outlines the LHM market outlook, typical feed chemistries from varying sources and the fundamental balance between purity versus capex and opex during flowsheet development. This process has been demonstrated with a case study.

Keywords: Lithium hydroxide, crystallisation, product purity, battery

1

Design Aims and Approach

- PURITY - Free from impurities
- SUSTAINABILITY - Low carbon footprint
- VALUE - High ratio of performance / cost

Design Approach

- Maximise purity
- Maximise yield
- Minimise CAPEX and OPEX costs
- Ease of operation with robust design

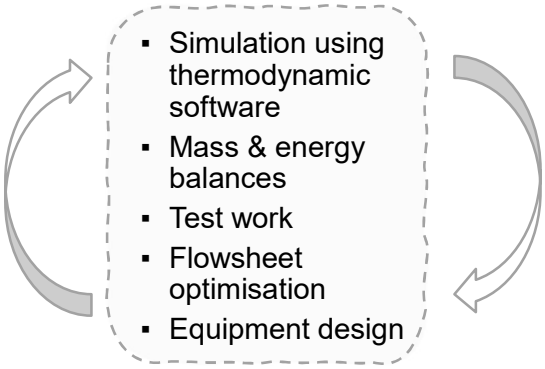

Evaporator / Crystalliser Fundamentals

2

EVAPORATION

- Produces a concentrate for discharge or further treatment
- Recovers clean water
- Handles tough liquors that biological and membrane treatment cannot handle

CRYSTALLISATION

- Thermal: Recovers clean water and solid waste or a usable product.
- Cooling crystallisation: recovery of a specific component
- Purification steps

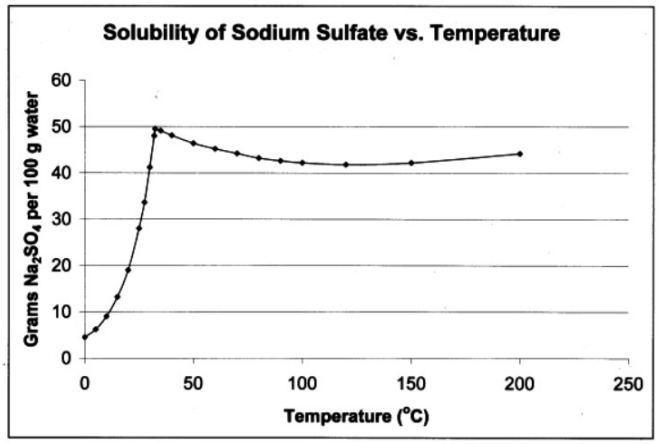

FALLING FILM EVAPORATOR

- Liquor re-circulated to top of heat exchanger
- Liquor heated as it falls as a film on inside of tube
- High heat transfer rates
- Low space requirements
- High turndown capability
- Not suitable for crystals or scaling liquors

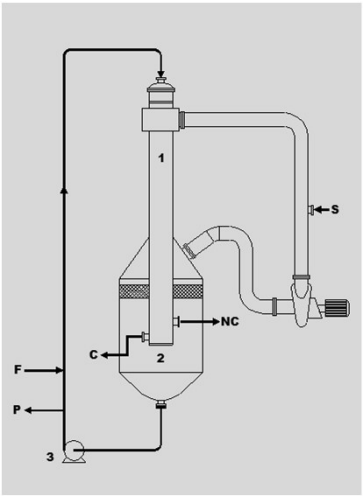

FORCED CIRCULATION- THERMAL

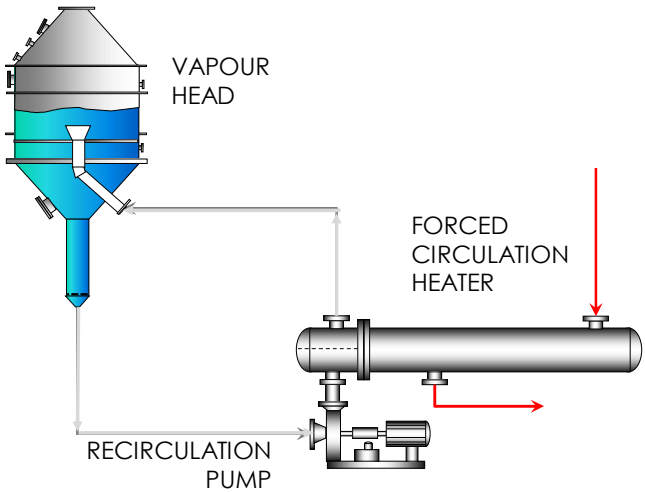

FORCED CIRCULATION- COOLING

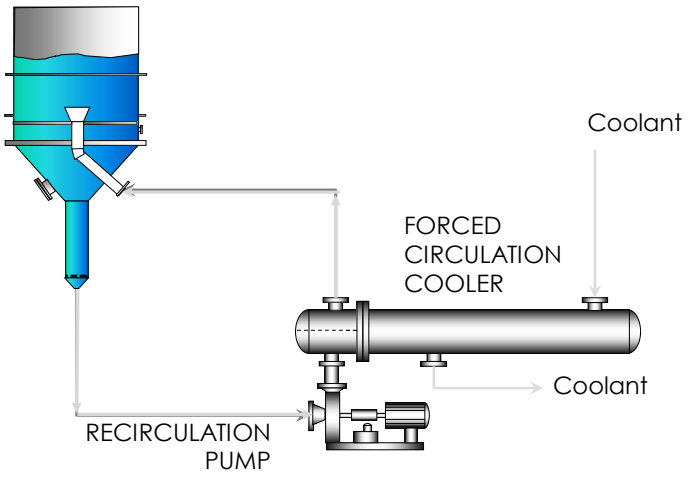

3

Purity

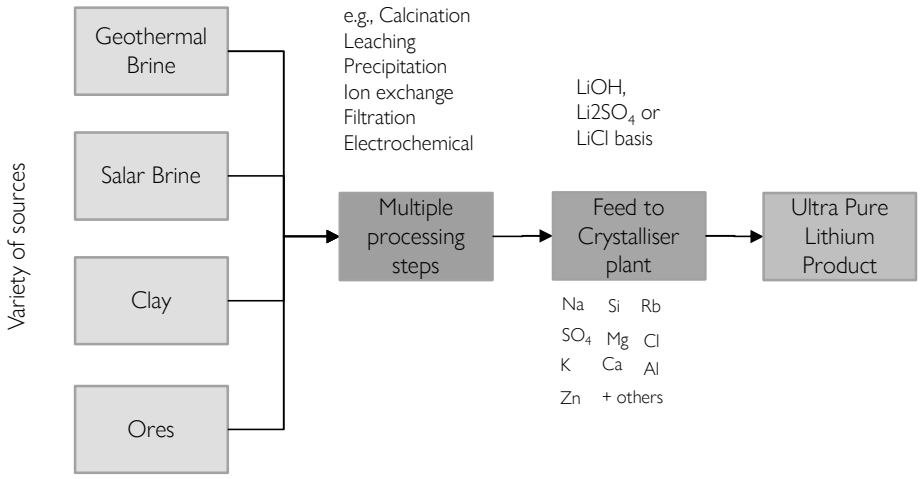

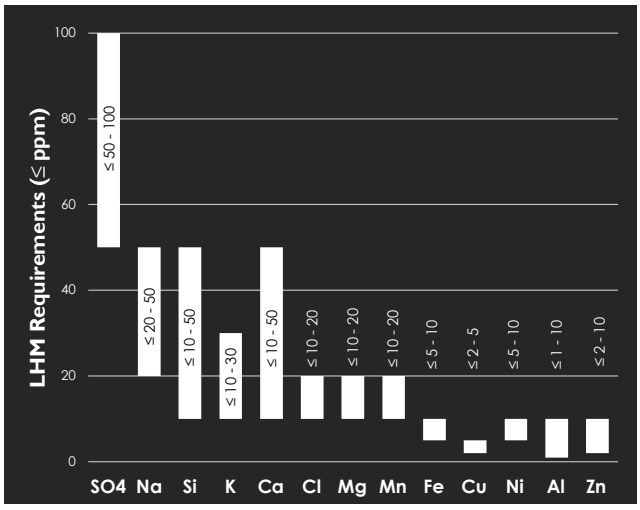

- Very low concentrations.
- Up to 3 nines LHM required (99.9% excl. CO_3).
- Future LHM purity may require as high as 4 nines (99.99% at < 100 total ppm impurities excl. CO_3).

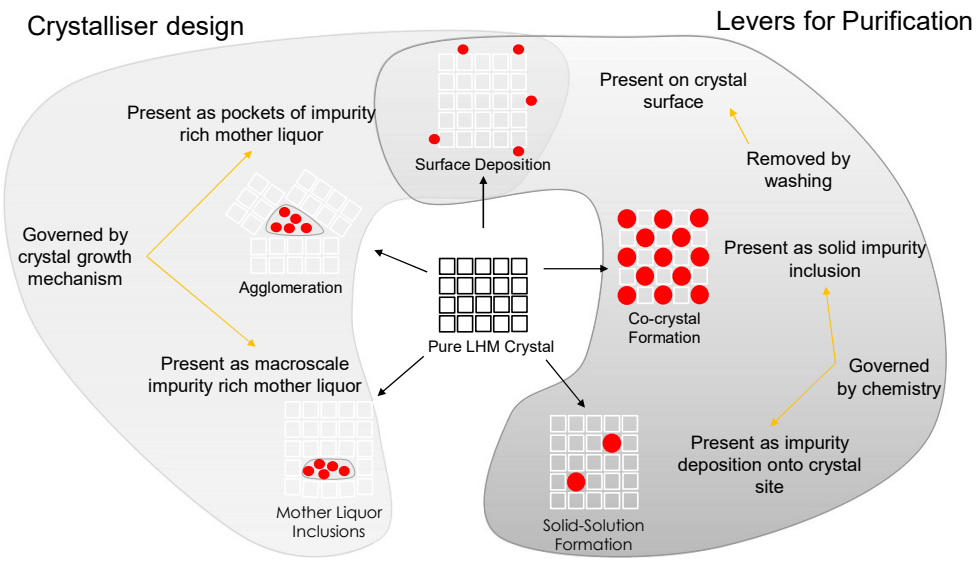
Crystalliser design
Levers for Purification
Present as pockets of impurity rich mother liquor
Surface Deposition
Present on crystal surface
Removed by washing
Governed by crystal growth mechanism
Agglomeration
Pure LHM Crystal
Co-crystal Formation
Present as solid impurity inclusion
Present as macroscale impurity rich mother liquor
Governed by chemistry
Mother Liquor Inclusions
Solid-Solution Formation
Present as impurity deposition onto crystal site

4

Case Study

Feed basis: Lithium sulphate **PLS** generated from traditional β-Spodumene sulphation route.

Range of main impurities presented in table below on a 10 g/L Li basis:

Component	Unit	Typical	Good	Excellent
Na	g/L	6-8	6	5
SO_4	g/L	70-80		
K	g/L	0.7-0.9	0.6	0.3
Cl	mg/L	< 100	70	< 40
Si	mg/L	10-20	10	< 5
Other typical trace level impurities include Ca, Mg, Cs, Zn, Al +…				

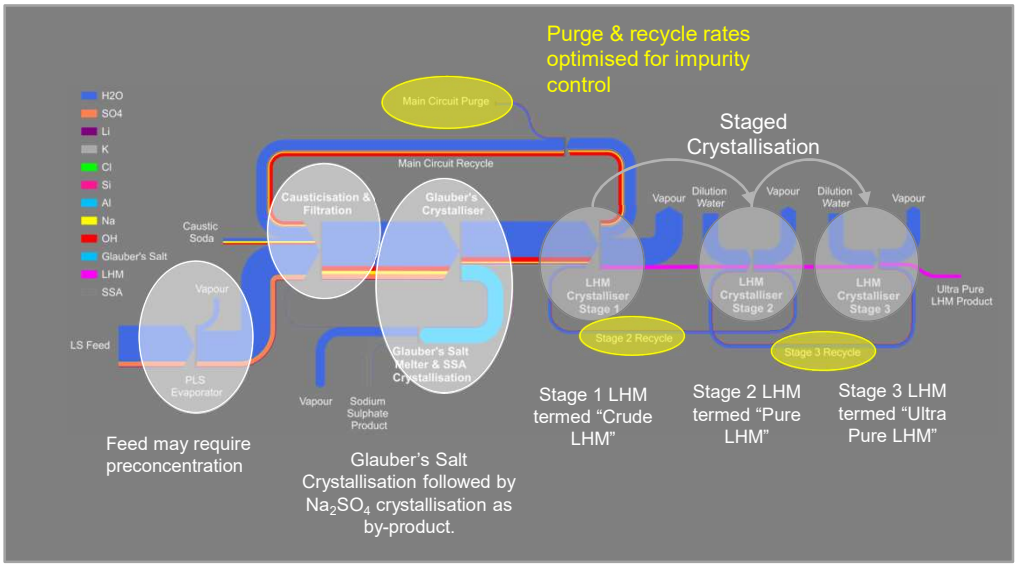

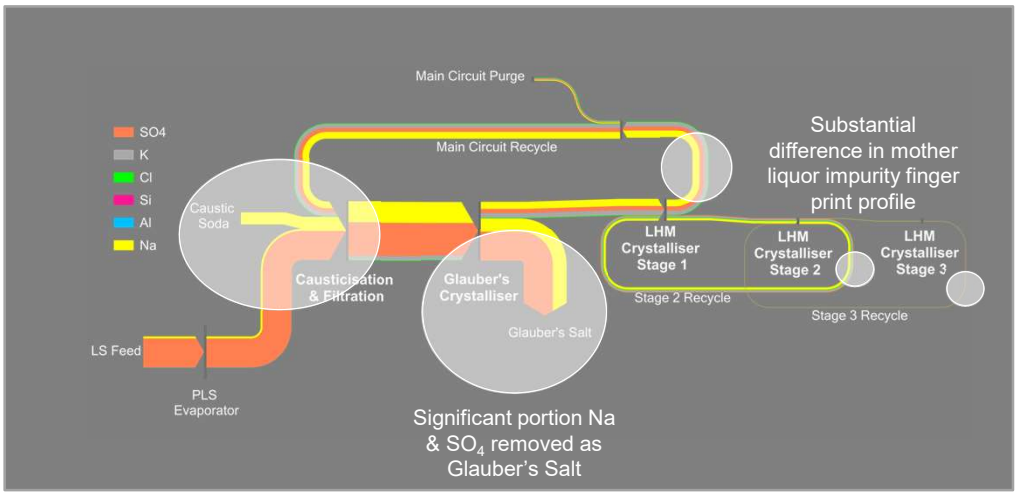
Main Circuit Purge
Main Circuit Recycle
SO4
K
Cl
Si
Al
Na
Caustic Soda
Causticisation & Filtration
Glauber's Crystalliser
Glauber's Salt
LS Feed
PLS Evaporator
LHM Crystalliser Stage 1
LHM Crystalliser Stage 2
LHM Crystalliser Stage 3
Stage 2 Recycle
Stage 3 Recycle
Substantial difference in mother liquor impurity finger print profile
Significant portion Na & SO_4 removed as Glauber's Salt

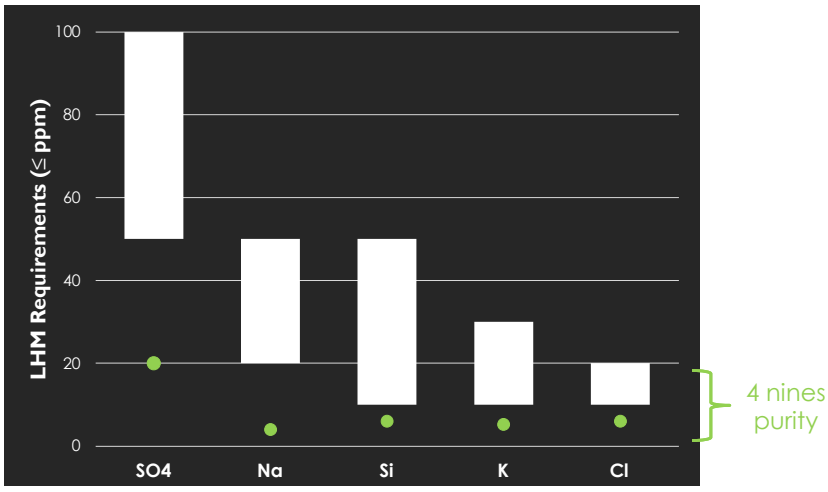
LHM Requirements (≤ ppm)
100
80
60
40
20
0
SO4
Na
Si
K
Cl
4 nines purity

5

Conclusions

CONCLUSIONS

- The requirements for LHM product purity are becoming ever more stringent.
- Well defined empirical impurity entrainment models along with test work validation helps us develop a robust flow sheet that can meet the desired product purities.
- JordProxa has expertise in the design of the flowsheets that can produce Ultra Pure LHM product with the current 3-nines and the future 4-nines purity from a variety of different feed compositions.

PROCESS MODELLING AND LIFE CYCLE ASSESSMENT: A CASE STUDY ON PRIMARY LITHIUM PRODUCTION

By

[1]Mike Dry, and [2]Laurens Tijsseling

[1]Arithmetek, Canada

[2]Minviro, England

Presenters and Corresponding Authors

Mike Dry
mike.dry@arithmetek.com

Laurens Tijsseling
laurens@minviro.com

ABSTRACT

Lithium is considered a critical metal to enable the transition from a fossil fuelled to an electric economy. It is estimated that lithium demand can grow up to 500% by 2050, compared to 2018 production. An increase in a demand could lead to higher lithium prices, meaning that previously considered uneconomic assets might become economically sustainable. However, when moving to an electric economy it is critical the improvement in downstream performance is not offset by an increase in environmental impacts from raw material extraction and refining.

To ensure holistic decision-making it is important that costs, revenue, carbon footprint, water scarcity footprint and other environmental impact categories are all considered throughout the iterative design phase. Process modelling can be used to evaluate the technical and economic feasibility of a project design, whilst life cycle assessment (LCA) can be used to quantify environmental impacts of technology options. LCA quantifies environmental impacts associated with all stages of a product, process, or activity.

In this study, process modelling paired with prospective LCA modelling is explored, the thesis being that such pairing enables earlier and much better-informed decisions about economic and environmental sustainability. Extraction of lithium from a salar brine is considered, followed by further processing into lithium hydroxide monohydrate via two options, namely the conventional solar evaporation route and a novel route using direct lithium extraction to separate lithium from the salar brine without evaporation, followed by selective lithium solvent extraction to concentrate the lithium into a pure lithium product. An integrated approach is presented that examines economic and environmental factors in evaluating the alternative technologies.

Keywords: Lithium, CO_2, water, environment, LCA, economics

INTRODUCTION

For the current drive towards electrification is to succeed, demand for the metals needed to make storage batteries must become vast. The lithium-ion battery, in various forms, is the leading contender for vehicle batteries, and the global demand for lithium in 2050 is expected to be almost ten times that of 2017[1]. This implies that many new lithium extraction projects must arise, along with the environmental challenges associated with all new mining ventures.

Holistic decision-making requires that costs, revenue, carbon footprint, water scarcity footprint and other environmental impact categories are all considered. Traditionally, life cycle assessment (LCA) is based on data from operating plants, but that data cannot be generated before the plant is operating. Leaving LCA to later in the development sequence when operating (or pilot-plant) data can be used means that technical decision making has already happened, and reversing major decisions is costly in terms of time and money. It would be preferable to have LCA input earlier in the project so that major decisions need not be reversed or adverse environmental consequences locked in. Process modelling can be used to evaluate the techno-economic feasibility of a project, whilst life cycle assessment (LCA) can be used to quantify its environmental impacts. LCA is a methodology for quantifying environmental impacts associated with all stages of a product, process, or activity that enables earlier and better-informed decisions about the economic and environmental sustainability of the project concerned.

The exercise presented here explores the pairing of techno-economics and LCA. Extraction of lithium from a salar brine by two technical routes is considered, with the lithium being extracted and recovered as lithium carbonate or lithium hydroxide, using conventional solar evaporation or direct lithium extraction without solar evaporation. An integrated approach is presented that examines economic and environmental factors for the alternative technologies.

METHODOLOGY

Life cycle assessment (LCA) is a scientific methodology to assess global environmental impacts associated with the life cycle of a product or process. Beyond this generic definition, LCA is a comprehensive and reliable tool that enables environmentally informed decision-making throughout all the stages of a project. Life cycle assessment makes it possible to evaluate indirect impacts arising from a product or processing system over its entire life cycle, providing information that otherwise may not be considered. A wide range of environmental impacts can be captured scientifically and quantitatively. This holistic approach generates information enabling informed decisions that avoid, for example, simple shifting of an environmental burden[2]. It must be noted that LCA is a powerful tool to determine impacts at a global scale, but it is less suitable for determining local impacts that are commonly investigated using environmental (and social) impact assessment studies.

LCA uses process data to quantify environmental impacts. One source of this data, which is not available when the operations under consideration do not yet exist, is actual operating plants. When the plant is yet to be built, process modelling can be used to generate plausible preliminary data[4]. An important caveat here is that, while process modelling is a very useful tool for project evaluation, it is beyond risky to use it in isolation. The assumptions used (for example recoveries, reagent consumptions, solid-liquid separation efficiencies) must be verified experimentally before major expenditure such as detailed engineering design is undertaken, and certainly before a decision is made to construct the actual plant. The exercise presented here uses process modelling to generate the preliminary data required to techno-economic evaluation and LCA for the two processing options examined.

Principles as outlined under ISO 14040[7] and ISO 14044[8] standards series were used in this study. They outline a four-step process, as shown in Figure 1.

The scope of a life cycle assessment study in the resource sector can be either:

- Cradle to gate: partial life cycle assessment study on product life cycle, from resource extraction to a defined end gate (e.g. lithium chemical delivered to the market).
- Cradle to grave or cradle to cradle: complete life cycle assessment study on product life cycle, from resource extraction throughout the use phase and evaluating end of life impacts (grave) or recycling pathways (cradle).

The life cycle assessment study presented here takes a cradle to gate approach. This means that the impacts are accounted for from resource extraction up to where the lithium product is ready for shipment to customers. The system boundaries used in this study are presented in Figure 2. The results of this life cycle assessment study are considered to be relevant input for rational decision making and ranking processing options but are not intended to communicate comparative assertions to the general public.

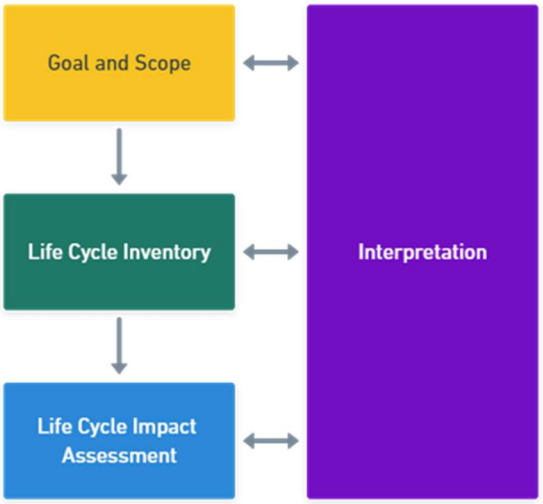

Figure 1 – LCA stages

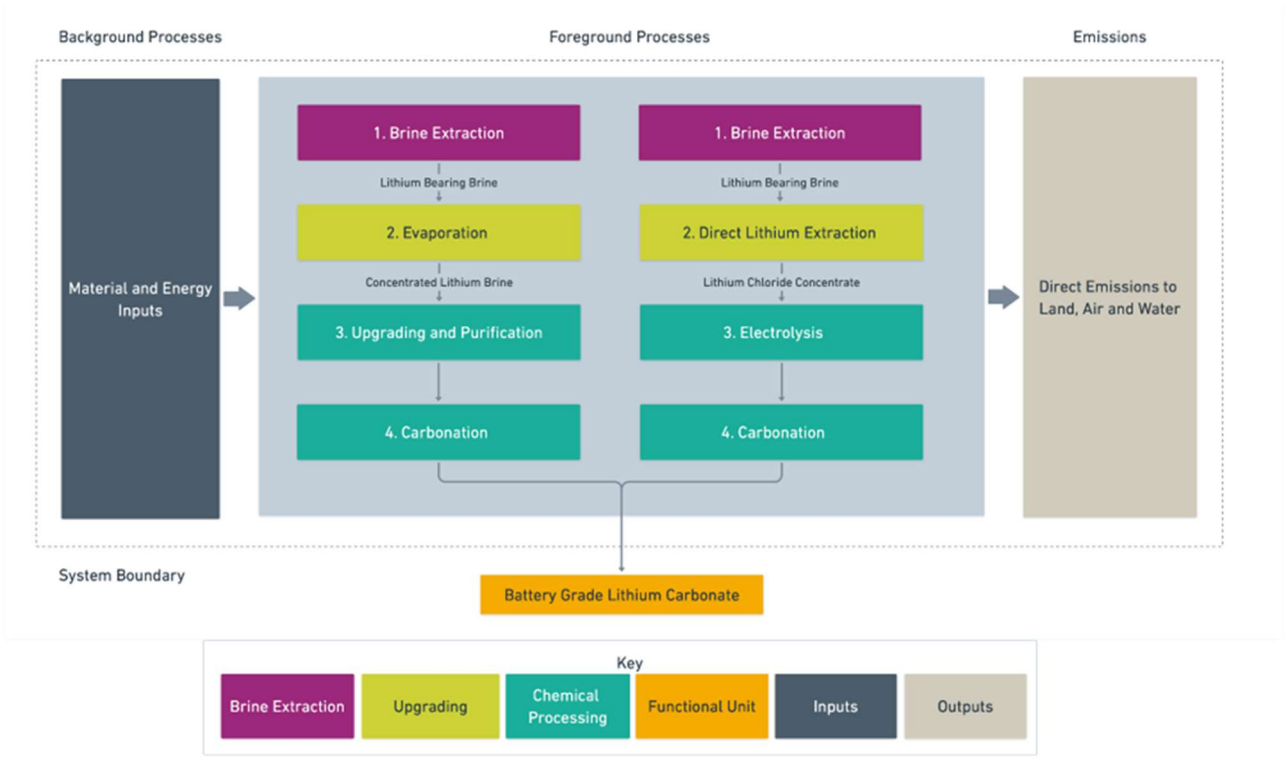

Figure 2 – System boundaries applied in this LCA study

LIFE CYCLE IMPACT ASSESSMENT

While there are other factors as well, the life cycle impact assessment categories evaluated in this study are climate change and water use.

Climate Change

Climate change is the term generally used to mean an increasing global temperature arising from the effect of "greenhouse gases" released by human activity. There is consensus that the increase in these emissions is having a noticeable effect on climate. Climate change is one of the major environmental effects of economic activity, and one of the most difficult to control because of its global scale[6]. The environmental profiles characterization model is based on factors developed by the UN's Intergovernmental Panel on Climate Change. Factors are expressed as GWP (Global Warming Potential) over various time horizons, the most common historically being 100 years, measured in the reference unit, kg CO_2 eq.

The Greenhouse Gas Protocol identifies three "scopes" of GHG emissions which have been included in this study. It should be noted, however, that scopes of emissions are not a framework inherent to LCA. The GHG Protocol defines scopes of emissions as:

- **Scope 1**: Direct GHG emissions (e.g. furnace off-gas, combustion of fuels)

- **Scope 2**: Indirect GHG emissions from consumption of purchased electricity, heat or steam (such as emissions embodied in grid power or embodied in steam at an industrial park).
- **Scope 3**: Other indirect emissions such as the extraction and production of purchased materials and fuels, transport-related activities in vehicles not owned or controlled by the reporting entity, electricity-related activities (for example transmission and distribution losses) not covered in scope 2, outsourced activities, and waste disposal. Scope 3 emissions can be either "upstream" or "downstream". In a cradle-to-gate LCA, "upstream" scope 3 must be included.

Water Use

The AWARE method is applied to quantify the environmental performance of products and operations regarding fresh water. This method was developed by Water Use in Life Cycle Assessment (WULCA), a working group of the UNEP-SETAC Life Cycle Initiative, on a water scarcity midpoint method for use in LCA and for water scarcity footprint assessments. This approach is based on the available water remaining per unit of surface area in any given watershed after human and ecosystem demands have been met, relative to the world average. The resulting characterization factor ranges between 0.1 and 100 and can be used to calculate water scarcity footprints[9]. A value close to 0.1 means that plenty of water is available in that region, whilst a water scarcity of 100 means that water in that region is extremely scarce. Units of the characterization factor are dimensionless, expressed in m^3 world eq. per m^3. It is important to note that this impact relates to the potential of water deprivation to humans or ecosystems, rather than direct water use by the project. Another way to think about this is that it is a life cycle impact assessment value, not an inventory flow. The water stress index for the project in this exercise is assumed to be 40 m^3 world eq. per m^3.

ALLOCATION

A difficulty in LCA is that, if a system produces multiple products, the impacts have to be divided between those products such that the distribution of the impacts between those products and the benefits of those products are allocated fairly; this is called allocation. It should follow a stepwise approach[8] and is not always easy. The two production pathways described in Figure 2 do not have any co-products, meaning that no allocation is required in the exercise presented here.

PROCESSES

This study extends a previous exercise[2], in which the extraction of lithium from a salar brine and from lithium bearing clay was examined. The source is the same salar brine as before (Table 1) and two processing options are examined:

- The conventional solar evaporation route from the previous exercise (the solar evaporation route).
- A novel route entailing the use of a lithium-ion sieve and lithium-selective solvent extraction (the DLE-SX route).

Table 1 – Hypothetical brine, ppm

Mg	4826
Ca	415
Na	487500
K	24900
Li	1960

Solar evaporation

The brine is concentrated by solar evaporation in a series of large ponds, causing mainly sodium chloride (initially) and potassium chloride (subsequently) to crystallize and settle to the bottom of the evaporation ponds. The settled salts are harvested periodically and disposed of on dumps. Depending on the composition of the brine, other salts such as calcium sulphate, borates and double salts can also crystallize. If the brine contains more than a small amount of magnesium, a lithium-magnesium double salt can crystallize, causing loss of lithium. In such cases the brine is treated with lime at some suitable point in the evaporation sequence, precipitating the magnesium as hydroxide and replacing it with calcium, to avoid that form of lithium loss. The first part of this circuit is illustrated in Figure 3 and the second in Figure 4.

Brine from the wellfield is limed, the resulting mixture of gypsum and magnesium hydroxide is settled out and the remaining brine is concentrated by solar evaporation. The solar evaporation is modelled as two steps, first crystallizing out sodium chloride and then crystallising out sodium and potassium chloride. (The two pond icons shown, of course, each represent multiple solar ponds.)

Hydrochloric acid is added to the evaporated brine to lower the pH and the acidified brine is warmed by heat exchange with steam, then passed through solvent extraction to remove the bulk of the boron. The boron-loaded organic phase is stripped with aqueous sodium hydroxide and the resulting strip solution is disposed of in a waste pond.

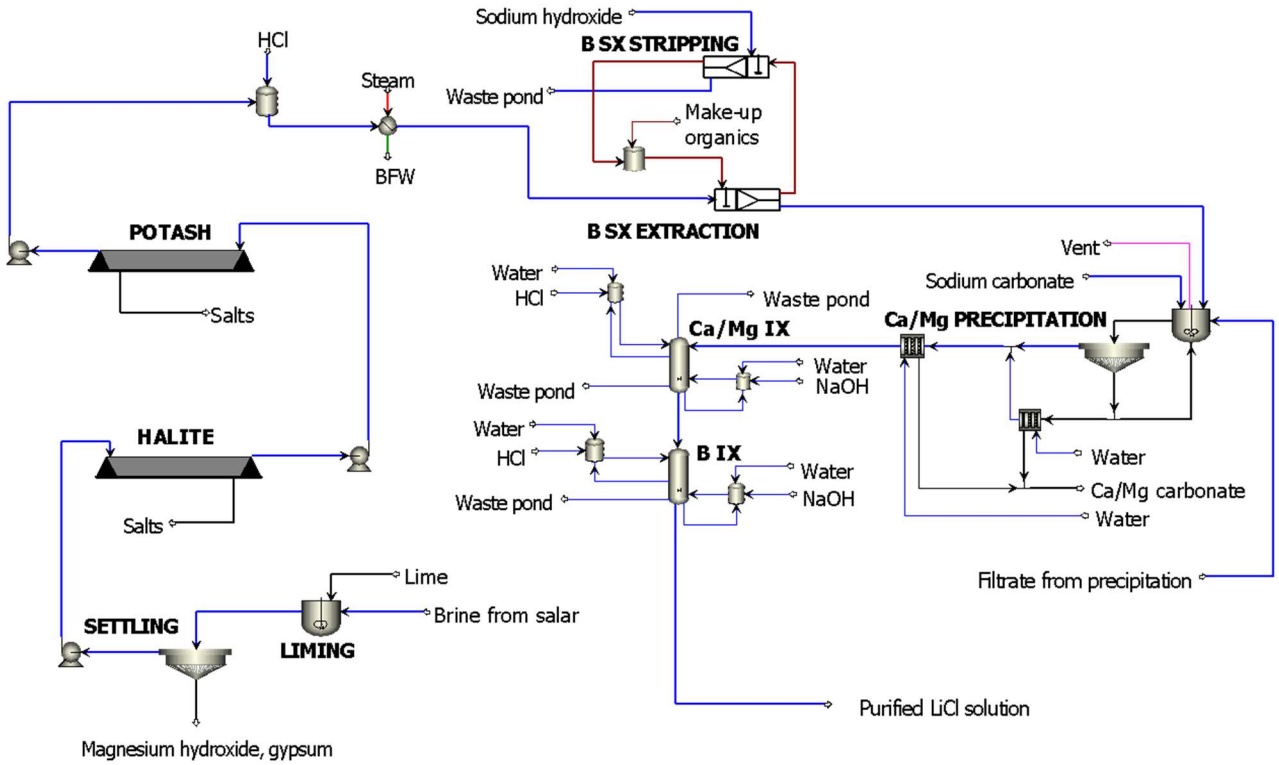

Figure 3 – Conventional circuit processing salar brine

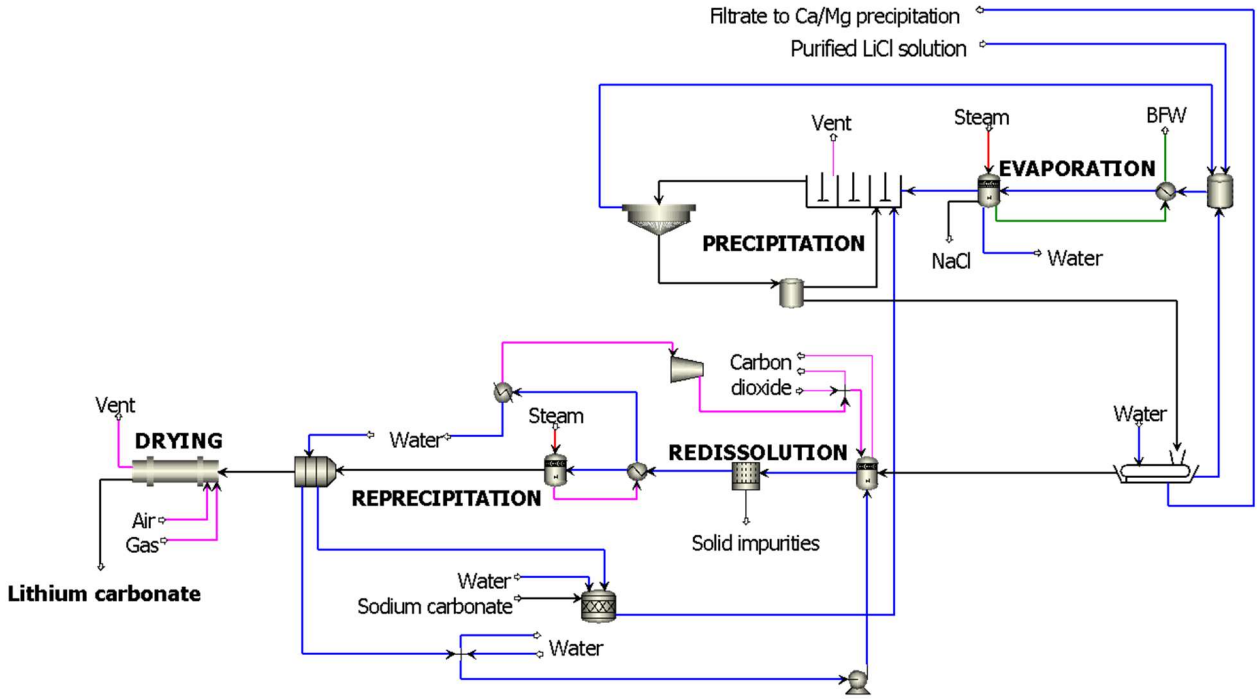

Figure 4 – Precipitation and refining of lithium carbonate

The boron-depleted brine is dosed with sodium carbonate to precipitate the bulk of the remaining calcium and magnesium, the precipitate being settled and filtered. The filter cake is washed with water and disposed of. The filtrate is passed through two ion exchange steps, first to remove residual calcium and magnesium, then to remove residual boron. In these ion exchange steps, the loaded resin is stripped with dilute hydrochloric acid and regenerated with dilute sodium hydroxide. The spent reagents are disposed of in the waste pond.

The purified brine is concentrated further by evaporation against condensing steam, with some of the remaining sodium chloride crystallizing and being removed. The concentrated brine is dosed with sodium carbonate, precipitating lithium carbonate that is recovered by thickening. Part of the thickener underflow is

recycled to the precipitation step as seed and the balance is filtered. The filter cake is washed with water and the filtrate is recycled to the Ca/Mg precipitation step in the front end of the circuit to bleed out impurities (Ca, Mg, B).

The washed filter cake is mixed with water and carbon dioxide at ambient temperature and somewhat elevated pressure (about 3 bar). The carbon dioxide reacts with the carbonate, forming bicarbonate and thereby re-dissolving the lithium. The addition of CO_2 is manipulated to re-dissolve the lithium carbonate while leaving impurities such as calcium carbonate undissolved. The bicarbonate solution is filtered, and the solid impurities are discarded. The filtrate is heated and depressurised, causing the aqueous bicarbonate to revert to carbonate and carbon dioxide, re-precipitating purified lithium carbonate that is recovered and washed with water in a centrifuge, then dried. The primary centrate is recycled to the redissolution step. The wash centrate and fresh water are used to dissolve solid sodium carbonate to make up the near-saturated solution of sodium carbonate that is used to precipitate lithium carbonate from the solution ex evaporation.

DLE-SX

The chemistry of processing salar brines via solar evaporation requires essentially all the divalent cations in the brine to be replaced with sodium. Where calcium hydroxide is used to remove magnesium, the magnesium is replaced by calcium that is later replaced with sodium, thus the magnesium is ultimately also replaced with sodium. The ratio of divalent cations to lithium determines the amount of sodium needed to replace the divalent cations, and the cost of the sodium accounts for an appreciable part of the overall cost of extracting lithium from salar brine. There is chemistry that selectively removes lithium in the presence of divalent cations, based on materials called lithium-ion sieves, one example being solid meta-titanic acid, which can selectively absorb lithium from brines containing high levels of calcium, magnesium and other cations[11,12]. The essential chemistry (bold denoting the solid phase) is:

$$\mathbf{H_2TiO_3} + H_2O + Li^+ \leftrightarrow \mathbf{LiHTiO_3} + H_3O^+$$

The crystal structure of the solid phase is such that the “holes” are small enough to allow only lithium or protons into the lattice, thus making the equilibrium highly selective for lithium.

Figure 5 and Figure 6 illustrate a circuit exploiting this chemistry. Incoming brine is mixed with recycled solution from the ion exchange purification stage and filtrate from the first precipitation of lithium carbonate, then passed through two counter-current stages of loading, where the lithium is absorbed into the lattice of the H_2TiO_3 sorbent, releasing protons. The loading reactors are held close to neutral (pH 7) by the addition of sodium or ammonium hydroxide. The resulting loaded sorbent (a mixture of H_2TiO_3 and $LiHTiO_3$) is washed with water in a counter-current decantation train, then stripped in a recirculating solution of lithium chloride (from the first thickener in the subsequent counter-current decantation train) that is held at about pH 2 by addition of concentrated hydrochloric acid into the circulating solution. The regenerated H_2TiO_3 is washed with water in a second counter-current decantation train, then recycled to the loading reactors.

A bleed from the circulating strip solution is filtered to capture and remove any entrained solids, the ensuing small loss of sorbent being replaced by fresh sorbent added to the stripping reactor. The pH of the resulting solids-free solution is raised, and ion exchange is used to remove the residual entrained divalent cations (mainly Ca^{2+}) not washed off the loaded sorbent in the counter-current decantation train preceding the stripping step. The resin is stripped with hydrochloric acid and regenerated with sodium hydroxide. The spent strip acid is recycled to the feed tank ahead of the ion exchange section. The spent regenerant is recycled to the feed tank ahead of the loading reactors via another counter-current decantation train.

The resulting purified solution of lithium chloride goes to the circuit illustrated in Figure 6. This circuit exploits a solvent extraction system that very selectively extracts lithium from solutions also containing other monovalent cations like sodium and potassium. The prime requirement is that the feed solution be free of divalent cations because these are extracted ahead of lithium. The preceding Li-ion sieve circuit extracts lithium and rejects divalent cations very selectively but does not concentrate the lithium overly and the lithium brine produced necessarily contains sodium cations.

The incoming LiCl brine is contacted with the organic solvent, the Li cations being extracted completely and very selectively. The pH is held at neutral by the addition of sodium hydroxide. The loaded organic solvent is then stripped with recycled sulphuric acid from the subsequent electrolysis step, in which the loaded strip liquor is passed to the anode side of a chlor-alkali type electrolysis cell. Oxygen is evolved at the anodes, releasing protons and thus regenerating sulphuric acid. Hydrogen is evolved at the cathode, generating OH^- ions that are balanced by Li^+ ions passing through the cation selective membrane. The anolyte, atter supplementation for minor losses with sulphuric acid and water (to replace the water decomposed by the production of oxygen and hydrogen) is recycled to the stripping step of the solvent extraction sequence. The catholyte is evaporated to crystallize lithium hydroxide monohydrate that is recovered by centrifugation and washing with part of the condensate from the evaporation step. The wash centrate and the balance of the condensate ex the evaporation step are recycled to the cathode side of the electrolysis stage. The washed lithium hydroxide is dried and becomes the product, or (not shown) can be treated with CO_2 to make high-grade lithium carbonate.

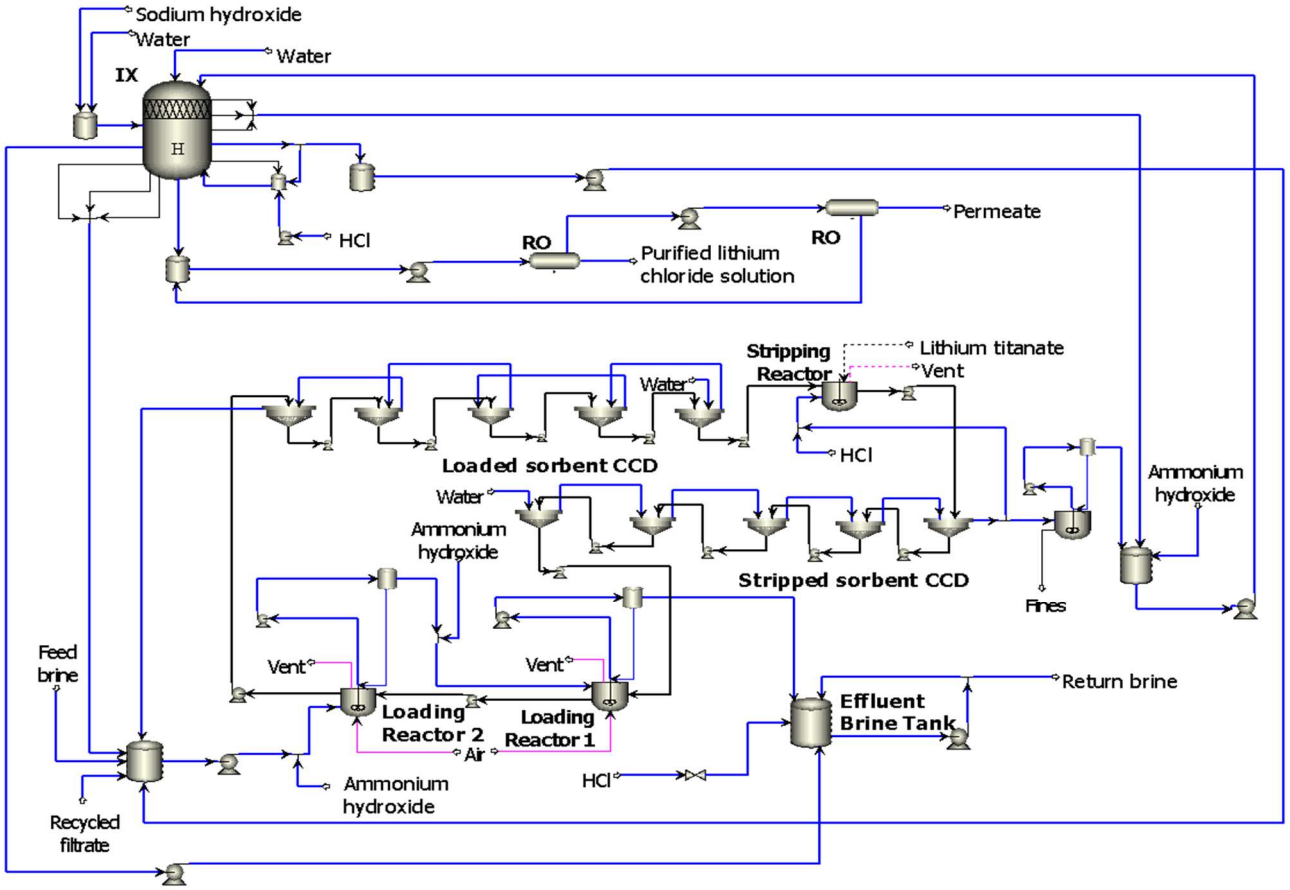

Figure 5 – Li-ion sieve circuit

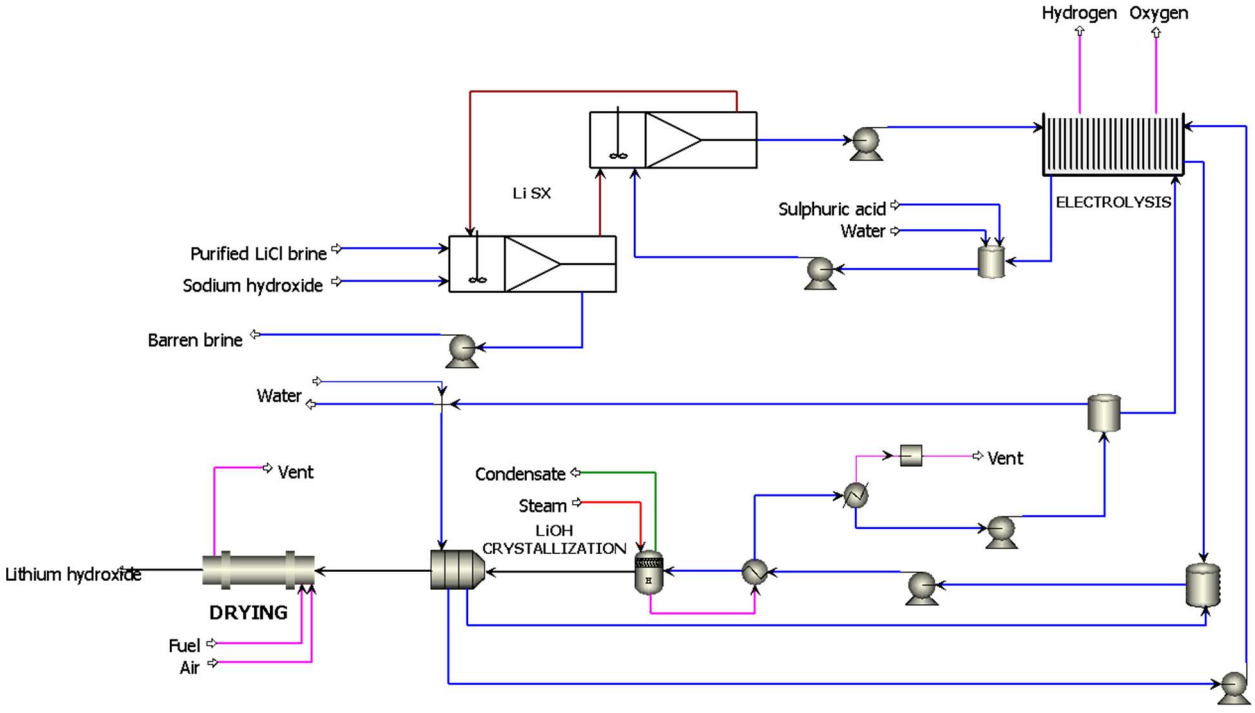

Figure 6 – Lithium hydroxide circuit

While admittedly still in their infancy, both the Li-ion sieve technology and the Li-selective solvent extraction technology have been tested reasonably extensively, up to pilot plant scale and engineering evaluations. For the purposes of the exercise presented here, these technologies are accepted as sound, but obviously both would require substantially more work to become commercial practice.

TECHNO-ECONOMIC RESULTS

The approach used for generating estimates of the capital and operating costs associated with the process routes in this exercise was to develop and analyse process models (mass-energy balances) for each, then to estimate the capital costs. The techniques used are presented in detail elsewhere[5]. Published data was used to estimate the capital costs.

Variable operating costs

Table 2 and Table 3 list the variable operating costs calculated for the two routes examined. The DLE-SX route would seem to have an advantage of about 30 percent over the established route, at an electricity cost of $0.05/kWh. At $0.1/kWh that advantage drops by about 5 percent.

Table 2 – Solar evaporation, variable costs per tonne LCE

Solar evaporation	Amount	Cost, $
Lime ($60/t CaO)	3596 kg	216
Hydrochloric acid ($200/t 32% HCl)	4633 kg	927
Sodium hydroxide ($450/t NaOH)	1630 kg	367
Sodium carbonate ($300/t Na_2CO_3)	21 kg	6
Utility steam ($20/t)	495 kg	10
Electricity ($0.05/kWh)	48 kWh	2
Fresh water ($2/m³)	53 m³	107
Sub-total reagent/utility cost per tonne LCE		1635
Li_2CO_3 precipitation and refining	Amount	Cost, $
Sodium carbonate ($300/t Na_2CO_3)	2238 kg	671
Carbon dioxide ($50/t CO_2)	42 kg	2
Utility steam ($20/t)	5526 kg	111
Electricity ($0.05/kWh)	52 kWh	3
Fresh water ($2/m³)	15 m³	29
Sub-total reagent/utility cost per tonne LCE		816
Combined reagent/utility cost per tonne LCE		2451

Capital and fixed operating costs

For both routes examined, the capacity was assumed to be 40 kilotons per year, with the product expressed as lithium carbonate equivalent (LCE). When the product is lithium carbonate, one tonne of product is one tonne LCE. When the product is lithium hydroxide monohydrate, one tonne of the product is 880.4 kg LCE. For this exercise, the capital cost associated with the solar evaporation route was taken from published information on the production of lithium carbonate from the Cauchari-Olaroz Salars in the Jujuy Province of Argentina[14]. For the route using lithium-ion sieve technology, selective solvent extraction and electrolysis, the capital cost was extrapolated from published information on the Lanxess Smackover project[15].

Table 4 lists the capital and fixed operating costs for the solar evaporation circuit. Table 5 shows the calculation of the capital cost for the Li-ion sieve route. The Standard Lithium project had three phases, capacity and cost of each as listed. Plotting the capital costs versus the design capacities for the three phases gives the plot shown in Figure 7, and fitting a power function through the data points gives the equation shown in the box on that graph. A capital cost for the Li-ion sieve route was calculated by scaling the costs for each phase - multiplying each capacity by 40000/209000 and using the equation in Figure 7 to calculate a scaled capital cost for each phase, then totalling the three numbers so calculated. The production wells were assumed to be the same for both cases.

The fixed operating costs were assumed to be the same for both routes, and to be those of the solar evaporation route. Table 6 shows the fixed operating costs.

Cash flow calculations

Cash flow calculations boil the various costs and revenues down to a set of simple numbers that show the relative economics of the options examined. The revenue for the two process routes would be the selling prices of lithium carbonate and lithium hydroxide monohydrate, respectively. Setting values for these numbers is not a trivial exercise. The values assumed for this exercise are thought to be plausible but are not claimed to be accurate; they are used only because cash flow modelling deals with revenues as well as costs, and therefore requires selling prices. Table 7 lists the assumptions used in the cash flow calculations.

Table 3 – DLE-SX, variable costs per tonne LCE

LiSTR	Amount	Cost, $
Sodium hydroxide ($450/t NaOH)	1099 kg	495
Hydrochloric acid ($200/t 32% HCl)	3204 kg	641
Make-up Li_2TiO_3 ($8000/t)	9 kg	74
Electricity ($0.05/kWh)	6 kWh	0
Fresh water ($1.61 per m³)	13 m³	25
Sub-total reagent/utility cost per tonne LCE		1236
Li SX-EW and LiOH crystallization	Amount	Cost, $
Sodium hydroxide ($450/t NaOH)	1119 kg	503
Sulphuric acid ($200/t H_2SO_4)	46 kg	12
Utility steam ($20/t)	83 kg	2
Natural gas ($400/t)	0.4 kg	0
Electricity ($0.1/kWh)	1818 kWh	91
Fresh water ($0.43 per m³)	12 m³	25
Sub-total reagent/utility cost per short ton LCE		633
Combined reagent/utility cost per tonne LCE		1868

Table 4 – Capital and fixed operating costs, solar evaporation route

Production wells	S50 million
Solar evaporation ponds and lithium carbonate plant	S565 million
Annual maintenance (3% of capex)	$16 million/y
Manpower, other fixed costs	$24 million/y

Table 5 – Capital and fixed operating costs, Li ion-sieve route

LiSTR data			At 40 kt/y LCE
Phase 1	9700 tpa LCE	$137 million	$181 million
Phase 2	8200 tpa LCE	$129 million	$169 million
Phase 3	3000 tpa LCE	$84 million	$110 million
Total	20900 tpa LCE	$350 million	$460 million
		Production wells	$50 million

Table 6 – Fixed operating costs

Annual maintenance (3% of capex)	$16 million/y
Manpower, other fixed costs	$24 million/y

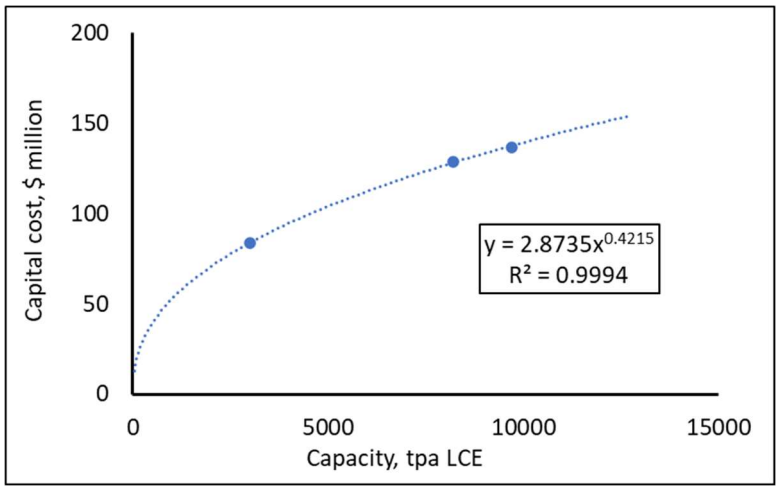

Figure 7 – Capex versus capacity, Standard Lithium project

Table 7 – Assumptions used for cash flow calculations.

Corporate tax rate	20%	Production in year 1	25%
Estimated capital cost	$600 M	Production in year 2	50%
Capital expenditure in year -1	50%	Production in year 3	75%
Capital expenditure in year 0	50%	Production after year 3	100%
Selling price for Li_2CO_3	S30000/t	Selling price for $LiOH•H_2O$	S36000/t

The capital and operating costs calculated for this exercise lead to the cash flow calculations presented next. Figure 8 shows the internal rates of return calculated for the two process routes. While both appear to offer attractive rates of return, the DLE-SX route appears to be stronger than the solar evaporation route.

Figure 9 shows the results of NPV (net present value) calculations for the two circuits, assuming a discount rate (annual cost of capital) of 10% in both cases on the left and 15% for the DLE-SX route on the right. The DLE-SX route appears to be superior at the same cost of capital as the solar evaporation route, but because the DLE-SX route is still unproven it might be prudent to assign it a higher cost of capital to account for the added technical risk compared to the other circuit that is well established. Making the cost of capital 5% higher for the unproven route essentially eliminates its advantage in terms of the NPV.

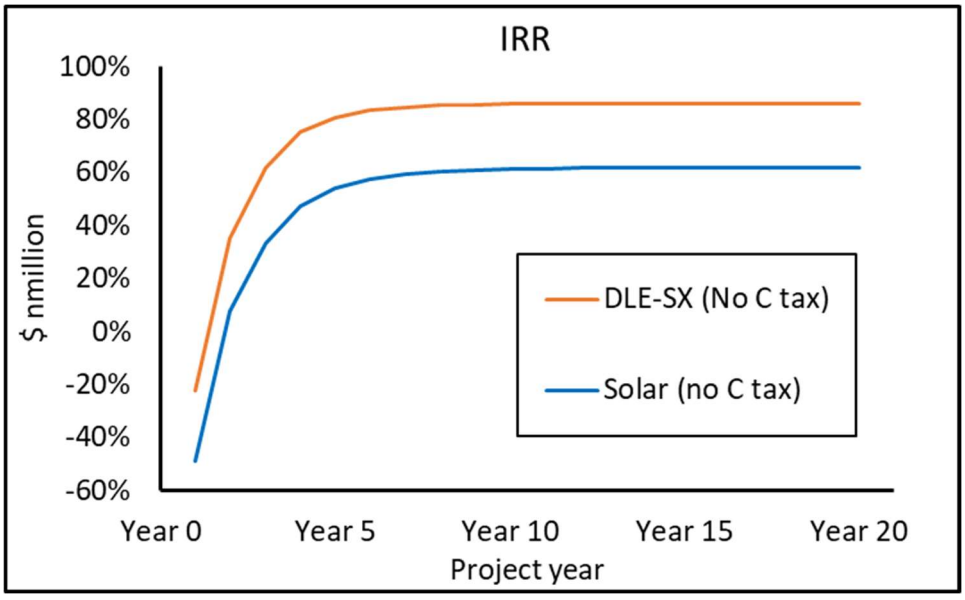

Figure 8 – IRR calculations

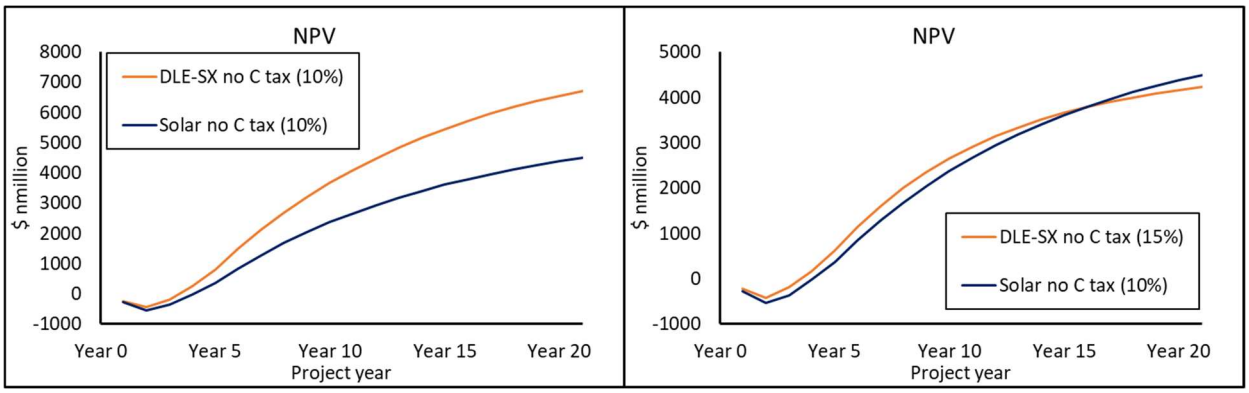

Figure 9 – NPV calculations

LIFE CYCLE IMPACT ASSESSMENT RESULTS

The above cash flow calculations ignore the impact of the LCA results, which are as follows.

Climate Change

Figure 9 shows the climate change impact for producing lithium hydroxide monohydrate via the conventional solar evaporation route. The total climate change impact is calculated to be 14.7 kg CO_2 eq. per kg LCE (lithium carbonate or equivalent).

- Total contribution of energy used in the process is 5.8 kg CO_2 eq. per kg LCE:
  - Steam, raised using of natural gas, contributes 5.7 kg CO_2 eq. per kg LCE.
  - Electricity contributes 0.1 kg CO_2 eq. per kg LCE.
- The use of reagents in the process, which in total contribute 9.1 kg CO_2 eq. per kg $LiOH•H_2O$, of which the contribution is as follows:
  - Lime contributes 4.3 kg Co_2 eq. per kg LCE
  - Hydrochloric acid contributes 1.3 kg CO_2 eq. per kg $LiOH•H_2O$.
  - Sodium hydroxide contributes 0.3 kg CO_2 eq. per kg $LiOH•H_2O$.
  - Sodium carbonate contributes 2.9 kg CO_2 eq. per kg $LiOH•H_2O$.

The relative impact of direct CO_2 emissions from the process to the atmosphere is negligible compared to the embodied impact of steam and reagents used in the process.

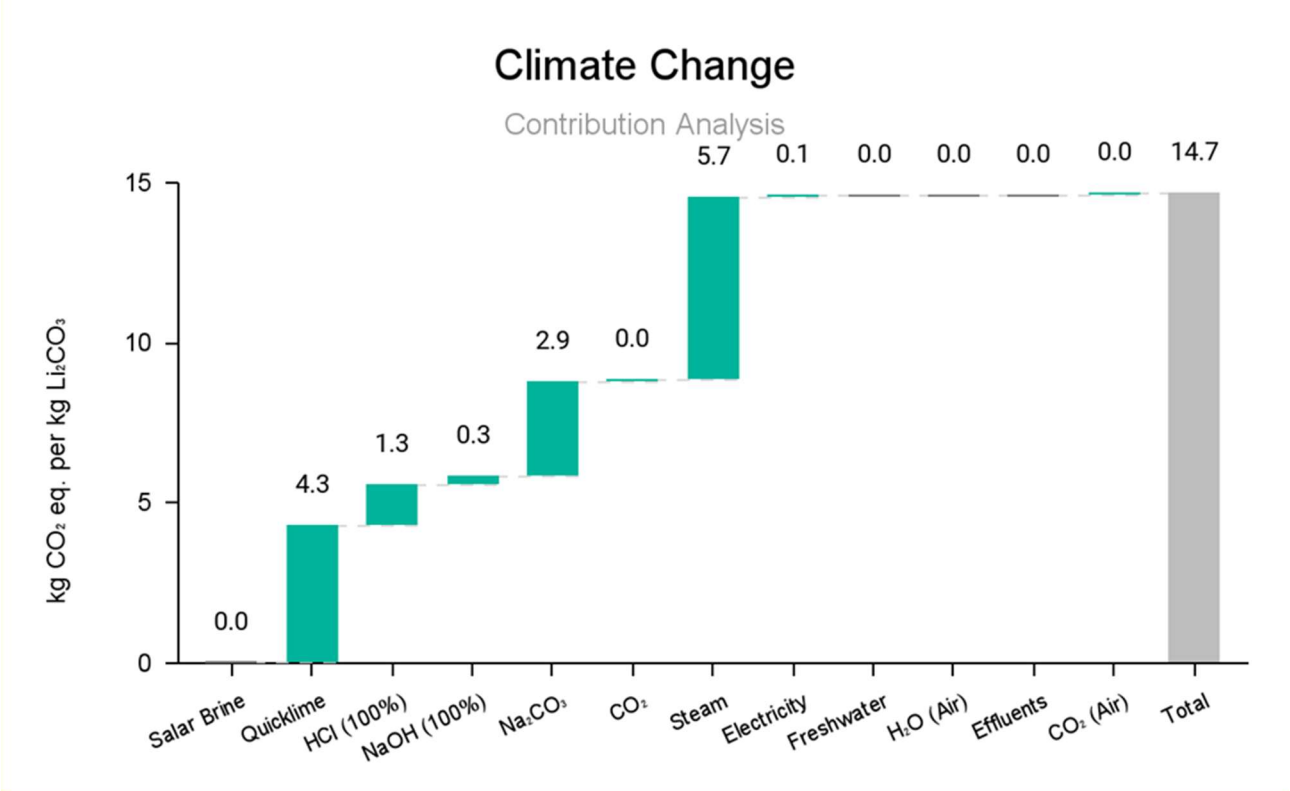

Figure 9 – Climate change contribution for the solar evaporation route

Figure 10 presents the climate change impact for the DLE-SX route. The total climate change impact for this route is 6.1 kg CO_2 eq. per kg LCE. The climate change impact is made up of the following factors:

- More than half of the climate change impact of lithium hydroxide produced via this route comes from the embodied impact of sodium hydroxide used in the process, which contributes 2.9 kg CO_2 eq. per kg LCE.
- Electricity, assumed to be produced on site from natural gas, contributes 1.2 kg CO_2 eq. per kg LCE.
- Hydrochloric acid used for direct lithium extraction contributes 0.9 kg CO_2 eq. per kg LCE.
- Direct hydrogen gas emissions from the production process contributes 0.3 kg CO_2 eq. per kg LCE.

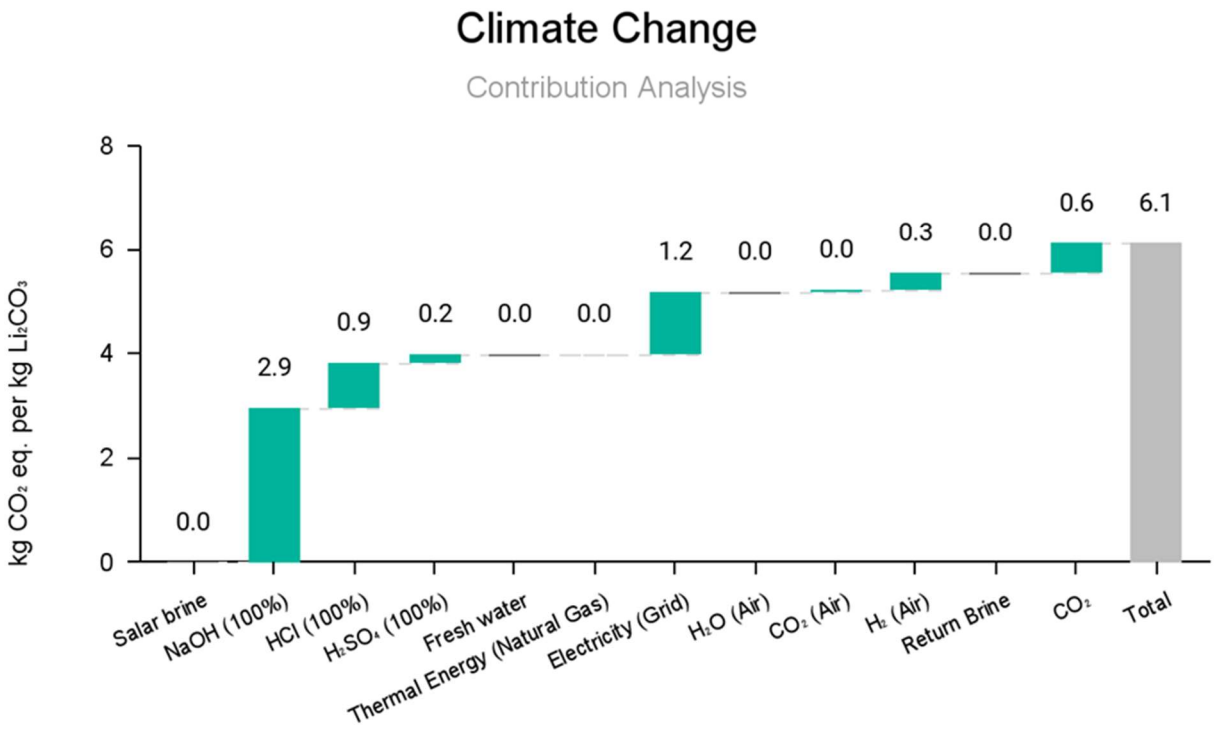

Figure 10 – Climate change contribution for the DLE-SX route

Comparing the results presented in Figure 9 and Figure 10, note that, overall, the DLE-SX route has fewer items contributing to the climate change impact. This could have to do with the lower technology readiness level of the DLE-SX route, in that its requirements for energy and consumables might be increase as the technology evolves further. Conversely, it is plausible that the DLE-SX route is really the better of the two.

A significant difference between the two routes is that in the DLKE-SX route, there being no evaporation of the salar brine, the lithium-depleted brine is returned to the salar. This does not contribute to the climate change impact but could conceivably affect the lithium content of the salar brine over time. The total waste from the DLE-SX route is much lower than the total waste from the solar evaporation route, per unit of lithium product, if the depleted brine returned to the salar is not considered a waste stream.

Figure 11 shows the climate change impact results for the solar evaporation and the DLE-SX routes, classified into scope 1, 2 and upstream scope 3 emissions. Scope 3 emissions make up most of the impact for both routes, which is a good example of why it is essential to use a life cycle assessment approach rather than just greenhouse gas inventory analysis. For the solar evaporation route, the upstream scope 3 emissions make up 67% of the total climate change impact. For the DLE-SX route, the scope 3 emissions account for 72% of the total climate change impact (of a smaller total than for the solar evaporation route). An interesting difference between the two routes is the relative contribution of scope 1 and scope 2 emissions. For the solar evaporation route, scope 1 emissions make up 33% of the climate change impact, whilst scope 1 emissions make up only 7% for the DLE-SX route. For the DLE-SX route, scope 2 emissions account for 21% of the total climate change impact, which for the solar evaporation route is less than 1%.

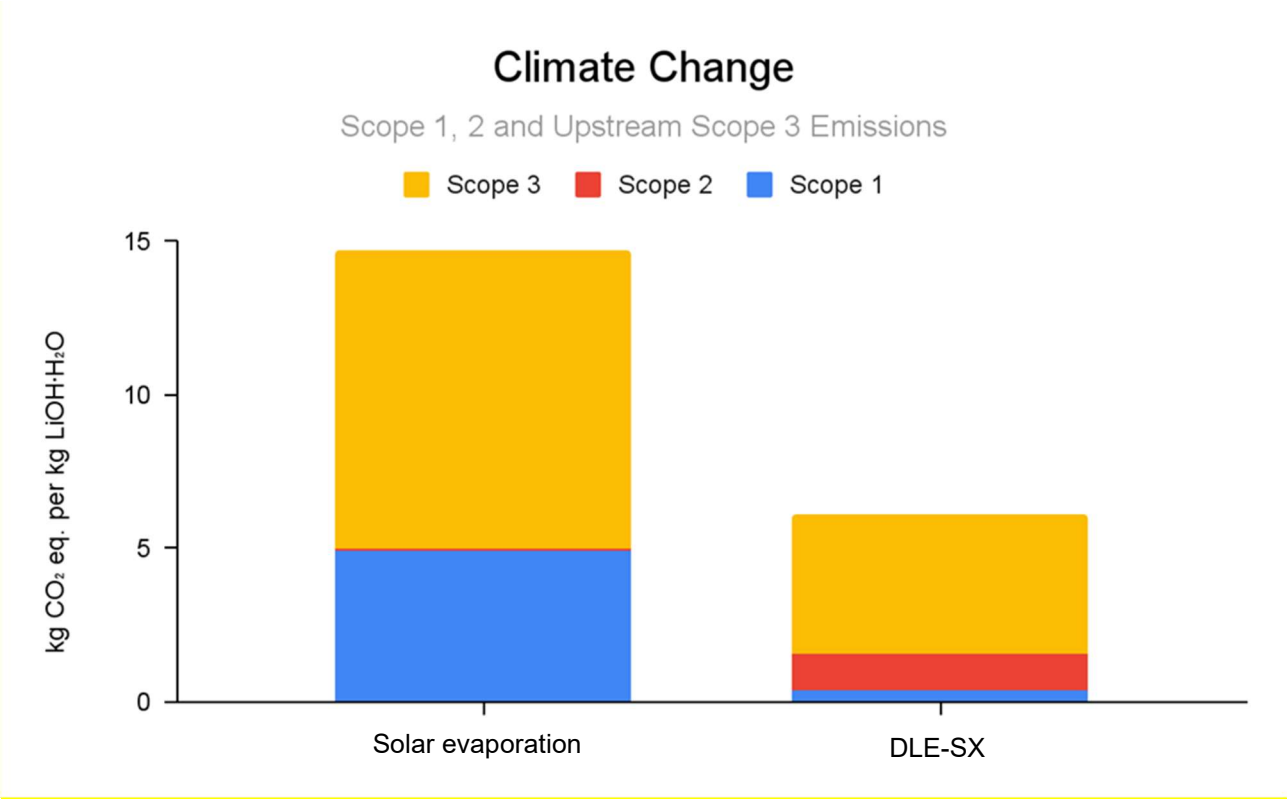

Figure 11 – Climate change impact as scope contributions

Carbon tax

Carbon taxes are a recent development that effectively add to the variable cost of a process, the amount depending on the carbon footprint of the process concerned. For this exercise, the assumption used is that the carbon tax will take the form of an amount at present, increasing annually into the future. The Canadian numbers[16] for this are $50 in 2022, escalating by $15/year from 2023 to 2030.

Figure 12 shows the impact of carbon tax on the IRR and NPV calculations as before. The symbols are the curves with the carbon tax and the lines are the NPV or IRR without the carbon tax. At the preliminary level of this exercise, the carbon tax makes no appreciable difference to the IRR for either process, while the NPV calculation indicates that the carbon tax does affect the economics of the conventional route to a small extent. This agrees qualitatively with the relative magnitudes of the two carbon footprints shown in Figure 11.

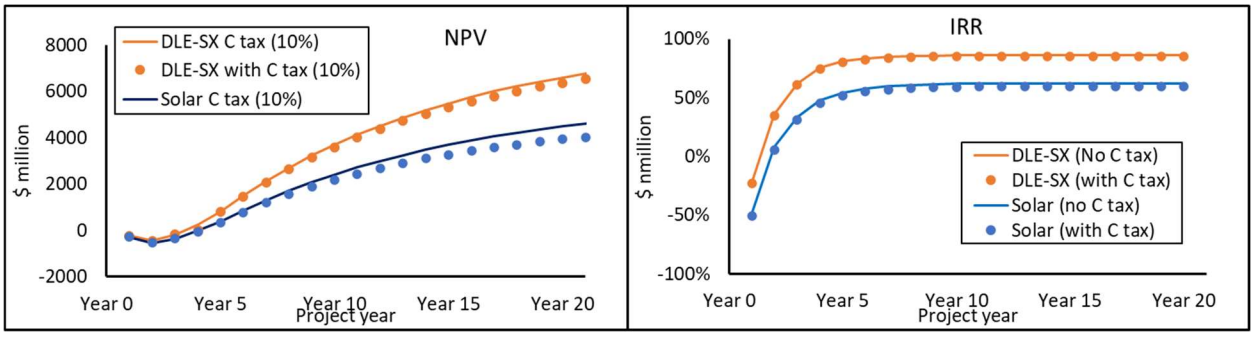

Figure 12 – Effect of C tax on IRR and NPV

Water Use

Figure 13 presents the water use calculated for lithium hydroxide monohydrate via the solar evaporation route, totalling at 24.0 m^3 world eq. per kg LCE. This total water use calculation accounts for direct use of fresh water on site, and embodied water impacts of consumables used. Water evaporated from the brine is considered as water used, as per the AWARE methodology which states that evaporated water is considered used. It is the direct H_2O emissions evaporated to air that account for most of the water impact: 20.3 m^3 world eq. per kg LCE. This value is relatively high due to the high water-scarcity footprint, which amplifies this value by a factor of 40. The relative water use impact of reagents such as hydrochloric acid and sodium carbonate is higher than the relative water use contribution from fresh water. By far the bulk of the water use, however, is evaporation from the solar ponds.

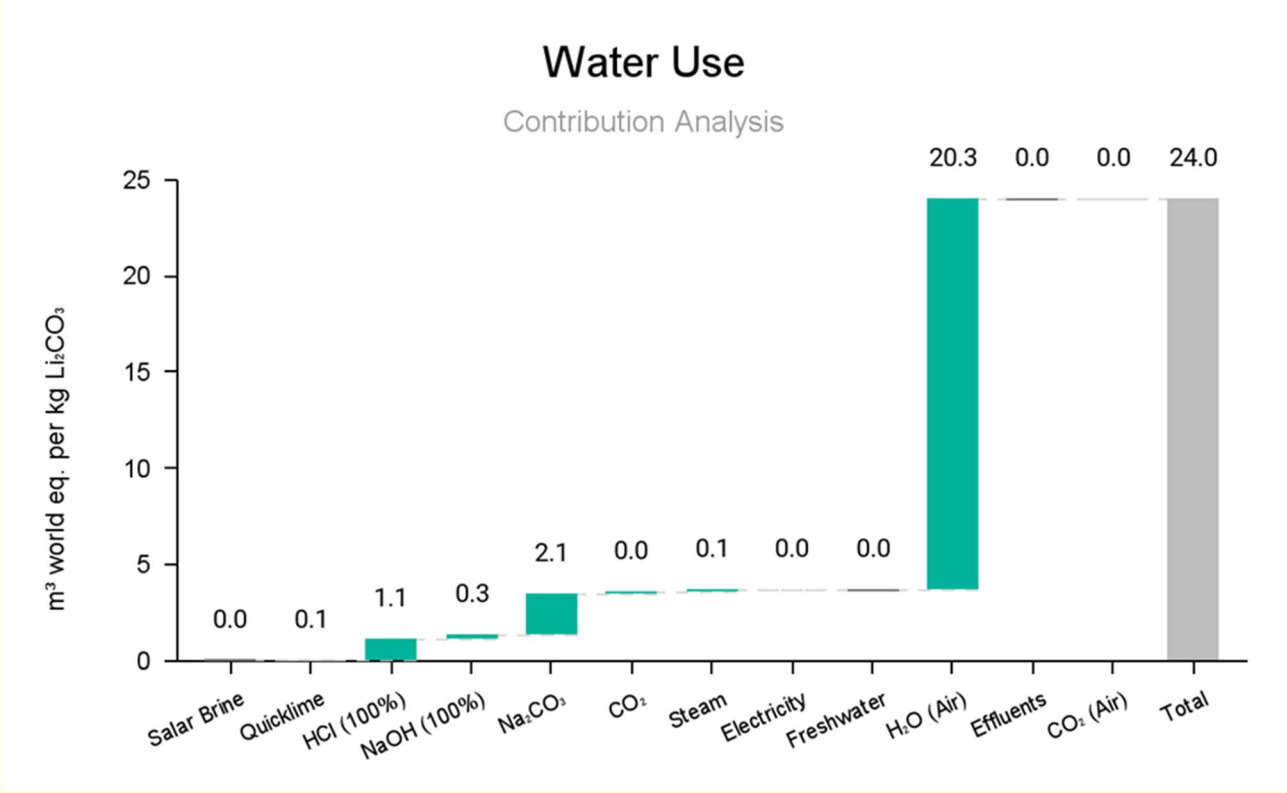

Figure 13 – Water use contribution for the solar evaporation route

Figure 11 presents the water use for the DLE-SX route. The water use for this route is one quarter of the value calculated for the solar evaporation route: 7.7 m^3 world eq. per kg LCE. Direct water emissions to air are much lower for this route, which can be attributed to the fact that the depleted brine brine returns to the aquifer and, in the AWARE methodology, is not considered used. The largest contributor to the water use impact is sodium hydroxide, which contributes 3.1 m^3 world eq. per kg LCE. That value is identical to the total freshwater input and direct water emissions that contribute to the water use impact via this route.

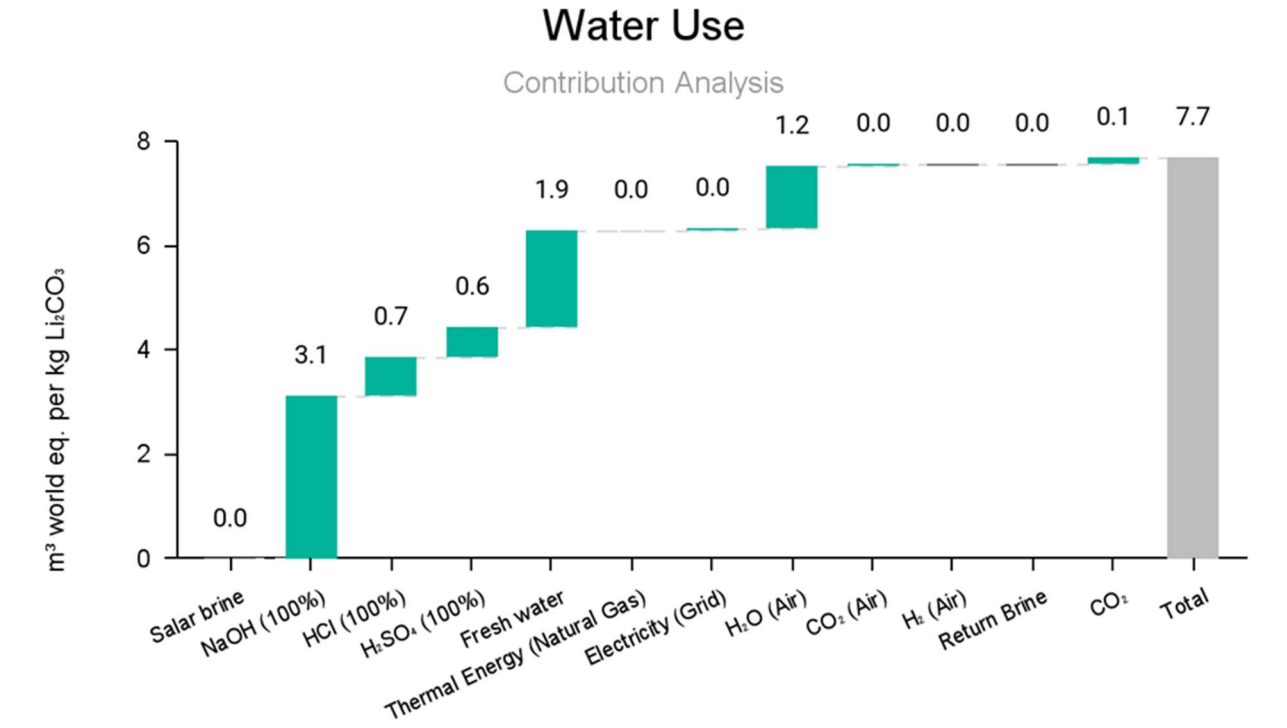

Figure 11 – Water use contribution for the DLE-SX route

Bringing the water footprint into the relevant business (cash flow) calculations is not currently possible in the same way as carbon tax brings the CO_2 footprint into these calculations. This is quite probably an aspect of

LCA that could be handled like CO_2, which would require consensus between the various stakeholders that may or may not be achievable – practioners of LCA might do well to add this to their efforts.

CONCLUSIONS

This paper explores the pairing of life cycle assessment and techno-economic evaluation to quantify and investigate the relationship between mineral resource project economics and environmental impacts when considering the production of lithium from a salar brine.

The techno-economic analysis indicates that direct extraction plus selective solvent extraction of lithium from the brine is potentially superior to the established route of solar evaporation, etc. However, adding a 5% risk premium to the cost of capital to allow for the technical risk associated with the novel process eliminates its apparent economic advantage. The 5% risk premium is a pure guess, meant to show the impact of such an assumption. What suc a risk premium should actually be is beyond the scope of this paper.

Depending on the production pathways, the climate change impact can range between 5.5 and 19.3 kg CO_2 eq. per kg $LiOH•H_2O$. The water use impact of the routes shown to range between 7.6 and 26.0 m^3 world eq. per kg $LiOH•H_2O$. Both for the climate change and water use impacts, the direct lithium extraction and electrolysis had the lowest impact and the solar evaporation route the highest.

At the levels used in this study, the carbon tax has a negligible impact on the economics of both process routes. That could mean that neither emits enough CO_2 to matter particularly, or, more probably, that the carbon tax levels are too low to appreciably influence the choice between these two process routes.

It is important to note that LCA results from any one project are not transferrable to other projects. Site specific factors play a major role.

The study shows the value of integrating life cycle assessment metrics into the early development phase. This enables environmentally informed decisions, that mitigate environmental impacts while the process flexibility is high.

REFERENCES

1. World Bank Group. Introducing Climate-Smart Mining. http://www.sonami.cl/v2/wp-content/uploads/2019/04/4.-Daniele-la-Porta.pdf (accessed 2020-11-07)
2. Dry, M. and Tijsseling, L. Process Modelling Based Prospective Life Cycle Assessment: A Case Study on Primary Lithium Production. Alta 2022 Conference, Perth, Australia, may 2022.
3. Pell, R., Tijsseling, L., Goodenough, K., Wall, F., Dehaine, Q., Grant, A., ... & Whattoff, P. (2021). Towards sustainable extraction of technology materials through integrated approaches. Nature Reviews Earth & Environment, 2(10), 665-679
4. Pell, R., Wall, F., Yan, X., Li, J., & Zeng, X. (2019). Mineral processing simulation based-environmental life cycle assessment for rare earth project development: A case study on the Songwe Hill project. Journal of environmental management, 249, 109353.
5. Dry, M. J. Early evaluation of metal extraction projects. Alta 2013, Perth, May 2013.
6. Horne, R. E., Grant, T. & Verghese, K. Life Cycle Assessment: Principles, Practice and Prospects. (Csiro Publishing, 2009).
7. International Organization for Standardization. ISO14040: 2006 Environmental Management. Life Cycle Assessment. Principles and Framework. 2006
8. International Organization for Standardization. ISO14040: 2006 Environmental Management. Life Cycle Assessment. Requirements and Guidelines. 2006
9. Boulay, A. M., Bare, J., Benini, L., Berger, M., Lathuillière, M. J., Manzardo, A., ... & Pfister, S. (2018). The WULCA consensus characterization model for water scarcity footprints: assessing impacts of water consumption based on available water remaining (AWARE). The International Journal of Life Cycle Assessment, 23(2), 368-378.
10. Dry, M. J. Extraction of Lithium from Brine – Old and New Chemistry. Critical Materials Symposium, EXTRACTION 2018, Ottawa, August 2018.
11. Dry, M. J. Lithium-ion sieve technology for recovery of lithium from brine. Alta 2020, Perth, Australia, November 2020.
12. https://www.standardlithium.com/projects/arkansas-smackover
13. Dry, M. J. Lithium from clay versus lithium from spodumene. Alta 2019, Perth, Australia, May 2019.
14. Lithium Americas, NI 43-101 Technical Report. Updated Feasibility Study and Mineral Reserve Estimation to Support 40 000 tpa Lithium Carbonate Production at the Cauchari-Olaroz Salars, Jujuy Province, Argentina. Date: October 19, 2020.
15. Standard Lithium Ltd., NI 43-101 Technical Report. Preliminary Economic Assessment of LANXESS Smackover Project. Date: August 1, 2019.
16. Government of Canada. https://www.canada.ca/en/environment-climate-change/services/climate-change/pricing-pollution-how-it-will-work/carbon-pollution-pricing-federal-benchmark-information.html

SIMULATING MASS AND CHEMSITRY BALANCE IN A DIRECT LITHIUM EXTRACTION PROCESS

By

Leslie Miller, and AJ Gerbino
OLI Systems, Inc. USA

Corresponding Author
A.J. Gerbino
Aj.gerbino@olisystems.com

Presenter
Leslie Miller
leslie.miller@olisystems.com

ABSTRACT

We use rigorous electrolyte thermodynamics, direct lithium extraction (DLE) media database with reaction kinetics, and a steady state process simulator to predict the mass, energy, and chemistry balance in lithium extraction from geological fluids. The electrolyte thermodynamic model is used to predict the brine properties at each step in the process. The DLE media database and reaction kinetics are used to predict lithium uptake by the adsorbent materials. A process simulator is used to predict the mass, energy, and chemistry balance in the overall process.

The electrolyte model contains the thermochemical data of key elements like Li, Na, K, Ca, Sr, Fe, Cl, CO3, SO4, H, OH, and B. It is used to calculate pH, density, buffer capacity, vapor pressure, activity coefficients, solids saturation, precipitation formation, and chemical demand. The electrolyte model is needed to predict the equilibrium state of the brines as it flows in and out of each process unit in the extraction and regeneration process. It is the most critical of the three tools.

We created a DLE media database with two approaches, empirical and rigorous, using experimental data from media providers to quantify lithium (and other ion) uptake as a function of contact time, pH, temperature, and brine chemistry. We back-calculate the media's formula using the moles of exchangeable sites available per gram of media. We also created a rate expression and a set of rate coefficients to calculate ion uptake as a function of temperature, pH and time. We have not developed media degradation parameters that could be used to optimize plant costs.

We used a steady-state process simulator with the electrolyte model and DLE media database to predict lithium extraction efficiency, contaminant ion uptake, solids deposition, chemical requirements, and LiCl extractant composition. We developed a full-plant simulation for several extraction plant designs, the essential parts of the plant are presented in this paper. Although we cannot present actual plant information due to the proprietary nature of the operations, we present a hypothetical plant design of a geological fluid and describe the sections of the extraction plant that are and are not simulated accurately at this time. The limitations we describe are mostly mass-transport-based, such as solids settling rates, media fouling, incomplete mixing, and membrane and ion exchange performance.

In summary, we have used the above three capabilities to design, with a relative accuracy, geological fluid extraction processes. This includes simulating critical unit operations like ion extraction and media regeneration, separation processes like ion exchange and membranes, predicting the formation of unwanted solids, and predicting the chemical and water demand under different process conditions.

Keywords: Direct Lithium Extraction, Lithium, process simulation

INTRODUCTION

Geologic fluids produced in geothermal and oil/gas production contain lithium at low concentrations compared to conventional sources of lithium like salars and ore. These low concentrations make the use of conventional extraction techniques such as evaporation or membrane technologies impractical. Many entrepreneurial startups and established mining companies have developed materials that selectively extract lithium directly from the brine, without taking up the other solutes (e.g., Na, Cl, Ca, Mg. etc.). The material, generally termed DLE media, is comprised of a porous magnesium oxide (MgOx) or titanium oxide (TiOx) matrix containing

positive-charge deficiencies. These materials are manufactured in ways that allow Li^+ and H^+ to diffuse and attach to sites in the media, but larger ions like Na^+, K^+, Ca^{+2}, to largely remain in the bulk fluid.

In DLE, lithium-containing brine contacts the protonated form of the media, allowing the ion-exchange reaction between Li^+ and H^+ to occur, the media is then separated from the brine and washed with acid to reverse the exchange, extracting lithium from the media. The resulting solution is an acid-containing pregnant liquor with lithium concentrations in the several thousands of mg/l.

With these new DLE processes, there is a strong demand to develop mass, chemistry, and energy balances around these techniques enabling designs of pilot and full-scale extraction plants. The challenge is that no predictive software tool exists to simulate the extraction process in any mechanistic way. This is in part because the extraction media vary by manufacturer, and therefore uptake rates, adsorption capacity, ion selectivity, and degradation rates vary.

OLI addresses these limitations by developing a semi-empirical thermodynamic and kinetic database that simulates direct lithium extraction and the larger process design. We use one of two approaches to simulate ion uptake, a kinetic-based uptake reaction (empirical) and an ion-exchange reaction with fixed selectivity coefficients (rigorous). We present our development of the kinetic database, and test it using the electrolyte model coupled with a process simulator to analyze a complete DLE plant.

APPROACH TO MODELING CATION ADSORPTION IN DLE MEDIA

We developed a private database containing two types of extraction mechanisms. The first uses a rate-based expression where adsorption is defined using a set of kinetic reactions (empirical). The equation below is the expression for Lithium uptake and release. Similar rate expressions are used for Na^+, K^+, Ca^{+2}, and Mg^{+2}. This approach does not use an equilibrium constant, although one can be back-calculated. We fixed the enthalpy of formation for each adsorption species so that there is negligible temperature change when the reaction proceeds.

$$HMedia + LiCl \leftrightarrow LiMedia + HCl$$

$$Rate\left(\frac{dLi^+}{dt}\right) = \left(\left[A_f * e^{B_f/T(K)} * (HIX^a * Li^b * H2O^c)\right] - \left[A_r * e^{B_r/T(K)} * (H3O^d * LiIX^e)\right]\right) * V_{liq}$$

The strength of the empirical approach is that adsorption and desorption extent is fit to measured data. The rate expression can be expressed to include the temperature, pH, and composition effects.

The second approach uses an equilibrium ion exchange reaction (rigorous). The papers we reviewed define the media as having two exchange sites per mole of central metal, e.g., H_2TiO_3. We evaluated four possible exchange reactions, an exchange of one mole M^{+1} per mole of media or an exchange of 0.5 mole M^{+2} per mole of media.

$$H_2Media + (Na, K, Li)^{+1} \overset{Q_{S1}}{\leftrightarrow} (Na, K, Li)HMedia + H^+$$

$$H_2Media + 2(Na, K, Li)^{+1} \overset{Q_{S2}}{\leftrightarrow} (Na, K, Li)_2Media + 2H^+$$

$$H_2Media + 0.5(Mg, Ca)^{+2} \overset{Q_{S3}}{\leftrightarrow} (Mg, Ca)_{0.5}HMedia + H^+$$

$$H_2Media + (Mg, Ca)^{+2} \overset{Q_{S4}}{\leftrightarrow} (Mg, Ca)Media + 2H^+$$

The strength of the rigorous approach is that it uses standard equilibrium reactions, a selectivity coefficient, and non-ideal interactions for each adsorbing ion. Thus, it incorporates temperature, concentration, and pH effects automatically.

Both approaches include adsorption with all ions if they are developed: H^+, Li^+, Na^+, K^+, Mg^{+2}, Ca^{+2}, Sr^{+2}, Ba^{+2}, Fe^{+2}, and Al^{+2}. The media molecular weight is defined by its molar exchange capacity (grams of media per mole of Li^+ adsorbed). The media enthalpy (for heats of reaction) is referenced to Na2TiO3. These values are not precise but are satisfactory for first-pass development. The enthalpy of reactions for H_2TiO_3 and Li_2TiO_3 species was adjusted to match adsorption vs. temperature data.

RESULTS – FITTING ADSORPTION AND DESORPTION DATA USING EMPIRICAL APPROACH

We used adsorption vs. time data from a private communication to define the reaction rate expression[i]. We set the media's formula weight to a value that would produce a lithium exchange capacity of 5 meq Li/g media (35 mg/g) and used the measured data to parameterize the kinetic coefficients. This data included concentration vs. time as temperature and pH varied. Then, using the brine composition, the experimental pH (5 and 8), temperature (20, 40, and 60C), and the concentration vs time plots to define the kinetic coefficients. Figure 1 is a curve fitting plot of adsorption rates on a proprietary DLE media.

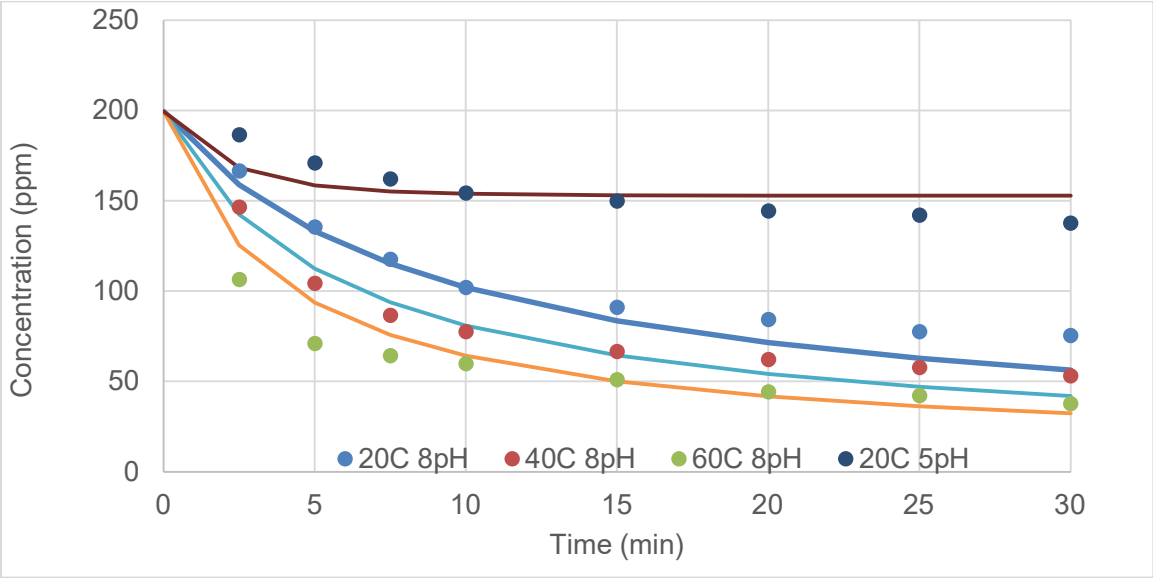

Figure 1 - Curve fitting of adsorption data vs time and temperature

We obtained good agreement with the measurements at pH 8, and limited alignment with data at pH 5. The best fit plots produced the following values. The reactants and products are measured in activities and the volume is in m^3.

$$Rate = \left(\left[3.4x10^{13} * e^{2112/T(K)} * (HIX^{1} * Li^{0.6} * H2O^{0})\right] - \left[2.8x10^{13} * e^{-97/T(K)} * (H3O^{1.19} * LiIX^{1.17})\right]\right) * V_{liq}$$

There were no uptake rates for Na^{+}, K^{+}, Mg^{+2}, and Ca^{+2}, so we used the lithium uptake rates for the other cations, and limited the extent to which these other ions adsorb to 1.5 mg/g (for Na and K) and 3 mg/g (for Mg and Ca).

RESULTS – FITTING MEASURED ADSORPTION AND DESORPTION DATA USING RIGOROUS APPROACH

Wang et al[ii] studied adsorption of metals from a heavy brine on their H_2TiO_3 media. Ion concentration for Ca^{+2}, Mg^{+2}, Na^{+}, K^{+}, and Li^{+} in the brine, was reported as 55, 58, 1.6, 0.5, and 1.56 g/l, respectively. They reported maximum adsorption capacities for these metals on their material at pH 8.8 and 25 C, this data is presented in Table 1.

Table 1 - Estimation of the equivalent weight of the media based on the different cation adsorption capacity.

Cation	Reported adsorption capacity in mg/g	Reported adsorption capacity meq /g	% of sites accessible to cation	TiO3 eq wt g/eq
H^{+} (stoichiometric)	20.43	20.43	100	**48.94**
Li^{+} (all sites)	36.3	5.24	25.6	
Li^{+} (site 1)		5.14	25.1	**194.6**
Li^{+} (site 2)		0.10	0.50	
Na^{+} (site 2)	1.93	0.08	0.40	
K^{+} (site 2)	1.99	0.05	0.25	
Mg^{+2} (site 2)	2.58	0.21	1.0	
Ca^{+2} (site 2)	3.53	0.18	0.86	

Li^+, Na^+, K^+, Mg^{+2}, Ca^{+2} (site 2)		**0.62**	**2.51**	**1604**

We created two sets of adsorption reactions to accommodate the two reported adsorption sites (site 1 and site 2) for Li^+, H^+, Na^+, K^+, Mg^{+2}, and Ca^{+2}. The first reaction (site 1) adsorbs Li^+ and H^+. It has a capacity of 5.14 meq/g and a formula weight of 194.6 g/mol. The second reaction (site 2) adsorbs all cations and has a capacity of 0.62 meq/g and formula weight of 1604 g/mol. The chemical reactions created were:

$$HMedia(1) + Li^{+1} \overset{Q_s}{\leftrightarrow} LiMedia(1) + H^+$$

$$HMedia(2) + (Li^{+1}, K^{+1}, Na^{+1}) \overset{Q_s}{\leftrightarrow} (Li, K, Na)Media(2) + H^+$$

$$HMedia(2) + 0.5(Ca^{+2}, Mg^{+2}) \overset{Q_s}{\leftrightarrow} (Ca, Mg)_{0.5}Media(2) + H^+$$

We then fit the experimental data (symbols) using selectivity coefficients. The results are shown in Figure 2. There is good fit for lithium (left plot) and reasonable fit above pH 7 for the other metals (right plot). The right plot fits can be improved by modifying the surface interaction parameters.

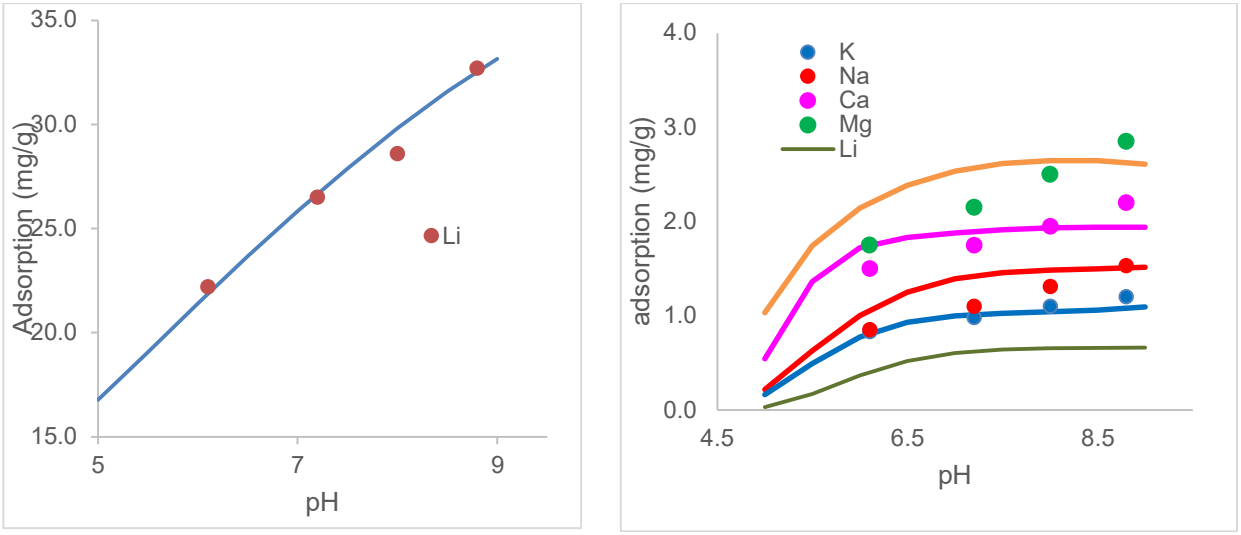

Figure 2 - Curve fitting Li, K, Na, Mg, and Ca adsorption on an HTiO3 media from a high concentration chloride brine

The computed selectivity coefficients (Q_s) for each metal were (log scale) -6.6, -4.4, -5.2, -6.8, and -6.8 for Li^+, Na^+, K^+, Mg^{+2}, and Ca^{+2}, respectively (before adjustment by activity coefficients). These values are based on the adsorption maximum values and the brine compositions reported by the authors. These selectivity coefficients are specific to the brine and the media. More intrinsic selectivity coefficients can be produced if the media is tested in simpler salt-water solutions like, NaCl-H_2O, KCl-H2O, $MgCl_2$-H_2O, and $CaCl_2$-H_2O.

We used the same parameters to simulate the adsorption data from Zhang et al[iii]. They produced a pure H_2TiO_3 and polyvinyl benzene treated H_2TiO_3, and studied lithium adsorption on that media. Figure 3 is a plot of the adsorption isotherm for the two materials. There is good agreement between the measurements and predictions for the pure H_2TiO_3 material but initially, poor agreement for the PVB-treated media. To compensate for this, we created a separate media, PVB-TiO_3. We calculated an equivalent weight for pure H_2TiO_3 media at 208 g/eq and for the PVB-TiO_3 media at 230 g/eq. The computed selectivity coefficients for the PVB-TiO_3 were (log scale) -6.8, -7.7, -6.9, -9.3, and -9.3 for Li^+, Na^+, K^+, Mg^{+2}, and Ca^{+2}, respectively (before adjustment by activity coefficients). Each of the metals are 1.1 log-unit lower than values shown above.

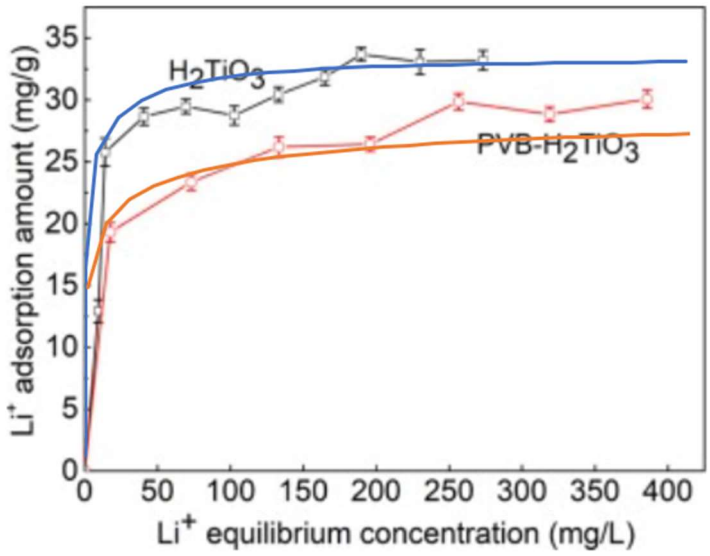

Figure 3 - Matching equilibrium sorption curve and capacity for a H_2TiO_3 and PVB-H_2TiO_3

Figure 4 is a plot of the calculated and measured adsorption vs. pH for the same materials. The model predicts lithium uptake quite well for the H_2TiO_3 media but not for the PVB-H_2TiO_3 media. It will be necessary to use different selectivity coefficients and equivalent weights for the commercial material as compared to the pure material.

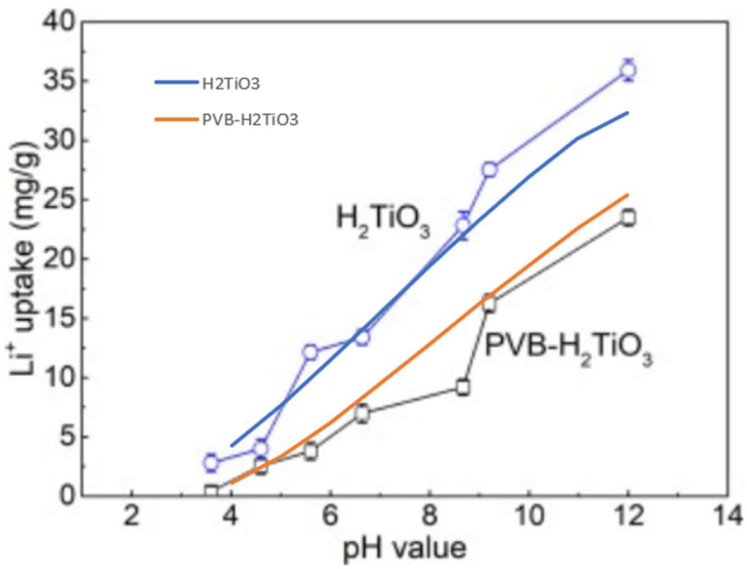

Figure 4 - Comparing simulated and reported uptake vs pH curves using parameters regressed for the equilibrium sorption curve

APPROACH TO SIMULATING THE DIRECT LITHIUM EXTRACTION PROCESS

Figure 5 is an image of the flow diagram used to simulate direct lithium extraction process with DLE media. The units represent a single contactor vessel undergoing four extraction process steps: lithium adsorption, brine rinsing, media regeneration with HCl, and a final rinse.

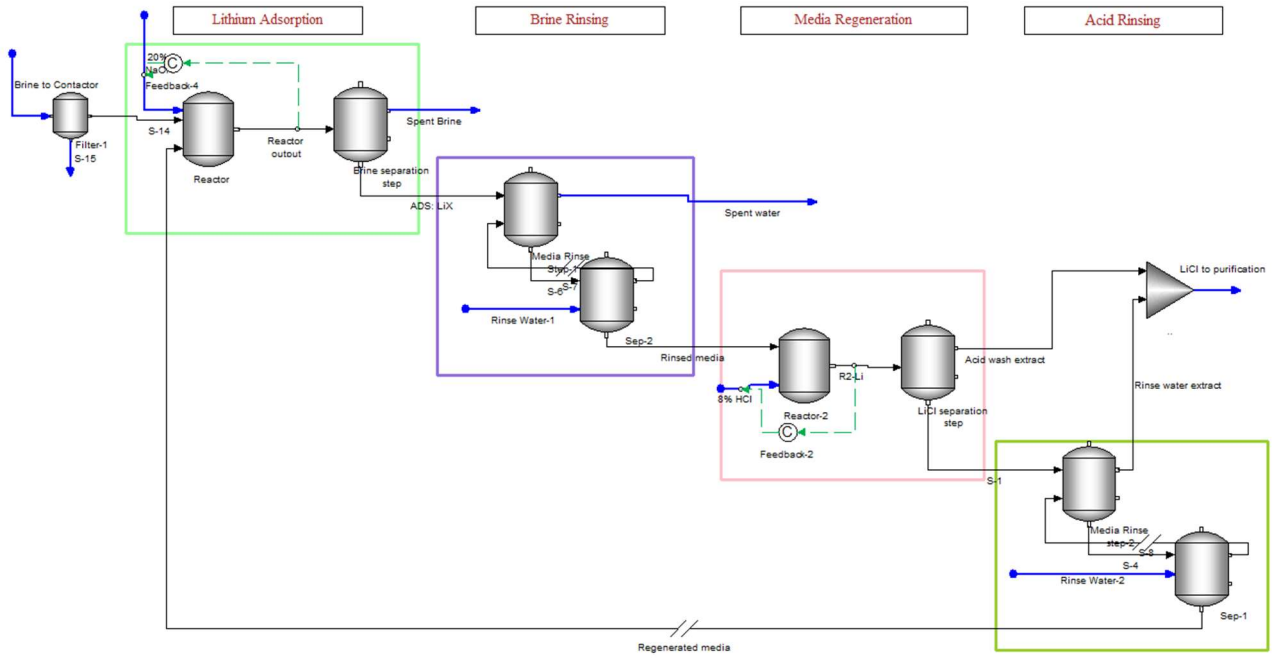

Figure 5 - Simulation flow diagram for testing the two DLE reaction approaches.

We simulated the lithium extraction process at 25 C and 1 atm using the above flow diagram with both the empirical and rigorous reaction methods. The following parameters were used for the modelling:

- Media mass / capacity reported in Table 1
- A generic Salton Sea brine composition (see below)
- Brine feed rate of 10 kg/min
- Lithium adsorption at pH 8 and controlled using 20% NaOH
- Lithium removal at pH 0.5 or 1 and controlled using 8% HCl
- Pure water at 5.5 g water/g media was used for rinsing brine off media
- Pure water at 2.5 g water/g media was used for rinsing acid off media to recover Li^+
- 10 wt% entrained liquid on the media at the start of each process step
- Filtered inorganic solids from the brine upstream of the extraction process

We then varied the following parameters:

- Brine to media mass ratio between 6 mg Li/g media (excess media) and 40 mg Li/g media (insufficient media). We expected to see a higher concentration of unwanted salts, Na, K, Mg, and Ca in the final extractant when using media in excess of lithium.

- Contact time for the adsorption and regeneration between 15 and 60 minutes (same value for each step). This is done for the empirical (kinetic) reactions only to study the impact on lithium uptake and on the final composition of the Li in the purification stream.

Figure 6 provides a visualization of the Na and Cl concentrations in the entrained liquid after each step. The jump in concentration following the regeneration is the Na release from the media and from the HCl added to release the lithium.

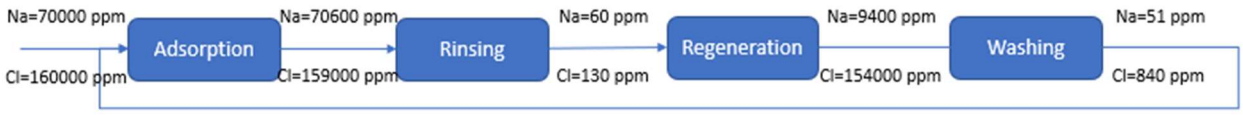

Figure 6 - impact of 10% entrainment on the sodium and chloride concentration in contact with the media through the four extraction steps

We used a generic Salton Sea brine in our simulation work. This brine has roughly half the ionic strength of the Wang et al brine, Table 2. The far-right column is the activity coefficient ratio between the generic Salton

Sea water and the Wang et al brine. It is based on the following equation, where Q' is the activity coefficient ratio. The equation is written reactants over products and the media phase is assumed to have unit activity:

$$Q' = \frac{\gamma_{M^{+z}}^{1/z} * \gamma_{H_2O}}{\gamma_{H_3O^+}}; \qquad ratio = \frac{Q'_{Salton\ Sea}}{Q'_{Wang\ et\ al\ brine}}$$

A ratio >1 indicates that metal adsorption from generic Salton Sea water is enhanced relative to the Wang et al brine. Lithium adsorption affinity is computed to be suppressed by 12% while Na^+, K^+, Mg^{+2}, and Ca^{+2} adsorption is computed to be enhanced, with K^+ adsorption enhanced by 7.2x. Uptake differences are further affected by the absolute metal concentrations in solution. Potassium concentrations for example are 17.6x greater in the generic Salton Sea brine. The effect of these differences is that the metal adsorption efficiency between the two brines will differ.

Table 2 - Comparison of the brines used to create the selectivity coefficients and to simulate lithium extraction.

	Brine composition (ppm)		Equivalent conc (eq/kg H_2O)		Activity coefficients (kg/mol)		Activity coefficient ratio
Ion	Wang et al	Generic Salton Sea	Wang et al	Generic Salton Sea	Wang et al	Generic Salton Sea	
H_2O	1000000	1000000	55.5	55.5	0.52	0.76	
H_3O^+	$3.0e^{-8}$	$1.9e^{-7}$	$1.6e^{-9}$	$1e^{-8}$	13.7	4.2	
Li^{+1}	1769	200	0.25	0.039	12.4	2.3	0.88
Na^{+1}	1814	70000	0.08	4.1	3	1.1	1.8
K^{+1}	567	10000	0.014	0.35	0.4	0.6	7.2
Mg^{+2}	67641	2000	5.6	0.22	28.6	1.5	1.3
Ca^{+2}	62583	20000	3.1	1.34	12	0.9	1.2
Sr^{+2}		650					
Ba^{+2}		100					
Fe^{+2}		20					
Cl^{-1}	319720	160000					
HCO_3^{-1}		15					
SO_4^{-2}		50					
BOH_3		1500					
SiO_2		10					
CO_2		50					
IS (m)	13.6	6.9					

RESULTS – SIMULATING EXTRACTION PROCESS USING EMPIRICAL REACTIONS

Table 3 contains the results for the empirical exchange simulation. The contact time is set to 30 minutes, the lithium to media mass ratio in the contactor is set to 20 mg/g. The adsorption step is set to pH 8, and the regeneration step is set to pH 0.5. The spent brine column contains the calculated lithium concentration of 71 mg/l. This represents 65% lithium capture. The simulated lithium concentration exiting to the purification process is 4872 mg/l and pH 1.9. Both values are after mixing the HCl extraction step with the pure water media washing step. The regenerated media is calculated to *still* contain lithium after the acid extraction. The final column shows that the regenerated media still contains 18.5 mg/g of lithium (50% of the available sites). This indicates that the HCl did not extract all the lithium. We suspect our kinetics may not be valid at very low pH's because there was no data to regress in this region.

Table 3 - Base case simulation using pH 8 in spent brine and pH 0.5 in LiCl to purification.

Species conc. (mg/l)	Feed Brine	Spent Brine	LiCl to purification	Regenerated media (mg/g)
Li^{+1}	200	73	4872	18.5
Na^{+1}	70000	70545	1250	<0.01
K^{+1}	10000	9943	230	<0.01
Mg^{+2}	2000	1981	124	<0.01
Ca^{+2}	20000	19836	484	<0.01
Ba^{+2}	100	35.5	<0.1	…
Cl^{-1}	159240	158971	26704	…
pH	5.1	8.0	2.0 (after rinsing)	…

Figure 7 is a plot of the lithium extraction efficiency as contact time and Li:Media loading vary. A minimum of 20 mg/g loading is required to achieve 75% removal efficiency. At this loading ratio, the contact time would be greater than 30 minutes. At 10 mg Li/g media loading, nearly 100% of the lithium is removed from the brine. This is not surprising, since at this loading only one in three of the available adsorption sites can be filled. This creates problems because the other ions are in excess and continue to adsorb on the sites that are available to them. The net effect is an enrichment of the impurities adsorbed relative to the lithium.

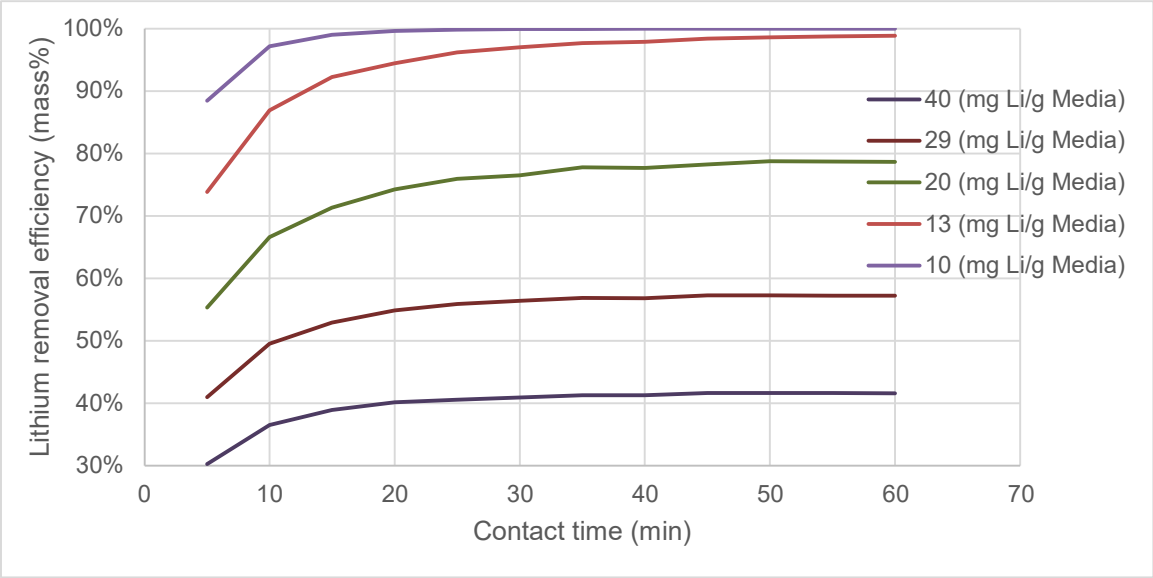

Figure 7 - Lithium extraction efficiency as a function of contact time and Li:Mg loading.

Figure 8 is a plot of the Li^+ concentration in the purification stream vs. contact time and Li:Media loading ratios. The lithium concentration increases with contact time for each of the Li:Media loading ratios except one. At the lowest ratio (10 mg Li/g Media), there is insufficient lithium remaining in the brine to occupy the available sites (above discussion). This has two effects, the first is that more HCl is needed to achieve the 0.5 pH, diluting the metals concentration in the purification stream. The second is that the impurities concentration in the purification stream increases relative to lithium. This is shown in Figure 9 where at low Li:Media loading ratio, there is a higher impurity:Li equivalent ratio in the purification stream. The increase is significant below the 20 mg Li^+/g media loading.

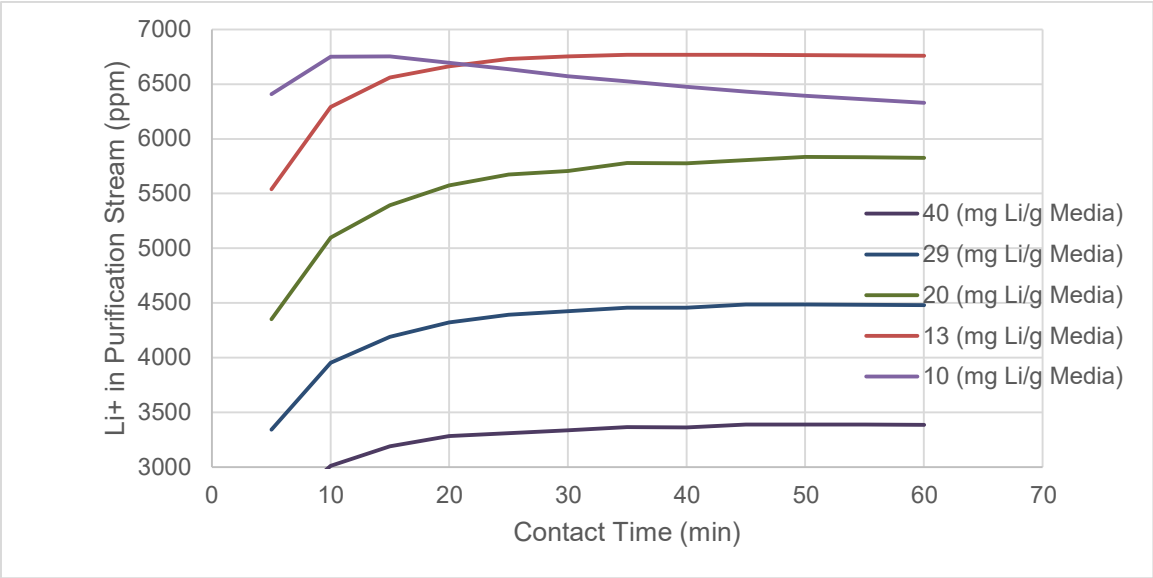

Figure 8 - Lithium concentration in the purification stream as a function of contact time in the extraction step and the Li:Media loading ratio.

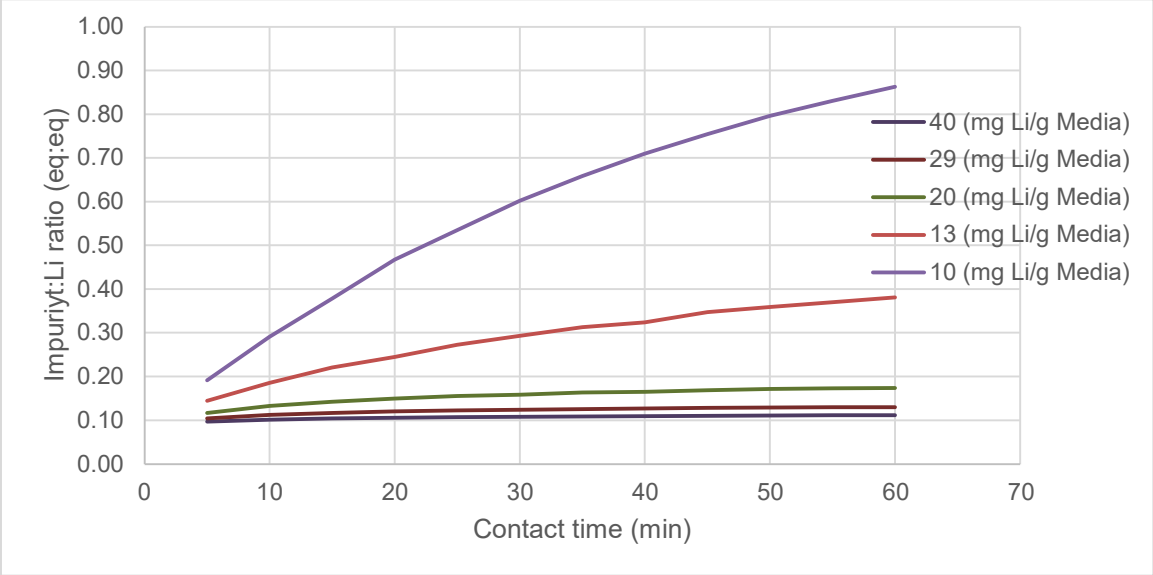

Figure 9 – The Impurity:Li ratio in the Purification stream as a function of contact time and Li:Media loading ratio

RESULTS – SIMULATING EXTRACTION-PROCESS USING RIGOROUS ION EXCHANGE

Table 4 contains the simulation results using the rigorous adsorption approach. The lithium loading is set to 20 mg Li/g media, the contactor pH for lithium extraction is set to pH 8, and the HCl recovery step set to pH 0.5. The software computes 15 ppm Li^{+} remaining in the spent brine, which is approximately 93% recovery. The slightly higher Na^{+} in the spent brine is from NaOH addition, and the lower cation concentration is from adsorption onto 10% of sites available to these ions. This simulation approach differs from the empirical approach in that reactions come to equilibrium.

Table 4 – Base case simulation using a Li/media load of 20 mg/g, a pH 8 for extracting lithium, and a pH 0.5 for removing the lithium.

Species conc. (mg/l)	Feed Brine	Spent Brine	LiCl to purification	Regenerated media (mg/g)
Li^{+1}	200	15	5094	1.3
Na^{+1}	70000	70270	2640	
K^{+1}	10000	9914	274	
Mg^{+2}	2000	19001	2409	
Ca^{+2}	20000	19790	13	
Ba^{+2}	100	0	0	
Cl^{-1}	159240	154977	38772	
pH	5.1	7.9	1.4 (after rinsing)	

Figure 10 is a plot of lithium concentration in the extracted purification and spent brine streams as a function of pH when the Li:Media loading is 20 mg/g. The pH where lithium is computed to be at its maximum concentration is 7.5. Above this pH, lithium concentration in the purification stream decreases. This is for three reasons; 1) the lower lithium concentration reduces the extent of the adsorption reaction; 2) the impurities continue to adsorb because they are not in limited concentrations; and 3) more HCl is used to bring the pH to 0.5, which dilutes the lithium in the purification stream.

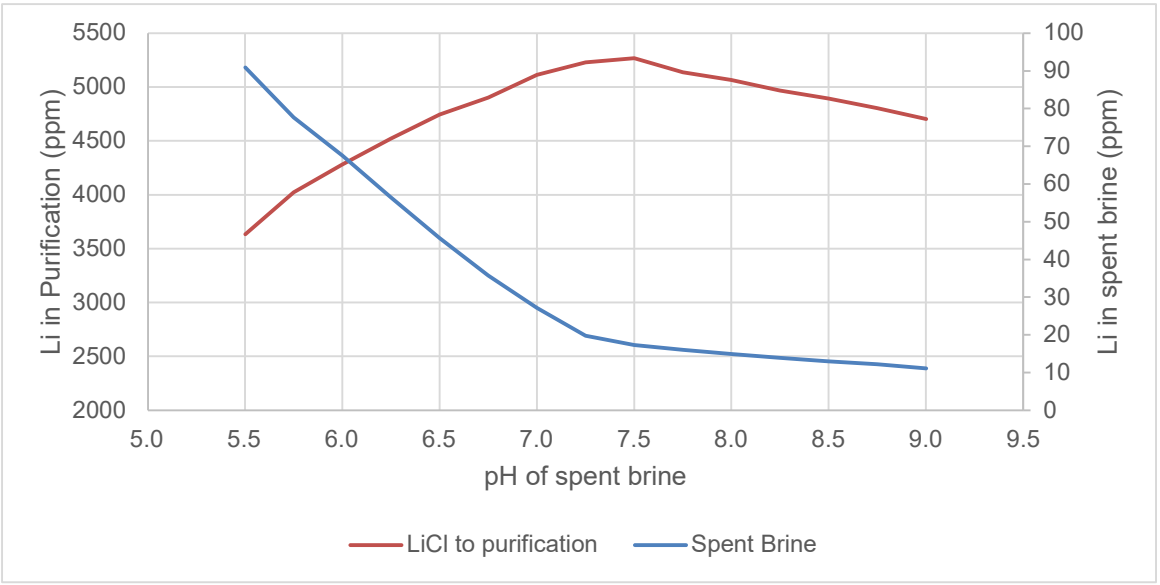

Figure 10 - Lithium concentration in *LiCl to purification* stream and spent brine as a function of target pH in the spent brine when the Li:Media loading is set to 20 mg/g.

Figure 11 is the computed lithium concentration in the *LiCl to purification* stream as the pH of the extraction step varies and as the Li:Media loading varies from 10 mg/g (excess media) to 40 mg/g (insufficient media). The highest Li^+ concentrations are computed to be at high Li:Media loadings and between pH 6.5 and 7. There is a marked decrease between the 27 and 20 mg/g loading at lower pH. At extraction above pH 7.5, there is no difference in loading effects above 20 mg/g.

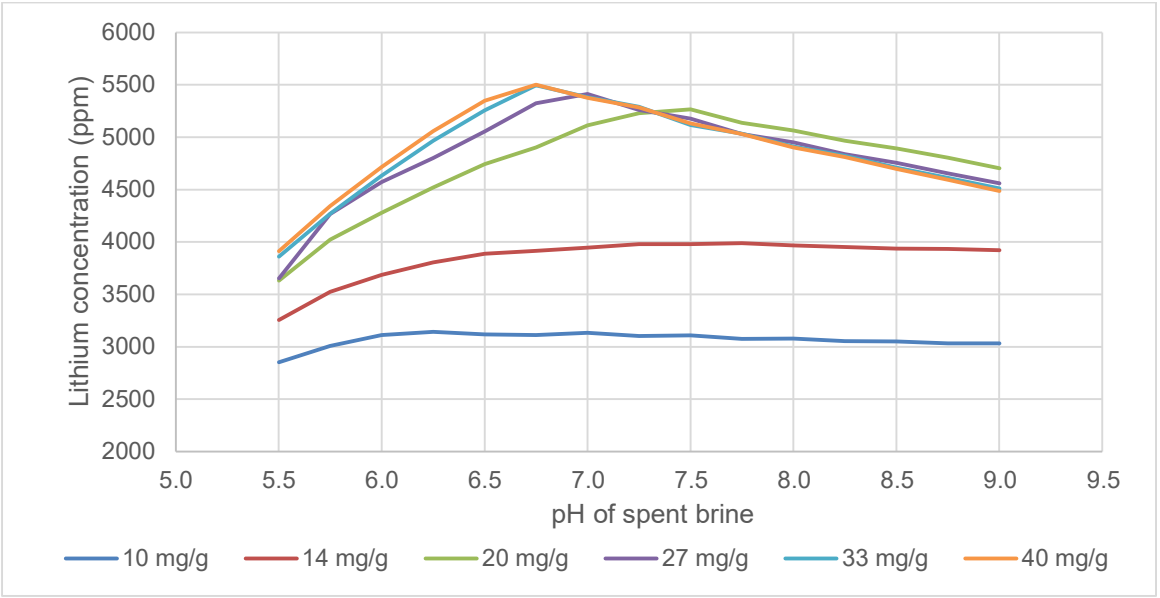

Figure 11 - Lithium concentration in purification stream as a function of spent brine pH and Li:Media loading

Figure 12 is a plot of the percentage of the feed brine Li^+ that is extracted. The 40 mg/g and 33 mg/g Li^+ loadings plateau above 6.7 pH, because the salinity effects on the Li^+ activity coefficient impacts overall adsorption. We will investigate this in future studies to determine the significance of ionic strength on lithium extraction. At loadings of 20 mg/g and lower, more than 90% of the Li^+ is computed to be extracted at pH 7.5 and higher.

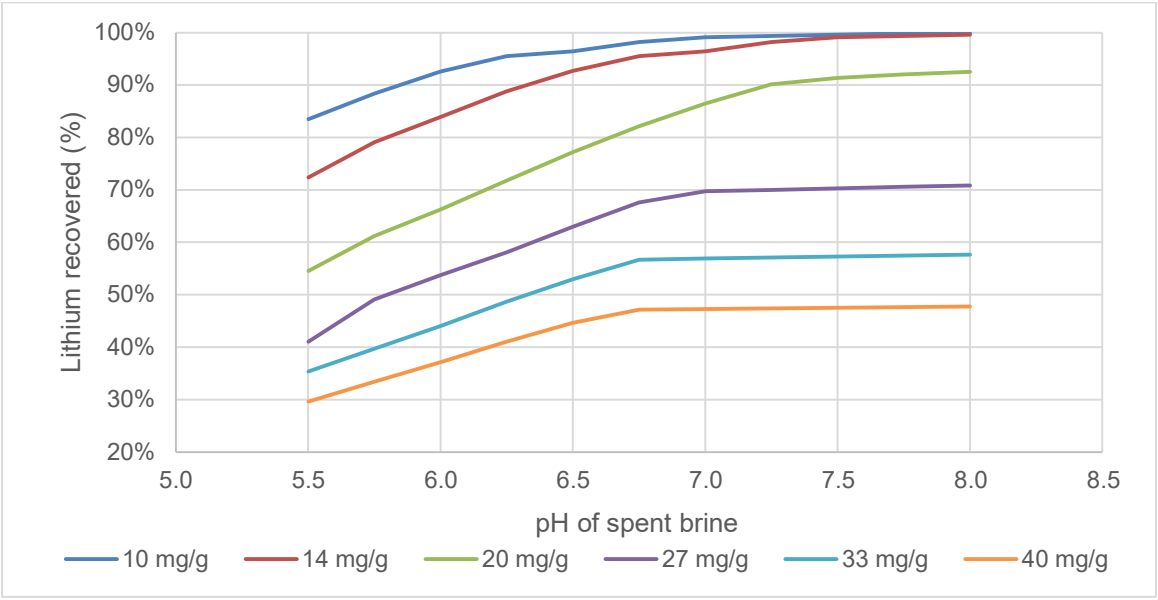

Figure 12 - Percent of lithium recovered from brine vs spent brine pH and Li:Media loading.

Figure 13 is the calculated impurity:Li ratio as a function of pH and Li:Media loading ratio. At low contactor pH, the impurity/Li ratio in the purification stream is low. The optimum ratio is calculated to be approximately 20 mg Li/g media loading. Below this ratio, there is insufficient lithium to extract to all available sites, but there are also additional sites for the impurities to adsorb. The worst-case scenario is the 10 mg/g loading. Compared to the 20 mg/g loading, there are twice as many sites for Na^{+}, K^{+}, Mg^{+2}, and Ca^{+2} to adsorb, and so their extraction is doubled. However, if we consider pH 7, there is only 15% additional lithium adsorbed when the loading is 10 mg/g vs 20 mg/g (Figure 12). Consequently, the impurity:Li ratio increases in the extraction.

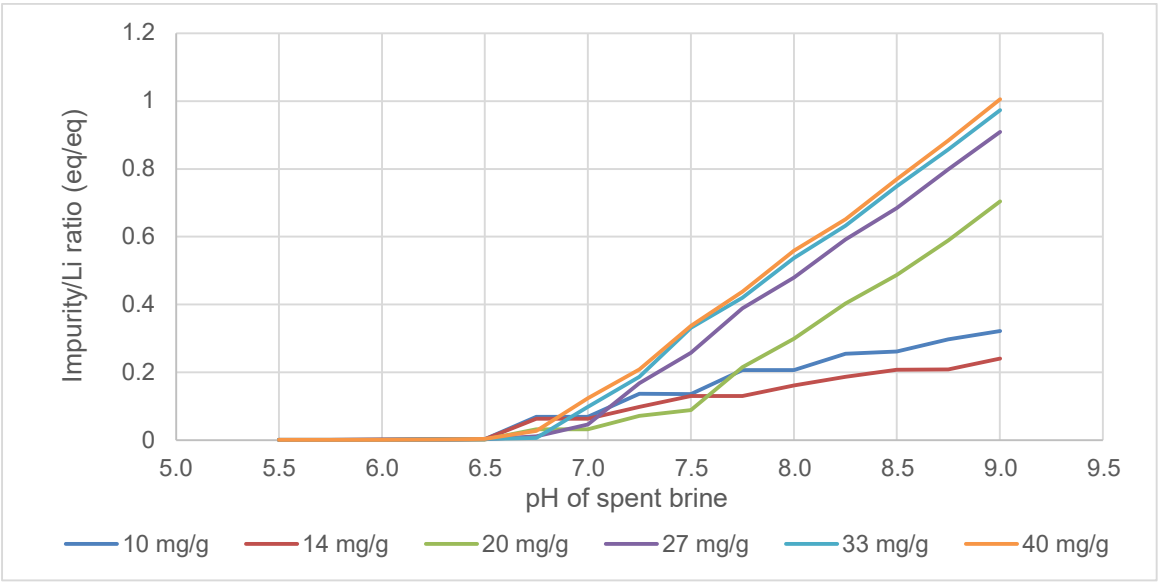

Figure 13 - Impurity:Li ratio in purification stream vs pH of spent brine and Li:Media loading

SUMMARY

We incorporated direct lithium extraction into a thermodynamic model to test whether it is feasible to simulate with precision the lithium extraction process. We used two modelling methods: empirical uptake and release calculations using proprietary media and kinetic reactions, and rigorous uptake and release using surface ion exchange reactions.

We can achieve reasonable curve fitting of laboratory uptake data using both approaches. We identified non-ideal adsorption vs. pH effects. This appeared in the kinetic and rigorous approach. These non-ideal adsorption behaviors should be resolved by using a more complex kinetic equation for the empirical approach and surface activity parameters for the rigorous approach. Both will be part of future work.

Finally, we used a process simulator to model the mass balance using the two uptake models (empirical and rigorous). We were able to predict in a semiquantitative way the impact of contact time, pH, and media reuse

(recycle) on overall process performance. Future work will focus on using more complex kinetic equations in the process simulation.

---

[i] Private communication

[ii] Wang, S. P, Li, X. Zhang, S. Zheng, and Y. Zhang. 2017. Selective adsorption of lithium from high Mg-containing brines using HxTiO3 ion sieve. Hydrometallurgy. Vol 174, pp 21-28. https://doi.org/10.1016/j.hydromet.2017.09.009

[iii] Zhang, T., J. Liu, Y. Yang, S. Lin, and P. Li. 2021. Preparation off granular titanium-type lithium-ion sieves and recyclability assessment for lithium recovery from brines with different pH values. Separation and Purification technology. Vol 267. https://doi.org/10.1016/j.seppur.2021.118613.

A ROBUST METHOD DEVELOPED FOR SPECIES ANALYSIS DURING A TYPICAL HYDROMETALLURGICAL TEST WORK PROGRAMME FOR PRODUCTION OF BATTERY GRADE PHOSPHORIC ACID – A MINTEK PACKAGE

By

Lebohang Hlatshwayo, Hlengiwe Mnculwane, Rasoul Hassanalizadeh

Mintek, South Africa

Presenter
Mothepane Happy Maboa
mothepanem@mintek.co.za

ABSTRACT

The current work evaluates the optimisation of an analytical method for the determination of fluoride and chloride impurities in a high phosphoric acid matrix. A typical battery grade acid is expected to contain meagre level of impurities to better enhance the capacity, voltage, specific energy, energy density, and thermal stability of lithium ion batteries, latter being the most crucial. Accurate determination of the species in the final product as well as streams generated throughout the three major phases of pre-treatment, solvent extraction and post-treatment is the only means to monitor the process effectiveness.

A robust inter-linked technique is required for preparation and analysis of various commodities and species during the process to meet the stringent impurity thresholds at each stage. These include determination of density, total suspended solids, P_2O_5, total organic carbon, critical base metals (arsenic, chromium, sulphur and boron), chloride and fluoride.

A precise determination of chloride and fluoride in the process is critical to ensure that the corrosiveness of the acid is minimised. The chloride and fluoride contents are expected not to exceed 20 and 10 ppm, respectively. These ions can be analysed using either ultraviolet-visible spectrophotometer (UV-Vis) or an ion chromatography. This paper therefore, details how analyses of such limited range were conducted, the development and optimization of the exclusion methods to suit the high phosphorus matrix of these samples. International certified reference material was used for validation purposes. The high phosphoric acid matrix resulted in challenges with both the UV-Vis and the Ion chromatography methods however, the ion chromatography exclusion method allowed for the determination of these ions at low concentrations. This comparative study showed good recoveries for both elements of interest (F^- and Cl^-) when using the ion chromatography exclusion method and the data obtained indicated good repeatability and reproducibility.

Keywords: Battery Grade Phosphoric Acid, Ion Chromatography, Exclusion, UV-Vis

INTRODUCTION

Phosphoric acid is a versatile industrial acid that finds numerous applications in the food and beverage industry. One of the primary uses of phosphoric acid, a colourless and odourless mineral acid, in the food industry is as a food additive and flavouring agent (1). It is commonly used in the production of carbonated soft drinks to provide a tangy taste and a slight acidic pH to balance the sweetness of the drink (2). Phosphoric acid also acts as a pH buffer in other food and beverage products such as jams, jellies, and sauces (3). The acidity of the acid helps to inhibit bacterial growth and prolong the shelf-life of the products (2).

Moreover, phosphoric acid is used in the food processing industry as a preservative and as a pH regulator. It is added to meat and poultry products to increase the water-holding capacity, resulting in juicier and more tender meat (3). Additionally, phosphoric acid is used in the production of cheese, yogurt, and other dairy products to lower the pH and create the ideal conditions for the growth of beneficial bacteria that contribute to the flavour and texture of the product (4).

Apart from these uses, phosphoric acid is also used in the food industry for its emulsifying and chelating properties (3). It is added to processed foods to stabilize emulsions, prevent separation of oil and water, and to enhance the texture of the food product. Phosphoric acid is also used as a chelating agent to remove minerals from food products, thereby preventing spoilage and rancidity (5).

Phosphoric acid is a critical component in the production of phosphatic fertilizers and industrial products due to its ability to react with phosphate rock and produce soluble forms of phosphate that are essential for plant growth (6). The acid is commonly used in the wet process of producing phosphoric acid, which involves the reaction of phosphate rock with sulphuric acid to produce phosphoric acid and gypsum as a by-product. The produced phosphoric acid is then neutralized with ammonia to form ammonium phosphate fertilizers such as mono-ammonium phosphate (MAP) and di-ammonium phosphate (DAP) (6).

In addition to its use in the production of fertilizers, phosphoric acid is also utilized in the production of various industrial products such as detergents (7), water treatment chemicals (8), metal surface treatment agents (9), and flame retardants (10). For instance, phosphoric acid is used as a rust inhibitor in the production of metal products by forming a protective layer on the metal surface. It is also used in the production of flame retardants due to its ability to release phosphorus that forms a protective layer on the surface of the material and prevents it from igniting (1).

Phosphoric acid has emerged as a key intermediate material in the production of lithium iron phosphate (LFP) for the battery material supply chain (11). The demand for LFP batteries has been increasing in recent years, driven by the growth of electric vehicles and the need for energy storage systems. Phosphoric acid is a vital component in the production of LFP cathode material, which is known for its long cycle life, stability, and safety. To meet the stringent purity requirements of the battery material supply chain, phosphoric acid used in LFP production must have ultra-high purity levels. Any impurities in the acid can have detrimental effects on the battery performance, resulting in reduced capacity, cycle life, and safety. Therefore, the production of ultra-high purity phosphoric acid is essential to meet the growing demand for LFP batteries (12).

Several methods have been developed to produce ultra-high purity phosphoric acid, including the solvent extraction method, the electrochemical method, and the ion exchange method. These methods involve the removal of impurities such as heavy metals, fluoride, and arsenic to ensure that the acid meets the purity standards required for LFP production.There are two primary flow sheeting methods used in industry for the production of phosphoric acid; the dry and the wet process (6, 13).

The wet-process phosphoric acid (WPA) usually contains impurities in combination with phosphoric acid. Some triggers to increased corrosiveness in technical phosphoric acids are fluorides, chlorides, and bromides. Care has to be taken while using phosphoric acids containing chlorides and at increased temperatures. The corrosion rate can increase more than 10-fold on a typical stainless steel grade when temperature slightly changes, even where only low amounts of chlorides are present in the acid, see Figure 1. High amounts of fluorides in combination with temperature increase may also have unpropitious effect on corrosive resistance, see Figure 2 (14).

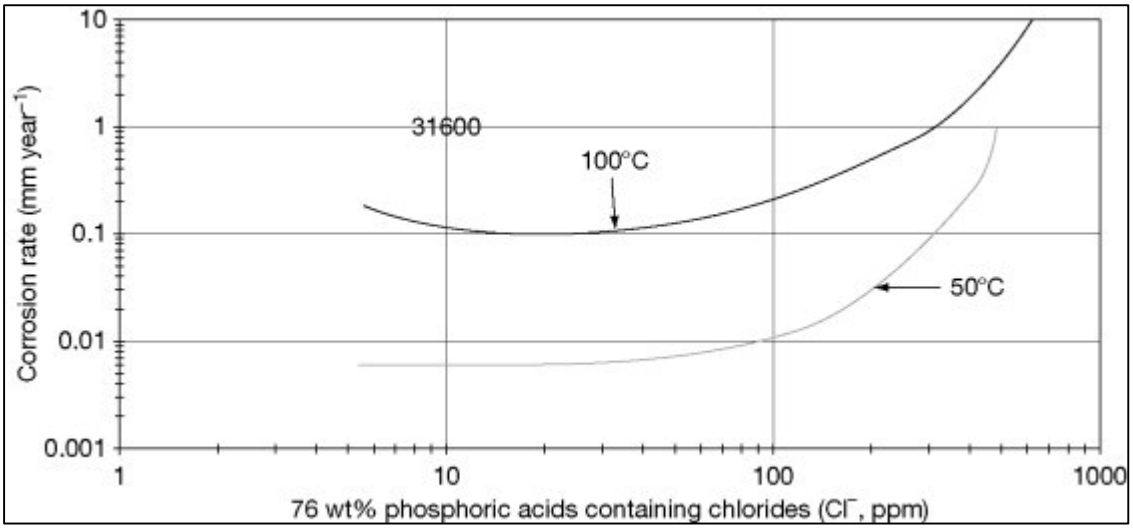

Figure 1: Corrosion rate for the stainless steel grade S31600 in phosphoric acid containing chloride (14)

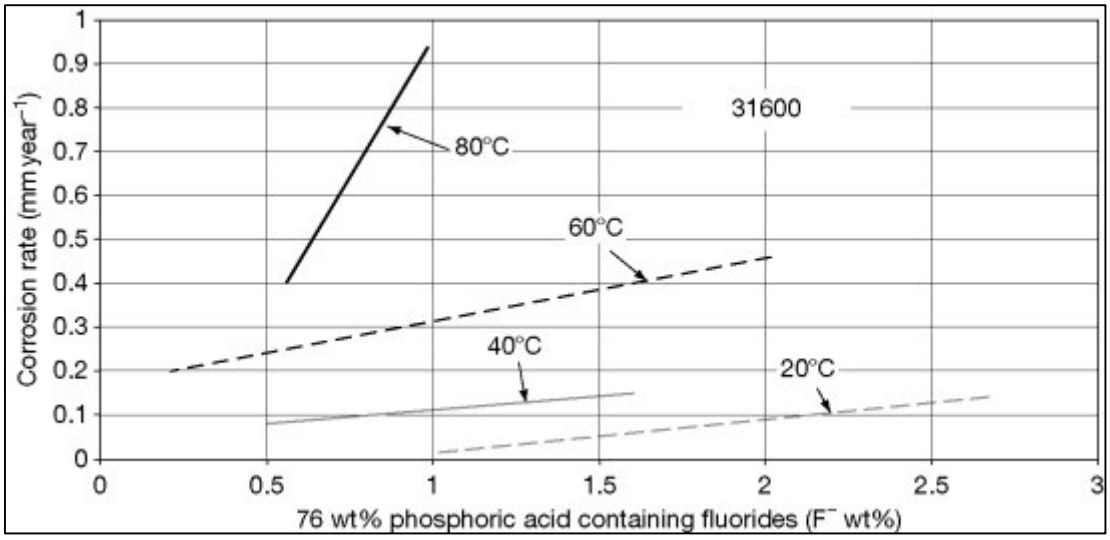

Figure 2: Corrosion rate for the stainless steel grade S31600 in phosphoric acid containing fluorides (14)

Ion chromatography (IC) is a widely used method for determining F and Cl levels in WPA (15, 16). IC has high sensitivity and selectivity, making it suitable for detecting very low levels of F and Cl in complex matrices. The technique separates and quantifies ions in a sample using ion-exchange resins and conductivity detection. IC is also relatively easy to use and requires minimal sample preparation, making it a popular choice for routine analysis of F and Cl in WPA.

Inductively coupled plasma mass spectrometry (ICP-MS) is another powerful analytical method for determining trace elements in complex matrices such as WPA (17). ICP-MS has high sensitivity, selectivity, and multi-element capability, making it suitable for analysing a wide range of elements, including F and Cl. The technique ionizes the sample using high-temperature plasma and measures the resulting ions using a mass spectrometer. ICP-MS also allows for the determination of isotopic ratios, which can provide additional information about the origin and fate of the elements in the sample (18).

The matrix effect of phosphoric acid can however be detrimental to ICP methods. The high concentration of phosphate ions in phosphoric acid can interfere with the determination of trace elements by ICP-MS by reducing ionization efficiency, producing polyatomic interferences, and increasing background noise. These effects can result in inaccurate and imprecise measurements of trace elements in phosphoric acid (19).

To overcome the matrix effect in ICP-MS analysis of phosphoric acid, several sample preparation techniques have been developed, including dilution, ion exchange, and sample digestion (20, 21). Dilution of the sample with a matrix-matched solution can reduce the concentration of interfering matrix elements, improving the accuracy and precision of the analysis. Ion exchange can remove interfering matrix elements selectively, allowing for more accurate and precise measurements of trace elements. Sample digestion can break down the matrix to release the target elements for analysis, but this technique requires more complex and time-consuming sample preparation (21).

The determination of trace anions by Ion Chromatography in phosphoric acid is nevertheless hindered by a large excess of phosphate ion. Diluting the concentrated sample overcomes the problem of a large concentration of the interfering matrix ions, but lacks the required sensitivity for the contaminant ions of interest. Therefore, trace inorganic anions need to be separated from the high concentration of phosphate prior to an ion-exchange separation (22).

It is worth noting that the concentration of phosphoric acid after the last defluorination and dechlorination stages is typically very high, often greater than 50% by weight (1). This is because the final purification steps involve the removal of impurities using carbon columns and/or ion exchange resins. These steps are designed to remove any remaining impurities, including fluoride and chloride ions, and to concentrate the phosphoric acid. The concentration of phosphoric acid before the final purification steps may vary depending on the efficiency of previous purification steps and the initial concentration of impurities. However, it is generally expected that the concentration will be lower before these steps and higher after them (10).

This report describes the theory, set up, and analytical procedure for the determination of fluoride and chloride at trace levels in 62% (w/w) phosphoric acid. An ion-exclusion column is used to separate the analyte ions from an excess of phosphate matrix ions. A selected fraction from the ion-exclusion separation is “cut” and sent to an anion-exchange concentrator column. The concentrated ions are then eluted onto a column set, on which the anions of interest are separated and detected by suppressed conductivity.

EXPERIMENTAL

This method addresses the challenge of determining trace concentrations of contaminant ions such as fluoride and chloride in a matrix composed of a high concentration of phosphate ion. This is accomplished in two steps: an ion-exclusion (ICE) pre-separation followed by injection of a portion of the ICE separation to an ion chromatographic (IC) separation. The ion-exclusion mechanism separates ionized species from non-ionized or weakly ionized species. This occurs because of a negatively charged hydration shell on the stationary phase surface called the Donnan membrane. The strong acid ions, such as chloride and fluoride, are excluded and elute first and the weakly ionized phosphate matrix ions (concentrate) are retained and elute later.

Equipment

- Thermo Scientific™ Dionex™ ICS-5000+ HPIC™ Ion Chromatography system consisting of:
    1. Gradient Pump, microbore configuration
    2. Conductivity Detector with a temperature controlled conductivity cell
    3. Enclosure with 2 Rheodyne® valves, PEEK™, rear loading
- Thermo Scientific™ Dionex™ Dionex RP-1 single piston pump
- Pressurizable Reservoir Chamber
- 1 Air pressure gauge, 0–171 kPa (0–25 psi) (for external water)
- Green PEEK tubing, diameter of 0.75 mm, to connect columns and make a 200 µl sample loop
- Thermo Scientific™ Dionex™ PeakNet™ Chromatography Workstation

The main operating parameters and/or conditions are presented in Table 1.

Table 1: Operating Conditions

Parameter	Conditions
Ion Exclusion	
Analytical Column	Dionex IonPac ICE-AS6, 9 x 250mm
Trap Column	Dionex IonPac AG10, 4 mm
Eluent	Deionized water from Millipore system, 18.2 MΩ·cm
Flow Rate	0.50 ml/min
Ion Chromatography	
Analytical Column	Dionex IonPac AS11-HC, 2 mm
Guard Column	Dionex IonPac AG11-HC, 2 mm
Concentrator Column	Dionex IonPac AG11-HC, 4 mm
Eluent	20 mM NaOH, step to 200 mM NaOH
Flow Rate	0.38 ml/min
Sample Volume	200 µl
Detection	Suppressed conductivity, Dionex Anion Self-Regenerating Suppressor (ASRS), AutoSuppression external water mode
Suppressor Current Setting	300 mA
Expected System Backpressure	16.5 MPa (2400 psi) (with concentrator column in line)
Expected Background Conductivity	2–3 µS

Reagents and standards

Deionized water from Millipore system, 18.2 MΩ·cm resistance, Sodium hydroxide, 50% (w/w) aqueous solution (Fisher Scientific) and Thermo Scientific™ Dionex™ Chloride and Fluoride 1000 mg/l.

The concentrated phosphoric acid sample is loaded via a pressurized reservoir into the 200 µl sample loop at a flow rate of 0.5 ml/min. This technique ensures that a representative sample of the concentrated phosphoric acid sample is loaded into the sample loop. It is important to pass at least 4 loop volumes through the sample loop to ensure reproducible sampling. The concentrated phosphoric acid sample is then delivered with the high-purity water carrier stream to the Dionex IonPac ICE-AS6. A Dionex IonPac AG10 is placed after the Dionex RP-1 pump to act as an anion trap column for the deionized water, illustrated in Figure 3.

The first portion of the ICE separation is sent to waste and disposed of properly, then the concentrator column is placed in-line with the ICE column and the portion eluted later is captured on the concentrator column. After some time, the 4-mm Dionex IonPac AG11-HC concentrator column is placed in-line with the 2 mm Dionex IonPac AS11-HC analytical column set and the concentrated ions (fluoride and chloride) are separated.

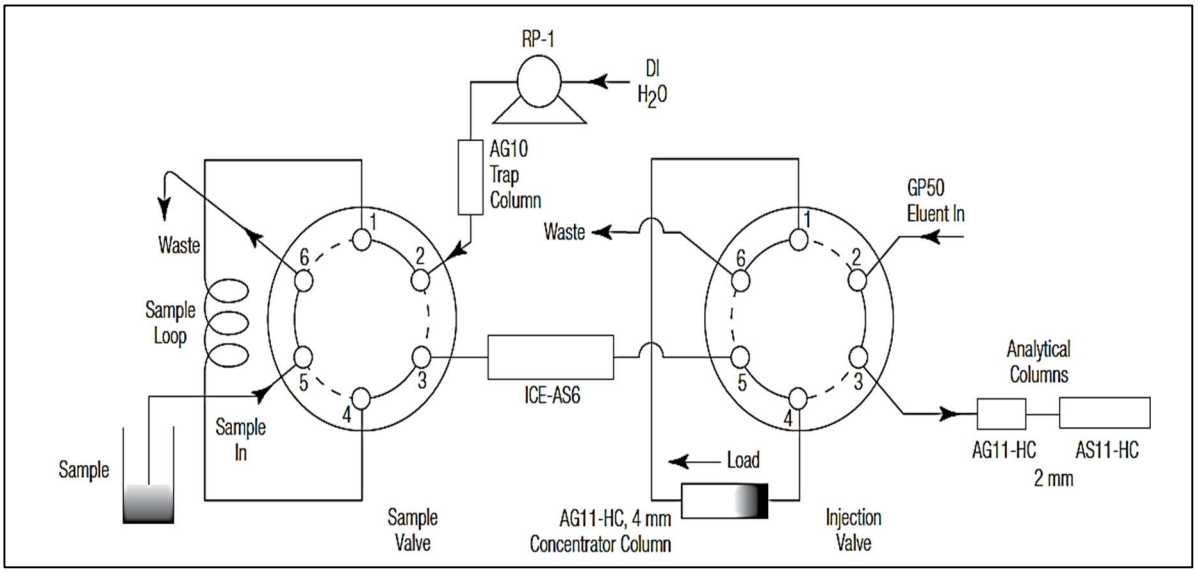

Figure 3: A schematic illustration the operation of the chromatography hardware

The IC separation utilizes the Dionex IonPac AS11-HC column with an isocratic eluent of 20 mM NaOH. The attractive feature of this separation is that phosphate elutes last. During the IC separation, the pressurized vessel is filling the sample loop for the next analysis. The deionized water rinses the Dionex IonPac ICE-AS6 column and associated tubing to ensure there is no contamination from the previous sample. After the phosphate has eluted from the column, the eluent concentration is stepped from 20 to 200 mM NaOH for 5 minutes. This ensures that the column is rinsed of residual phosphate. The method returns the system to equilibrate at 20 mM NaOH for the next injection.

Calibration

Four calibration standards (Table 2) at low concentration levels, similar range to the expected concentrations in the samples were prepared by diluting the working standard.

Table 2: Calibration Standards

Anion	Evaluation Type	Level 1	Level 2	Level 3	Level 4
Fluoride, mg/l	Area	0.78125	3.125	12.50	50.00
Chloride, mg/l	Area	0.78125	3.125	12.50	50.00

RESULTS AND DISCUSSIONS

A representative blank is presented in Figure 4. It was found that after concentrated phosphoric acid had been in the sample loop pathway, several cycles of deionized water were required to completely rinse away the high concentration of phosphate matrix ions. A blank was established by running ten replicates and obtaining reproducible results. These levels, which were quantified based on a calibration curve for these ions in deionized water, were found to be below the concentrations expected for high-purity grade concentrated phosphoric acid. A small amount of phosphate was detected in the blank, as carryover from previous injections. However, this is not expected to significantly impact sample analysis.

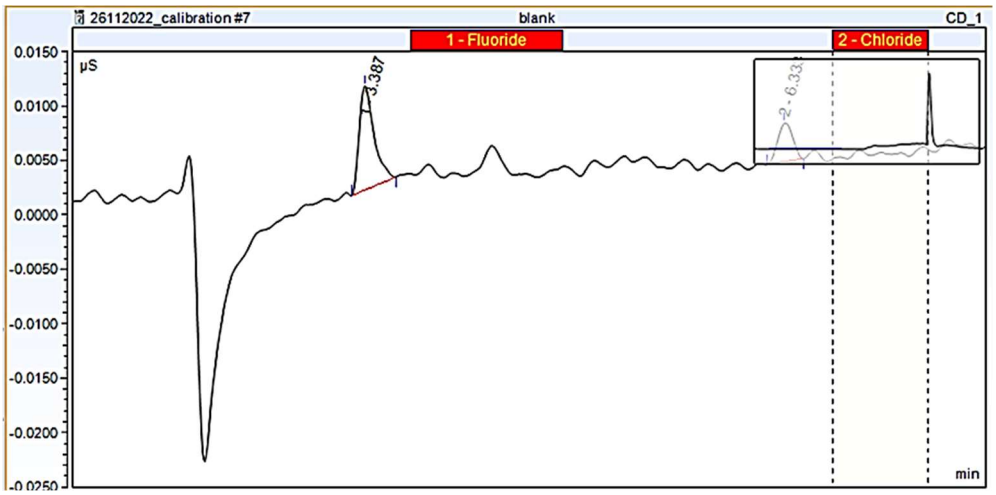

Figure 4: Representative Blank

To verify proper quantification of analytes in the phosphoric acid matrix, fluoride and chloride standards with increasing concentrations were analysed. Chromatograms for the analysis of standards in 60% (w/w) phosphoric acid is shown in Figure 5. The large phosphate matrix (peak 5) is well separated from the anions of interest. Any residual phosphate left in the column was eluted with the high eluent concentration.

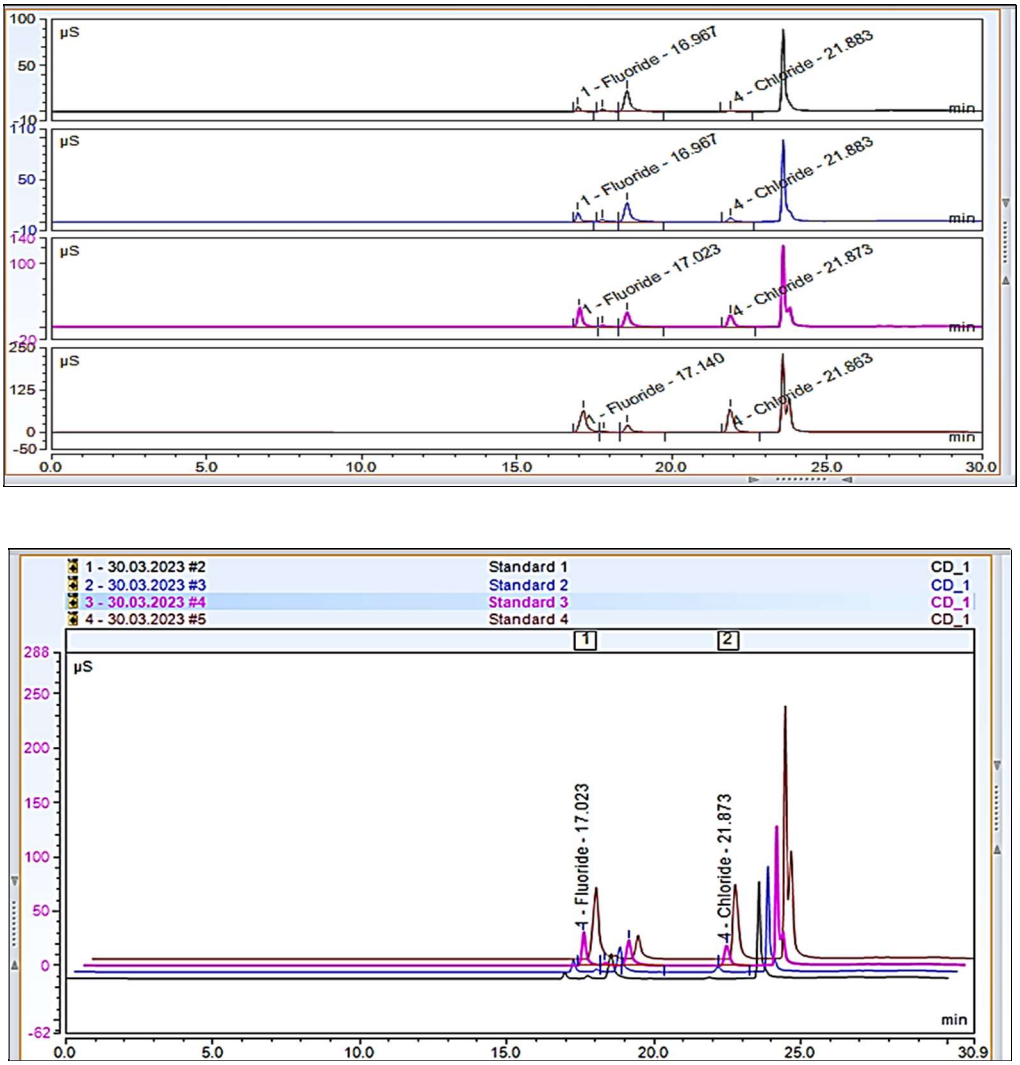

Figure 5: Calibration Standards

To assess method reproducibility, retention time precision was calculated from standards and samples spiked with known quantities of the anions injections. The retention time was reproducible for all injections with an average of 17.087 and 22.053 minutes for fluoride and chloride respectively.

Calibration curves are presented in Figures 6 and 7. Fluoride and chloride yielded coefficients of determination (r^2) values 0.9986 and 0.9999 respectively.

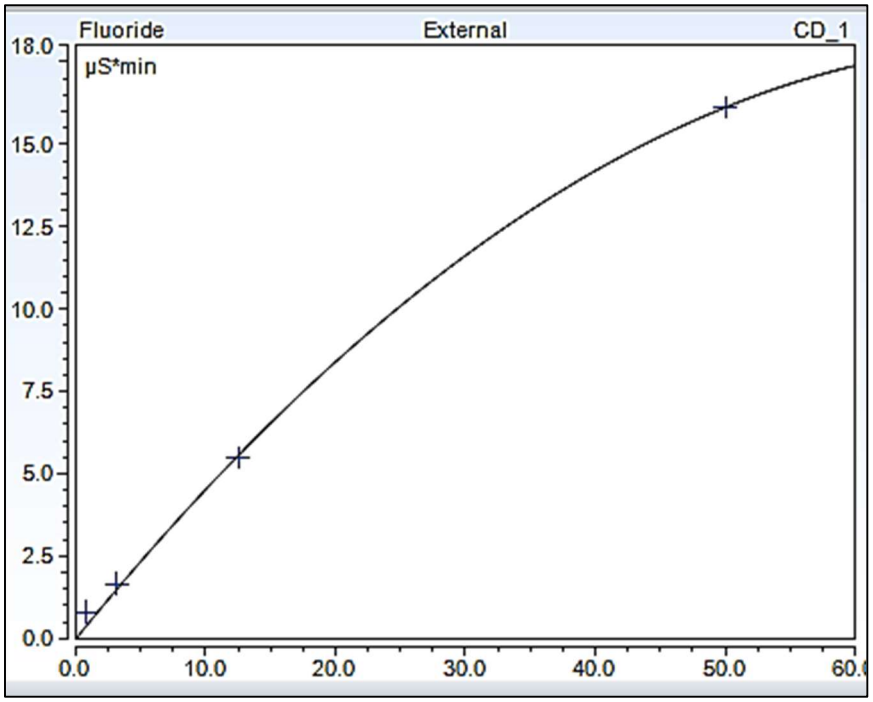

Figure 6: Fluoride Calibration Curve

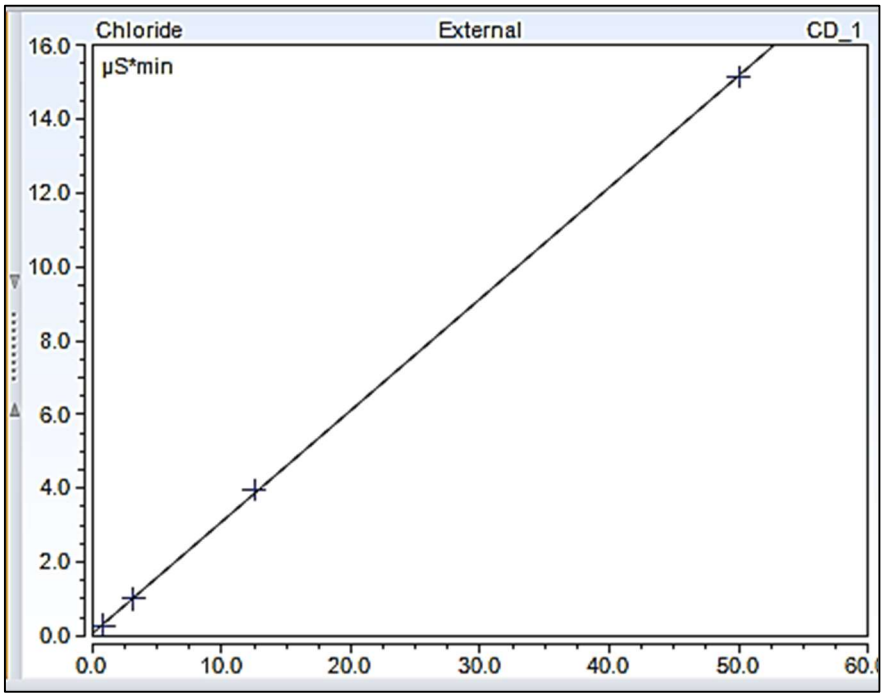

Figure 7: Chloride Calibration Curve

Method detection limits (MDLs) were calculated using the standard deviation of ten replicate injections multiplied by the Student's *t*-value for the 99.5% confidence level. MDLs for fluoride and chloride are in the low µg/l range. The calculated MDLs for this method are well below the maximum limit of impurity guidelines for phosphoric acid established by semiconductor equipment and materials international (SEMI) for the purest grade of phosphoric acid, as shown in Table 3.

Table 3: Method detection limits for trace anions in phosphoric acid

Anion	*MDL (µg/l)
Fluoride	1.10
Chloride	0.40

*Method Detection Limit = (SD) x (ts)99.5% where (ts) is for a single-sided Student's *t*-test distribution for n = 10.

To determine method precision, a sample of a battery grade 62% phosphoric acid was analysed by this method. A chromatogram is shown in Figure 8. The large phosphate matrix (peak 5) is well separated from the anions of interest.

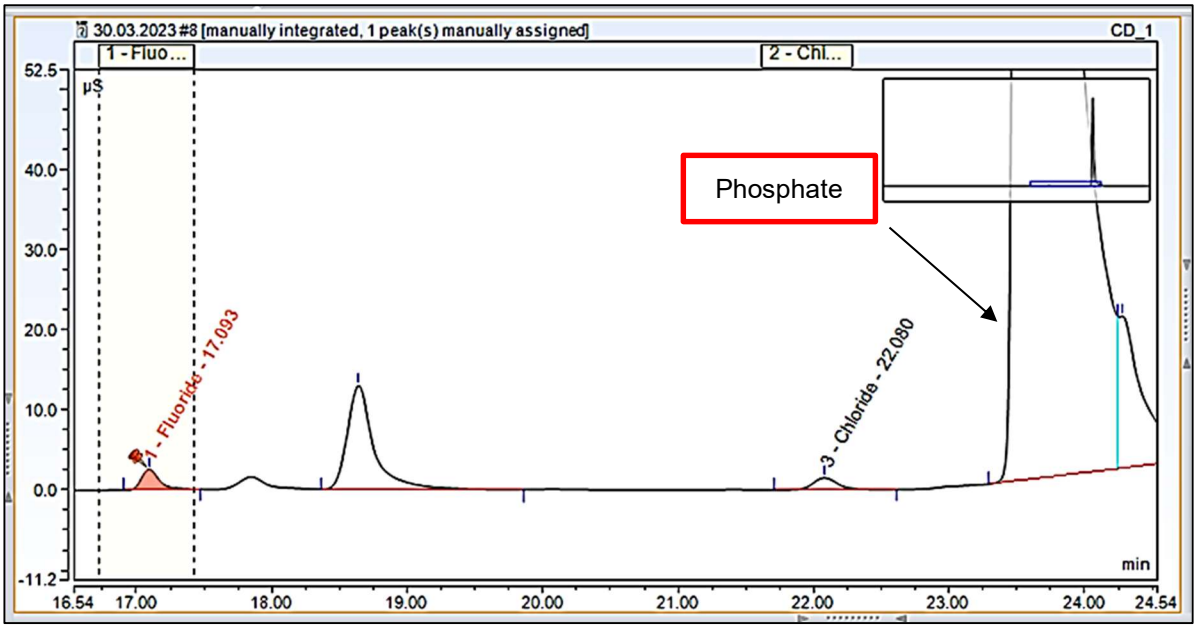

Figure 8: Determination of trace anions in high purity 62% phosphoric acid.

For six replicates, a relative standard deviation (RSD) of less than 5% was obtained for 87 µg/l fluoride and 150 µg/l chloride. Results are presented in Table 4. This sample was spiked with known concentrations and sent to be analysed by an external laboratory for verification purposes and results from the verification analysis are presented in Table 5.

Table 4: Determination of trace anions in battery grade 62% phosphoric acid

Anion	Fluoride	Chloride
Battery grade 62% phosphoric acid	**µg/l**	**µg/l**
	90	148
	85	148
	87	153
	88	151
	85	156
	84	145
+	86.5	150.2
STD Deviation	2.25	3.97
%RSD	2.61	2.64
Certified Value, mg/l	<1	<2

Table 5: Spike recovery of trace anions in battery grade 62% phosphoric acid

Anion	Spike, mg/l	Value obtained, mg/l	%Recovery	External lab. Value, mg/l
Fluoride	10	10.9	109	13.5
Chloride	10	9.0	90.0	9.1

CONCLUSIONS

The method development was a success, the study showed good recoveries for both elements of interest (F^- and Cl^-) using the ion chromatography exclusion method and the data obtained indicated good repeatability and reproducibility at low concentrations. The large phosphate matrix was well separated from the anions of interest. More international certified reference materials will be sourced and used for validation purposes.

ACKNOWLEDGMENTS

The authors would like to thank the staff and management of Mintek for provision of data to prepare this paper.

REFERENCES

1. Gilmour R. Phosphoric acid: purification, uses, technology, and economics: CRC Press; 2013.
2. Caballero B, Finglas P, Toldrá F. Encyclopedia of food and health: Academic Press; 2015.
3. Akoh CC. Food lipids: chemistry, nutrition, and biotechnology: CRC press; 2017.
4. Sodini I, Remeuf F, Haddad S, Corrieu G. The relative effect of milk base, starter, and process on yogurt texture: a review. Critical reviews in food science and nutrition. 2004;44(2):113-37.
5. Schorr M, Valdez B. Phosphoric acid industry: problems and solutions: BoD–Books on Demand; 2017.
6. Becker P. Phosphates and phosphoric acid: raw materials, technology, and economics of the wet process. revised and expanded: Marcel Dekker, Inc.; 1989.
7. Geeson MB, Cummins CC. Phosphoric acid as a precursor to chemicals traditionally synthesized from white phosphorus. Science. 2018;359(6382):1383-5.
8. De Boer MA, Wolzak L, Slootweg JC. Phosphorus: reserves, production, and applications. Phosphorus recovery and recycling. 2019:75-100.
9. Kadoma Y. Surface treatment agent for dental metals using a thiirane monomer and a phosphoric acid monomer. Dental materials journal. 2002;21(2):156-69.
10. Green J. A review of phosphorus-containing flame retardants. Journal of fire sciences. 1992;10(6):470-87.
11. Satyavani T, Kumar AS, Rao PS. Methods of synthesis and performance improvement of lithium iron phosphate for high rate Li-ion batteries: A review. Engineering Science and Technology, an International Journal. 2016;19(1):178-88.
12. Liu X, Gao Z, Cheng J, Gong J, Wang J. Research progress on preparation and purification of fluorine-containing chemicals in lithium-ion batteries. Chinese Journal of Chemical Engineering. 2022;41:73-84.
13. Schorr M, Lin I. Wet process phosphoric acid production problems and solutions. Industrial minerals. 1997;355:61-71.
14. Revie RW. Uhlig's corrosion handbook: John Wiley & Sons; 2011.
15. Ramteke L, Sahayam A, Ghosh A, Rambabu U, Reddy M, Popat K, et al. Study of fluoride content in some commercial phosphate fertilizers. Journal of Fluorine Chemistry. 2018;210:149-55.
16. Smee BW, Hall G, Koop D. Analysis of fluoride, chloride, nitrate and sulphate in natural waters using ion chromatography. Journal of Geochemical Exploration. 1978;10(3):245-58.
17. Guo W, Jin L, Hu S, Guo Q. Method development for the determination of total fluorine in foods by tandem inductively coupled plasma mass spectrometry with a mass-shift strategy. Journal of Agricultural and Food Chemistry. 2017;65(16):3406-12.
18. Beauchemin D. Inductively coupled plasma mass spectrometry. Analytical chemistry. 2008;80(12):4455-86.
19. Agatemor C, Beauchemin D. Matrix effects in inductively coupled plasma mass spectrometry: A review. Analytica Chimica Acta. 2011;706(1):66-83.
20. Masson P, Dalix T, Bussière S. Determination of Major and Trace Elements in Plant Samples by Inductively Coupled Plasma–Mass Spectrometry. Communications in Soil Science and Plant Analysis. 2010;41(3):231-43.
21. Becker JS, Boulyga SF, Pickhardt C, Becker J, Buddrus S, Przybylski M. Determination of phosphorus in small amounts of protein samples by ICP–MS. Analytical and Bioanalytical Chemistry. 2003;375(4):561-6.

22. Michalski R. Ion Chromatography as a Reference Method for Determination of Inorganic Ions in Water and Wastewater. Critical Reviews in Analytical Chemistry. 2006;36(2):107-27.

MODELLING OF MULTICOMPONENT ION EXCHANGE IN LITHIUM ION BATTERY RECYCLING

By

Tobias Wesselborg, Sami Virolainen, [2]Tuomo Sainio

LUT University (Lappeenranta), Finland
[2]LUT University (Lahti), Finland

Presenter and Corresponding Author

Tobias Wesselborg
tobias.wesselborg@lut.fi

ABSTRACT

Lithium ion batteries are applied in various mobile devices and utilized as power source in electronic vehicles (EVs) due to various advantages such as their high energy density, large operating temperature range and sensible discharge resistance [1]. Recycling of spent LIBs has been reviewed by various researchers and new processes for metal recovery from LIBs have been suggested to recover valuable materials.

Although ion exchange offers advantages and potential in metal recovery due to its high selectivity, ion exchange has only played a minor role in LIB recycling. Recently, our research group proposed a process to remove impurity metals via ion exchange while producing high purity Co/Li/Ni containing battery grade raffinate [2]. Aminomethyl phosphonic acid functional chelating resin (Lewatit TP 260) offers great potential for this process as it shows high affinities towards the impurity metals (Al, Cu, Fe and Mn) and low affinities towards the valuable target metals (Co, Li and Ni) [2].

As part of the process development towards a continuous ion exchange process for metal recovery from LIBWL, equilibrium data is required to model and optimize the process. To our knowledge, the available literature lacks LIB metal equilibrium data at higher concentrations and acidities. Additionally, the literature also lacks in thermodynamic data to describe nonidealities of resin and aqueous phase which makes modeling of ion exchange processes in LIB recycling challenging. In this research, single metal sorption curves have been measured at LIB metal concentration range and high acidity for the first time. Equilibrium data was obtained via batch equilibrium experiments in test tubes using chelating resin Lewatit TP 260 in protonated form at three adjusted pH values (0, 1 and 1.8) and two temperatures (22°C and 60°C). Ion exchange and metal uptake were enhanced with increased temperature and increased pH. Three equilibrium models have been tested to model the equilibrium data and to gain model parameters to predict ion exchange equilibria of multi metal solutions.

In ion exchange from concentrated solutions, the charges of the functional groups must be balanced by the mixture of counter-ions. Physical adsorption isotherm models cannot thus be applied. In principle, the stoichiometric equilibrium of an ion exchange reaction can be described using the mass action law (MAL). Here, MAL was used with the assumption of ideal behavior in the electrolyte and the resin phase. In addition, two explicit equilibrium models were used to describe the experimental data. The non-ideal competitive adsorption (NICA) model by Kinniburgh et al. [3] was rewritten for the case of ion exchange (NICA-IX). The two fitted model parameters for each species i are the affinity constant K_i and the non-ideality constant h_i. When setting h_i equal to 1, the NICA-IX model reduces to the ideal competitive ion exchange model. Neither MAL, ideal competitive ion exchange model, nor NICA-IX models could explain the effect of the proton concentration with a fixed set of model parameters when the acid concentration changes 10 or 100 times, *i.e.* 1-2 steps on the pH scale. However, the experimental equilibrium data for an individual metal at a given pH was well correlated using the NICA-IX model.

The results help to understand ion exchange in concentrated battery metal solutions and provide a useful tool to estimate the equilibria of multi component solutions with chelating resin Lewatit TP260. The model also helps to reduce elaborate experimental work during process design and development of a continuous ion exchange process for battery metals purification.

References:

[1] P. Meshram, A. Mishra, Abhilash, R. Sahu, *Chemosphere*. **2020**, *242*, 125291. DOI: 10.1016/j.chemosphere.2019.125291.

[2] S. Virolainen, T. Wesselborg, A. Kaukinen, T. Sainio, *Hydrometallurgy*. **2021**, *202*, 105602. DOI: 10.1016/j.hydromet.2021.105602.

[3] D. G. Kinniburgh, W. H. Van Riemsdijk, L. K. Koopal, M. Borkovec, M. F. Benedetti, M. J. Avena, *Colloids Surfaces A Physicochem. Eng. Asp.* **1999**, *151* (1–2), 147–166. DOI: 10.1016/S0927-7757(98)00637-2.

Keywords: lithium ion battery, recycling, ion exchange, modelling, process development

Background

Background

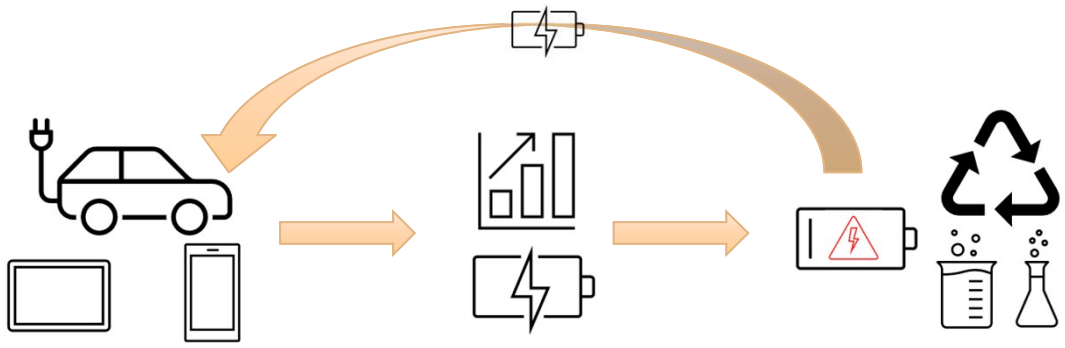

Possible recycling process

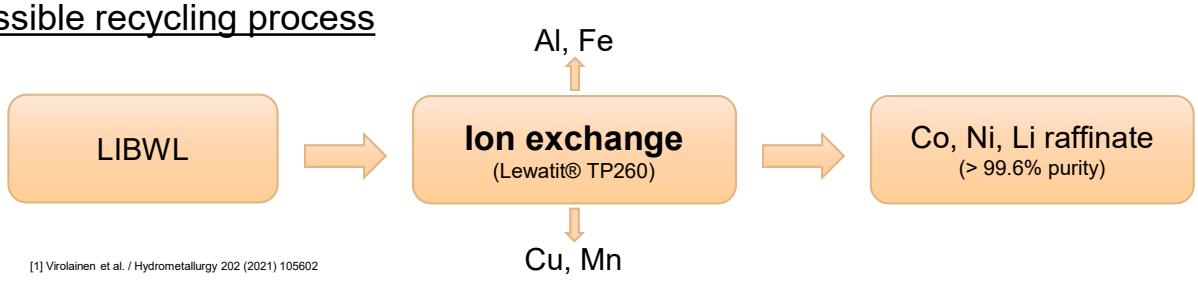

[1] Virolainen et al. / Hydrometallurgy 202 (2021) 105602

Background

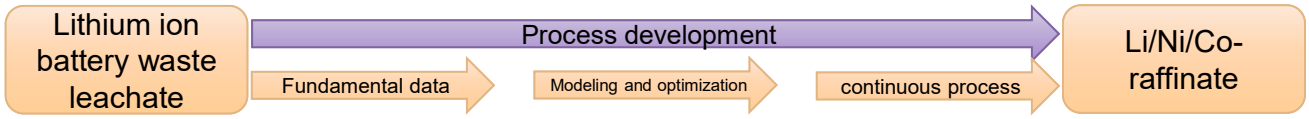

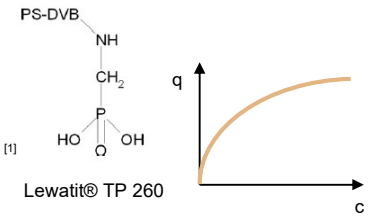

$$0 = \frac{\partial c}{\partial t} + \frac{(1-\varepsilon)}{\varepsilon}\frac{\partial q}{\partial t} + \frac{Q}{\varepsilon A_{col}}\frac{\partial c}{\partial z} - D_{ax}\frac{\partial^2 c}{\partial z^2}$$

$$q = f(c, T, pH, \dots)$$

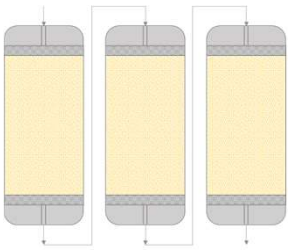

- Literature lacks in LIB metal equilibrium data at higher concentrations and acidities

[1] Virolainen et al. / Reactive & Functional Polymers 73 (2013) 647–652

Methodology, experimentals, theory on modelling of ion exchange

Methodology and experimentals

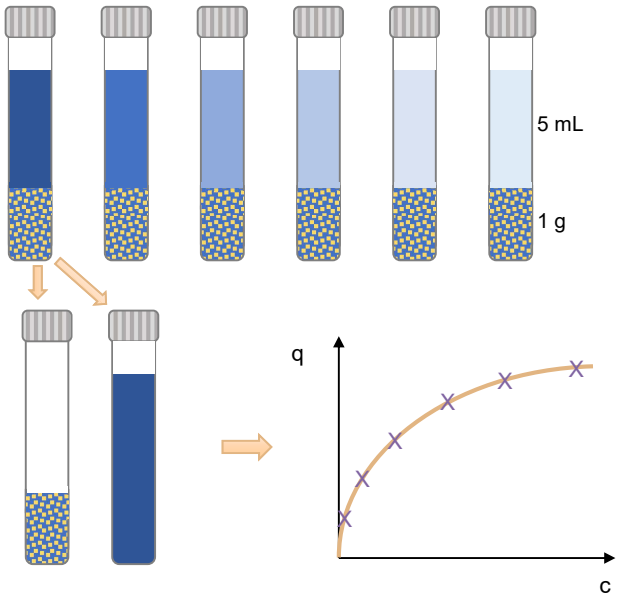

- Batch equilibrium experiments at 22°C and 60°C
- Resin phase: Lewatit® TP 260 in protonated form, functional group: AMPA
- Aqueous phase: LIB metals at varied concentrations in sulfate media
- Adjusted pH values: 0, 1 and 1.8
- Intermittent pH adjustment with NaOH and H_2SO_4 until pH is constant
- Digestion of dried loaded resin
- Analytics: ICP-MS and AAS

Example: Experimental results for the ternary system Cu+Na+H

Due to brevity, the measured equilibrium data is exemplarily shown for the ternary system with cation species Cu^{2+}, Na^{+} and H^{+}. First, second and third column show the uptakes of Cu, Na and H, respectively. First and second row show the uptake of cation species at 22°C and 60°C, respectively.

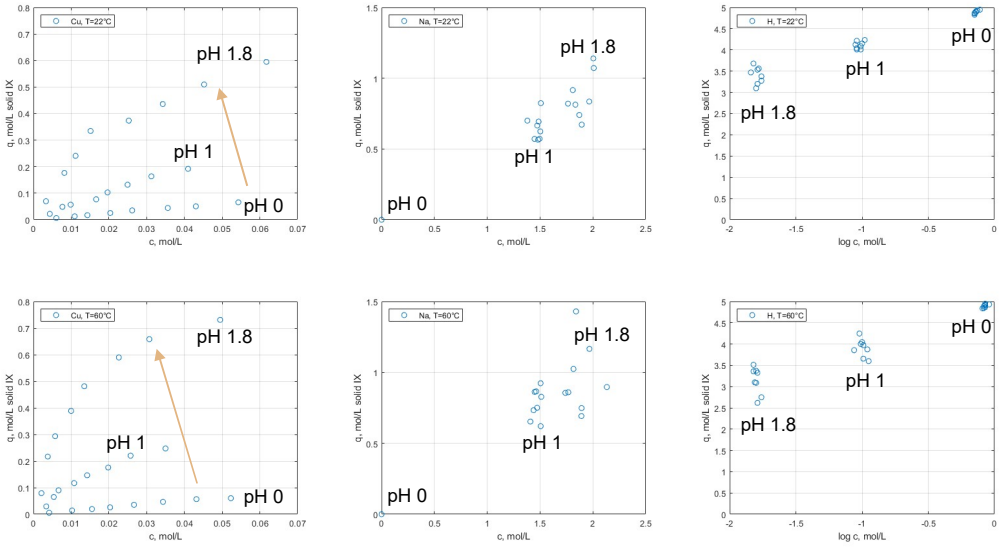

Three isotherms for uptake of Cu at a constant pH can be identified. The metal uptake increases with the increase of pH and temperature. The effect of temperature is enhanced with higher pH values.

- Metal uptake is enhanced with increased pH and increased temperature

Example: Experimental results for the ternary system Cu+Na+H

Due to brevity, the measured equilibrium data is exemplarily shown for the ternary system with cation species Cu^{2+} Na^{+} and H^{+}. First, second and third column show the uptakes of Cu, Na and H, respectively. First and second row show the uptake of cation species at 22°C and 60°C, respectively.

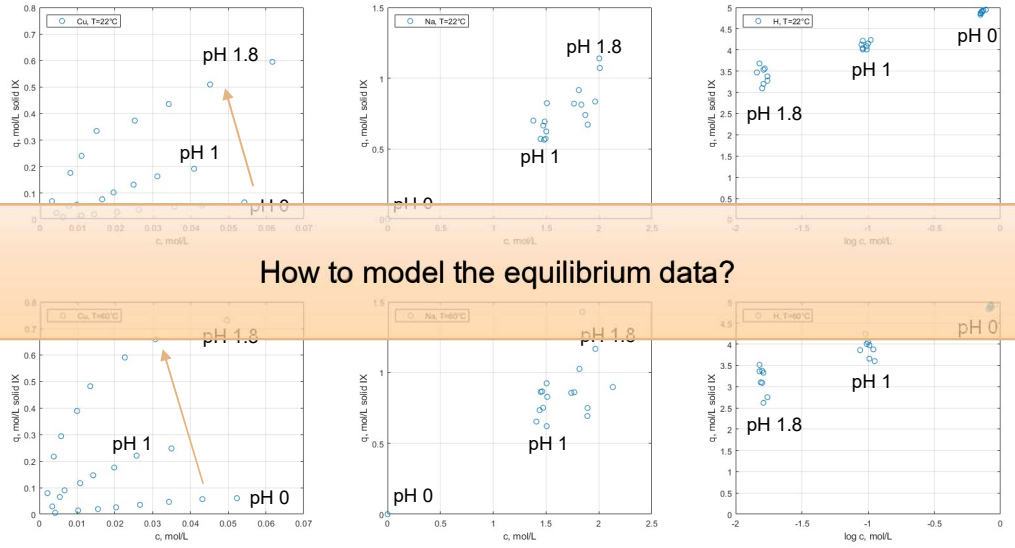

How to model the equilibrium data?

Three isotherms for uptake of Cu at a constant pH can be identified. The metal uptake increases with the increase of pH and temperature. The effect of temperature is enhanced with higher pH values.

- Metal uptake is enhanced with increased pH and increased temperature

Modelling methodology

- Idea: Model each LIB metal separately and use determined model parameters to model the multi metal solution (LIBWL)
  - Each system is a ternary system and consists of three cation species (one LIB metal, Na and H)
  - One binary cation system: Na and H to determine model parameters for Na
- Assumptions:
  - Model parameters for each cation species are independent
  - Proton concentration via pH measurement: α(H)≈c(H)
  - Only phosphonic acid group participates in IX, i.e. amine group is always protonated due to low pH and calculation of $q_{H,exp}$ via mole balance
- OF: minimizing sum of squared error (i.e. method of least squares)

Theory on modelling of ion exchange (IX)

- Characteristics of IX in comparison to physical adsorption:
  - Charge balance (i.e. electroneutrality applies): $\Theta_i = \frac{|z_i| \cdot q_i}{|z_r| \cdot q_{max}}$
  - All sites are permanently occupied: $\sum_j |z_j| q_j = |z_r| q_{max}$
  - Competition between ions, i.e. the system has at least two cations or anions

- Thus, physical adsorption isotherm models cannot be applied.
  - Freundlich $q_i = K c_i^{\frac{1}{n}}$ and Langmuir $q_i = \frac{q_{max} K_i c_i}{1 + K_i c_i}$
  - Competitive Langmuir $q_i = \frac{q_{max} K_i c_i}{1 + \sum K_j c_j}$

Mass Action Law (MAL)

- Stoichiometric equilibrium of an ion exchange reaction:
  - E.g. $Cu^{2+} + 2\underline{H}^{+} \rightleftharpoons \underline{Cu}^{2+} + 2H^{+}$
- MAL: $K_{CuH} = \left(\frac{\alpha(\underline{Cu})}{\alpha(Cu)}\right)^1 \cdot \left(\frac{\alpha(H)}{\alpha(\underline{H})}\right)^2$
  - Literature also lacks in thermodynamic data to describe nonidealities of resin and aqueous phase.
  - Simplification: $K_{CuH} = \left(\frac{c(\underline{Cu})}{c(Cu)}\right)^1 \cdot \left(\frac{c(H)}{c(\underline{H})}\right)^2 = \left(\frac{q(Cu)}{c(Cu)}\right)^1 \cdot \left(\frac{c(H)}{q(H)}\right)^2$

Please note:
After simplification, K_{CuH} does not represent the thermodynamic equilibrium constant; K_{CuH} is the selectivity coefficient.

  - Fitted model parameter: K_{CuH}

Non Ideal Competitive Adsorption isotherm model for IX

- Physical adsorption model rewritten for IX
- NICA-characteristics[1]:
  - Explicit model
  - Affinity constant $K_i \neq$ f(pH)
  - Nonideality is considered
    - h_i is an ion specific non-ideality parameter ($0<h_i\leq 1$)
    - p describes the adsorption site heterogeneity

- NICA: $q_i = \Theta_{i,t} \cdot \frac{h_i}{h_H} \cdot q_{max,H}$

  with $\Theta_{i,t} = \frac{(K_i c_i)^{h_i}}{\sum_i (K_i c_i)^{h_i}} \cdot \frac{\left[\sum_i (K_i c_i)^{h_i}\right]^p}{1+\left[\sum_i (K_i c_i)^{h_i}\right]^p}$

- IX characteristics are applied:

  $\sum_j |z_j| q_j = |z_r| q_{max}$ and $\Theta_i = \frac{|z_i| \cdot q_i}{|z_r| \cdot q_{max}}$

- NICA-IX:

  $$q_i = |z_r| q_{max} \frac{h_i (K_i c_i)^{h_i}}{\sum |z_j| h_j (K_j c_j)^{h_j}}$$

- Fitted model parameters: K_i, h_i
  - Per definition: $\log_{10} K_H = 0$ and $h_H = 1$

[1] D.G. Kinniburgh et al. / Colloids Surfaces A: Physicochem. Eng. Aspects 151 (1999) 147-166

Ideal Competitive Ion Exchange Model

- Equation is obtained by setting $h_i = 1$ in NICA-IX model
  - NICA-IX: $q_i = |z_r| q_{max} \frac{h_i (K_i c_i)^{h_i}}{\sum |z_j| h_j (K_j c_j)^{h_j}}$

- Ideal Competitive Ion Exchange Model: $q_i = \frac{|z_r| q_{max} K_i c_i}{\sum |z_j| K_j c_j}$

- Fitted model parameter: K_i

Experimental and modelling results using MAL, ideal competitive ion exchange and NICA-IX models with a fixed set of model parameters

Results for MAL, ideal competitive ion exchange model and NICA-IX at T=22°C

Example: Li

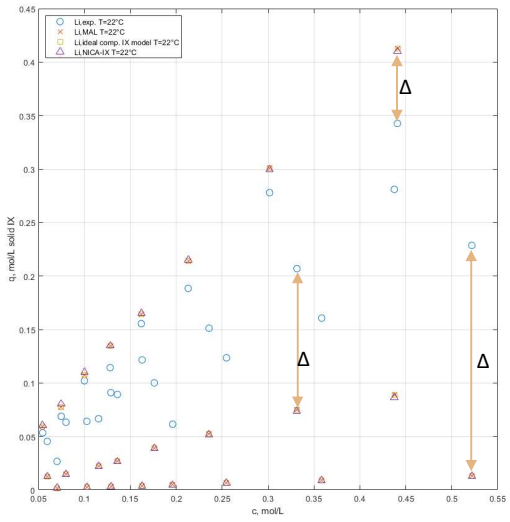

Please note:
Calculated results are not presented as solid lines because the metal (Li) uptake also depends on the pH and Na concentration in the aqueous phase.

- Exemplarily, the experimental and modeled results for Li at 22°C are shown.
  - Due to brevity, only the LIB metal uptake is shown. Corresponding uptakes of Na and H are not shown for the ternary systems (LIB metal + Na + H).
- The experimental data is not well explained by the models.
  - Deviations between experimental and modeled data are highlighted exemplarily.
  - The models cannot explain the effect of the proton concentration with a fixed set of model parameters when the acid concentration changes 10 or 100 times, i.e. 1-2 steps on the pH scale.

Results for MAL, ideal competitive ion exchange model and NICA-IX at T=22°C

Example: Mn

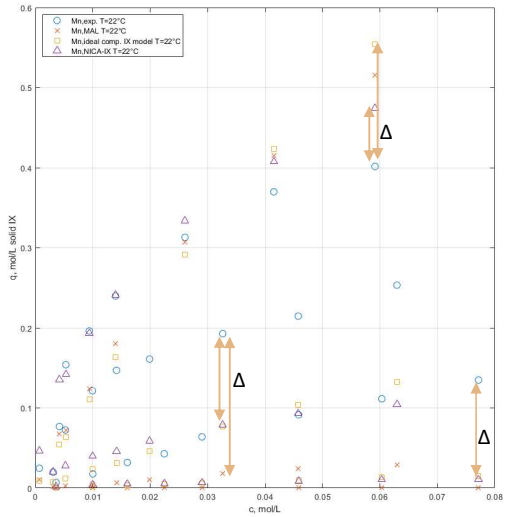

Please note:
Calculated results are not presented as solid lines because the metal (Mn) uptake also depends on the pH and Na concentration in the aqueous phase.

- Exemplarily, the experimental and modeled results for Mn at 22°C are shown.
  - Due to brevity, only the LIB metal uptake is shown. Corresponding uptakes of Na and H are not shown for the ternary systems (LIB metal + Na + H).
- The experimental data is not well explained by the models.
  - Deviations between experimental and modeled data are highlighted exemplarily.
  - The models cannot explain the effect of the proton concentration with a fixed set of model parameters when the acid concentration changes 10 or 100 times, i.e. 1-2 steps on the pH scale.

Results for MAL, ideal competitive ion exchange model and NICA-IX at T=22°C

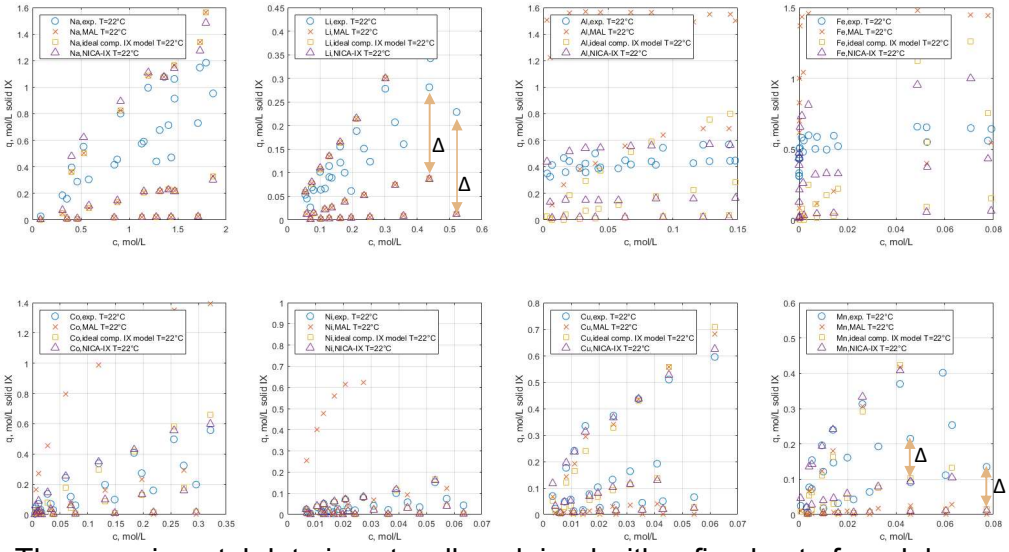

Due to brevity, only the LIB metal uptake is shown. Corresponding uptakes of Na and H are not shown for the ternary systems (LIB metal + Na + H). Uptake of H is not shown for the binary system (Na + H).

- The experimental data is not well explained with a fixed set of model parameters, differences are highlighted for Li and Mn exemplarily.

Results for MAL, ideal competitive ion exchange model and NICA-IX at T=60°C

With increased temperature (T=60°C), similar observations are made. The experimental data is not well correlated with the models, too.

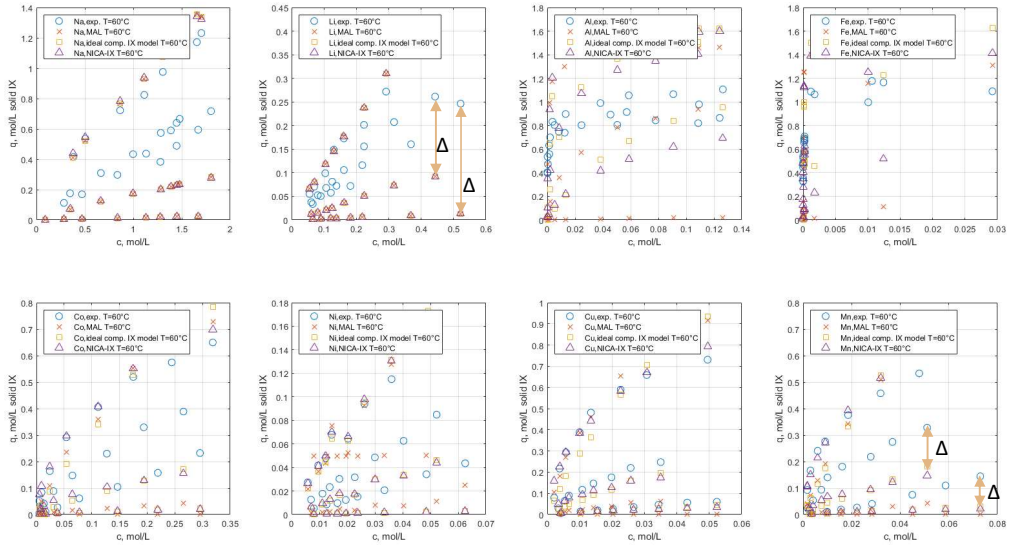

Due to brevity, only the LIB metal uptake is shown. Corresponding uptakes of Na and H are not shown for the ternary systems (LIB metal + Na + H). Uptake of H is not shown for the binary system (Na + H).

- The experimental data is not well explained with a fixed set of model parameters, differences are highlighted for Li and Mn exemplarily.

Modelling results using NICA-IX with a linear correlation of $\log_{10} K_i$ and pH

An approach, how to model large changes in acid concentration

- Observation: At a given pH, the explicit NICA-IX model correlates well with the experimental data
  - NICA-IX: $q_i = |z_r| q_{max} \frac{h_i (K_i c_i)^{h_i}}{\sum |z_j| h_j (K_j c_j)^{h_j}}$
- Idea: linear correlation for log K_i and pH
  - $\log_{10} K_i = a_i \, pH + b_i$
- Fitted model parameters: a_i, b_i and h_i

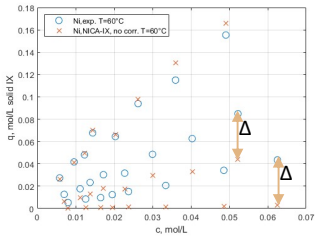

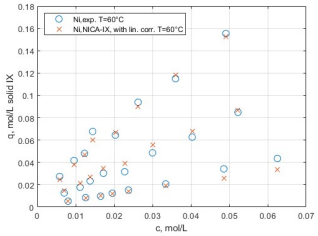

The upper graph shows the experimentally measured uptake of Ni at 60°C and the modeled uptake using the NICA-IX model with a fixed set of model parameters. Deviation between experimental and modeled value are highlighted. The lower plot shows the experimental of Ni at 60°C and modeled uptake using NICA-IX with a linear correlation for the affinity constant and corresponding pH value.

Example: Comparison of NICA-IX without and with correlation for log K at T=60°C

First row: Experimental and modeled data for Ni, Na and H at 60°C using the NICA-IX model with a fixed set of model parameters.

Second row: Experimental and modeled data for Ni, Na and H at 60°C using the NICA-IX model with a linear correlation for the affinity constant and the corresponding pH value.

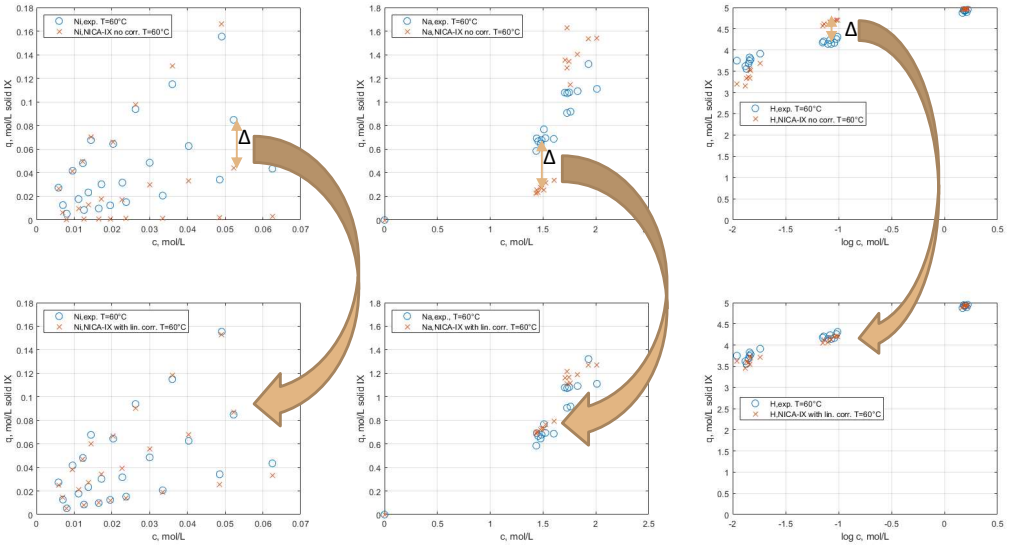

Improvement of the modeled results are highlighted exemplarily for a datapoint at pH 1.

Example: Comparison of NICA-IX without and with correlation for log K at T=60°C

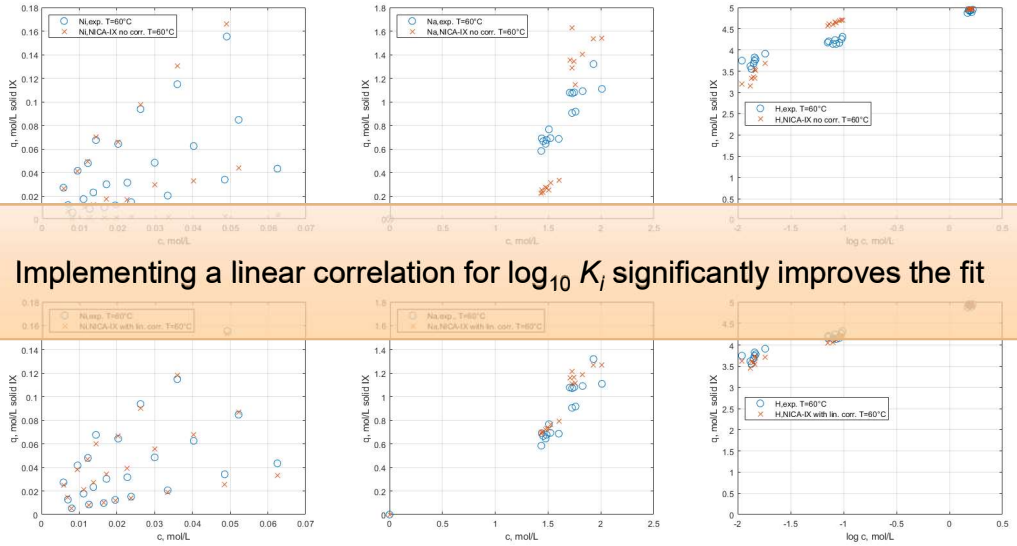

Implementing a linear correlation for $\log_{10} K_i$ significantly improves the fit

Results for system Na+H using NICA-IX with log K_i = f(pH, T)

First and second column show the experimentally measured and modeled uptakes of Na and H, respectively. First and second row show the experimentally measured and modeled uptake of cation species at 22°C and 60°C, respectively.

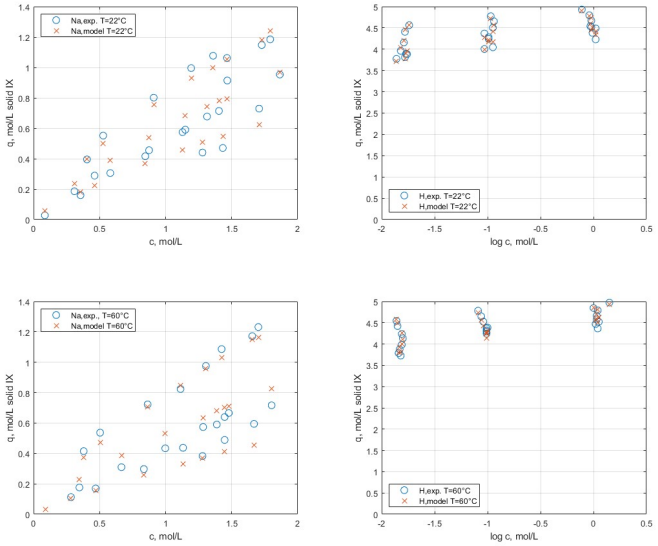

Uptake of Na is enhanced with increasing pH. Only minor effect of temperature on the sorption are observed.

- Good agreement between the experimentally measured and modelled equilibrium data for the binary system (cation species: Na^+, H^+) is achieved.

Results for system Li+Na+H using NICA-IX with log K_i = f(pH, T)

First, second and third column show the experimentally measured and modeled uptakes of Li, Na and H, respectively. First and second row show the experimentally measured and modeled uptake of cation species at 22°C and 60°C, respectively.

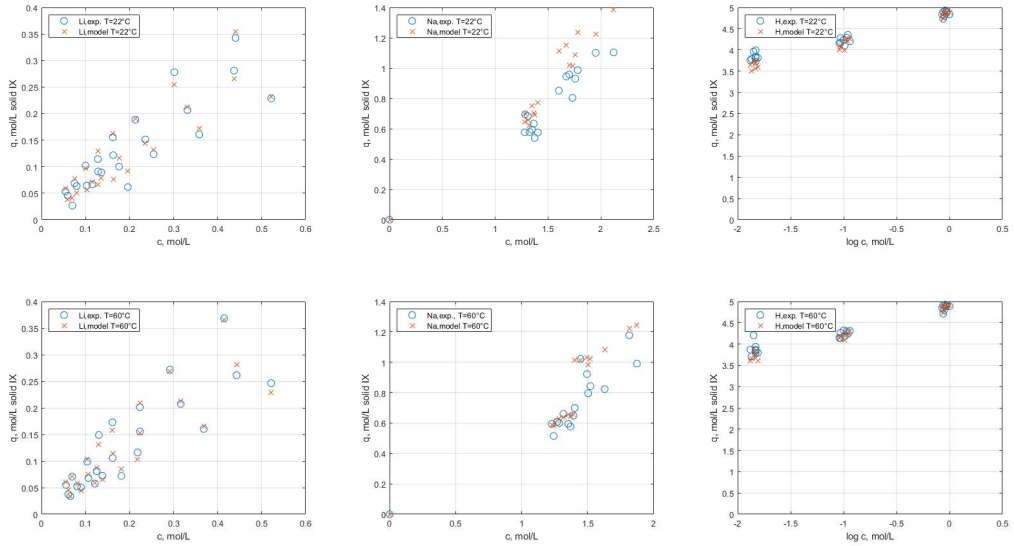

Uptake of Li is enhanced with increasing pH. Only minor effect of temperature on the sorption are observed.

- Good agreement between the experimentally measured and modelled equilibrium data for the ternary system (cation species: Li^+, Na^+, H^+) is achieved.

Results for system Ni+Na+H using NICA-IX with log K_i = f(pH, T)

First, second and third column show the experimentally measured and modeled uptakes of Ni, Na and H, respectively. First and second row show the experimentally measured and modeled uptake of cation species at 22°C and 60°C, respectively.

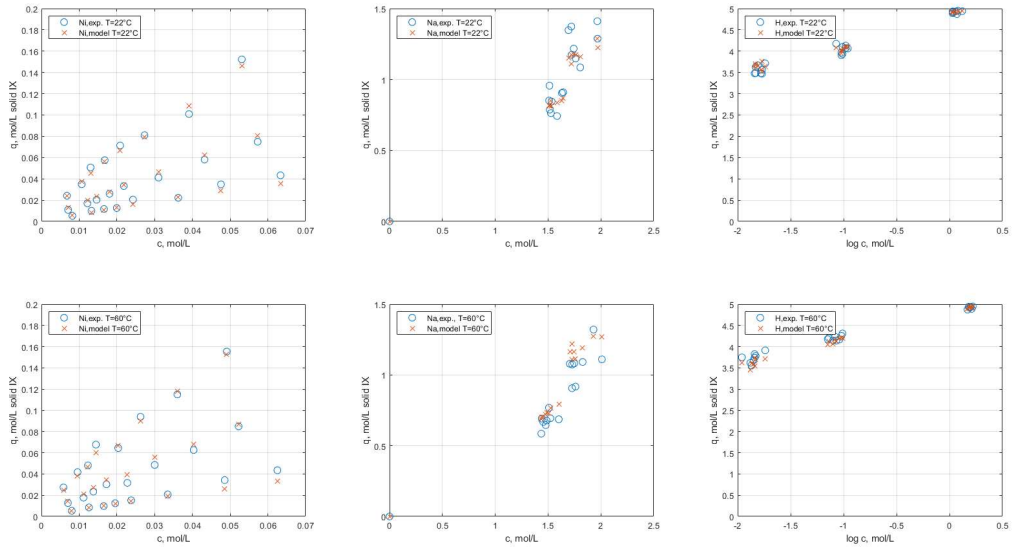

Uptake of Ni is enhanced with increasing pH. Almost no effect of temperature on the sorption are observed.

- Good agreement between the experimentally measured and modelled equilibrium data for the ternary system (cation species: Ni^{2+}, Na^+, H^+) is achieved.

Results for system Co+Na+H using NICA-IX with log K_i = f(pH, T)

First, second and third column show the experimentally measured and modeled uptakes of Co, Na and H, respectively. First and second row show the experimentally measured and modeled uptake of cation species at 22°C and 60°C, respectively.

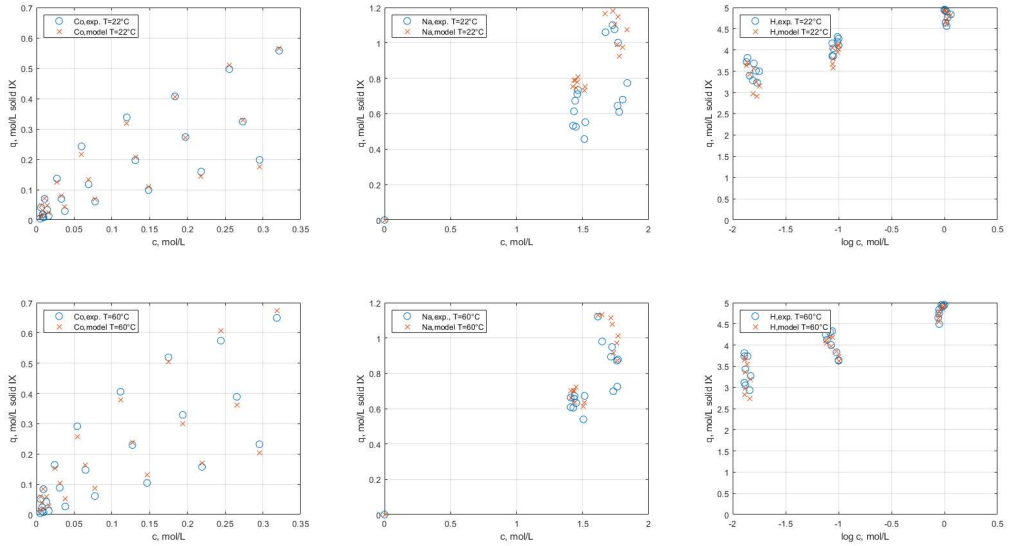

Uptake of Co is enhanced with increasing pH. Only minor effect of temperature on the sorption are observed.

- Good agreement between the experimentally measured and modelled equilibrium data for the ternary system (cation species: Co^{2+}, Na^{+}, H^{+}) is achieved.

Results for system Cu+Na+H using NICA-IX with log K_i = f(pH, T)

First, second and third column show the experimentally measured and modeled uptakes of Cu, Na and H, respectively. First and second row show the experimentally measured and modeled uptake of cation species at 22°C and 60°C, respectively.

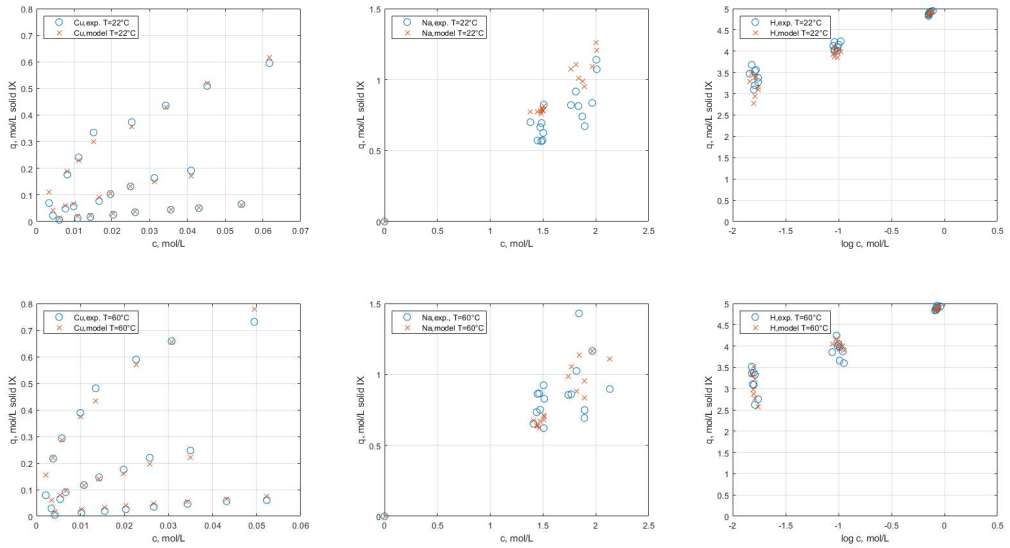

Uptake of Cu is enhanced with increasing pH. Higher temperature promotes the uptake of Cu. The effect of temperature is enhanced with increasing pH.

- Good agreement between the experimentally measured and modelled equilibrium data for the ternary system (cation species: Cu^{2+}, Na^{+}, H^{+}) is achieved.

Results for system Mn+Na+H using NICA-IX with log K_i = f(pH, T)

First, second and third column show the experimentally measured and modeled uptakes of Mn, Na and H, respectively. First and second row show the experimentally measured and modeled uptake of cation species at 22°C and 60°C, respectively.

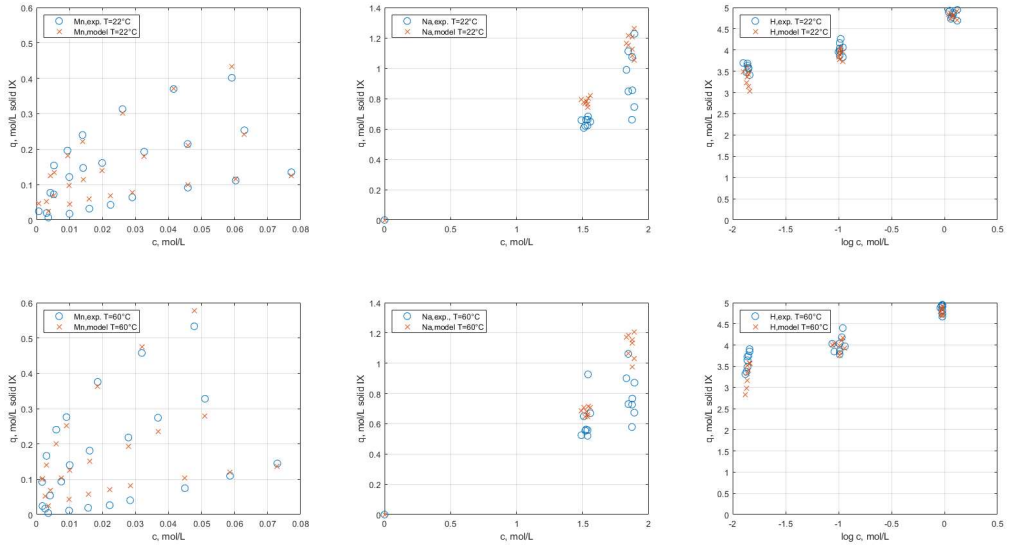

Uptake of Mn is enhanced with increasing pH. Higher temperature promotes the uptake of Mn. The effect of temperature is enhanced with increasing pH.

- Good agreement between the experimentally measured and modelled equilibrium data for the ternary system (cation species: Mn^{2+}, Na^{+}, H^{+}) is achieved.

Results for system Al+Na+H using NICA-IX with log K_i = f(pH, T)

First, second and third column show the experimentally measured and modeled uptakes of Al, Na and H, respectively. First and second row show the experimentally measured and modeled uptake of cation species at 22°C and 60°C, respectively.

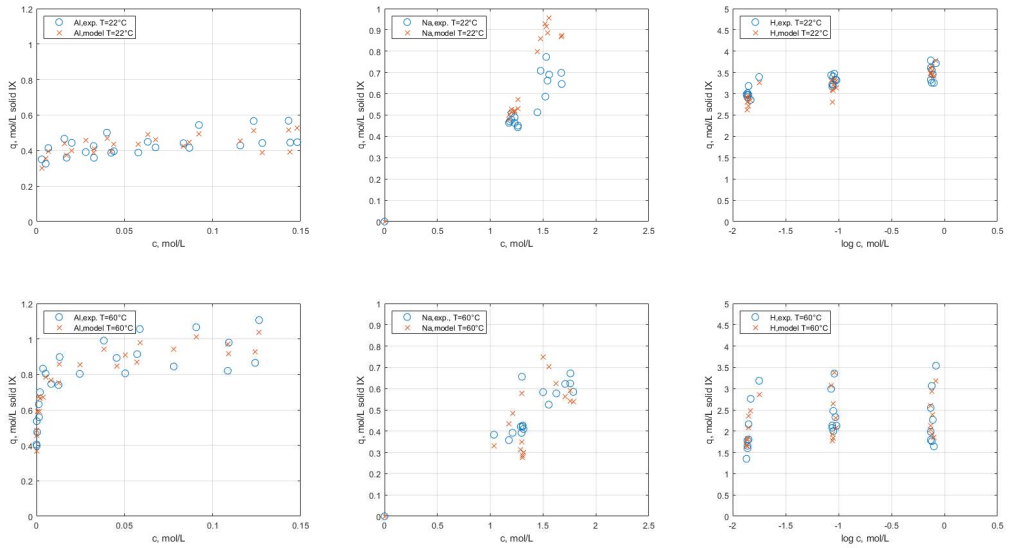

Chelating resin TP260 shows strong affinity towards Al with minor effect of the pH. Higher temperature promotes the uptake of Al.

- Good agreement between the experimentally measured and modelled equilibrium data for the ternary system (cation species: Al^{3+}, Na^{+}, H^{+}) is achieved.

Results for system Fe+Na+H using NICA-IX with log K_i = f(pH, T)

First, second and third column show the experimentally measured and modeled uptakes of Fe, Na and H, respectively. First and second row show the experimentally measured and modeled uptake of cation species at 22°C and 60°C, respectively.

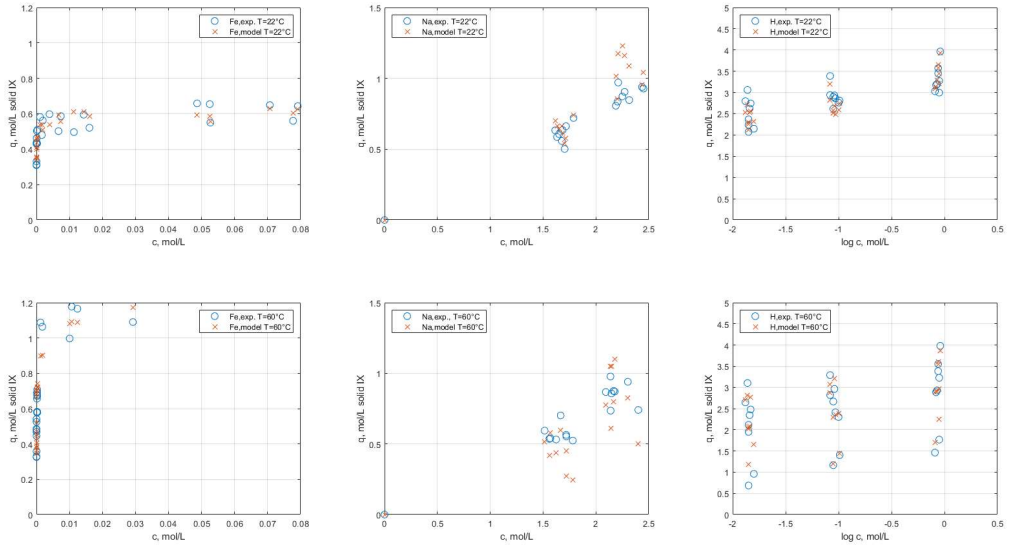

Chelating resin TP260 shows very strong affinity towards Fe. Only minor effects of pH on the uptake of Fe are observed. Higher temperature promotes the uptake of Fe.

- Good agreement between the experimentally measured and modelled equilibrium data for the ternary system (cation species: Fe^{3+}, Na^{+}, H^{+}) is achieved.

Results for modelling of multicomponent (LIBWL) IX equilibria with nine cations (H, Na, Li, Co, Ni, Cu, Mn, Fe, Al)

Notes on the multicomponent equilibrium (LIBWL) measurements and modelling

- Experimental procedure for LIBWL equilibrium data like in single equilibrium metal measurements
  - Obtained aqueous phase equilibrium concentration is used to calculate resin phase concentration
  - Experimentally measured solid phase composition is compared to the modeled one
  - pH range was 0 – 1.8 including values between 0 and 1 as well as 1 and 1.8 to see if model calculation is correct
  - LIBWL:

	Al	Co	Cu	Fe	Li	Mn	Ni
c [g/L]	1.5	16.8	2.1	0.8	2.5	2.1	2.0

- NICA-IX with log K_i = f(pH, T) is still an explicit model
  - Advantage: input values are concentrations of aqueous phase and corresponding resin phase concentration is calculated

Results for modelling of multicomponent (LIBWL) IX equilibria using the gained model parameters at T=22°C

Chelating resin TP260 was contacted with synthetic LIBWL. Graph shows the experimentally measured and modeled uptake of cation species at 22°C.

Region for uptake of LIB metals is highlighted.

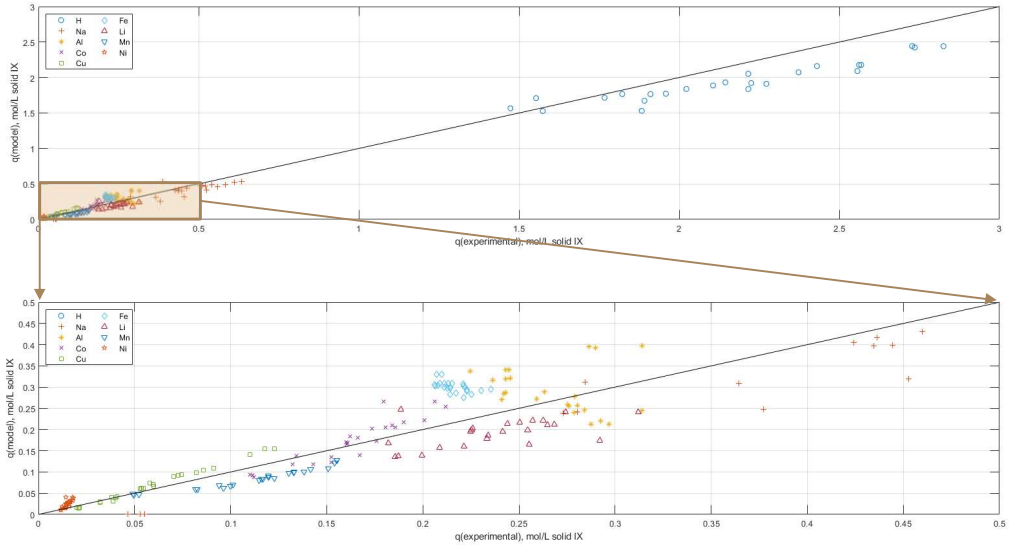

The experimental and modeled data correlate well.

- The model and experimental data for synthetic LIBWL with nine cations correlate well.

Results for modelling of multicomponent (LIBWL) IX equilibria using the gained model parameters at T=60°C

Chelating resin TP260 was contacted with synthetic LIBWL. Graph shows the experimentally measured and modeled uptake of cation species at 60°C.

Region for uptake of LIB metals is highlighted.

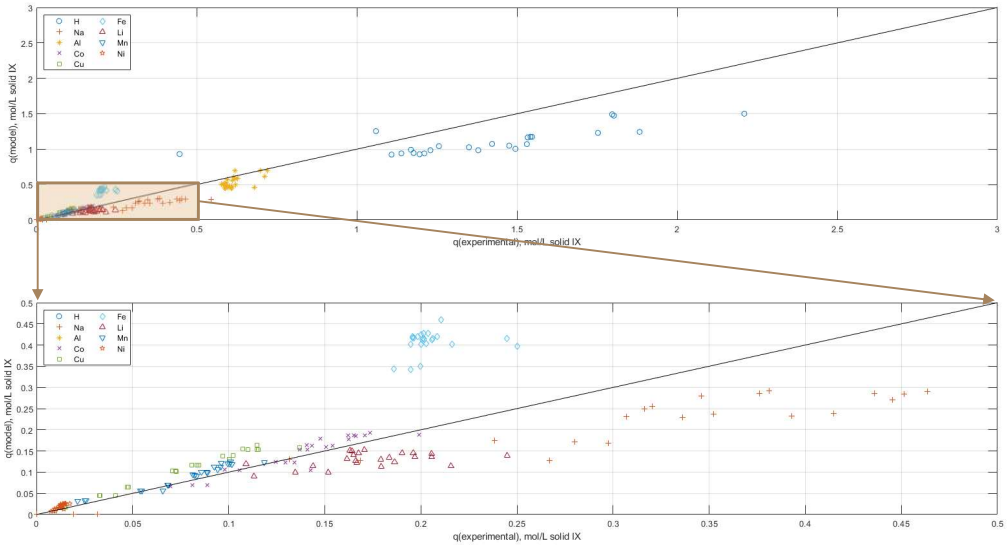

The experimental and modeled data correlate well. Overestimation of Fe uptake is explained by the very strong affinity of TP260 towards Fe. The model predicts a higher uptake of Fe than physically possible as TP260 took almost all Fe from the aqueous phase.

- The model and experimental data for synthetic LIBWL with nine cations correlate well.

Summary, Conclusion and Outlook

- Equilibrium data for the chelating resin Lewatit® TP260 and LIB metals at higher concentrations and acidities was measured for three pH values at 22°C and 60°C
- MAL, ideal competitive ion exchange model and NICA-IX with a fixed set of parameters cannot explain the equilibrium data
- A semi-empirical model (NICA-IX with lin. correlation of $\log_{10} K_i$ and pH) is suggested and explains the equilibrium data for the single metals well
- Calculated resin phase composition for a given liquid phase with nine cations (synthetic LIBWL) correlates well with the experimental data
- Data and model will help in process development of LIB recycling processes

Acknowledgement

- Financial support:
  - BATix, funded by Steel and Metal Producers' Fund

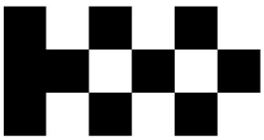

Teknologiateollisuuden
100-vuotissäätiö

- Supervisors and co-authors:
  - Prof. Tuomo Sainio
  - Dr. Sami Virolainen

A STUDY ON THE RECYCLING OF LITHIUM-ION BATTERIES FROM NEWLY GENERATED RECHARGEABLE SMALL ELECTRONIC DEVICES

By

Mooki Bae, Hyunju Lee, Hyeon-ji JO, Sookyung Kim and Yosep Han

Korea Institute of Geoscience and Mineral Resources (KIGAM), Republic of Korea

Presenter and Corresponding Author

Mooki Bae
muki.bae@kigam.re.kr

ABSTRACT

In 2021, the global home appliance market size increased by 8% compared to 2020, reaching an all-time high of about $360 billion. In particular, rechargeable and non-rechargeable small appliances grew by about 21% compared to the same period last year, and are expected to grow by 2.5% annually until 2030. Nevertheless, an effective treatment process and method for future waste resources have not been established. In general, the pretreatment process of large waste batteries such as electric vehicle batteries goes through the steps of physical disassembly - residual value evaluation - classification - waste battery discharge (deactivation), and then is introduced into the crushing process. In the case of small electronic devices, because they are so small, physical treatment (dismantling and discharging) reduces the efficiency of the entire process. In addition, undischarged waste batteries have a risk of fire or explosion when small rechargeable electronic devices are directly shredded. Among electric vehicles and medium/large home appliances, products that include batteries are processed through a discharge system to prevent fires and explosions during pre-recycling, but remarkably small-sized wireless and rechargeable electronic products (wireless earphones, robot vacuum cleaners, Bluetooth audio devices, smart watch, etc.) requires the development of a preprocessing system for small home appliances that does not require physical disassembly and discharge systems.

In this study, a safe crushing technology was researched through a pretreatment system customized for small equipment, and hydrometallurgical research was conducted to recover cobalt, lithium, nickel, etc. from black powder containing valuable metals generated through pretreatment.

A fire-resistant shredder for small electronic devices was manufactured to be shredded in an inert gas atmosphere, and the effect of the type and partial pressure of gas on fire during crushing was investigated. In the air, sparks and fire occurred due to contact between the cathode active material and oxygen, but no fire occurred in the shredded material. However, since a fire due to an explosion can be expected when crushing more than a pilot scale, crushing was carried out in a nitrogen and carbon dioxide atmosphere. The crushing was performed while changing the nitrogen partial pressure to 85%, 90%, and 95%, and at 85%, no spark occurred during crushing, but a fire occurred in the crushed material after completion of crushing. Even at a nitrogen partial pressure of 90%, sparks did not occur during crushing and a fire occurred in the crushed material. At a nitrogen partial pressure of 95%, no sparks or fire occurred. In the case of carbon dioxide, the experiment was conducted while changing the partial pressure by 10%, 20%, and 30%. Sparks and fires did not occur during crushing under 10-30% conditions, and the crushed materials were also in a stable state.

The chemical components of the crushing product obtained through the pretreatment are shown in the table below.

Table. Chemical compositions of crushed material

Sample	Chemical composition (wt%)						
waste battery sample	Ni	Co	Mn	Li	Cu	Al	Carbon
	16.55	4.62	5.22	3.05	3.25	3.73	30.1

Nickel, cobalt, manganese, lithium, copper, aluminum, and graphite are the main components in anode and cathode materials, and fine black powder obtained through classification of 0.2 mm or less contains a large amount of nickel, cobalt, lithium, and manganese. Valuable metals in black powder were effectively separated through flotation, and as a result, high-quality black powder concentrate was obtained, and efficient recovery and low energy generation (relative CO_2 emission reduction) can be expected in the hydrometallurgical process.

Keywords: Recycling, Lithium-ion battery, Small electronic device, Safe crushing technology

Contents

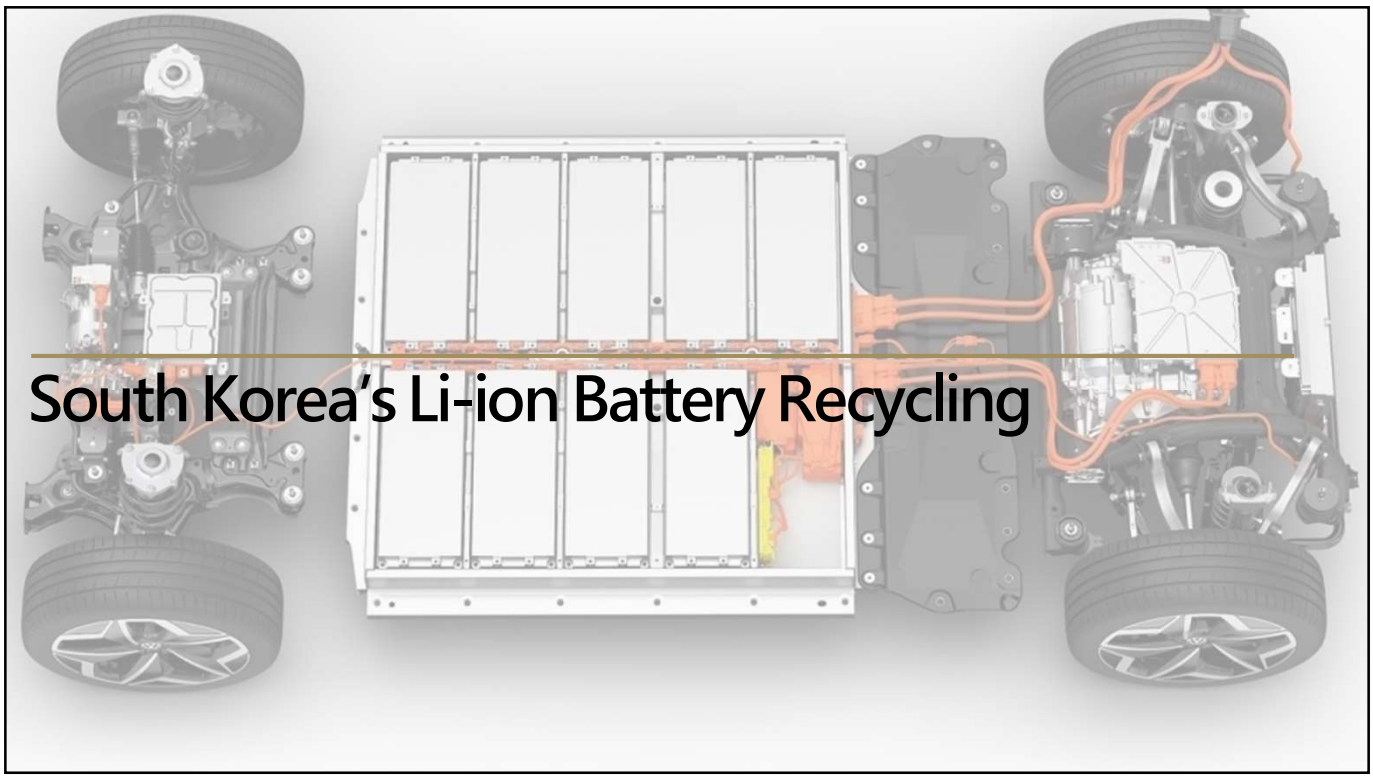

South Korea's Li-ion Battery Recycling

Battery Recycling

Recycle vs. Re-Use

Korean battery circular economy is classified into **recycling** (extracting and recycling rare metals by decomposing waste batteries into cells) and **reuse** (using waste batteries in their original form for other purposes), and there are differences in necessary facilities and requirements.

RECYCLING		RE-USE
• A method of extracting and recycling rare metals by decomposing waste batteries in cell units	Definition	• How to use waste battery modules and packs as ESS or UPS
• Small IT device battery	Target	• Medium and large batteries (electric vehicle batteries, etc.)
• Waste battery discharge system required • Required to secure recovery process technology	Requirements	• Waste battery diagnosis and analysis equipment • Advantageous for ESS production and operation know-how
• Reduction of raw material cost • Sales $600-900/24kWh battery packs by extracting metals	Expected Effects	• No need to dismantle the module and cell • Stable dismantling process and low cost

Battery Recycling

Korea's Battery Recycling Industry

The size of the South Korean battery recycling market was $170 million in 2020, and it is expected to grow at a compound annual rate of 6.1% until 2025, reaching $220 million. Accordingly, the disposal of used electric vehicle batteries is estimated to increase from 100 units in 2019 to 79,000 units in 2029.

Battery Market Forecast

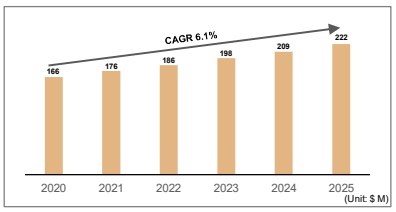

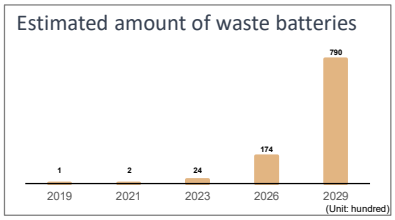

Flow sheet for Battery recycling

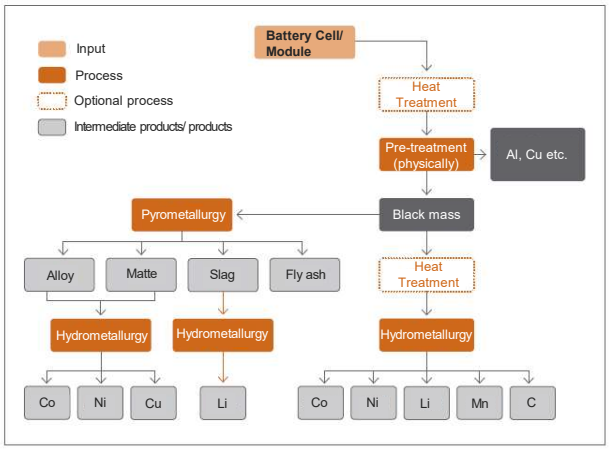

Battery Recycling

Comparison of Large and Small Battery Recycling Processes

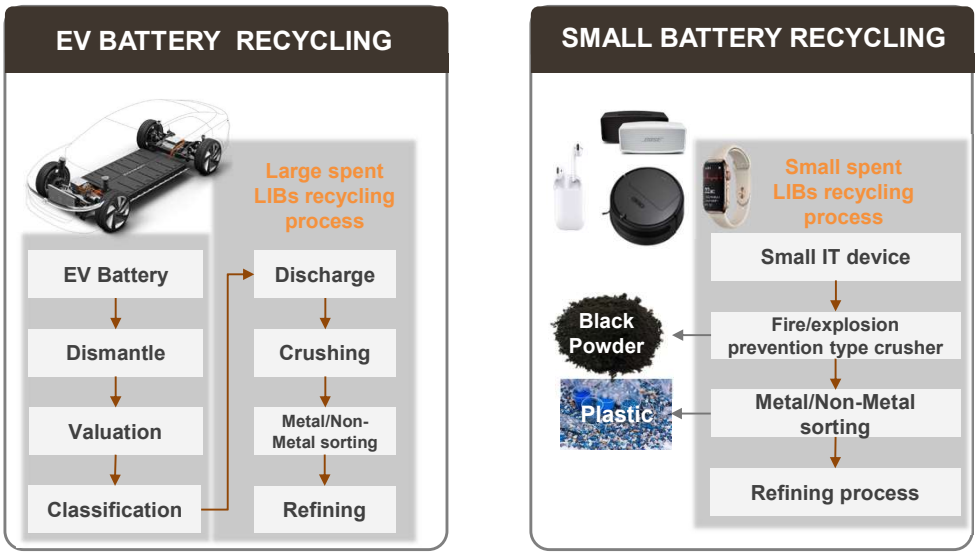

LIBs Recycling R&D

Research on Pre-treatment for Small Electrical Appliances(on-going)

Development of technology for stable dismantling of small waste electrical and electronic products including lithium-ion batteries and the optimal separation process for plastic-metal materials

WHY? Explosion and fire problems during pre–treatment

HOW? **Development of fire/explosion prevention type crusher**

Establishment of customized pretreatment system for future waste

LIBs Recycling R&D

Experimental part 1: Development of Stable Shredding Technology

✓ **Battery shredding**

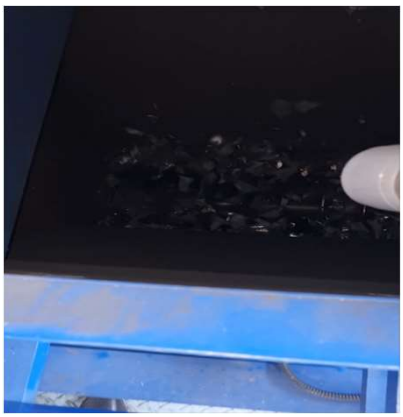

✓ **Causes of fire and explosion**

Fire	• Combustion of organic materials/electrolyte by sparks caused by short circuit • Heat generated by thermit reaction by Al separation film and cathodic oxide-white smoke • During charging and discharging, unconverted energy generates heat and burns
Explosion	• By burning oil vapor • By thermit reaction – explosive • Pressure increase due to oil vapor combustion • Increased pressure due to gas generation by oxide and carbon reaction

LIBs Recycling R&D

Experimental part 1: Development of Stable Shredding Technology

✓ **Stable shredder development**

LIBs Recycling R&D

Experimental part 1: Development of Stable Shredding Technology

✓ **Log C-pH Diagram**

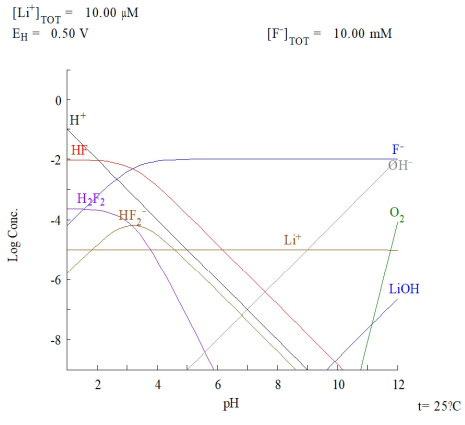

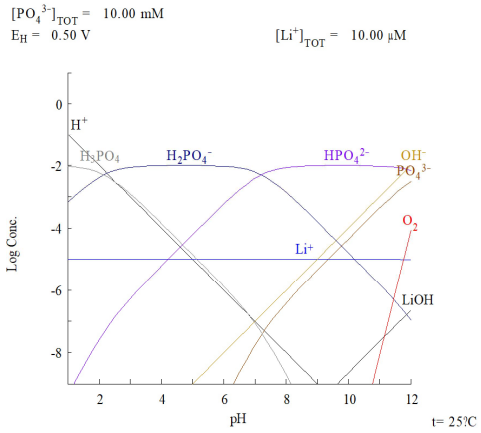

$LiPF_6 + H_2O \rightarrow LiF \cdot HF + HF \uparrow + POF_3 \uparrow$

$POF_3 + H_2O \rightarrow H[PO_2F_2]$

$H[PO_2F_2] + H_2O \rightarrow H[PO_3F] + HF \uparrow$

$H_2[PO_3F] + H_2O \rightarrow H_3[POF] + HF \uparrow$

LIBs Recycling R&D

Experimental part 1: Development of Stable Shredding Technology

✓ **Samples information**

No	Robot Vacuum					Handheld Vacuum				
	Weight(g)				Total	Weight(g)				Total
	Battery	Plastic	Ferrous	PCB		Battery	Plastic	Ferrous	PCB	
1	0.199	2.375	0.857	0.146	3.577	0.778	2.037	0.163	0.037	3.015
2	0.198	2.742	0.321	0.099	3.360	0.405	1.817	0.314	-	2.536
3	0.672	1.531	0.243	0.192	2.638	0.586	2.440	1.234	0.037	4.297
4	0.201	1.934	0.383	0.115	2.633	0.460	2.431	0.310	0.036	3.237
5	0.218	2.086	0.415	0.164	2.883	0.265	2.210	0.164	0.030	2.669
6	0.199	1.616	0.332	0.033	2.180	0.105	2.346	0.250	0.087	2.788
7	0.428	2.522	0.428	0.145	3.523	0.251	2.522	0.402	0.046	3.221
8	0.213	2.087	0.399	0.170	2.869	0.382	2.506	0.346	0.054	3.288
9	0.221	2.011	0.532	0.195	2.959	0.242	2.063	0.646	0.033	2.984
10	0.426	2.437	0.862	0.103	3.828	0.270	1.813	0.291	0.016	2.390
11	0.193	2.099	1.446	0.166	3.904	0.243	2.056	0.218	0.025	2.542
12	0.191	1.513	0.410	0.072	2.186	0.562	2.498	1.237	0.016	4.313
13	0.583	1.666	0.362	0.173	2.784	0.283	1.905	0.369	0.012	2.569
14	0.642	1.605	0.171	0.148	2.566	0.705	2.025	0.428	0.055	3.213
15	0.692	2.892	0.141	-	3.725	0.177	0.403	0.191	0.010	0.781
Av.	**0.352**	**2.074**	**0.487**	**0.137**	**3.050**	**0.381**	**2.071**	**0.438**	**0.035**	**2.925**
wt%	**11.53 %**	**68.01 %**	**15.96 %**	**4.50 %**		**13.02 %**	**70.87 %**	**14.96 %**	**1.21 %**	

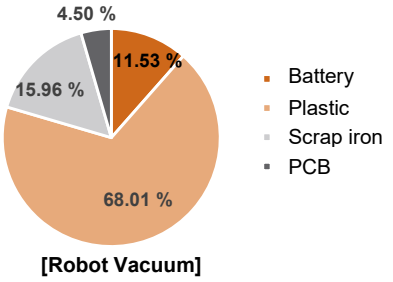

[Robot Vacuum]

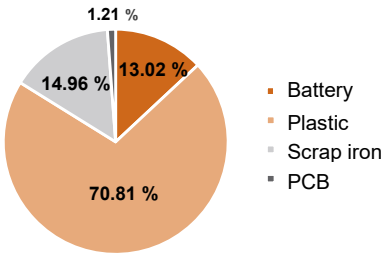

[Handheld Vacuum]

LIBs Recycling R&D

Experimental part 1: Development of Stable Shredding Technology

✓ **Stable shredder development**

- Conducting a shredding experiment with a spent batteries secured after disassembling small waste appliances
- To derive stable crushing conditions in an inert gas

[Separated LIBs]

[Lab scale shredder]

[Gas, Salt water injection system]

LIBs Recycling R&D

Experimental part 1: Development of Stable Shredding Technology

✓ **Experimental Results**

Atmosphere	Contents		
	Spark	Fire	Note
Atmospheric	O	X	Spark long time
Nitrogen 85%	X	O	Shredded product fire
Nitrogen 90%	X	O	Shredded product fire
Nitrogen 95%	X	X	-
Carbon dioxide 10%	X	X	-
Carbon dioxide 20%	X	X	-
Carbon dioxide 30%	X	X	-

- Sparks continuously occur for about 30 sec. in atmospheric shredding conditions
- N_2 85%, 90% partial pressure shredding product fire and stable shredding in N_2 95%
- CO_2 atmosphere is possible at all partial pressures (10-30%) for stable shredding

[Atmospheric shredding]

[Nitrogen 85% shredding]

LIBs Recycling R&D

Experimental part 1: Development of Stable Shredding Technology

✓ **Compositions of shredded LIBs samples**

Name	Chemical composition(%)								
	Li	Ni	Co	Mn	Fe	P	Cu	Al	C
Un-fired sample	3.54	21.6	6.07	6.62	0.41	0.48	0.33	0.20	35.5
Sample on fire	1.95	10.4	3.74	3.28	0.47	2.83	0.80	1.59	-

- The occurrence of fire during the shredding process has an effect on the decrease in the concentration of Co, Ni, and Li
- Therefore, the pretreatment process is reduced through proper atmosphere control without the discharge process

[Atmospheric shredding]

[Nitrogen 85% shredding]

LIBs Recycling R&D

Experimental part 2: Efficient Separation Technology for Electrode Active Materials

✓ **Particle size analysis of black powder**

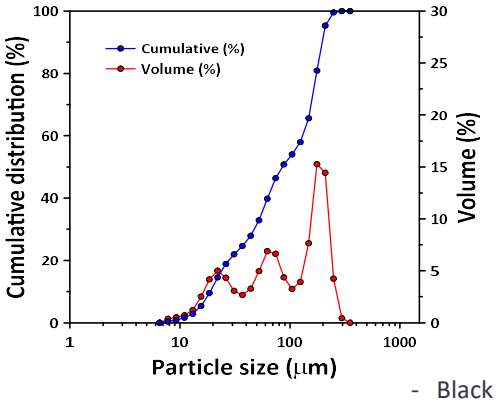

✓ **Composition of lithium-ion batteries(NCM)**

Cathode material (%)			
Ni	Co	Mn	Li
16.55	4.62	5.22	3.05
Other metal and carbon (%)			
Cu	Al	Carbon	
3.25	3.73	30.1	

- Black powder recovered after classification of ground spent LIBs
- Recovered black powder is divided into the cathode material containing Ni, Co, Mn, and Li, and the portion separated into metals or carbon

LIBs Recycling R&D

Experimental part 2: Efficient Separation Technology for Electrode Active Materials

- Since the material is in a powdered state, no pretreatment process, such as density or electrostatic separation, is performed before flotation

[Denver D12 laboratory flotation machine]

[Experimental conditions]
- Agitation 1500 rpm
- Time 0.5, 1, 2, 4 min
- Pulp density 1% (w/w)
- Flocculant conc. 0, 0.75, 1.5, 3 (kg/ton)
- Foaming agent conc. 1.5 (kg/ton)

$$\text{Recovery}(\%) = \frac{c(f-t)}{f(c-t)} \times 100 \text{ ; >90\%}$$

Impurities ; <2.0%

[Recovery efficiency of metals]

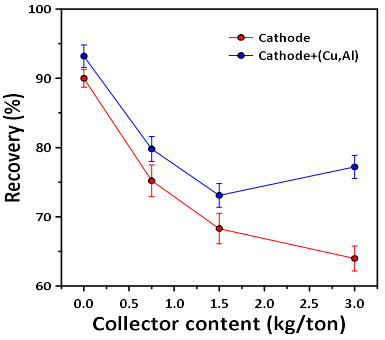

[Composition of carbon after flotation]

Carbon (%)				
Feed	Collector content (kg/ton)			
	0 (natural floatability)	0.75	1.50	3.00
30.1	22.6	8.93	5.74	3.67

LIBs Recycling R&D

Experimental part 2: Efficient Separation Technology for Electrode Active Materials

✓ **TGA analysis**

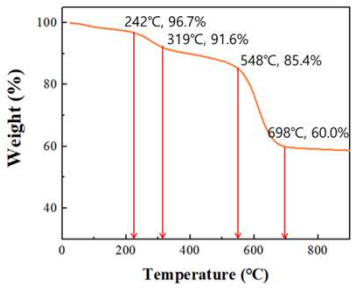

[feed]

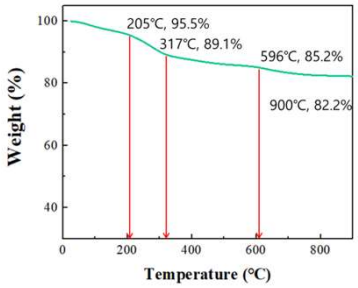

[sink]

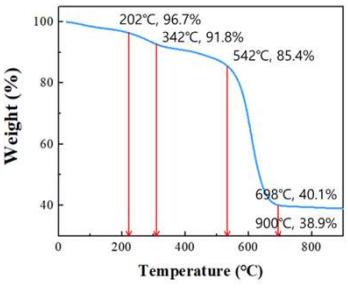

[floating]

- Feed sample contains a relatively high amount of carbon and binder
- Sink samples showed a decrease in carbon and binder content, whereas floating samples showed a significant increase in binder and carbon content

LIBs Recycling R&D

Experimental part 2: Efficient Separation Technology for Electrode Active Materials

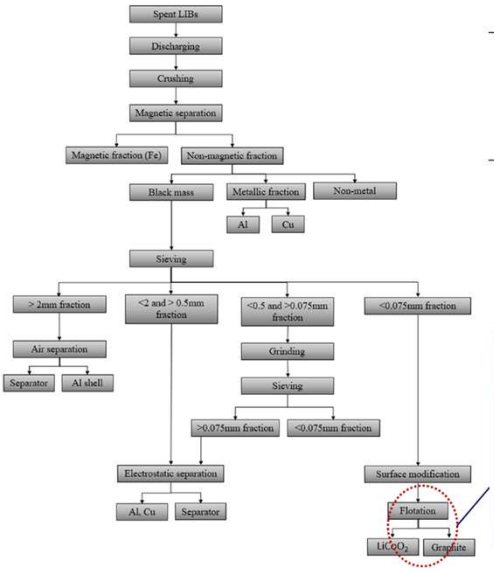

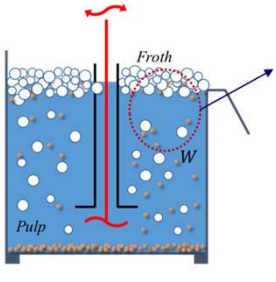

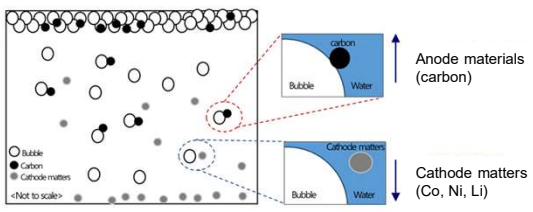

- Due to the presence of a significant amount of active material in micro-sized black powder, selective separation based on the surface hydrophobicity characteristics of the particle-bubble is possible
- In some cases, pre-treatment involving specific gravity and electrostatic separation may be necessary, and floatation separation is carried out through reverse floatation process (with the target material sinking and impurities floating)."

Conclusions

- ✓ **Stable pre-processing system for newly generated small electronics**

  N_2 85%, 90% partial pressure shredding fire and stable in N_2 95%
  CO_2 atmosphere is stable shredding (partial pressures 10-30%)

- ✓ **Valuable metals (Ni, Co, Mn, Li) in black mass were effectively separated through flotation**

  Reverse floatation process for separation of anode materials (floating, carbon) and cathode materials (sinking, Ni, Co, Mn, Li)

LITHIUM ION BATTERIES IN THE CIRCULAR ECONOMY – NEW DEVELOPMENTS FROM CSIRO

By

[1]Thomas Rüther, [1]Adam Christensen, [2]Gavin Collis, [1]Owen Lim, [3]Andreas Monch, [1,4]Oliver Pohl, [1]Yanyan Zhao

[1]CSIRO Energy, Australia
[2]CSIRO Manufacturing, Australia
[3]CSIRO Mineral Resources, Australia
[4]Swinburne University, Australia

Presenter and Corresponding Author

Thomas Ruether
Thomas.ruether@csiro.au

ABSTRACT

The estimated 2030 global demand for lithium-ion battery (LIBs) is expected to be around 3 TWh, nearly 10 times the demand of 2020. Large volumes of LIBs are entering national economies, including Australia's and beyond Battery electric Vehicles (BEV), are expected to support electrical grid stability and renewable energy adoption.

The implementation of the new technology needs to be accompanied by the principles of sustainability and circular economy, hence innovative End of Life (EoL) solutions are required for the expected large volume resource streams. The estimated EoL LIBs in Australia is expected to exceed 140,000 t by 2030 according to a 2020 report by the Battery Stewardship Council. To address this need, CSIRO's Electrochemical Energy Storage team at Clayton VIC has, over the past five years, developed an overarching project that will advance various aspects of LIB recycling.

For delegates from various backgrounds, this presentation covers three main topics (i) the greenhouse gas emissions, energy inputs and costs associated with producing and recycling lithium-ion cells for the three most common cathode chemistries: NMC, NCA and LFP (ii) overview of progress in key science areas – second life of LIBs and CSIRO's proprietary lithium salt recovery process, now entering into the pilot scale phase and (iii) opportunities for further development, collaboration and investment.

References

R. E. Ciez and J. F. Whitacre, Examining different recycling processes for lithium-ion batteries, Nature Sustainability 2019, 148, 148–156.
Battery Stewardship Council, Australian Battery Market Analysis, Report June 2022 (accessible online bsc.org.au).

Growth of Battery Capacity Demand

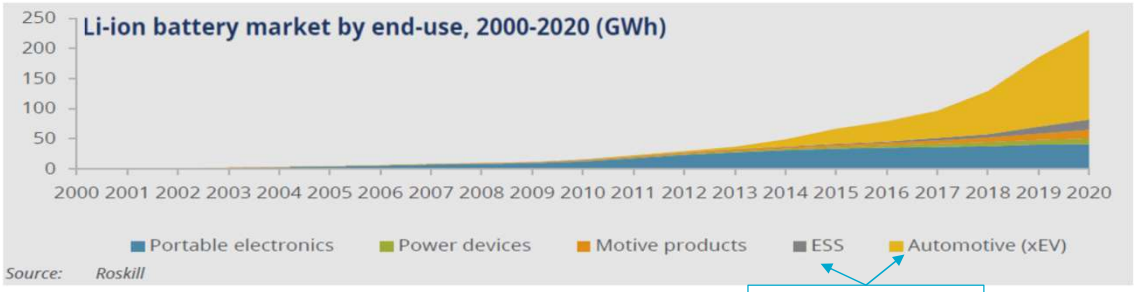

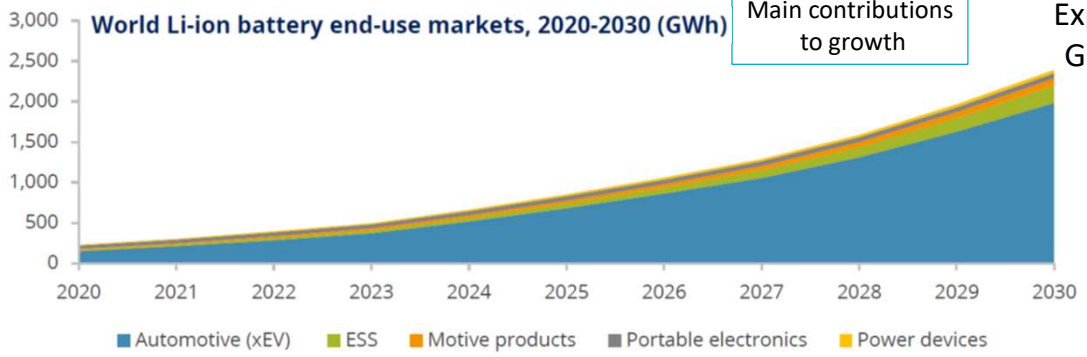

Main contributions to growth

Expected Growth 10 x

Competition LIB – NMH – NiCd

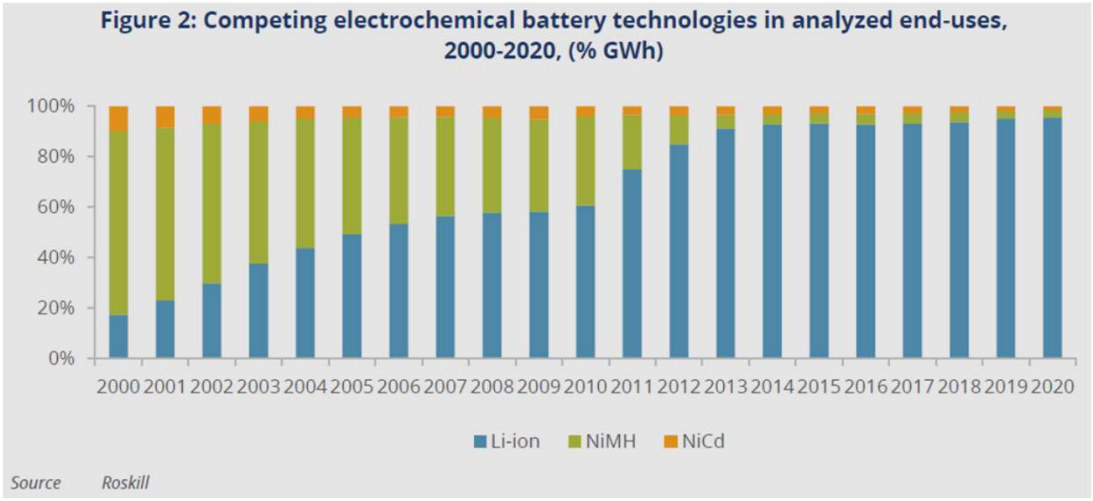

NMH: Decline in HEVs
NiCd: Environmental regulations

Cost of Production

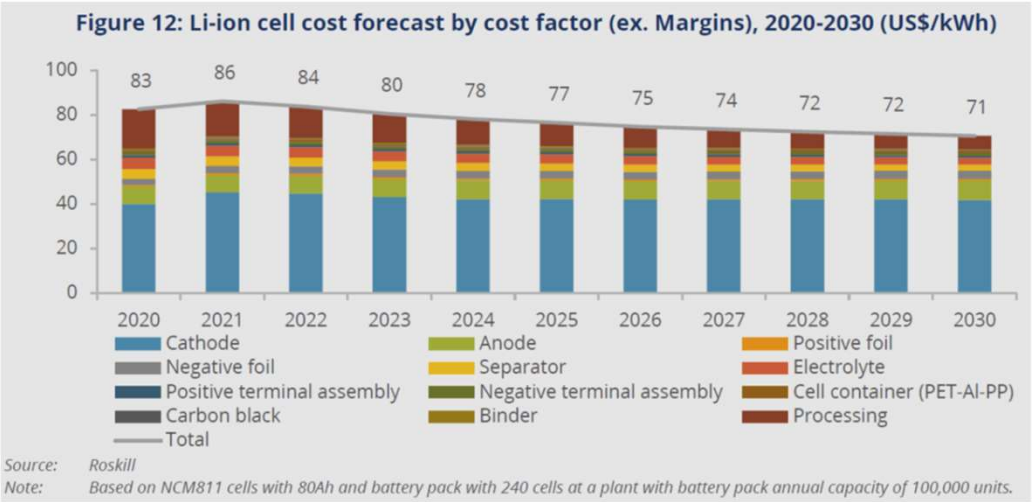

Cathode is largest cost contributor
Changes mainly due to processing costs

The obvious questions arising…

Source of batteries

Supply of key materials

What does this mean for GHG emissions

How do we deal with the emerging waste stream, do we have an EoL strategy ??

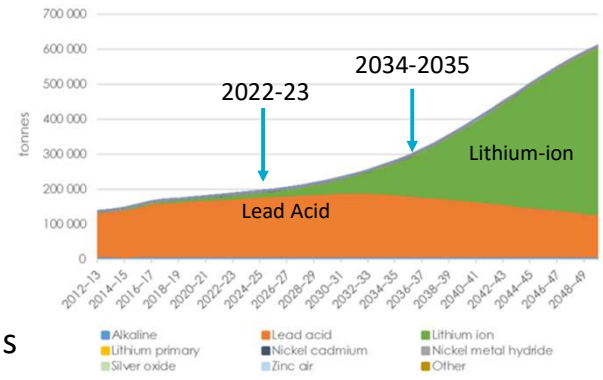

Projected EoL Lithium ion batteries in Australia:

~ 100,000 tonnes by 2034-35.

SOURCE: Battery stewardship Council

Supply of LIBs

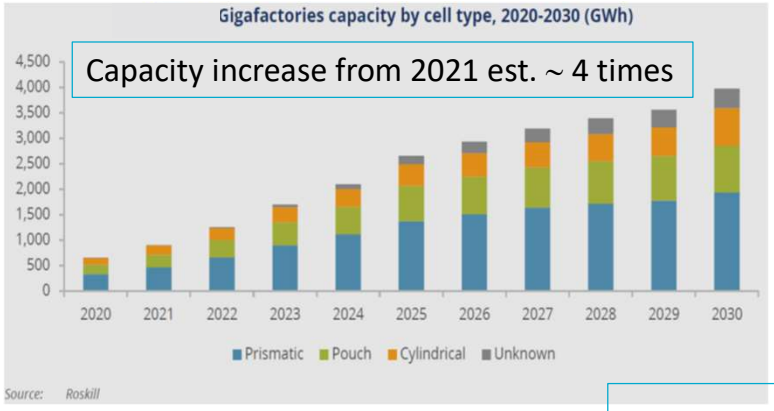

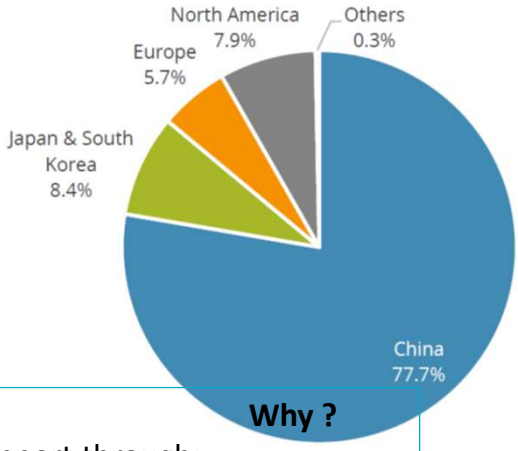

Why ?

EU:
Attracted Asian manufacturers
Gov. strategic support
Move towards Green Economy

CH Gov. support through:

- R&D funding
- Subsidies for manufacturers
- Financing of charging stations
- Priority registration over ICE vehicles

Battery Manufacturing GHG Emissions

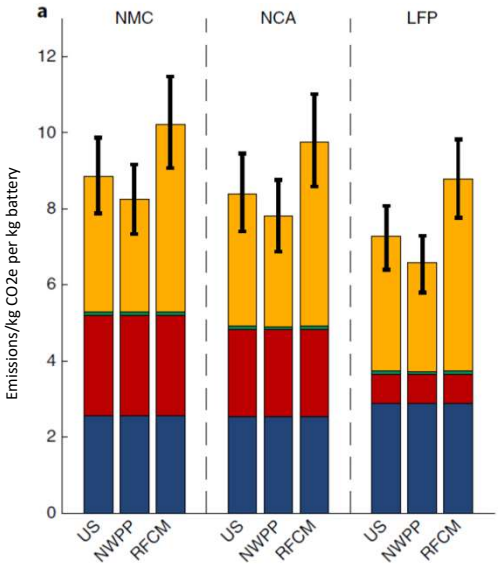

Source: Ciez et al. Nature Sustainability, 2019, 2, 148–156

Materials account for 50-60% of GHG-e

Variations:

- Cathode material
- Location of Manufacture

Production of commodities in kg CO2-e/kg

- Copper 1.4
- Aluminium 6.7
- Iron/Steel 1.5

Source: IEA 2022

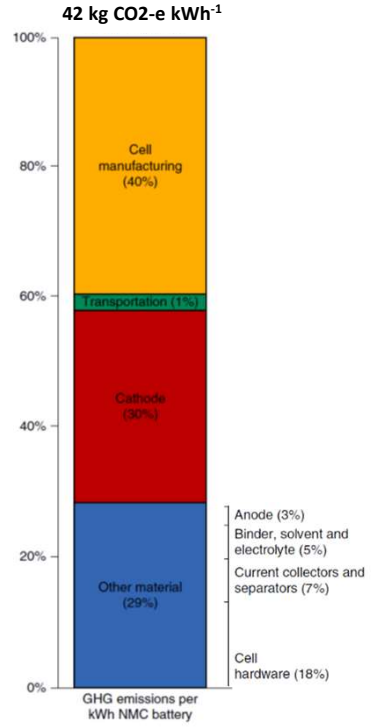

Cell Chemistry	Spec. Energy Wh kg^{-1}	Total Materials GHG-e kg CO_2e kg^{-1}	Manufacturing GHG-e kg CO_2e kg^{-1}
NMC	210	4.4	3.0
NCA	190	4.1	4.1
LFP	100	3.7	2.9
LMO*	114	5	1

Data for cylindrical cells except *

NMC: Nickel Manganese Cobalt Oxide

NCA: Nickel Cobalt Aluminium oxide

LFP: Lithium Iron Phosphate

LMO: Lithium Manganese Oxide

How beneficial is LIB Recycling?

GHG-e and E-consumption

- Pyrometallurgy – net Increase
- Hydrometallurgy – net Decrease
- Direct cathode recycling – net Decrease
- Cathode chemistry decides

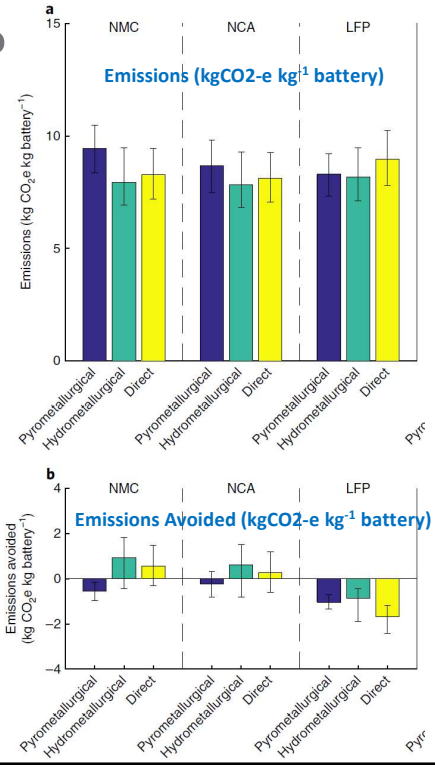

Raw material

	demand/Mt 2020	demand/Mt 2030	production/Mt 2020
Li	0.380	2.3 (6 x)	0.41
Co	0.021	0.17 (8 x)	0.14
Ni	0.1295	1.45 (11 x)	2.5
Cu	0.319	2.38 (7 x)	20.0
Al (foil)	0.194	1.42 (7.5 x)	16.5
Nat. Gr	<0.4	1.77 (4.4 x)	0.96

Sources: Roskill 2022, US Geological Survey, IEA, Int. Aluminium

LIB Recycling Pathway

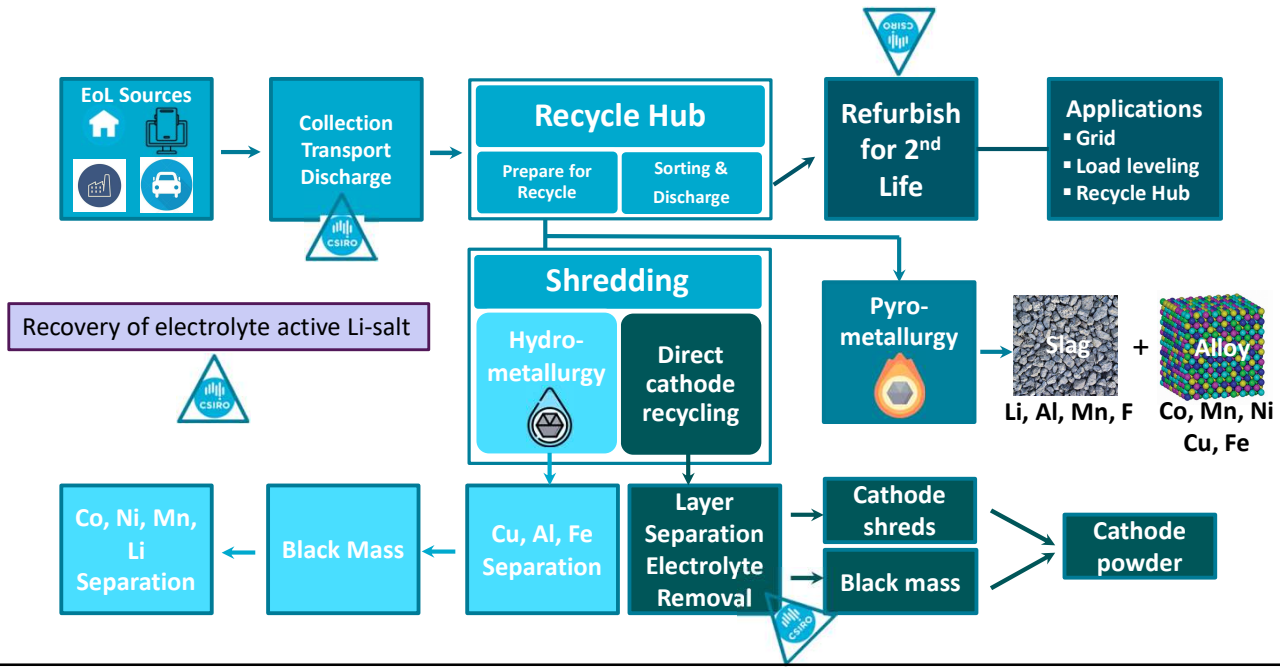

Demonstration Discharging Batteries

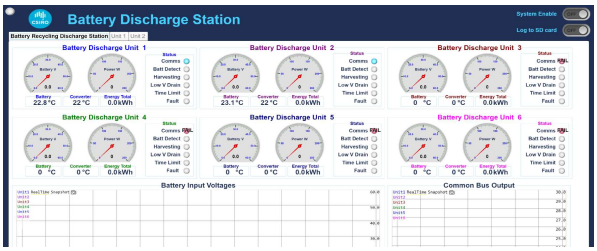

- **Demo for various packs, i.e. 48V unit, total of 0.6kWh removed**
- **Energy can be fed into grid or facility mains**
- **Unit reached < 0.1 V**
- **Demo built with common power electronics and hardware**
- **Scalable depending on facility requirements**
- **Industry Partner Project**

Brisbane (Sept 2018)

- EoL LIBs can contain 50-80% of initial energy
- Damage or short circuit create fire hazards
- Multiple different form factors complicate this energy removal

Demonstration Battery Second Life / Reuse

- **Real-life demonstrations (5kW) showing viability can dissuade consumer concerns**
- **Developed versatile battery management system (BMS)**
- **System is battery chemistry agnostic**
- **Industry Partner Project Demo: EV EoL batteries**
- **PV into battery and then grid export**
- **Large pack development for office/commercial load support with PV input**

Standards for LIB packs EoL @ 70-80% capacity

…likely to be fit for other purposes after "health check"

…but true hurdles, Certification Regulations Warranties

Demonstration Battery Shredding

- 1st Demo of its kind in AUS
- Custom built for High Safety operation
- Dry shredding
- Total nitrogen atmosphere
- Optical Chamber monitoring
- IR Temperature monitoring
- Interchangeable hopper & receiving vessels
- Can be used as experimentation platform

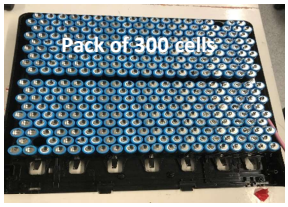

Optical and Thermal Monitoring of process

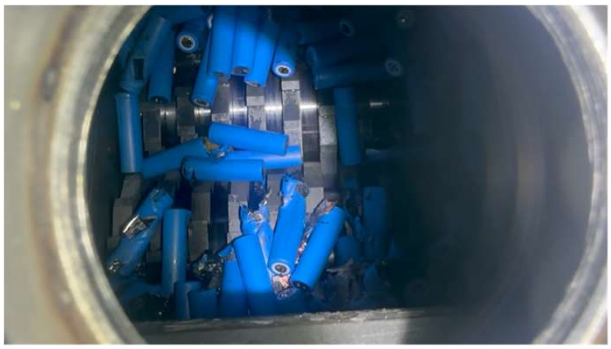

Demonstration Lithium Salt Recovery

Material Use ↔ **Economics** ↔ **Monetary**

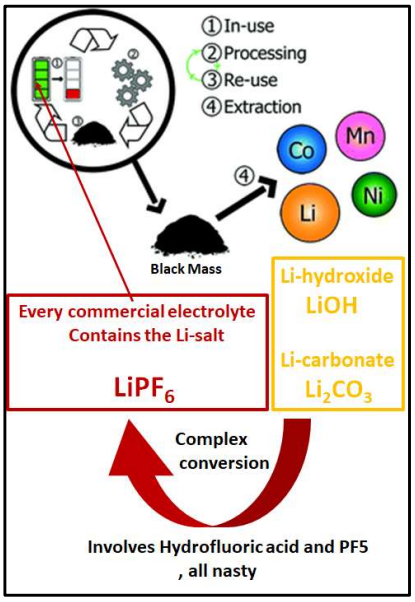

Component	Spot Price 7/20 US$/t	Spot Price Nov/21 US$/t
Electrolyte solution	**132000**	**150000**
$LiPF_6$	7400	59300
Li_2CO_3	7250	28000
LiOH	9500	30000
Nickel	13070	20900
Cobalt	28500	63000

Sources: Metals, Trading economics
$LiPF_6$, OilChem China,
Electrolyte Solution, Alibaba

$LiPF_6$ and Battery Materials Recovery Process

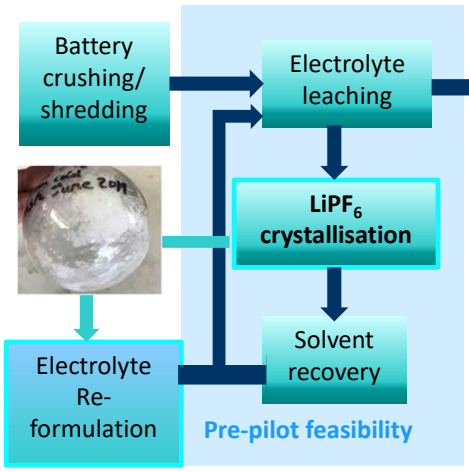

- **Aim:** practical, economic, sustainable process
- **Apply:** benign methodologies
- **Avoid:** environmentally questionable solvents
  high vacuum & temperature processing
  extensive waste volumes
- **Achieve:** an ideal solution for manufacturers and recyclers

✓ Retrofitting to existing recycling processes
✓ Scalable with off-the-shelve chem. eng. equipment
✓ Product obtained in high yield and quality
✓ Can be directly used in manufacture of electrolytes
✓ Material streams can be recirculated

Process Status

- ✓Patent entered National Phases
- ✓Numerous experiments conducted
  - **Process Variables tested (up to 30 g lab scale):**
    - Conditions for effective crystallization
    - Process Temperature
    - Recovery from partially decomposed electrolyte
  - **Phase and Product Analysis**
    - Identification of components in liquid phases
    - Confirmation of Li-salt composition (NMR, EA)
    - Recovery yield >> 80% (based on 1M Electrolyte)
- ✓Battery testing
  - Use of commercial electrode materials
  - Rate testing
- ✓Techno-economic Analysis

A REVIEW OF HYDROMETALLURGICAL FLOWSHEETS CONSIDERED FOR THE TREATMENT OF BLACK MASS

By

Niels Verbaan and Roxanne Naidoo

SGS Natural Resources, Lakefield ON, Canada

Presenter and Corresponding Author

Niels Verbaan
niels.verbaan@sgs.com

ABSTRACT

Recycling of lithium-ion batteries has generated significant attention in recent years due to the increase in demand of EV's. This paper focusses on the hydrometallurgical treatment of the black mass stream produced from the battery shredding operations. Many flowsheet configurations exist and are reported by recycling companies. Typically, flowsheets can be characterized by a) complete metal separation via solvent extraction, electrowinning and/or crystallization operations and b) direct production of battery pre-cursor material. This paper will provide a review of some of the flowsheets considered by current companies and will comment on feed characterization, leach chemistry, SX circuits considered and product recovery circuits.

Keywords: black mass, cobalt, nickel, lithium, sodium sulphate

INTRODUCTION

SGS Canada is a leading supplier of testing services to the mining and metallurgical industries and operates metallurgical laboratories out of Canada, Chile, Mexico, South Africa and Australia. Several clients of SGS (such as Neometals, Aleon Renewable Metals, Coherent Corporation, and H.C. Starck Tungsten) are existing battery recycling firms or are developing technologies to support battery recycling. While researching the overall industry it became apparent that many technologies exist for the hydrometallurgical treatment of black mass. The authors therefore decided to document their review and presented their work to the EV Battery Recycling and Re-use Conference held in Detroit[1] in March 2023. This paper provides further detail and information to this review. The review is not intended to be exhaustive but does show the wide variety of process routes under current consideration.

The use of lithium-ion batteries (LIBs) is expected to increase in the near future due to the increased use of electric vehicles (EVs), which use LIBs as the power source. Figure 1 shows the predicted sales of EVs and the EV market penetration up to 2035. LIBs are also widely used in portable electronic devices (e.g. cellular phones and laptops). The popularity of LIBs is due to their high energy density, high voltages and low weight-to-volume ratio. With the increased usage of LIBs comes the requirement to recycle these batteries. Current feedstock to recycling facilities consists to a large extent of manufacturing scrap (cell or precursor cathode active material, pCAM), and a lesser extent of End-of-Life (EOL) batteries. As the usage of LIBs increases and more EOL LIBs become available, the feedstock to recycling facilities is expected to change from off-spec (i.e. scrap) to EOL material as is shown in Figure 2. As battery chemistries are changing rapidly due to ongoing developments of new batteries with improved performance or due to metal shortages (i.e. cobalt), it is safe to assume that the metal ratios (Ni:Co:Mn) contained in EOL batteries are significantly different from what may be the primary battery chemistry at the time of recycling.

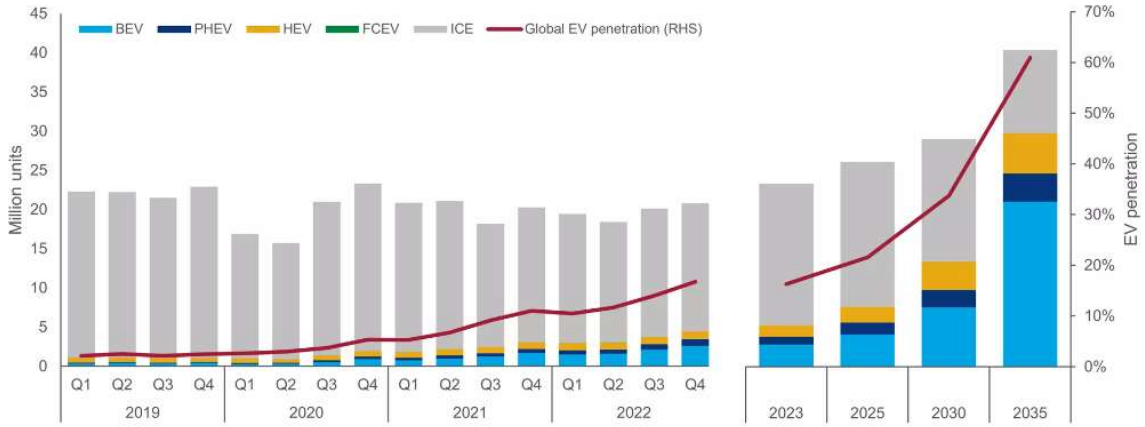

Figure 1 Vehicle Sales Forecast[2]

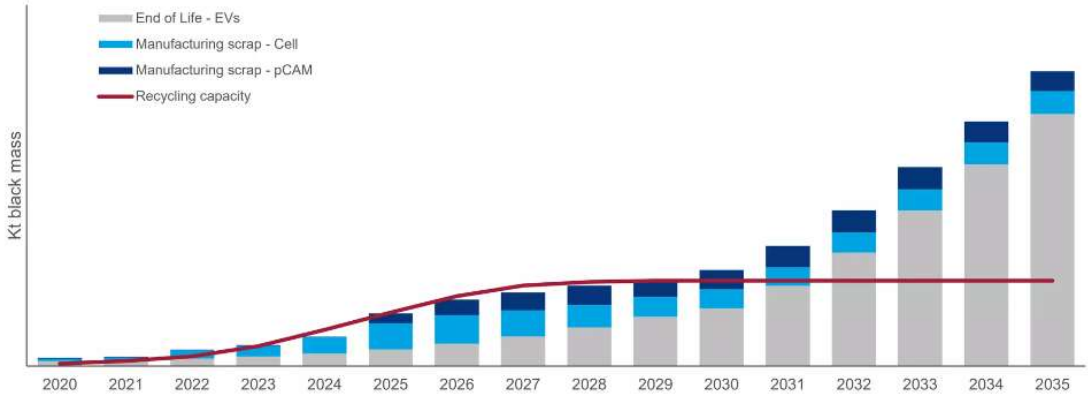

Figure 2 Feedstock and Recycling Capacity in North America[2]

Conceptually, a typical battery recycling flowsheet consists of a mechanical step (shredding) where plastics are separated from the metallics (aluminum and copper foils) and the black mass.

Duessenfeld[3] reports that around 57% (see also Figure 3) of their input LIB mass consists of black mass. This paper focusses on the hydrometallurgical treatment options of the black mass stream.

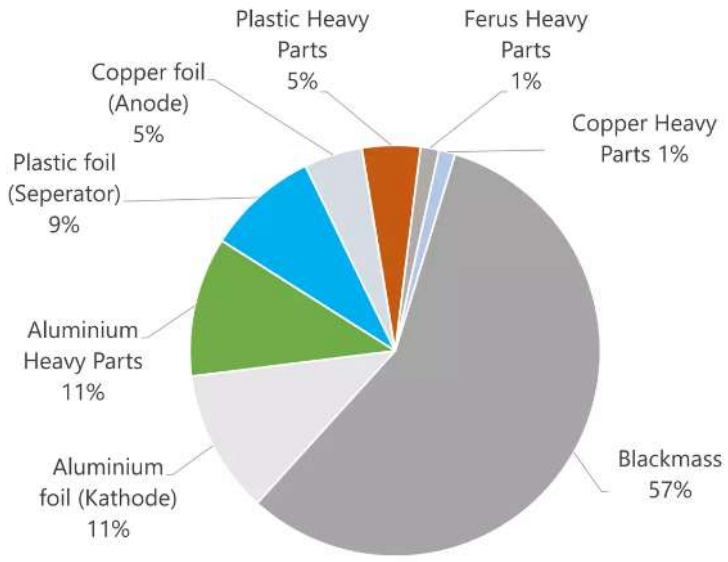

Figure 3 Duesenfeld Mechanical (shredding) Output[3]

BLACK MASS FEED CHARACTERISATION

1.1 Components of LIBs

LIBs consist of various components as shown in Figure 4. The general design of a LIB cell consists of a copper foil current collector, a porous anode which is made of graphite, a porous separator comprised of polypropylene or polyethylene, a porous cathode consisting of active material mixed with conductive carbon and a polymeric binder such as polyvinlylidene fluoride (PVDF) and an aluminum foil current collector. The porous anode, porous cathode and separator are soaked in an electrolyte solution which consists of a lithium salt (such as $LiPF_6$, $LiBF_4$, $LiCF_3SO_3$ and $Li(SO_2CF_3)_2$) which is dissolved in a mixture of organic solvents. Some organic solvents which are typically used are dimethyl carbonate (DMC), ethyl methyl carbonate (EMC), ethylene carbonate (EC), cyclohexylbenzene, polypylene carbonate (PC) diethyl carbonate (DEC), dimethyl sulfoxide (DMSO)[4][5].

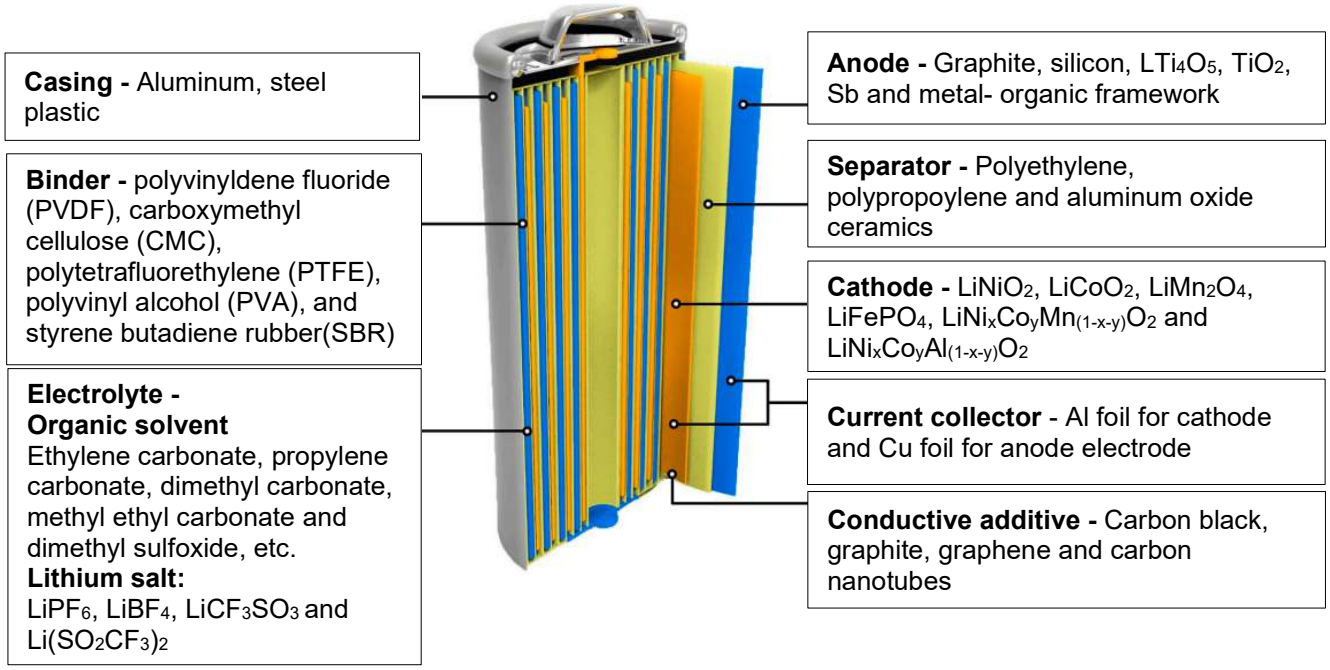

Figure 4: Structure of typical cylindrical LIB[6]

1.2 Black mass processing steps

The spent LIBs are first subjected to discharging and dismantling before various stages of mechanical recovery. However, before the mechanical separation, the LIBs can be subjected to pyrolysis. Pyrolysis is a process whereby the black mass is heated to temperatures of approximately 500-700°C after separation from the shredded material to remove the electrolyte components via thermal decomposition[7]. During the pyrolysis process, the fluorine-containing components are removed. The mechanical recovery stages can include dry crushing, drying sieving, and sorting[8].

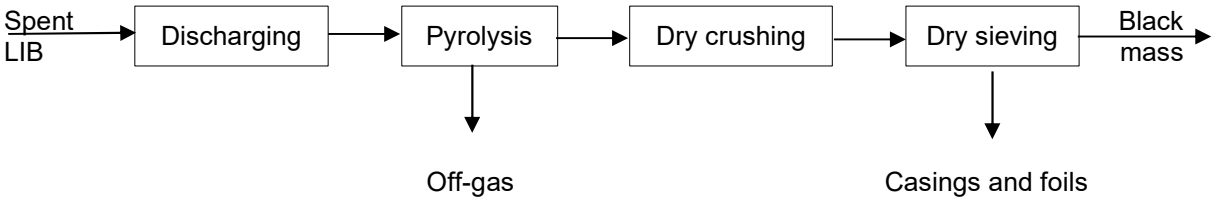

Figure 5: Production of black mass

1.3 Composition of black mass

The black mass is a combination of cathode and/or anode electrode powders which consist of lithium metal oxides, lithium iron phosphates (cathode) and graphite (anode). A list of the major cathode chemistries for LIBs is detailed below[9][10]:

1. $LiMn_2O_4$ - Lithium manganese oxide (LMO)
2. $LiFePO_4$ - Lithium iron phosphate (LFP)
3. $LiNi_{0.3}Mn_{0.3}Co_{0.3}O_2$ - Lithium nickel manganese cobalt oxide (NMC111)
4. $LiNi_{0.6}Mn_{0.2}Co_{0.2}O_2$ - Lithium nickel manganese cobalt oxide (NMC622)
5. $LiNi_{0.8}Mn_{0.1}Co_{0.1}O_2$ - Lithium nickel manganese cobalt oxide (NMC811)
6. $LiNi_{0.8}Co_{0.15}Al_{0.05}O_2$ - Lithium nickel cobalt aluminium oxide (NCA)
7. $LiNi_{0.5}Mn_{0.3}Co_{0.1}O_2$ - Lithium nickel manganese cobalt oxide (NMC532)
8. $LiCoO_2$ – Lithium cobalt oxide (LCO)

Table 1 below shows the detailed analyses of black mass samples which SGS is currently working on. The composition of the black mass can be classified as containing either high cobalt or high nickel-containing samples. The composition of cobalt ranges from 17-22% Co for the high cobalt samples and the composition of nickel ranges from 13- 17% Ni for the high nickel samples. The Li content ranges from 3.0- 3.7% Li for all black mass samples. Typical moisture content is 2-5% and particle size ranged from a fine K80 of ~ 30 µm to a K80 of several 100 µm.

Table 1: Detailed chemical analyses of different black mass samples

	High cobalt				High nickel	
	Black Mass 1	**Black Mass 2**	**Black Mass 3**	**Black Mass 4**	**Black Mass 5**	**Black Mass 6**
Element	%	%	%	%	%	%
Ni	6.79	5.09	6.58	10.6	17.0	12.83
Co	17.1	22.1	21.2	18.6	3.67	4.46
Mn	4.65	3.14	3.68	2.89	3.02	4.19
Li	3.39	3.32	3.36	3.74	3.11	3.03
Cu	0.22	1.18	0.55	0.72	1.38	2.37
Zn	-	-	0.03	0.01	<0.004	0.006
Fe	0.10	0.68	0.37	0.21	0.04	0.03
Al	2.50	2.04	1.21	1.54	1.42	0.5
Ca	0.04	0.28	0.12	0.05	0.02	0.02
Mg	0.04	0.14	0.24	0.10	0.01	0.01
Na	0.06	0.28	0.06	-	0.05	0.06
Cr	0.01	0.04	0.003	0.00	<0.00	0.002
C	38.4	26.4	36.8	37.0	45.5	47.8
F	-	-	1.62	1.75	2.48	2.05

RECYCLING PROCESS CONSIDERATIONS

As illustrated in this paper, many processing routes exist for the treatment of black mass streams. While this paper focusses on the hydrometallurgical treatment, it should be noted that dedicated pyrometallurgical processes have also been developed for the treatment of black mass. A good example is Umicore's operation in Hoboken (Belgium) which operates a 7000 t/a facility with stated plans to expand.

Most of the hydrometallurgical flowsheets incorporate a reductive leach process using sulphuric acid and hydrogen peroxide, though some exceptions exist such as the chloride based flowsheet described by Ehren[11]. Hydrogen peroxide is both a reductant (to reduce the $LiNi_xCo_yMn_{(1-x-y)}O_2$) and an oxidant (to oxidize the metallic copper foil). All flowsheets include one or several steps to remove impurities such as copper, fluoride, iron, aluminum, zinc and manganese.

Many flowsheets under consideration lead to the production of sodium sulphate as a waste or by-product. Sodium sulphate is produced when soluble metals are loaded (SX) or precipitated using sodium-based chemicals. Two moles of NaOH are required to load or precipitate one mole of nickel. Taking the Black Mass Sample 5 from Table 1, one can calculate that around 2.4 tonnes of $Na_2SO_4.10H_2O$ or 1.0 tonne of Na_2SO_4 is produced for each tonne of black mass processed. While salt splitting (into dilute NaOH and H_2SO_4) is a viable technical option, this is still considered an expensive option. Therefore, the use of ammonia (NH_4OH) is considered a potentially viable alternative and leads to the production of ammonium sulphate which can be a feed source in the fertilizer industry.

The recycling projects reviewed for this paper can be grouped as follows:

- Complete separation of metals (Mn | Co | Ni | Li)
- Direct production of battery precursor material (MnCoNi | Li).

Complete separation of metals is usually accomplished via solvent extraction and/or electrowinning and can be used to produce a metal sulphate crystal or metal cathode. When individual metal sulphates are produced, these require further treatment for the production of cathode active materials, including blending of sulphate salts in the correct ratio, dissolving these in water and reacting the metal sulphate liquor with sodium hydroxide or sodium carbonate to produce solid metal hydroxide or carbonate and sodium sulphate[12]. Therefore, the production of an intermediate metal product requiring re-dissolution and reaction with a sodium-based reagent will lead to additional production of sodium sulphate (in addition to the sodium sulphate produced during the processing of black mass). Flowsheets capable of producing a mixed metal hydroxide without an intermediate will therefore lead to lower production of sodium sulphate.

There are several entry points to the LIB recycling business. Types of companies include dedicated recycling companies (with IP, such as Li-Cycle and others), automotive and battery companies, chemical reagent companies (such as Solvay) and trading companies. It is also worth noting that while mining projects employ mining guidelines and regulations, especially relating to public disclosure (TSX, ASX, etc.), recycling projects do not share the same industry guidelines. They are in effect chemical plants. Mining projects offer the opportunity to dispose of or store waste streams in dedicated tailing storage facilities (TSF). Recycling projects typically do not offer such opportunities.

BLACK MASS TREATMENT FLOWSHEETS

Complete Separation (Mn | Co | Ni | Li | Na/NH_4)

Li-Cycle, Lithion, Neometals and the Veolia-Solvay JV all have in common that complete separation of Mn, Co, Ni and Li is targeted. All four projects use a sulphuric acid / hydrogen peroxide based leach flowsheet to produce a pregnant leach solution and a graphite based leach residue, but differ from one another on how the pregnant leach solution is treated. Table 2 summarizes the liquor treatment unit operations and the sections below provide additional detail.

In all cases presented here, additional treatment will be required to produce precursor cathode active material from metal sulphate or metal products. The additional treatment is likely to consist of blending, water leaching (sulphate salts) or acid leaching (metal) followed by neutralization with NaOH or Na_2CO_3 to produce metal hydroxides or carbonates and sodium sulphate.

Table 2: Summarized Unit Operations – Complete Separation Mn | Co | Ni | Li | Na/NH_4

Company	Leach Chemistry	Copper Separation and Recovery?	Impurity (FeAl) Removal	NCM Separation / Recovery Process	NCM Products	Waste alkali?	Lithium Recovery and Product
Li-CyCle	H_2SO_4/H_2O_2	CuS / CuSX-EW	Precipitation (NaOH, lime) of $Al(OH)_3$, $Fe(OH)_3$	Sequential SX of Mn, Co and Ni, with $MnCO_3$ precipitation from MnSX strip and metal sulfate crystallization from CSX and NSX strip liquors	Separate $MnCO_3$, $CoSO_4.7H_2O$, $NiSO_4.6H_2O$	$Na_2SO_4.10H_2O$	Li_2CO_3 Precipitation with Na_2CO_3
Lithion	H_2SO_4/H_2O_2 (internal recycled MnO_2 and Al powder)	CuS (Na_2S or H_2S)	Precipitation (NaOH) of $Al(OH)_3$, $Fe(OH)_3$	Column SX. CoMnSX (Cyanex 272) to separate CoMn | LiNi. Loaded organic is scrubbed with strip liquor bleed. CoMn are stripped together with pH 1 H_2SO_4. Cobalt is electrowon from CoMn strip liquor producing Co Metal (cathode) and MnO_2 (anode). Spent electrolyte is returned to stripping. Nickel is precipitated with NaOH from the CoMnSX raffinate to produce $Ni(OH)_2$	Co Metal, MnO_2, $Ni(OH)_2$	$Na_2SO_4.10H_2O$ fed to electrolysis (production of H_2SO_4 and NaOH)	Li_2CO_3 Precipitation with Na_2CO_3
Neometals	H_2SO_4/H_2O_2	CuSX (LIX84I). Salting out Crystallization of CuSO4.5H2O from strip liquor via addition of H2SO4	Precipitation of $Al(OH)_3$, $Fe(OH)_3$ with NH_4OH and oxidant (if required for oxidation of Fe_2 to Fe_3)	CoMnSX (Cyanex 272 / Ionquest 801 / D2EHPA) is used to separate CoMn|LiNi. Mn is extracted from CoMnSX Strip liquor with Co preloaded organic (D2EHPA). Co-preloading is done by contacting stripped organic with purified cobalt stream. Final product liquors are crystallized to $CoSO_4.7H_2O$ and $MnSO_4.H_2O$ CoMnSX raffinate advances to NiSX (LIX84I or Versatic 10), with crystallization of $NiSO_4.6H_2O$ from strip liquor	Separate $MnSO_4.H_2O$, $CoSO_4.7H_2O$, $NiSO_4.6H_2O$	No. Production of Ammonium Sulphate	NiSX raffinate is treated by IX to remove divalents. LiSX (Cyanex 936, 926, 923, LIX54, LIX55, Mextral 54-100 or mixtures) to separate Li|NH_4. Li strip liquor treatment to produce final Li product (Li_2SO_4 liquor)
Solvay / Veolia	H_2SO_4/H_2O_2 (Solvay Interox Technology)	CuSX (Acorga), IX, CuEW. Production of Cu Cathode	Precipitation of $Al(OH)_3$, $Fe(OH)_3$ with NaOH or NH_4OH	Impurity SX (D_2EHPA) to separate CuFeAlMn | CoNiLi. Co SX (Cyanex 272) to separate Co | Ni Li. Crystallization of $CoSO_4.7H_2O$ NiSX (Versatic 10)) to separate Ni | Li Na/NH_4. Crystallization of $NiSO_4.6H_2O$	Separate $CoSO_4.7H_2O$, $NiSO_4.6H_2O$	unknown which alkali is used	LiSX (Cyanex 936P) to separate Li|Na/NH_4. Li strip liquor treatment to produce final Li product (LiOH / Li_2CO_3)

Li-Cycle

Li-Cycle is a Canadian-based company that focusses on LIB resource recovery and recycling. LIB recycling at Li-Cycle is a patented[5] process which involves various hydrometallurgical steps. The processing plant is expected to have a capacity of 35 000 tonnes of black mass per year and once fully operational is expected to produce lithium carbonate (8500 tonnes/annum), nickel sulphate (48 000 tonnes/annum) and cobalt sulphate (7500 tonnes/annum) [8]. Li-Cycle uses a hub and spoke model with a central hub (Rochester, NY) plant processing black mass produced at several spoke sites spread out over North America.

A simplified block flow diagram for the hydrometallurgical Li-Cycle process is illustrated in Figure 6 below. The BFD is an interpretation of the published patent and investor presentations[13] and generally follows a conventional metal separation flowsheet. The reagents in red text are possible reagents which can be used in the process plant, however, the actual process may employ a variation of the reagents listed above.

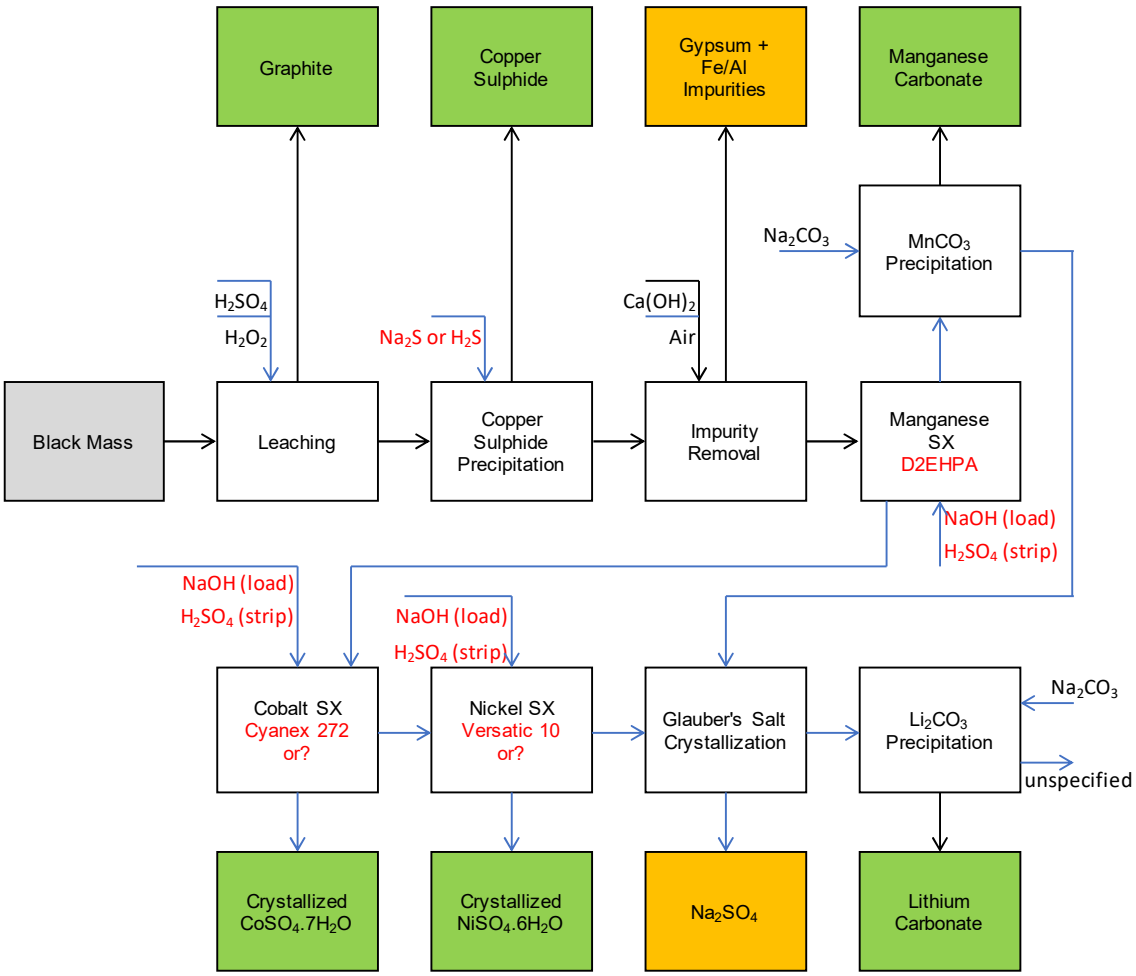

Figure 6: BFD for hydrometallurgical treatment of black mass – Li-Cycle

The pregnant leach solution (from a sulphuric acid/hydrogen peroxide leach) is subjected to copper sulphide precipitation using precipitants such as sodium sulphide or hydrogen sulphide. The solution is further purified removing iron and aluminum and based on the published production of gypsum it is assumed that calcium-based reagents such as lime are used. Of the projects reviewed, Li-Cycle is the only project using calcium-based reagents and producing gypsum. Presumably, this is driven by the improved fluoride removal performance when CaF_2 is produced.

After iron and aluminum removal the solution then undergoes manganese solvent extraction, presumably using D2EHPA. The manganese can be stripped from the organic extractant using sulphuric acid. The manganese in the loaded strip liquor is then precipitated using sodium carbonate to form a manganese carbonate. The raffinate produced from manganese solvent extraction advances to cobalt solvent extraction. Cyanex 272 is believed to be used as an extractant to extract Co from nickel, lithium and sodium contained in the Mn raffinate stream. Cobalt loaded organic is stripped using sulphuric acid and the resultant loaded strip liquor is crystallized to form cobalt sulphate. Cobalt raffinate is then subjected to nickel solvent extraction presumably using Versatic 10 to separate nickel from sodium and lithium sulphate. Sulphuric acid is used to strip the nickel loaded organic phase and the resultant loaded strip liquor is crystallized to produce nickel sulphate. Sodium sulphate is removed from the system via Glauber's salt crystallization. The mother liquor produced after crystallization is then processed to produce lithium carbonate via precipitation using sodium carbonate.

The assumed use of D2EHPA in the Li-Cycle flowsheet ensures that the liquor advancing into cobalt and nickel solvent extraction is clean and impurities such as zinc should be picked up as well. The use of calcium in impurity removal is surprising as it leads to the production of gypsum, but also produces a gypsum saturated liquor advancing into the D2EHPA SX circuit. While D2EHPA is able to extract calcium, removal is typically not quantitative and extracted calcium can lead to gypsum precipitation in scrubbing and stripping when sulphuric acid is used.

Li-Cycle has reported that the Rochester hub is on track for commissioning in 2023, with 90% of process equipment ordered and 65% of detailed engineering completed[14].

Neometals

Neometals is an emerging, battery materials producer and has developed a proprietary hydrometallurgical process for the recycling of EOL LIBs. The process is looking at the recovery of valuable materials from consumer electronic batteries (lithium cobalt oxide cathodes) and nickel-rich electric vehicle and stationary storage battery chemistries (lithium-nickel-manganese-cobalt cathodes)[15]. Based on the patent by Beer[16] and other publications[17], a simplified block flow diagram of the Neometals LIB recycling process has been drawn up and is shown in Figure 7. The Neometals flowsheet was piloted at SGS Canada in 2019-2020.

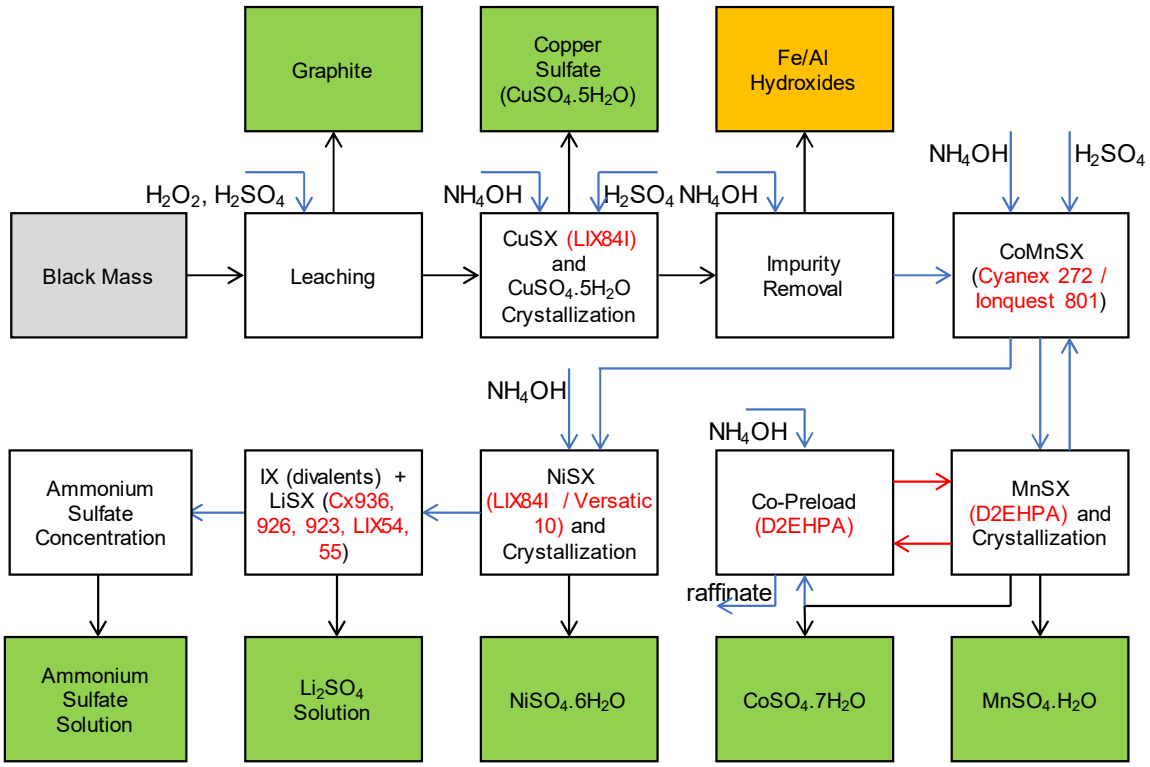

Figure 7: BFD for hydrometallurgical treatment of black mass – Neometals

In the Neometals hydrometallurgical flowsheet, sulphuric acid is used in combination with hydrogen peroxide to leach the black mass, leaving graphite in the leach residue. The pregnant leach solution is subjected to copper solvent extraction. A copper extractant such as LIX84-I (as identified by Beer[16]) can extract copper at relatively low pH values and could be a possible copper extractant used in the process. The copper is stripped from the organic phase and the loaded strip liquor is then crystallized to form copper sulphate crystals. The raffinate produced from the copper solvent extraction step is then subjected to iron and aluminum removal via hydroxide precipitation using ammonium hydroxide. After iron and aluminum removal the solution is then subjected to cobalt and manganese solvent extraction, extracting both cobalt and manganese by a single extractant such as Cyanex 272, Ionquest 801 or PC88-A[16]. Both cobalt and manganese are stripped from the organic phase. Manganese is then extracted from the loaded strip liquor using a cobalt loaded extractant such as D2EHPA and is stripped using sulphuric acid. Thereafter the strip liquor advances to manganese sulphate crystallization. The purified manganese SX raffinate is split into two streams. A portion of the stream is recycled to cobalt pre-loading and is loaded onto D2EHPA, the second portion of the stream advances to cobalt sulphate crystallization.

The raffinate stream produced from the combined manganese cobalt SX advances to nickel solvent extraction. Typical nickel extractants such as LIX 84-I and Versatic 10 are possibly used as extractants for nickel solvent extraction. The nickel is stripped off the organic phase and the loaded strip liquor is subjected to nickel sulphate crystallization. The raffinate solution produced after nickel

solvent extraction is further purified using ion exchange to remove divalent impurities. Lithium is recovered via solvent extraction from the purified solution. Possible extractants for lithium recovery are Cyanex 936, 926, 923, LIX 54 and LIX55. The raffinate obtained from lithium solvent extraction is directed to a step whereby the ammonium sulphate is preconcentrated.

While the operation of multiple sequential SX circuits can be challenging and carry-over of organic should be avoided, Neometals plans to use activated carbon coalescers to avoid extractant carry-over from circuit to circuit. The Neometals circuit is unique in that it avoids the production of sodium sulphate and uses ammonia in place of sodium-based reagents. Consequently, ammonium sulphate is produced as a potential feed source for the fertilizer industry. Care must be taken to avoid the formation of nickel ammonium sulphate double salts in nickel solvent extraction circuits using ammonia.

Lithion

Lithion is a battery recycling company located in Canada. The company has developed patented[18] technology for LIB recycling and commissioned an industrial-scale demonstration plant in January 2022. The capacity of its first commercial scale plant is expected to be 7500 metric tonnes per annum[19]. Lithion's goal is to install more than 20 recycling plants over the next 15 years. The Lithion hydrometallurgical flowsheet consists of leaching, impurity removal, upgrading and electrowinning as shown in Figure 8.

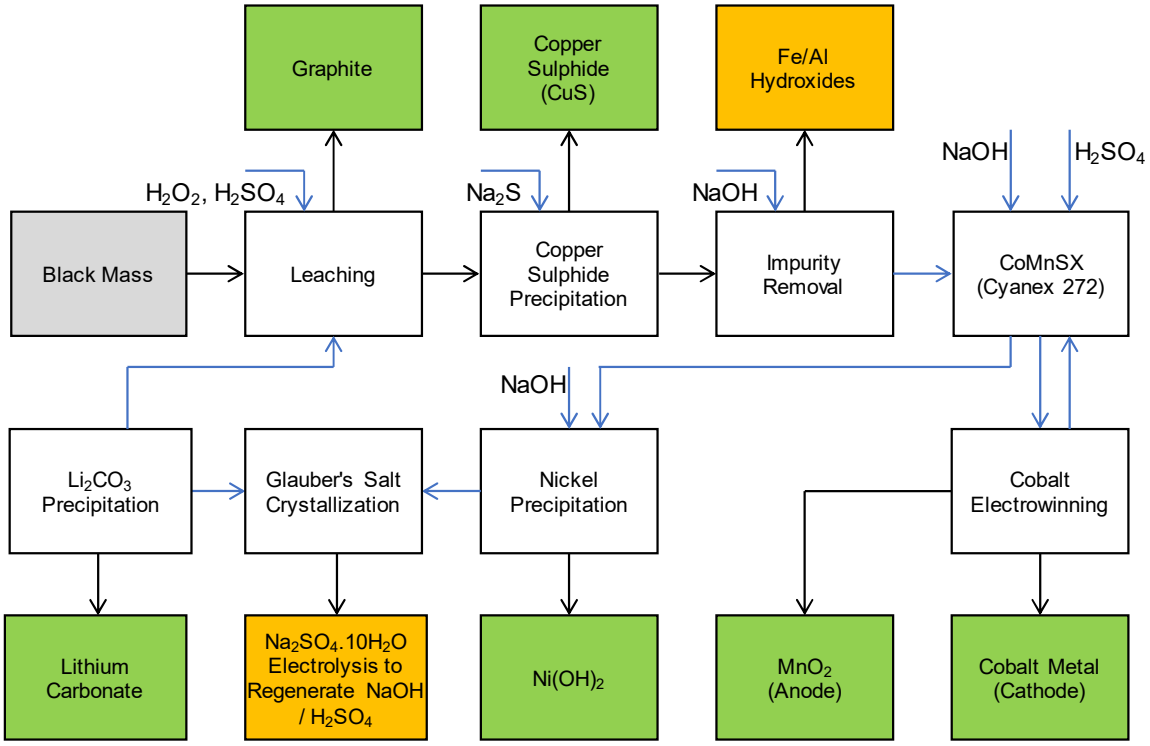

Figure 8: BFD for hydrometallurgical treatment of black mass – Lithion

The pregnant leach solution (after H_2SO_4/H_2O_2 leaching) is subjected to copper sulphide precipitation using sodium sulphide. The copper free solution is then passed to impurity removal where sodium hydroxide is used to remove iron and aluminium via hydroxide precipitation. The purified solution is subjected to solvent extraction where cobalt and manganese are extracted together using Cyanex 272 as the extractant. The loaded organic phase is stripped and the loaded strip liquor is passed onto an electrowinning step, where cobalt metal is plated at the cathode and manganese oxide is produced at the anode. The raffinate stream produced from CoMn SX is then subjected to nickel hydroxide precipitation using sodium hydroxide as a precipitant. After the nickel is removed sodium sulphate is formed via Glauber's salt crystallization. The hydrated sodium sulphate is subjected to electrolysis to produce sodium hydroxide and sulphuric acid for recycling. Lithium carbonate is precipitated from the mother liquor.

The use of electrowinning to separate cobalt from manganese is energy efficient as the same electric current is used to reduce cobalt to cobalt metal at the cathode and for manganese oxidation (to Mn^{4+}) at the anode. According to the published patent, the electro-separation of cobalt and manganese is

performed in an undivided cell, which may lead to reduced efficiencies since optimal conditions (pH, temperature, current density) for cobalt electrodeposition and MnO_2 precipitation are different. Moreover, suspended MnO_2 particles could be incorporated into the cobalt deposit.

Solvay-Veolia

In 2020[20] Solvay and Veolia announced their partnership on a circular economy consortium to offer new solutions that promise better resource efficiency for critical metals used in lithium-ion electric vehicle (EV) batteries. Solvay & Veolia have not published specific information on the hydrometallurgy process, except for a simple description[21] which forms the basis of the BFD shown in Figure 9.

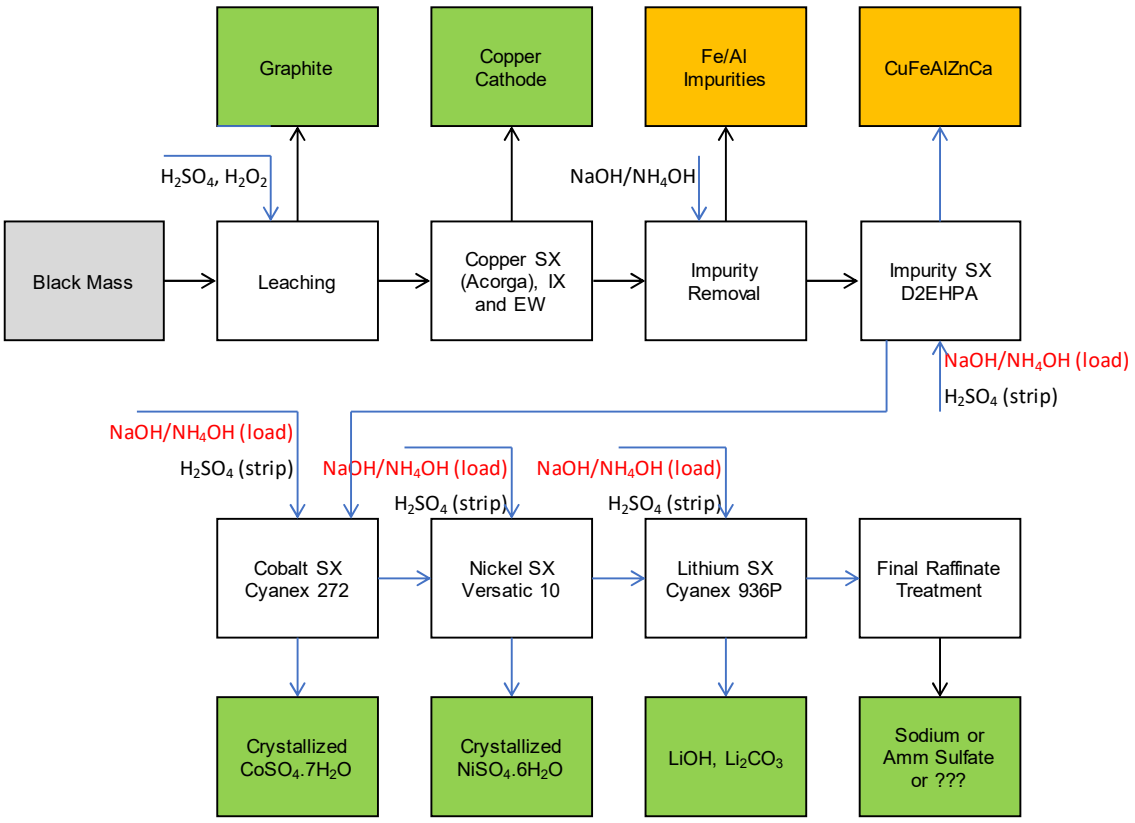

Figure 9: BFD for hydrometallurgical treatment of black mass – Solvay/Veolia

Sulphuric acid in combination with hydrogen peroxide is used to leach the black mass. The pregnant leach solution is subjected to various impurity removal and upgrading steps via solvent extraction. Throughout the flowsheet, Solvay solvent extraction reagents are used to separate each metal:

- Acorga to extract copper
- D2EHPA to extract manganese (and presumably impurities such as zinc)
- Cyanex 272 to extract cobalt
- Versatic 10 to extract nickel
- Cyanex 936 to extract lithium.

Sodium hydroxide or ammonium hydroxide are possibly used as pH modifiers. Depending on the reagent used either a sodium sulphate or ammonium sulphate stream is produced as a by-product of the process. As stated above the operation of multiple sequential SX circuits using all different reagents can be complex and care must be taken to avoid organic carry-over from one circuit into the other.

Separation using electrowinning

Various companies are proposing to use electrochemistry as a basis to separate and it is worthy to mention even though little information is provided publicly.

Aqua Metals is a US based company headquartered in Reno, Nevada and has its origins in lead battery recycling and holds several patents[22] related to its AquaRefining™ technology, based on the use of methane sulfonic acid as a solvent. Aqua Metals has indicated it has filed a provisional patent, also using AquaRefining technology, for recovering high-value metals from recycled lithium-ion batteries. It is noted that the authors of this paper were not able to locate this provisional patent. Aqua Metals provided a simplified BFD (shown in Figure 10) of its proposed process at a recent conference in the USA[23]. It is worth noting the less than common order of metal recovery: copper – lithium – nickel – cobalt – manganese.

Figure 10: Block Flow Diagram – Aqua Metals[23]

Partial Separation (Mn Co Ni | Li | Na/NH_4). Direct Production of Precursor Material

NorthVolt, Coherent Corporation and RecycLiCo all have in common that partial separation of Mn, Co, Ni and Li is targeted, producing a mixed metal hydroxide, carbonate or battery precursor material directly from black mass leach liquors offering the advantage of reduced production of waste products such as sodium sulphate. A variation of this process route appears to be applied by Redwood Materials which has indicated it produces a mixed Ni/Co sulphate product stream, which will require additional processing (and associated production of sodium sulphate) for direct production of battery precursor material. Not all leach chemistry details are available for these projects, but Northvolt, RecycLiCo and Redwood appear to use a sulphuric acid based leach flowsheet with reductants to produce a pregnant leach solution and a graphite based leach residue. Each differs from one another on how the pregnant leach solution is processed. Table 2 summarizes the liquor treatment unit operations and the sections below provide additional detail.

Table 3: Summarized Unit Operations – Partial Separation Mn Co Ni | Li | Na/NH_4

Company	Leach Chemistry	Copper Separation and Recovery?	Impurity (FeAl) Removal	NCM Separation / Recovery Process	NCM Products	Waste Alkali	Lithium Recovery and Product
Northvolt	H_2SO_4/H_2O_2	CuSX	Precipitation (NCM Hydroxide) of $Al(OH)_3$, $Fe(OH)_3$	Metal salts (sulfates or hydroxides) are added to adjust NCM ratio. NCM are precipitated together with NaOH. Minimim co-precipitation of impurities (Li,P,F, Mg, Na, Ca) due to use of concentrated liquors. Filtrate contains unprecipitated NCM and impurities	Battery Precursor Material ($NiCoMn(OH)_2$))	$Na_2SO_4.10H_2O$	Li_2CO_3 Precipitation with Na_2CO_3
Coherent	not disclosed	not disclosed	not disclosed	NCM are precipitated simultaneousy	cathode precursor	not disclosed	not disclosed
RecycLiCo	$H_2SO_4/SO_2/Al$	assumed grouped with Impurity Removal	Precipitation of Fe/Al hydroxides with recycled LiOH	Precipitation of Mixed (NiCoMn) hydroxide/carbonate with Li_2CO_3.	Mixed metal hydroxide/carbonate	N/A. LiOH and Li_2CO_3 used throughout	Electrodialysis to produce LiOH and H_2SO_4 for recycle
Redwood	H_2SO_4/Reductant	CuSX, $CuSO_4$	not disclosed	While undisclosed, it is assumed that SX with H_2SO_4 strip is applied	Mixed Ni/Co Sulphates	not disclosed	Li_2SO_4

Northvolt

Northvolt is a Swedish battery developer and manufacturer, specializing in lithium-ion battery technology for electric vehicles. Northvolt has a factory in Skellefteå, northern Sweden, part of Northvolt's plan to increase production capacity to 32 gigawatt-hours by 2023. Its headquarters for research and development is in Västerås, Sweden. Northvolt has developed LIB recycling technology in-house and its technology is patented[24].

The Northvolt hydrometallurgical flowsheet consists of leaching, copper removal, impurity removal, NMC ratio adjustment, NMC precipitation, residual NMC precipitation for internal recycling, Glauber's salt crystallization and lithium recovery as lithium carbonate. A simplified block flow diagram is shown in Figure 11.

Northvolt uses a reductive acid leach with sulphuric acid and hydrogen peroxide to produce a PLS rich in Ni, Mn, Co and Li as well as impurities such as Cu, Fe, Al, F and Zn. Copper contained in the

PLS is recovered via SX-EW or IX. The copper free solution is then passed to impurity removal where recycled NMC hydroxide is used to remove iron and aluminum via hydroxide precipitation. While not explicitly identified one of the patent examples also used IX to control impurities such as zinc.

The concentration of Ni, Co and Mn in the purified solution is subsequently adjusted by the addition of individual metal sulphate salts to a total metal concentration of 1.55 mol/L and the ratio of Ni:Co:Mn in the target precursor material. NMC is subsequently precipitated together using NaOH (the patent also identifies LiOH and NH_4OH). The inventors[24] claim that by adjusting (i.e. increasing) the metal concentration, selectivity against key impurities is introduced during NMC precipitation at relatively low pH. This leaves unprecipitated Ni, Co and Mn in the filtrate together with ionic impurities. The residual NMC is precipitated with NaOH and recycled upstream (acid neutralization, impurity removal). After the NMC is removed sodium sulphate is formed via Glauber's salt crystallization. Lithium carbonate is precipitated from the mother liquor.

Within a separate patent[25] co-authored by Northvolt personnel, a variation of the Northvolt process route is described. The process variation is based on solvent extraction and crystallization of metal sulphates from strip liquors. Residual metal contents in the crystallizer mother liquor are subsequently precipitated and returned upstream as a source of alkalinity in precipitation circuits.

Since battery precursor material is produced directly from black mass leach liquor, the overall production of the waste stream (in this case sodium sulphate) is reduced. However, due to the need to adjust the NMC ratio by the addition of individual nickel, cobalt or manganese sulphates, individual separation of these metals on a fraction of the overall metal stream will still be required.

The use of NMC hydroxides in impurity removal may lead to NMC metal losses, since impurity precipitation is typically carried out at pH 3-5, a range where the re-dissolution of metal hydroxides is slow.

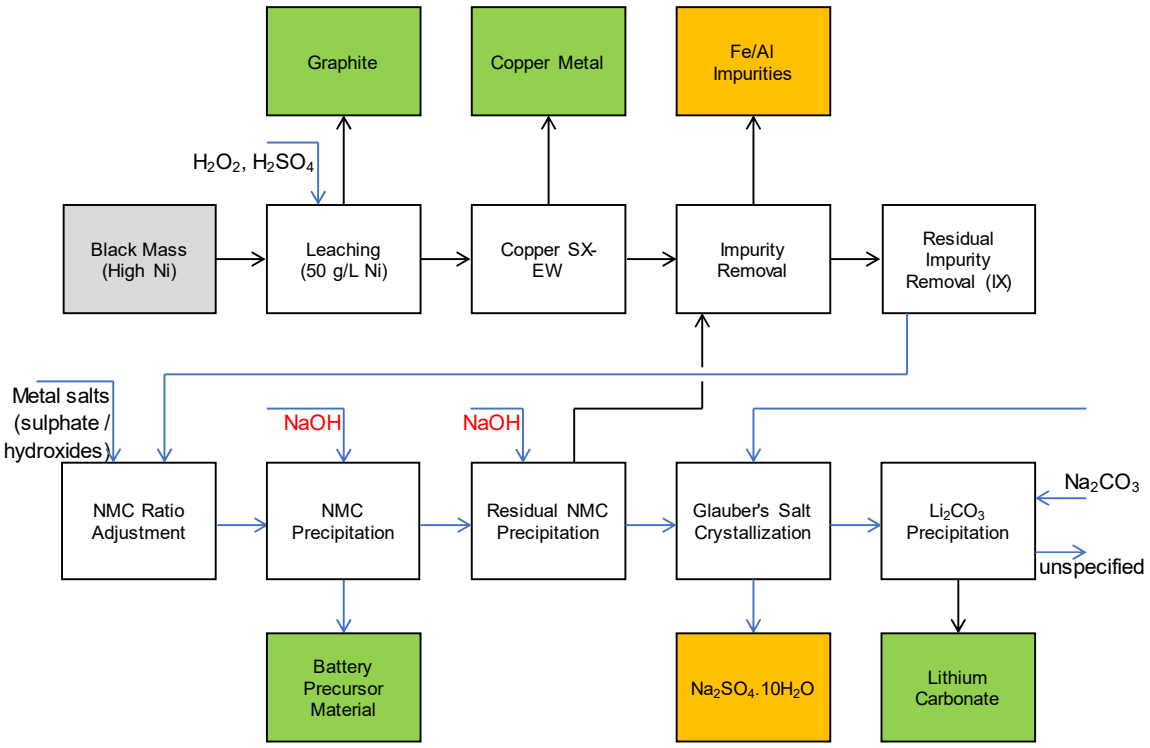

Figure 11: BFD for hydrometallurgical treatment of black mass – Northvolt

Coherent

Coherent Corporation (formerly II-VI Incorporated) is an American manufacturer of optical materials and semi-conductors and is head quartered in Saxonburg, Pennsylvania. Coherent has developed a Streamlined Hydrometallurgical Advanced Recycling Process (SHARP) described in a white paper by Nazari[26]. While the white paper does not reveal much process information, it describes a hydrometallurgical process consisting of black mass leaching, impurity removal and direct production of battery precursor material. A simple conceptual BFD is shown in Figure 12.

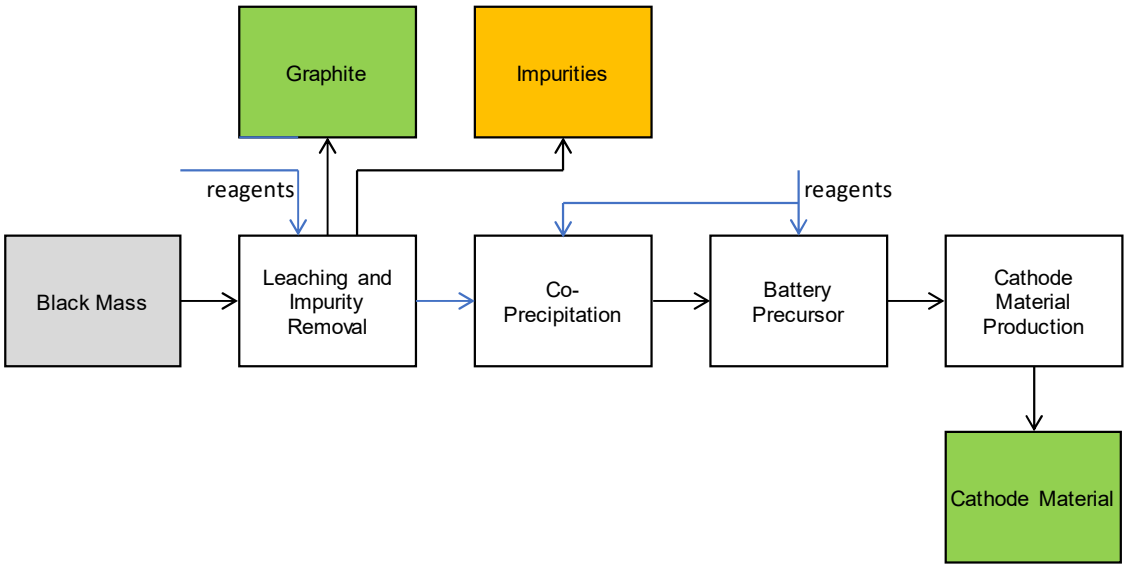

Figure 12: BFD for hydrometallurgical treatment of black mass – Coherent

RecycLiCo

RecycLiCo, formerly known as American Manganese, is a publicly-traded company listed on the TSX venture exchange. The company has developed and patented[27] technology for the recycling of battery cathode waste. The technology has been described in several journal articles[28][29]. Combined these sources of information form the basis of the flowsheet description below (Figure 13). RecycLiCo recently announced that its demo plant has operated for "thousands of person hours" producing battery grade lithium carbonate and high nickel pCAM[30].

Jung et al[29] describe a reductive sulphuric acid leach process using SO_2 gas as reductant. Typical leach conditions included 10% solids, 0.8M H_2SO_4 and SO_2 addition to ORP of 350 mV leading to metal extractions of over 99%. The authors opined that leaching with SO_2 resulted in a much smaller volume of leachate than leaching with H_2O_2. Impurities are removed via the addition of recycled LiOH and NMC were precipitated together with Li_2CO_3 (presumably also recycled internally). While the authors looked at precipitation with LiOH, it was found that this was not practical due to the high resulting dilution when 1M LiOH is used. In place of LiOH, the authors used Li_2CO_3. The authors reported that a 177% stoichiometric addition of Li_2CO_3 was required to recover over 99.5% of contained nickel and cobalt and that the final Ni/Co precipitate containing elevated levels of Li_2CO_3 indicating poor reactivity of the Li_2CO_3 used.

The nickel and cobalt free filtrate containing 10 g/L Li advances to lithium electrodialysis in a three-compartment cell to regenerate LiOH and H_2SO_4. When operated at a current density of 204 A/m^2, 0.8 M LiOH was generated in a single pass.

The RecycLiCo process appears able to process black mass, producing precursor material directly without the production of sodium sulphate due to the internal recycling of LiOH and Li_2CO_3 formed by electrodialysis of Li_2SO_4. Obvious concerns exist around the cost of operating the electrodialysis cell. High recycling rates of LiOH and poor utilization of Li_2CO_3 will contribute to increased electrical costs.

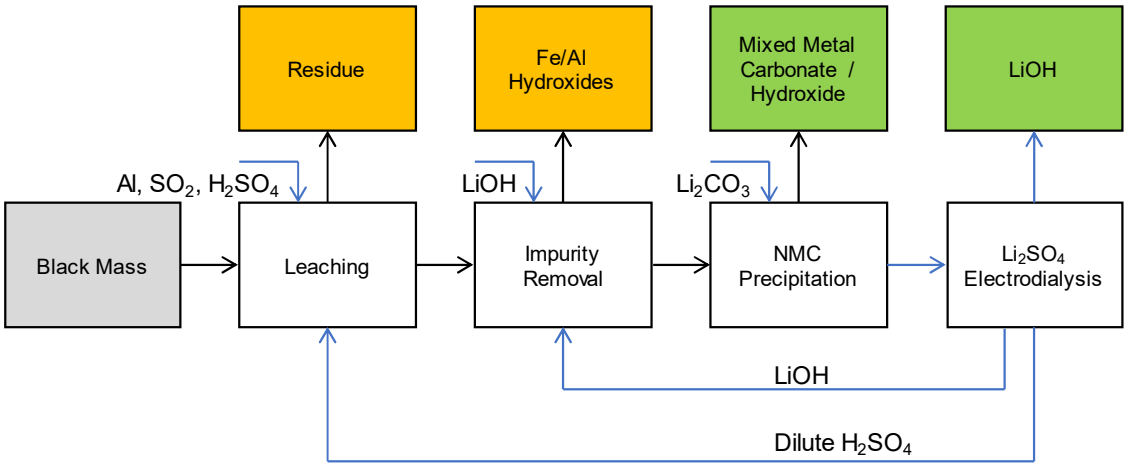

Figure 13: BFD for hydrometallurgical treatment of black mass – RecycLiCo

Redwood Materials

Redwood Materials is an American company headquartered in Carson City, Nevada. The company aims to recycle LiBs and produce battery materials for electromobility and electrical storage systems. Not much information on its processing flowsheet is available publicly except for what is posted online[31]. A simple conceptual BFD is shown in Figure 13. The flowsheet indicates the separate production of copper sulphate, mixed nickel/cobalt sulphate and lithium sulphate. This implies that a sulphate based leach process is used and that solvent extraction with sulphuric acid stripping is employed to produce separate copper and mixed nickel/cobalt streams. The production of an intermediate sulphate stream also implies that additional processing steps (water leaching, neutralization with NaOH, production of Na_2SO_4) are required to produce precursor cathode active materials. Insufficient detail is provided to comment on the behavior of impurities within this flowsheet.

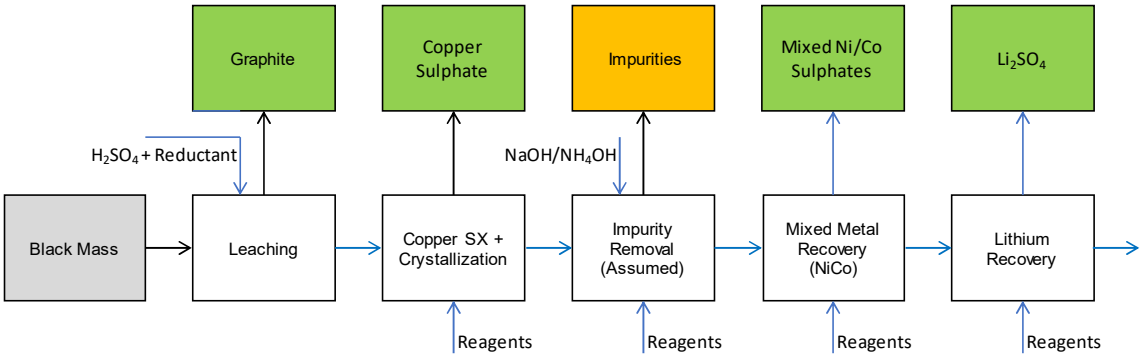

Figure 14: BFD for hydrometallurgical treatment of black mass – Redwood Materials

FINAL THOUGHTS: ISSUES, OPPORTUNITIES AND CONCLUSIONS

The developments in battery chemistries are rapid and technologies developed today for the treatment of current battery chemistries need to be able to adapt quickly to changing feedstocks. While the current recycling need is primarily for off-spec material, this will change to end-of-life materials.

While this review is far from exhaustive and other authors have provided significantly more comprehensive reviews[32][33], it is clear that developments are rapid and not all developments reported in this or other papers will have a successful outcome. The companies must conduct thorough and rigorous testing (including pilot and demonstration style piloting) to evaluate the robustness and operability of the processes developed and their ability to handle constantly changing feedstocks.

The ability to produce precursor cathode active material directly is of interest, as it provides the opportunity to limit the production of waste streams such as sodium sulphate. However, this means

that the recycler needs to continuously adapt its process to meet the ever-changing battery chemistry needs.

REFERENCES

1. N. Verbaan, 2023. “Review of Hydrometallurgical Flowsheets for Treatment of Black Mass”. EV Battery Recycling & Reuse USA 2023 Conference, Detroit.

2. M. Reid, 2023. “Can recycling fill the raw material supply gap?”. EV Battery Recycling & Reuse USA 2023 Conference, Detroit.

3. T. Bußmann, 2023. “Eco friendly recycling of lithium ion batteries”. EV Battery Recycling & Reuse USA 2023 Conference, Detroit.

4. L. Dario, M. Vaccari, M. Lagnoni, M. Orefice, F. Mathieux, J. Huisman, L. Tognotti and A. Bertei, "A comprehensive reviw and classification of unit operations with assessment of outputs quality in lithium-ion battery recycling.," *Journal of Power Sources,* p. 546, 2022.

5. A. Kochlar and T. G. Johston, 2020. "Process, apparatus, and system for recovering materials from batteries". United States Patent US 2020/0078796.

6. W. Yu, Y. Guo, S. Xu, Y. Yang, Y. Zhao and J. Zhang, "Comprehensive recycling of lithium-ion batteries: Fundamentals, pre-treatment, and perspectives," *Energy Storage Materials,* pp. 172-220, 2023.

7. A. Vanderbruggen, G. Eligiusz, R. Blannin, K. Bachman, R. Serna-Guerrero and M. Rudolph, "Automated mineralogy as a novel approach for the compositional and textural characterisation of spent lithium-ion batteries," *Minerals Engineering,* 2021.

8. D. L., D. Pirrie, M. Power, I. Corfe, J. Kuva, S. Lukkari, Y. Lahaye, L. X. and A. Butcher, "The sampling and phase characterisation of black mass," *Proceedings of WCSB10,* pp. 397-409, 2022.

9. X. Duan, W. Zhu, Z. Ruan, M. Xie, J. Chen and X. Ren, "Recycling of Lithium Batteries - A review," *Energies,* pp. 1-23, 2021.

10. O. Winjobi, Q. Dai and J. Kelly, *Update of Bill-of-Materials and Cathode Chemistry addition for Lithium-ion Batteries in GREET 2020,* 2021.

11. P. Ehren. 2022. “Production of lithium hydroxide and lithium carbonate”. US Patent: US 11,339,481 B1

12. S. Ahmed, P. Nelson, K. Gallagher, N. Surarla, D. Dees. 2017. “Cost and energy demand of producing nickel manganese cobalt cathode material for lithium ion batteries”. Journal of Power Sources 342 (2017), p733-740

13. Li-Cycle Investor Presentation, 2022. “People, Planet, Profit”. April 2022

14. J Muccioli, 2023. “LIB Material Recovery Technology as a Sustainable and Scalable Solution”. EV Battery Recycling & Reuse USA 2023 Conference, Detroit.

15. Neometals, "Lithium ion battery recycling," Available: https://www.neometals.com.au/our-projects/core-projects/recycling/. Accessed 16 April 2023

16. G. Beer and M. Urbani, 2022. "Battery Recycling Process". USA Patent US2022/0017989 A1, 20 January 20, 2022.

17. G. Beer, 2022. "Development of the Neometals Lithium-Ion Battery Recycling Process", ALTA 2022.

18. D. Morin, C. Gagne-Bourque, E. Nadeau and B. Couture, "Lithium-ion batteries recycling process". United States Patent US 11,508,999 B2, 22 November 2022.

19. Lithion, "Lithion Plants," 2023. https://www.lithionrecycling.com/lithium-ion-battery-recycling-plant/. Accessed 23 April 2023.

20. Solvay, 2020. https://www.solvay.com/en/press-release/veolia-partnership-renew-life-cycle-electric-car-batteries. Accessed April 24, 2023

21. Solvay. https://www.solvay.com/en/solutions-market/batteries/recycling. Accessed April 24, 2023

22. S. Clarke, R. Clarke, M. Hurwitz, M. King, S. Mould. 2016. “Devices and method for smelterless recycling of lead acid batteries”. US Patent: US 2016/0294024 A1

23. S. Cotton. 2023. “Building a recycling infrastructure that accounts for both optimism and caution”. EV Battery Recycling & Reuse USA 2023 Conference, Detroit.

24. A. Mahmood, R. Sjödahl, E. Nehrenheim, R. Jensen. 2022. “Process for cathode active material precursor preparation”. International Patent Application WO 2022/167662 A1

25. R. Fraser, E. Stamatiou, M. Machado, H. von Schroeter, A. Mahmood. 2021. “Process for Producing Crystallized Metal Sulphates”. US Patent US 10,995,014 B1

26. G. Nazari. 2022. “A Streamlined Hydrometallurgical Advanced Recycling Process (SHARP) Technology for LiB Waste. White paper retrieved from https://ii-vi.com/product/lithium-ion-battery-recycling/ . Accessed April 25, 2023

27. N. Chow, J. Jung, A. Nacu, D. Warkentin. 2018. “Processing of cobaltous sulphate/dithionate liquors derived from cobalt resource”. International Patent Application WO 2018/089595 A1

28. J. Jung, N. Chow, D. Warkentin, K. Chen, M. Melashvilli, Z. Meseldzija, J Pang-Chieh Sui, J. Zhang. 2020. “Experimental study on recycling spent lithum-ion battery cathode materials”. Journal of the Electrochemical Society, 167, 160558

29. J. Jung, N. Chow, D. Warkentin, A. Nacu, M. Melashvilli, A. Cao, L. Khorbaladze, Z. Meseldzija, J Pang-Chieh Sui, J. Zhang. 2021. “A novel closed loop process for recycling spent Li-ion battery cathode materials”. International Journal of Green Energy

30. RecycLiCo. https://recyclico.com/press-releases/. Last accessed April 24, 2023

31. Redwood Materials. https://www.mobilityengineeringtech.com/component/content/article/ae/pub/features/articles/46827. Last accessed April 26, 2023

32. G. Tian, G. Yuan, A. Aleksandrov, T. Zhang, Z. Li, A. Fathollahi-Fard, M. Ivanov. 2022. “Recycling of spent lithium ion batteries: A comprehensive review for identification of main challenges and future research trends”. Sustainable Energy Technologies and Assessments 53 (2022) 102447

33. R. Wagner-Wenz, K. Berberich, A Weidenkaff, A. van Zuilichem, L. Göllner-Völker, L. Schebek. 2022. “Recycling routes of lithium-ion batteries: A critical review of the development status, the process performance and life-cycle environmental impacts”. MRS Energy & Sustainability.

LEWATIT® ION EXCHANGE RESINS FOR THE RECOVERY, REFINING AND RECYCLING OF CRITICAL BATTERY METALS

By

Dirk Steinhilber, [2]Lydia Tang, [2]Rajeev Bavaraju

LANXESS Deutschland GmbH, Liquid Purification Technologies, Koeln, Germany
[2] LANXESS Pty Ltd., Granville, NSW, Australia

Presenter and Corresponding Author

Dirk Steinhilber
dirk.steinhilber@lanxess.com

ABSTRACT

The growing demand for high purity battery lithium, nickel, cobalt and copper, requires efficient methods for the purification of those metals, to meet the high purity specifications of battery producers. Lewatit® ion exchange resins are crucial for many different metals processing applications. This paper will especially focus on the evolving application of the recycling of battery metals, which enables the reduction of carbon footprint and cost savings.

Recycling and refining of battery metals
Metal concentrates can be obtained by various operations e.g. hydrometallurgical mining of ores and recycling of cathode materials from lithium ion batteries (LIBs). Recycling of end of life batteries is based on battery discharge, mechanical separation and leaching of the black mass which is composed of graphite and Li, Ni, Co, Mn. The obtained concentrates often contain impurities like Al, Zn, Fe and Cu and need to be purified. High-purity metal concentrates can be produced by the use of selective Lewatit® resins. Selective chelating resins like Lewatit MDS TP 260, Lewatit® TP 272 and Lewatit® VPOC 1026 are especially suited for these separation tasks because of their high selectivity and loading capacity towards impurities, which ensures efficient removal below the specification limit. At the same time the resins show low interaction towards valuable and concentrated battery metals, which pass the resin bed in high yield and recovery.

Recovery of battery metals
The resin in pulp (RIP) technology is a very promising recovery approach, because battery metals can be extracted and concentrated from ore pulps, directly after leaching, without the need for CAPEX-intensive countercurrent decantation processes. To achieve high throughput within the continuous RIP process we developed our Lewatit® MonoPlus TP 209 XL. The resin shows high mechanical stability and low attrition rates which leads to savings in resin top-up demand. The large bead size up to 0.9 mm facilitates an efficient screening and sieving during resin-feed separation once the loading cycle is completed. Recovery of nickel in presence of high concentrations of ferric and cobalt can be achieved with Lewatit® MDS TP 220. Thanks to its small size and, in turn, short diffusion paths, the resin exhibits fast kinetics during exchange and regeneration. This results in higher capacity utilization and longer service lives with lower chemical requirements for regeneration as compared to conventional resins.

Waste water treatment
Waste water streams generated by battery metals processing plants can for instance be efficiently treated by Lewatit® MonoPlus TP 207. This resin selectively removes toxic heavy metals in the presence of high concentrations of other constituents of the waste water, e.g., hardness. Valuable heavy metals can additionally be recovered and recycled from the resin by selective regeneration.

In conclusion Lewatit® ion exchange resins provide benefits including up to two times longer cycle times compared to conventional resins combined with savings on regeneration chemical costs. Excellent exchange kinetics ensures contaminant removal down to trace levels and yields pure battery metal concentrates. Additionally, Lewatit® chelating resins possess high resilience towards osmotic and mechanical stress and ensure long resin lifetimes.

Keywords: Selective Lewatit® chelating resins, recovery, refining and recycling of battery metals

Strong growth of battery market growth driven by e-mobility & renewables

Key drivers

Megatrends driving the battery market

- Global awareness of global warming pushing for adoption of green solutions (CO_2 emissions reduction)
- Widespread introduction of **renewable energies** (stationary storage)
- **Population increase** and **city growth** challenging mobility and energy solutions (e-mobility)

Li-Ion battery is key technology for new concepts of mobility and energy

E-mobility drives demand for battery chemicals

Global lithium-ion and materials demand forecast from EV sales, 2015–2030 (thousand of tonnes, GWh)

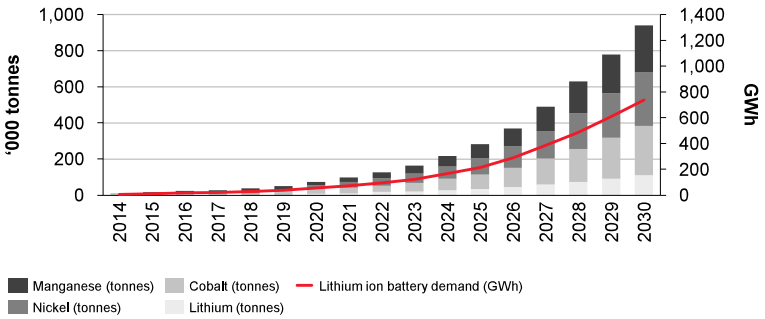

Source: Bloomberg New Energy Finance

LANXESS is offering products and solutions for Li-ion Batteries

LANXESS activities in Li-ion battery materials

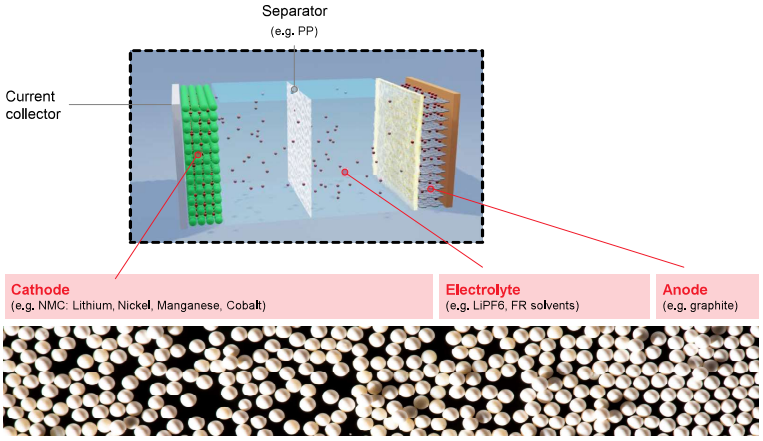

Explanation

Cathode and Anode

- Lewatit® ion exchange resins for extraction, refining and recycling of battery grade cobalt, nickel, and lithium
- Bayoxide® for the purification of LiCl, LiOH, $NiSO_4$ and $CoSO_4$ concentrates

Electrolyte

- Lewatit® ion exchange resins for the purification if $LiPF_6$ electrolyte

Monodisperse droplet generation by jetting process

Stable scaffolds for demanding metals processing applications!

Formation of monodisperse droplets

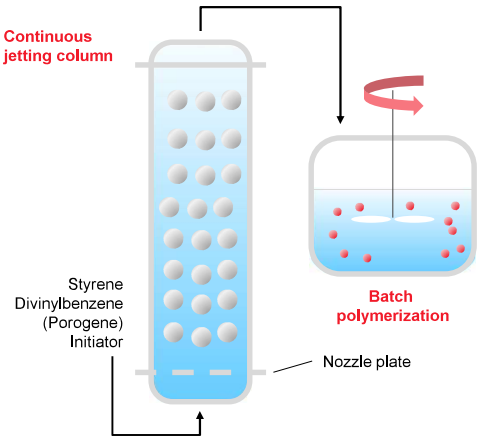

Description

- Continuous process
- Raw materials are fed through a nozzle plate at the bottom of the column
- The resulting monomer jet is chopped into droplets of the same size
- Particle size can be controlled by adjustment of the whole width of the nozzle plate
- The droplets formed at the bottom start to encapsulate as they proceed to the column head
- Polymerization of the monodisperse encapsulated droplets is completed afterwards

The structure of macroporous resins

Small opaque beads are actually of a highly permeable sponge-like structure

Microscopic image

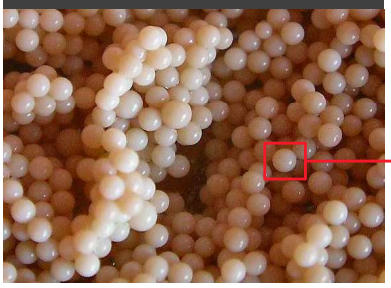

SEM

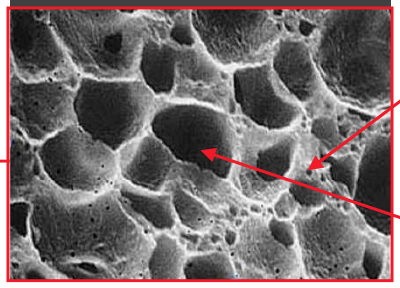

Schematic structure

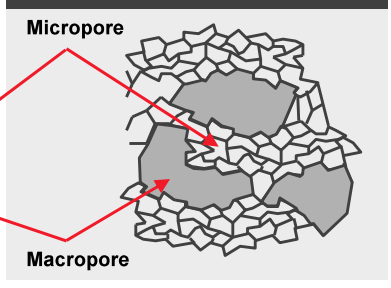

Functional groups

A strong portfolio of solutions for critical separation challenges

Solvent impregnated resins	Selective chelating resins		Anion exchange resins
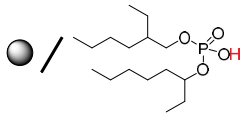	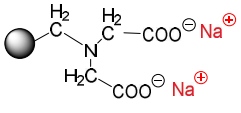	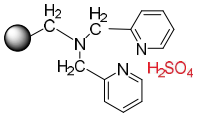	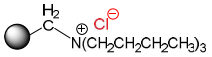
D2EHPA impregnated Lewatit® VP OC 1026	Iminodiacetic acid (IDA) e.g. Lewatit® MonoPlus TP 208	Bispicolylamine (BiPicA) e.g. Lewatit® MonoPlusTP 220	Tri-n-butylammonium Lewatit® TP 106
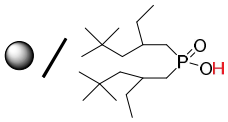	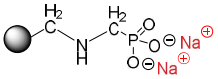	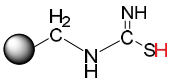	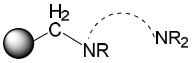
Cyanex 272 impregnated Lewatit® TP 272	Aminomethylphosphonic acid (AMPA) Lewatit® MonoPlus TP 260	Thiourea Lewatit® MonoPlus TP 214	Complex amine Lewatit® A 365(weak base) Lewatit® TP 107 (strong base)

Key properties of ion exchange resins

Precise control of resin parameters for critical separation challenges

- Functional group (type of chelating)
- Polymer Matrix (styrenic or acrylic)
- Morphology (gel or macroporous)
- Crosslinking
- Bead size (mono- vs. heterodisperse)
- Kinetics
- Resin swelling

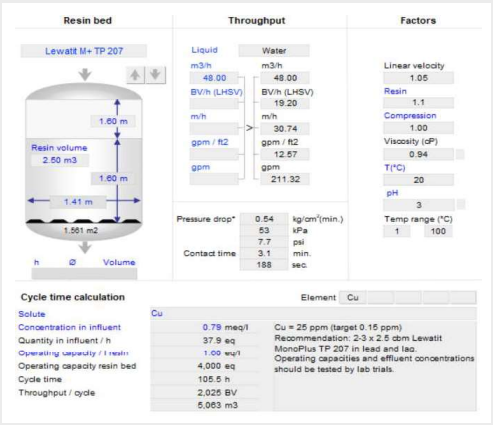

Lewatit® ion exchange resins in applications for purification and refining of battery materials

A strong portfolio of solutions for the preparation critical battery materials

	Nickel and Cobalt					Copper				Lithium	$LiPF_6$
	Recovery fixed bed	Recovery Resin in pulp	Conc. purification	Separation	Waste water	Recovery resin in pulp	Recovery fixed bed	Waste water	Conc. purification	Brine purification	Purification
Lewatit® M+ TP 209 XL	✓	✓			✓	✓					
Lewatit® M+ TP 207	✓		✓		✓		✓	✓			
Lewatit® VPOC 1026			✓								
Lewatit® TP 272			✓								
Lewatit® M+/MDS TP 220			✓	✓			✓	✓			
Lewatit® M+/MDS TP 260			✓		✓		✓		✓	✓	
Lewatit® M+/MDS TP 208										✓	
Lewatit® M+ TP 214			✓								
Lewatit® TP 308			✓							✓	
Lewatit® MP 62 WS			✓								✓
Bayoxide® E IN 30			✓							✓	

Lithium ion battery material life cycle

Lewatit® is a crucial part in the recycling flow sheet!

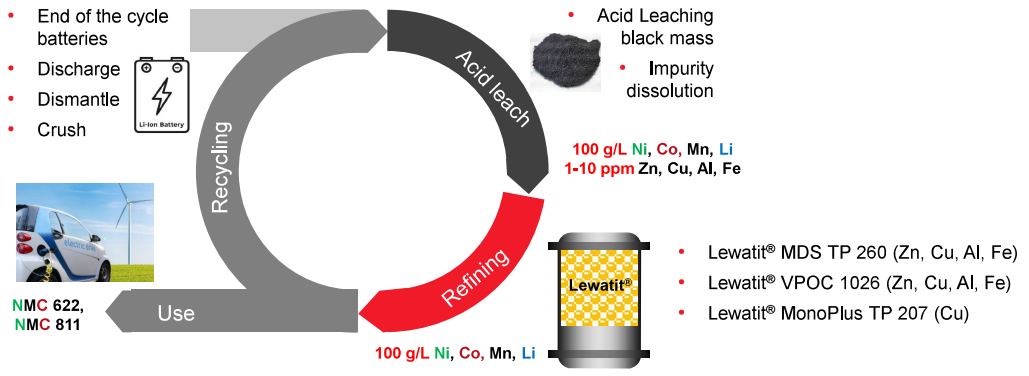

Ion exchange resins for high purity lithium extraction – lithium recovery from brines

A strong portfolio of solutions for the preparation battery grade lithium!

Lewatit® ion exchange resins are required in the most critical places within the flow sheet

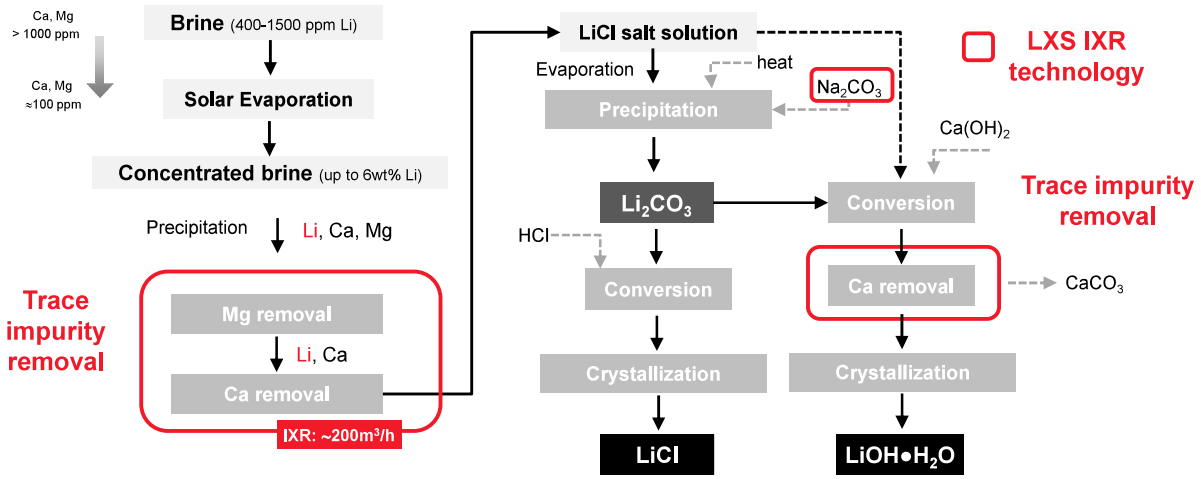

Functional groups for the selective removal of calcium magnesium from lithium brines

Iminodiacetic acid (IDA)	Aminomethylphosphonic acid (AMPA)
Lewatit® MonoPlus/MDS TP 208	Lewatit® MonoPlus/MDS TP 260
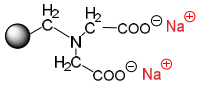 ▪ **MonoPlus TP 208** (650 µm) ▪ **MDS TP 208** (390 µm)	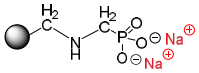 ▪ **MonoPlus TP 260** (630 µm) ▪ **MDS TP 260** (420 µm)
▪ Removal of Ca, Mg and other multivalent cations ▪ Usually used for lithium sulphate and chloride brines ▪ Not prone towards ferric fouling	▪ Adsorption of Ca, Mg, Al and other multivalent metals ▪ Mainly used in lithium hydroxide purification ▪ Fe loading needs to be considered

Surface area calculation

Resins with small particle size

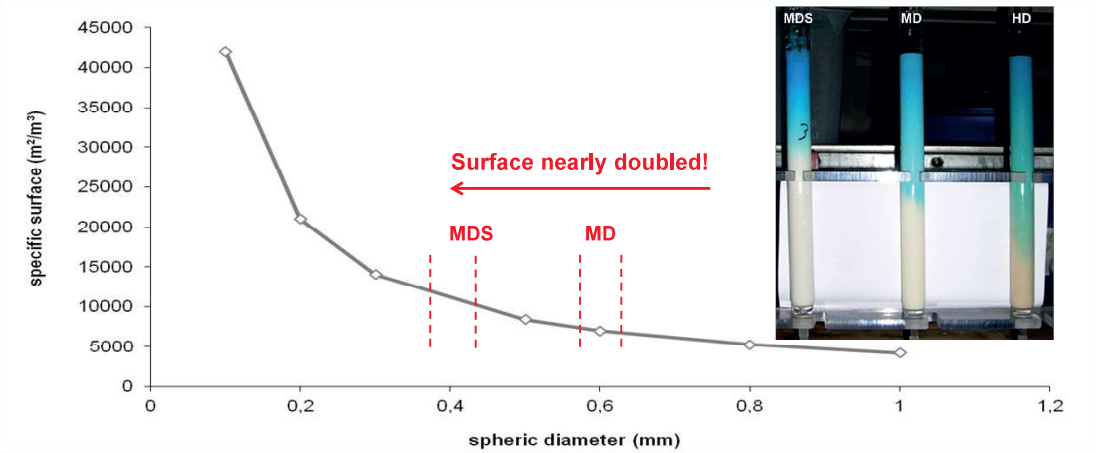

Advantages of monodisperse IX resins

Higher osmotic & mechanical stability of MD resins due to an innovative manufacturing process

Osmotic shock test (OST)

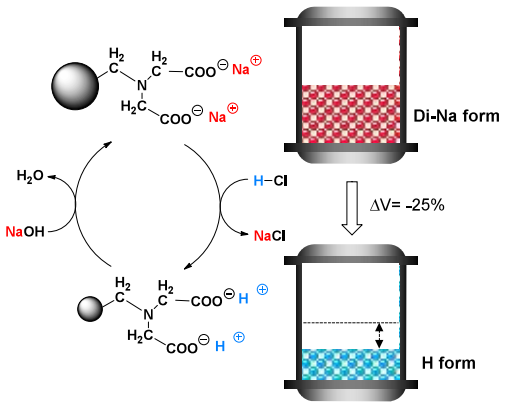

Example: Lewatit® MonoPlus TP 208

Whole perfect beads

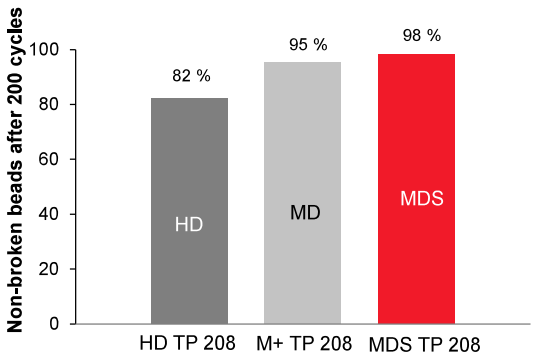

Total Capacity[1] of Lewatit® HD, MD to MDS

MDS resins have significantly higher total capacity!

Reduction of bead size leads to higher substitution grade

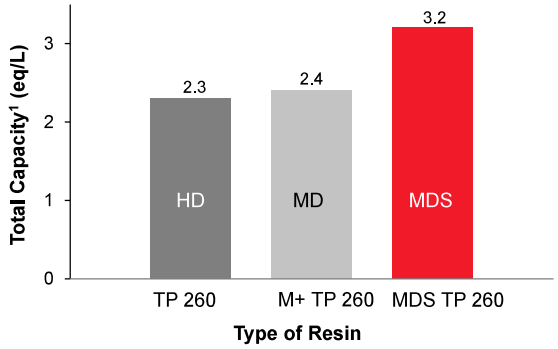

1. Total Capacity = number of charge equivalents by functional groups per liter of resin
MDS: MonoDisperse Small; MD: MonoDisperse; HD: HeteroDisperse

Calcium capacity from LiCl brines

Lewatit® MDS TP 208 has the highest operating capacity and the lowest leakage!

Softening lithium chloride brine to 1 ppm Ca breakthrough

Op. Conditions	
Resin in Na form	
$CaCl_2$	10 ppm as Ca
LiCl	61.1 g/L (10 g Li/L)
NaCl	60 g/L as NaCl
pH	9
SV	10 BV/h
Temp	60°C
Breakthrough	1 ppm Ca
Op. Capacity	
Competitor 1	2.7 g Ca/L
Competitor 2	3.7 g. Ca/L
Lewatit® M+TP 208	8.3 g Ca/L
Lewatit® MDS TP 208	10.6 g Ca/L

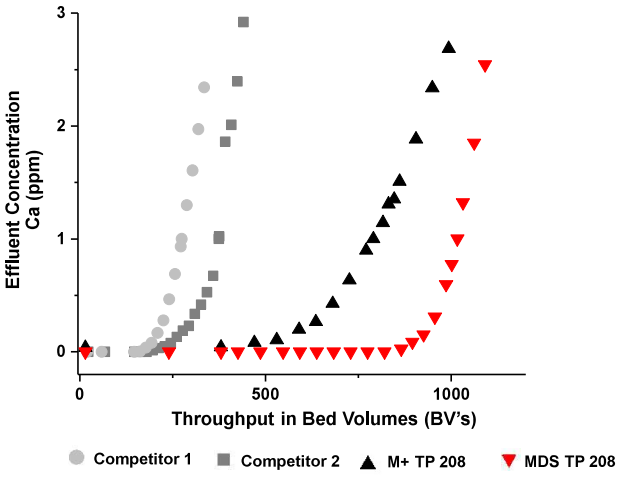

Calcium capacity from LiCl Brines

MDS TP 208 can achieve less than 20 ppb hardness in the treated brine

Lewatit® MonoPlus TP 208 vs. MDS TP 208

Op. Conditions

Resin in Na form

$CaCl_2$, feed	10 ppm as Ca
LiCl, feed	61.1 g/L (10 g/L as Li)
NaCl, feed	60 g/L as NaCl
pH	9
SV	10 BV/h
Temp	60°C
breakthrough	100 ppb Ca

Op. Capacity

M+ TP208	5,2 g Ca/L
MDS TP 208	9,0 g Ca/L

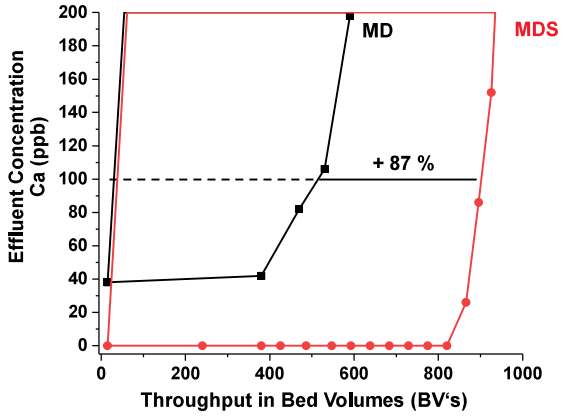

Barium capacity from LiCl brines

Lewatit® MDS TP 208 has the highest operating capacity and the lowest leakage!

Softening lithium chloride brine to 1 ppm Ba breakthrough

Op. Conditions	
Resin in Na form	
$BaCl_2$	10 ppm as Ba
LiCl	10 g/L as Li
NaCl	60 g/L as NaCl
pH	9
SV	10 BV/h
Temp	60°C
Breakthrough	1 ppm Ba
Op. Capacity	
Competitor 1	0.23 g Ba/L
Lewatit® M+ TP208	0.29 g Ba/L
Lewatit® MDS TP208	0.48 g Ba/L

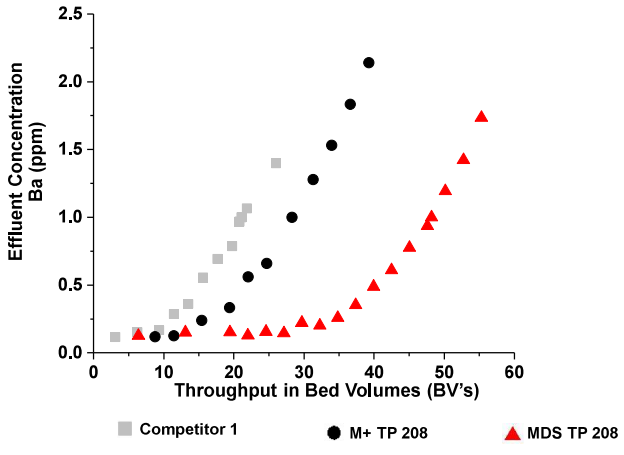

Lithium recovery by selective regeneration of trial product

Efficient separation between lithium and calcium by split elution, high lithium yield!

More than 70% of co-loaded lithium can be recovered by split elution

Loading conditions	
Resin in Na form	
$CaCl_2$, feed	10 ppm as Ca
LiCl, feed	61.1 g/L (10 g Li/L)
NaCl, feed	60 g/L as NaCl
pH	9
SV	10 BV/h
Temp	60 °C
Regeneration conditions	
HCl	1.5%
SV	1.5 BV/h

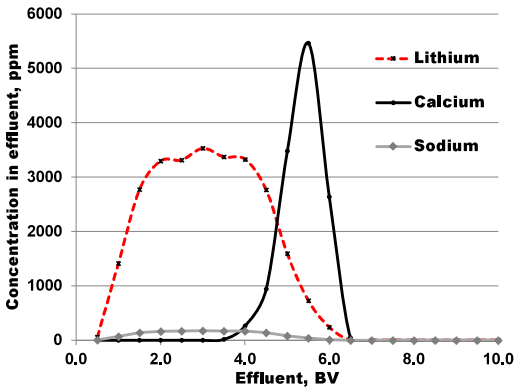

Calcium capacity from low concentrated LiCl brines

TP 308 has the highest operating capacity and the lowest leakage!

Softening lithium chloride brine to 1 ppm Ca breakthrough

Op. Conditions	
Resin in Na form	
$CaCl_2$	2000 ppm
LiCl	1000 ppm
NaCl	5000 ppm
pH	8
SV	10 BV/h
Temp	60°C
Breakthrough	10 ppm Ca
Op. Capacity	
Competitor 1	1.3 eq. Ca/L
Competitor 2	1.6 eq. Ca/L
Lewatit TP 308	2.0 eq. Ca/L

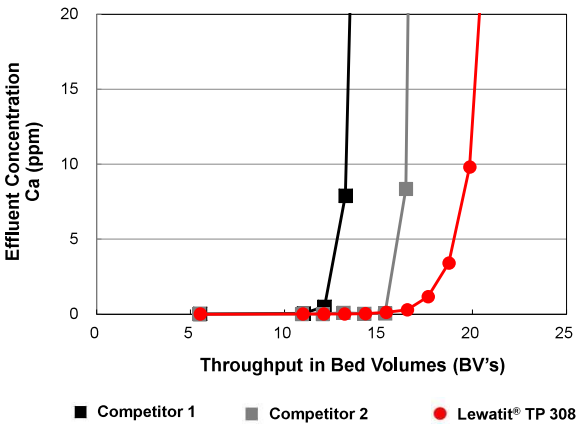

Calcium capacity from LiOH brines

MDS TP 260 has the highest operating capacity but is kinetically limited

Softening lithium hydroxide brine to 1 ppm Ca breakthrough

Op. Conditions

Resin in Na form

$CaCl_2$	10 ppm as Ca
LiOH	30 g/L (8.7 g/L as Li)
pH	12
SV	10 BV/h
Temp	60°C
breakthrough	1 ppm Ca

Op. Capacity

M+ TP 208	6,4 g Ca/L
MDS TP 208	8,8 g Ca/L
M+ TP 260	4,7 g Ca/L
MDS TP 260	9,8 g Ca/L

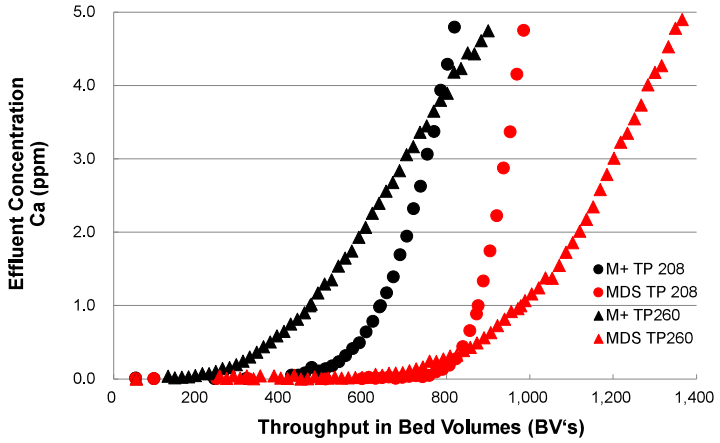

Silica removal from $NiSO_4$, $CoSO_4$, LiCl, and LiOH concentrates by use of Bayoxide® E IN 30

Bayoxide® has a low silica leakage in various battery metal concentrates

Nickel sulfate

	Co	Fe	Ni	Si
Feed silicate	970	0	81550	78.9
Effluent silicate	445	0	65250	2.1
Removal %	54%	n/a	20%	97%

Lithium chloride

	Fe	Li	Si
Feed silicate	0	14070	68.8
Effluent silicate	0	13535	0.01
Removal %	n/a	4%	100%

Lithium hydroxide

	Fe	Li	Si
Feed silicate	0	7715	24.8
Effluent silicate	0	5145	0.01
Removal %	n/a	33%	100%

10 g of Bayoxide were added to 40 mL of concentrate and shaken for 20 h. After decantation and filtration through 0.4 µm filter, ICP analysis performed.

Generic RIP process flowsheet of Ni, Co recovery

Lewatit® ion exchange resins are required in the most critical streams within the flow sheet

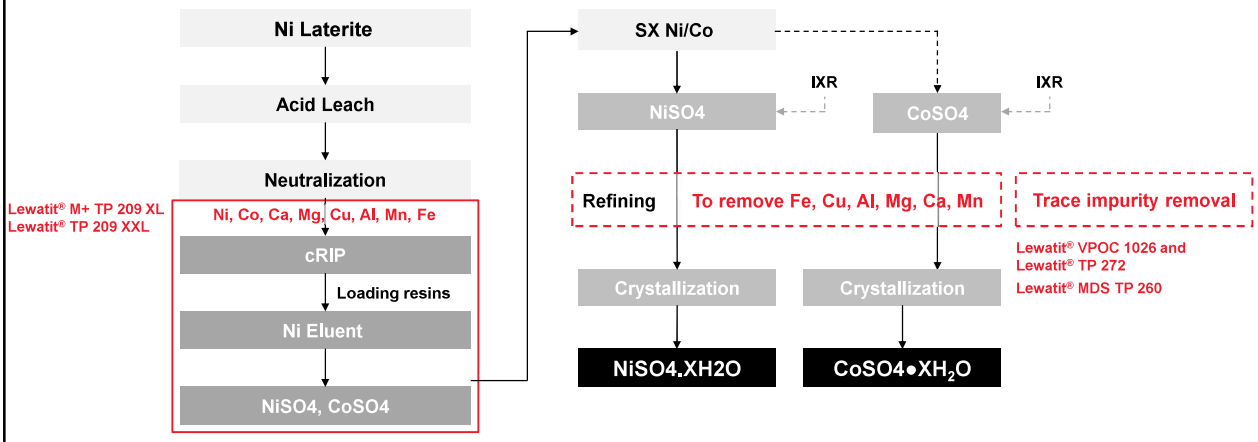

Principle of resin in pulp (RIP) employing Lewatit® MonoPlus TP 209 XL

Bead size, stability and capacity are crucial resin parameters for the resin in pulp process!

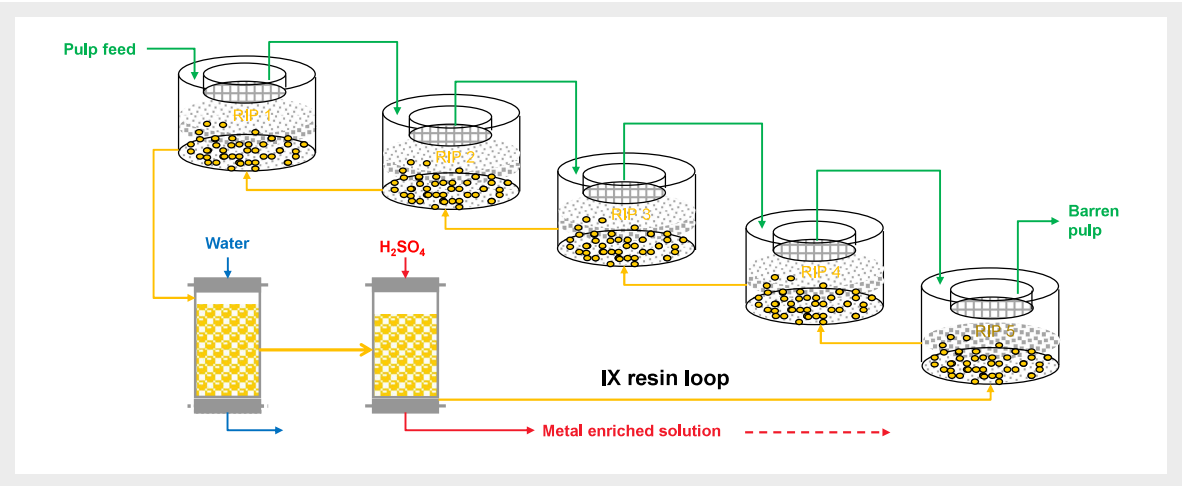

Special selective resin for RIP mining applications

Lewatit® MonoPlus TP 209 XL meets the needs for resin in pulp processes

Requirements for RIP

- Big bead diameter
- Very good kinetics in uptake and desorption
- High mechanical stability

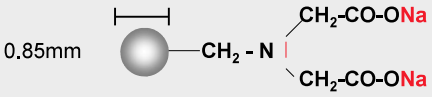

Lewatit®
MonoPlus TP 209 XL

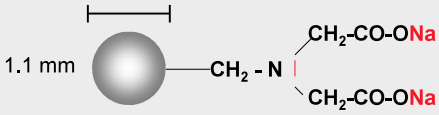

Lewatit®
TP 209XXL

Example

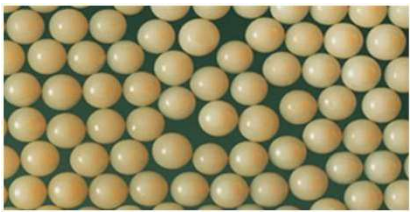

Mechanical stability test

Lewatit® MonoPlus TP 209 XL has superior mechanical stability compared to competition shown by various tests methods!

Attrition Test

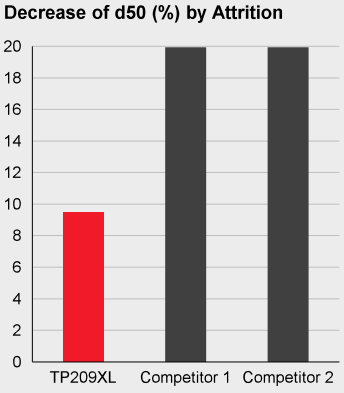

Roll Test

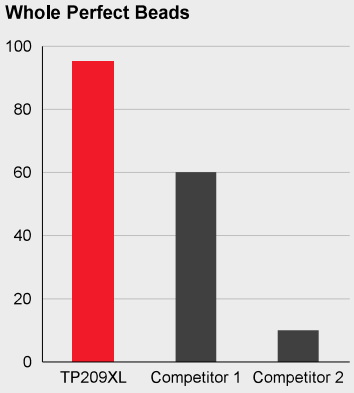

Ball Mill Test

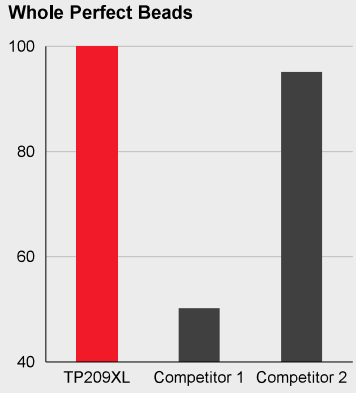

Nickel recovery in presence of high concentration of ferric using Lewatit® MDS TP 220

The resin has a high selectivity for nickel over ferric and cobalt!

Nickel	2.6 g/L
Ferric	17 g/L
pH	1.8
Temperature	r.T.
Specific velocity	10 BV/h

Other application fields

- Purification of cobalt electrolytes (nickel/cobalt separation)
- Copper recovery at low pH (<2)
- Separation of nickel and copper from chromium (III) and ferric solutions
- Selectivity Series: Cu^{2+}> UO_2^{+}> Pb^{2+} > Ni^{2+}> Fe^{3+}> Zn^{2+}>Co^{2+}> Cd^{2+}> Fe^{2+}>>>Cr^{3}

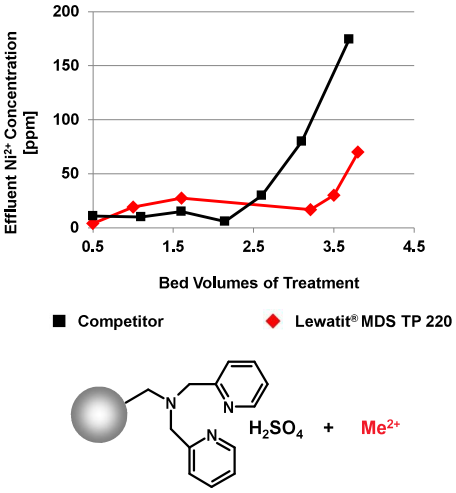

Lewatit® TP 272 – A Cyanex®1 doped resin

Immobilized Cyanex®1 272 as an alternative to solvent extraction

Loading

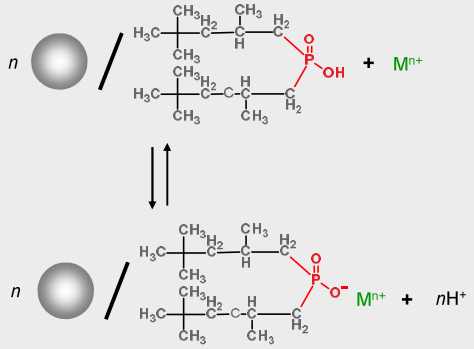

pH dependency of SX with Cyanex®1 272

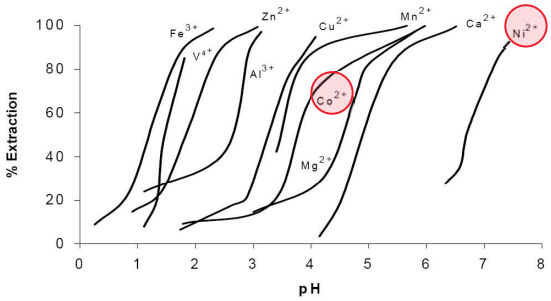

1 Product of Cytec Industries Inc., Woodland Park, NJ (USA)

Lewatit® TP 272 for Ni/Co separation

A selective resin for cobalt over nickel!

Loading

Nickel	≈ 80 g/L
Cobalt	≈ 990 mg/L
$(NH_4)_2SO_4$	≈ 50 g/L
pH adjustment	ammonia
pH	≈ 5,0
Temperature	≈ 65°C
Specific velocity	3 BV/h

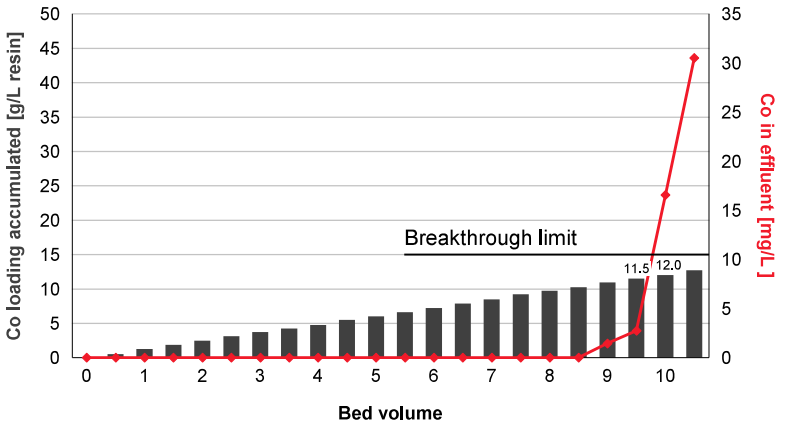

Selectivity series of Lewatit® VP OC 1026

The resin has a high selectivity for impurities over nickel and cobalt

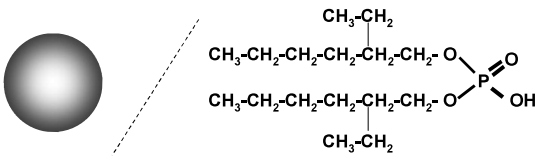

Lewatit® VP OC 1026
(Solvent impregnated resin)

Decomplexing pH

D pH	Cations
< 1	Ti^{4+} , Fe^{3+} , In^{3+} , $Sn^{2+/4+}$, Sb^{3+} , Bi^{3+} ,VO^{2+} , Be^{2+}
1 – 2	Al^{3+} , Zn^{2+} , Pb^{2+} , Cd^{2+} , La^{3+} , Ce^{3+} , Ca^{2+}
2 – 3	Mn^{2+} , Cu^{2+} , Fe^{2+}
3 – 4	Co^{2+} , Ni^{2+} , Mg^{2+}
> 4	Li^{+} , NH^{4+}

Selectivity series

Ti^{4+} > Fe^{3+} > In^{3+} > $Sn^{2+/4+}$ > Sb^{3+} > Bi^{3+} > VO^{2+} > Be^{2+} > Al^{3+} > Zn^{2+} > Pb^{2+} > Cd^{2+} > Ca^{2+} > Mn^{2+} > Cu^{2+} > Fe^{2+} > Co^{2+} > Ni^{2+} > Mg^{2+} > Cr^{3+} >>> Alkalis > H+

Selectivity series of Lewatit® VPOC 1026

The resin has a high selectivity for impurities over nickel and cobalt!

Ni^{2+} and Co^{2+} Concentrate Purification

- Lewatit® VP OC 1026 efficiently removes Zn^{2+} and Fe^{3+} from nickel and cobalt electrolytes
- Fe^{3+} can be stripped efficiently using HCl
- In case other bivalent ions such as Mg^{2+} is envisioned, a combination of Lewatit® VPOC 1026 and TP 272 is recommended

Asorption Isotherm

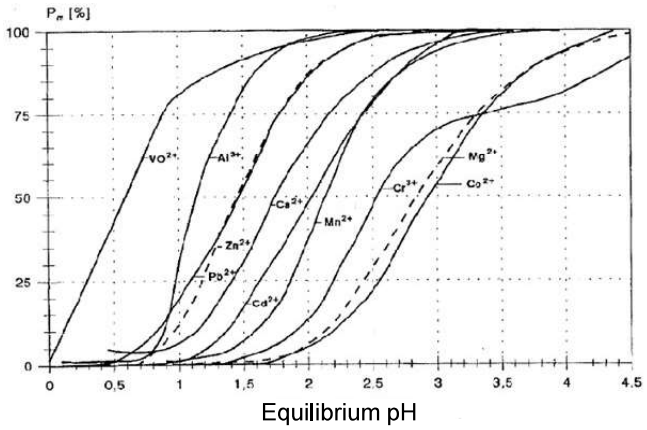

Ion exchange resins for high purity cobalt refining

Zink and copper removal from cobalt electrolyte

Lewatit® IXR are required in the most critical places within the flow sheet

Co+Ni 30 g/L
Zn 8 mg/L

Feed Nickel- and Cobalt Carbonate

LXS IXR technology

Acid Leaching and Iron Removal

Adjustment pH 3.5

Ni, Co, Zn, Cu

Copper Removal — Lewatit® MonoPlus TP 207

Ni, Co, Zn

60 °C
Zn < 1 ppm

Zn Removal — Lewatit® VPOC 1026

Ni, Co,

Cobalt Nickel Separation — Lewatit® MDS TP 220

Electrowinning

IXR: applied 10 cbm scale

The principle of copper electrorefining

When copper is transferred from the anode to the cathode, soluble impurities (e.g., Sb, Bi) are accumulating in the electrolyte and may have a negative effect on the cathode **quality**

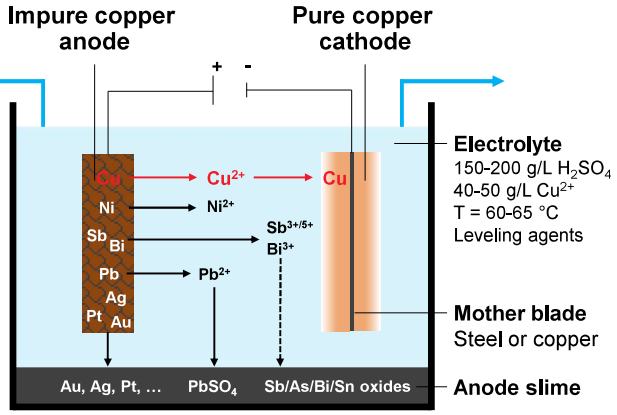

Example for anode composition

Metal	ppm.
Pb	1,300
Ni	4,000
As	700
Sb	100
Bi	120
Se	500
Te	70
Ag	1,000
Au	5

Source: B. E. Langner (2011), *Understanding Copper*

- A variety of other impurities (metals) are present in the anode
- During electrolysis these impurities are liberated along with copper
- Metals more precious than Cu precipitate to form anode slime along with other insoluble sulfates and oxides
- Less precious metals (at least partially) remain dissolved

Purification of a copper electrolyte for electrorefining

High selectivity towards Sb and Bi. Regeneration with the use of concentrated HCl

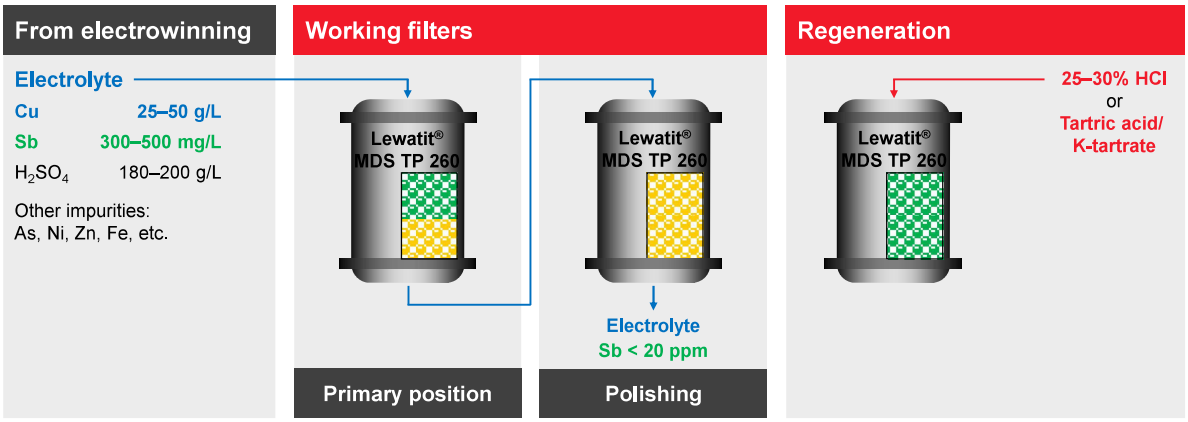

HF removal from $LiPF_6$ electrolyte

Pure electrolytes free of acid by Lewatit® MP 62 WS

Operation

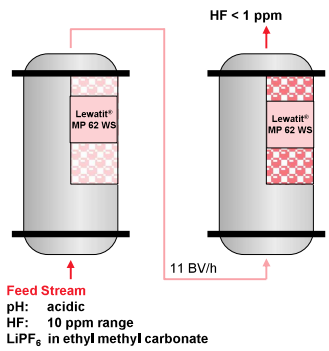

Regeneration

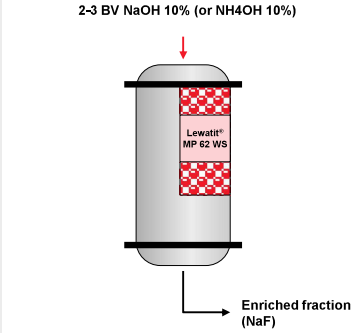

- HF generated by hydrolysis of $LiPF_6$
- Operating capacities up to 1 eq/L and more possible at high HF feed concentration
- At low feed concentrations operating capacities between 0.5 eq/L and 1 eq/L g/L

33 03.05.2023

Disclaimer

Health and Safety Information: Appropriate literature has been assembled which provides information concerning the health and safety precautions that must be observed when handling the LANXESS products mentioned in this publication. For materials mentioned which are not LANXESS products, appropriate industrial hygiene and other safety precautions recommended by their manufacturers should be followed. Before working with any of these products, you must read and become familiar with the available information on their hazards, proper use and handling. This cannot be overemphasized. Information is available in several forms, e.g., material safety data sheets, product information and product labels. Consult your LANXESS representative in Germany or contact the Regulatory Affairs and Product Safety Department of LANXESS Deutschland GmbH or - for business in the USA - the LANXESS Corporation Product Safety and Regulatory Affairs Department in Pittsburgh, PA, USA.

Regulatory Compliance Information: Some of the end uses of the products described in this publication must comply with applicable regulations, such as the FDA, BfR, NSF, USDA, and CPSC. If you have any questions on the regulatory status of these products, contact – for business in the USA- , the LANXESS Corporation Regulatory Affairs and Product Safety Department in Pittsburgh, PA, USA or for business outside US the Regulatory Affairs and Product Safety Department of LANXESS Deutschland GmbH in Germany.

The manner, in which you use and the purpose to which you put and utilize our products, technical assistance and information (whether verbal, written or by way of production evaluations), including any suggested formulations and recommendations are beyond our control. Therefore, it is imperative that you test our products, technical assistance and information to determine to your own satisfaction whether they are suitable for your intended uses and applications. This application-specific analysis must at least include testing to determine suitability from a technical as well as health, safety, and environmental standpoint. Such testing has not necessarily been done by us. Unless we otherwise agree in writing, all products are sold strictly pursuant to the terms of our standard conditions of sale. All information and technical assistance is given without warranty or guarantee and is subject to change without notice. It is expressly understood and agreed that you assume and hereby expressly release us from all liability, in tort, contract or otherwise, incurred in connection with the use of our products, technical assistance, and information.

Any statement or recommendation not contained herein is unauthorized and shall not bind us. Nothing herein shall be construed as a recommendation to use any product in conflict with patents covering any material or its use. No license is implied or in fact granted under the claims of any patent.